UNIVERSIDAD AUTÓNOMA DE MADRID

DEPARTAMENTO DE BIOQUÍMICA

Tesis Doctoral

The identification of new familial pheochromocytoma/paraganglioma genes using whole exome sequencing

IÑAKI COMINO MÉNDEZ

Madrid, 2015

DEPARTAMENTO DE BIOQUÍMICA

FACULTAD DE MEDICINA

UNIVERSIDAD AUTÓNOMA DE MADRID – UAM

The identification of new familial pheochromocytoma/paraganglioma genes using whole exome sequencing

Tesis Doctoral presentada por:

Iñaki Comino Méndez

Licenciado en Biología y Licenciado en Bioquímica por la Universidad de Navarra (UN)

Máster en Biotecnología por la Universidad Autónoma de Madrid (UAM)

Directores de la Tesis:

Dr. Alberto Cascón Soriano

Investigador del Grupo de Cáncer Endocrino Hereditario (CNIO)

Dra. Mercedes Robledo Batanero

Jefa del Grupo de Cáncer Endocrino Hereditario (CNIO)

GRUPO DE CÁNCER ENDOCRINO HEREDITARIO

PROGRAMA DE GENÉTICA DEL CÁNCER HUMANO

CENTRO NACIONAL DE INVESTIGACIONES ONCOLÓGICAS (CNIO)

Dr. Alberto Cascón Soriano, Investigador del Grupo de Cáncer Endocrino Hereditario del Centro Nacional de Investigaciones Oncológicas (CNIO), como codirector,

Dra. Mercedes Robledo Batanero, Jefa del Grupo de Cáncer Endocrino Hereditario del Centro Nacional de Investigaciones Oncológicas (CNIO), como Profesora Honoraria del Departamento Biología Molecular de la Universidad Autónoma de Madrid y como codirectora y

Dr. Miguel Campanero García, Científico Titular del Departamento de Biología del Cáncer del Instituto de Investigaciones Biomédicas "Alberto Sols" CSIC-UAM, como Tutor,

CERTIFICAN:

Que **Don Iñaki Comino Méndez**, Licenciado en Biología y Licenciado en Bioquímica por la Universidad de Navarra, ha realizado la presente Tesis Doctoral **"The identification of new familial pheochromocytoma/paraganglioma genes using whole exome sequencing"** y que a su juicio reúne plenamente todos los requisitos necesarios para optar al **Grado de Doctor**, a cuyos efectos será presentada en la Universidad Autónoma de Madrid, autorizando su presentación ante el Tribunal Calificador.

Y para que así conste se extiende el presente certificado,

Madrid, Febrero 2015.

V^{o}B^{o} codirector:	V^{o}B^{o} codirectora:	V^{o}B^{o} Tutor:
Dr. Alberto Cascón Soriano	Dra. Mercedes Robledo Batanero	Dr. Miguel Campanero García

La presente Tesis Doctoral se realizó en el Centro Nacional de Investigaciones Oncológicas (CNIO) de Madrid entre los años 2010 y 2015 bajo la supervisión del Dr. Alberto Cascón Soriano y la Dra. Mercedes Robledo Batanero.

Las siguientes becas, ayudas y proyectos han permitido la realización de esta Tesis Doctoral:

● Beca Lanzadera promovida por el Centro de Investigación Biomédica en Red de Enfermedades Raras (CIBERER) (Unidad 706). Período: 2010-2011

● Beca de Investigación Biomédica "Severo Ochoa" promovida por la Fundación Ferrer Investigación (Convocatoria 2011). Período: 2011-2013

● Proyecto PS09/00942 del Fondo de Investigación Sanitaria (FIS) del Instituto de Salud Carlos III dirigido por el Dr. Alberto Cascón Soriano. Periodo: 2010-2012.

● Proyecto PI12/00236 del Fondo de Investigación Sanitaria (FIS) del Instituto de Salud Carlos III dirigido por el Dr. Alberto Cascón Soriano. Periodo: 2013-2015.

RESUMEN/ABSTRACT

RESUMEN

Los feocromocitomas (PCC) son tumores neuroendocrinos, desarrollados a partir del tejido cromafín de la médula adrenal, que suelen causar hipertensión arterial por sobre-secreción de catecolaminas. Los paragangliomas (PGL) son PCCs, en su mayoría secretores y con un gran riesgo de malignizar, que se desarrollan a partir de paraganglios localizados fundamentalmente en la región intra-abdominal o torácica. Algunos PGLs pueden desarrollarse en la región de la cabeza y el cuello, y en esa localización suelen comportarse como masas benignas no secretoras. Los PCCs presentan una incidencia anual en población española de 2 casos por millón de habitantes y son por tanto una enfermedad rara. Tanto la secuenciación masiva del genoma completo, como la limitada a las regiones codificantes (secuenciación exómica, SE), se han convertido a lo largo de los últimos años en herramientas de gran utilidad para el descubrimiento de genes de susceptibilidad responsables de enfermedades mendelianas. De este modo, el objetivo principal de esta tesis doctoral fue la identificación de nuevos genes de susceptibilidad implicados en el desarrollo de PCC/PGL mediante el uso de la SE aplicada a 3 proyectos independientes. En el primer proyecto, se llevó a cabo la SE de tres pacientes no relacionados, con antecedentes familiares de la enfermedad y sin mutaciones en ninguno de los genes conocidos. Los pacientes fueron seleccionados como candidatos para el estudio debido a que sus correspondientes tumores presentaban perfiles de expresión muy homogéneos. El filtrado y posterior análisis de los datos de secuenciación permitió identificar mutaciones germinales patogénicas en el gen *MAX* en los tres pacientes. Además, la pérdida de heterocigosidad del alelo silvestre, la ausencia de proteína MAX en los tumores y el descubrimiento de otras 5 mutaciones en pacientes aquejados de la enfermedad permitió demostrar que *MAX* constituía un nuevo gen supresor de tumores asociado con el desarrollo de PCC hereditario. En un segundo trabajo, el estudio de una serie compuesta por más de 1500 pacientes no relacionados permitió establecer tanto la prevalencia de las mutaciones en *MAX* en pacientes con PCC/PGL (1,12%), como el fenotipo asociado a dichas mutaciones. Por último, con el objeto de determinar la patogenicidad de las variantes con significado desconocido halladas en el gen *MAX*, se llevó a cabo un estudio funcional de las mismas en células de PCC de rata (PC12) y se implementó una herramienta de predicción *in silico* basada en el consenso de 5 predictores. En el segundo proyecto, los candidatos a estudio mediante SE (3 tríos paciente/madre/padre) fueron seleccionados en base a la presencia de una característica fenotípica poco frecuente en pacientes con PCC/PGL: policitemia idiopática. Durante el análisis de los datos, se publicó el descubrimiento de mutaciones somáticas post-zigóticas en el gen *EPAS1* en pacientes con PCC/PGL múltiple y policitemia idiopática. El análisis de *EPAS1* en los correspondientes tumores de los pacientes seleccionados para la SE, reveló la presencia de mutaciones somáticas en mosaico en el gen *EPAS1* en todos ellos. Además, el estudio de una serie adicional de tumores identificó mutaciones somáticas en tumores de pacientes sin policitemia. Finalmente, se identificó la ganancia de la región 2p como exclusiva de tumores con mutación en *EPAS1*. En el tercer proyecto, se llevó a cabo una selección de pacientes basada en la presencia de tumores múltiples (más de 5) como indicador de la existencia de una enfermedad hereditaria. Durante el filtrado de las variantes encontradas en uno de los pacientes seleccionados, se identificó una mutación en el gen *MDH2*, implicado en el ciclo de Krebs. La ausencia de RNAm, proteína y actividad enzimática malato deshidrogenasa, así como el diagnóstico de la enfermedad en un pariente portador de la variante permitió concluir que el gen *MDH2* es un nuevo gen supresor tumoral responsable de susceptibilidad a desarrollar PCC/PGL. La identificación de este segundo gen de susceptibilidad a desarrollar PCC/PGL demuestra la eficacia de la SE en la identificación de nuevos genes responsables de enfermedades mendelianas.

ABSTRACT

Pheochromocytomas (PCCs) are neuroendocrine tumors arising from the medulla of the adrenal gland that usually cause hypertension due to oversecretion of cathecolamines. On the other hand, paragangliomas (PGLs) are normally secretor tumors with high risk of malignancy that arise from the paraganglia of the intra-abdominal or thoracic regions. Some PGLs arise in the head and neck region, usually as benign, non-secretor tumors. PCC/PGL is a rare disease, with an incidence in the Spanish population of approximately 2 cases per million habitants. High-throughput techniques such as whole-genome sequencing (WGS) and whole-exome sequencing (WES) are nowadays widely applied to discover susceptibility genes involved in mendelian diseases. Thus, the main objective of this thesis was to identify new genes related to the susceptibility to develop PCC/PGL by applying WES in three independent projects. In the first project, we applied WES to three unrelated patients with a family history of disease testing negative for mutations in the major PCC/PGL susceptibility genes. The three patients were selected because they shared a common homogeneous transcriptional profile, suggesting a common underlying genetic alteration. The variant filtering process and the posterior analysis of the WES data allowed us to identify pathogenic germline mutations in the *MAX* (MYC associated factor X) gene in all three patients. Moreover, loss of heterozygosity of the wild type allele, loss of the protein in the tumors and the identification of *MAX* mutations in additional patients with the disease, together indicated that *MAX* constitutes a novel tumor suppressor gene. In a posterior international collaborative study, we recruited more than 1500 unrelated patients and established the prevalence of *MAX* mutations to be 1.12%; we also characterized the associated phenotype. Finally, we developed a functional model to determine the pathogenicity of variants of unknown significant (VUS) found in *MAX*. This model was implemented based on a consensus *in silico* prediction obtained from five algorithms available online. In the second project, the selection of three trios (patient/mother/father) was based on the presence of a very infrequent phenotypic characteristic in patients suffering for PCC/PGL: idiopathic polycythemia. While the analysis of the WES data was underway, a study was published reporting the presence of somatic post-zygotic mutations in the gene *EPAS1* (*HIF2A*) in patients presenting multiple PCC/PGL and idiopathic polycythemia. Our posterior screening for *EPAS1* mutations in the tumors from the index patients revealed the presence of somatic mutations in all of them. In addition, the analysis of an additional series of tumors identified somatic mutations in tumors from patients without polycythemia. Finally, we indentified a gain of the chromosomic region 2p exclusive to tumors harboring *EPAS1* mutations. In the last WES Project, we selected patients based on the presence of multiple (more than five) tumors as phenotypic marker of hereditary disease. We identified a splice-site mutation affecting the *MDH2* gene involved in the Krebs cycle. The observed absence of the messenger RNA, protein and malate dehydrogenase enzymatic activity, as well as the positive diagnosis for the disease of a family member, led us to conclude that *MDH2* is a novel tumor suppressor gene implicated in susceptibility to develop PCC/PGL. The identification of this second susceptibility gene implicated in PCC/PGL development demonstrates the efficacy of WES in discovering susceptibility genes involved in Mendelian diseases.

INDEX

ABBREVIATIONS

5-mC - 5-methylcytosine

CIMP - CpG island methylator phenotype

CNS - Central nervous system

COSMIC - The catalogue of somatic mutations in cancer

CT - Computed tomography

FDG – Fluorodeoxyglucose

GWAS - Genome wide association studies

HGP - Human genome project

INDELs - Small insertions and deletions

LOH - Loss of heterozygosity

MIGB - Metaiodobenzylguanidine

MRI - Magnetic resonance imaging

NGS - Next generation sequencing

PCC - Pheochromocytoma

PET - Positron emission tomography

PGL - Paraganglioma

SNPs - Single nucleotide polymorphism

UPD - Uniparental disomy

VUS - Variants of unknown significance

WES - Whole exome sequencing

WGS - Whole genome sequencing

α-KG - α-ketoglutaric acid

ccRCC - Clear-cell renal cell carcinoma

HLRCC - Hereditary leiomyomatosis and renal cell cancer

PHPT - Primary hyperparathyroidism

MTC - Medullary thyroid cancer

MEN - Multiple endocrine neoplasia

SCLC - Small-cell lung cancer

NF1 - Neurofibromatosis type 1

HB - Hemangioblastoma

GIST - Gastrointestinal stromal tumors

VHL - von Hippel-Lindau

INTRODUCTION

1. GENERAL ASPECTS OF THE DISEASE

Pheochromocytomas (PCCs) are rare neuroendocrine tumors that arise from the chromaffin cells of the adrenal medulla, and usually cause secondary hypertension via over secretion of catecholamines. On the other hand, paragangliomas (PGLs) are secreting or non-secreting tumors that develop from paraganglia of the sympathetic or parasympathetic chains, respectively. PCCs and PGLs share their origin in the neural-crest, and though they are usually benign, between 10 and 15% develop distant metastases in embryologically different tissues such as bone, liver, lungs or lymph nodes.

1.1 HISTORY

The adrenal glands were first described in 1563 by Eustachius in the study *Opscula anatomica*[1], in which he established their division into cortex and medulla. It was not until 1855 that Addison described the pivotal role of the adrenal glands in releasing hormones (e.g. catecholamines) in response to stress in patients with tuberculosis[1]. Almost thirty years later, in 1884, the first diagnosis of what was later to become known as PCC was reported in a 18 year-old woman from a small village near Lahr in Germany[2]. The patient was admitted to hospital because of palpitations, anxiety, vomiting, headache, and muscle weakness. Ten days later, she died and the autopsy revealed two adrenal tumors that were initially diagnosed as sarcoma and adrenal angiosarcoma. Interestingly, one century later this case was reviewed by Neumann *et al*.[3] who concluded that the patient, diagnosed at an early age and presenting with bilateral adrenal tumors (PCCs), was really the first reported case of multiple endocrine neoplasia (MEN) type 2. The descriptive term PCC was formulated in 1912 by the pathologist Ludwig Pick because of its colourful reaction in fixatives containing chromic acid salts, something lately corroborated by Manasse[4]. The term PGL had been adopted previously, in 1908, by Alezais and Peyron to describe extra-adrenal chromaffin tumors arising from paraganglia.

1.2 EPIDEMIOLOGY

Together, PCCs and PGLs have an overall annual incidence of 2 per million in the Spanish population and 3-8 per million in the United States[5], and although their prevalence is unknown it has been estimated to lie between 1/6500 and 1/2500 in the United States[6]. However, these figures are probably under-estimates, taking into consideration the high frequency of incidental diagnoses from autopsies[7,8]. Of note, PCC is the most common endocrine tumor diagnosed in children, despite the fact

that the mean age at diagnosis is approximately 43 years[9]. Thus, between 10 and 20% of patients affected with the disease are diagnosed during childhood, which is usually associated with a genetic germline alteration[10-12]. No difference is seen between males and females in the incidence of pheochromocytoma.

1.3 CLINICAL PRESENTATION

Patients suffering from PCC/PGL can present with a variety of nonspecific symptoms that may suggest other diseases. Given the frequent finding of incidental masses in autopsies, the identification of signs and symptoms of PCC/PGL has become one of the most challenging aspects in the clinical management of the disease[7,8].

The most frequent symptoms of catecholamine-secreting PCCs/PGLs are sustained or paroxysmal hypertension, headaches, sweating and palpitations. Less frequent are pallor, anxiety or panic attacks, fever, nausea and vomiting[6,13]. Patients with non-secreting PGLs in the intra-abdominal region suffer from hydroureteronephrosis or renal hypertension due directly to the tumor mass. In patients with non-secreting head and neck PGLs, unilateral hearing loss, pulsate *tinnitus,* hoarseness, cough, headache, difficulty swallowing, tongue mobility problems or feeling of pharyngeal fullness can be found, depending on the size and location of the tumor[6,13].

As mentioned above, one of the main differences between PCCs and PGLs is the anatomical location of the tumor, which is also related to the underlying germline alteration. Whereas 70% of tumors appear in the adrenal medulla, around 30% present as highly vascular masses within sympathetic and, more rarely, parasympathetic paraganglia distributed along the paravertebral and paraaortic axis. The main anatomical locations of PGLs are (Figure 1):

a) **Abdominal and retroperitoneal sympathetic paraganglia** (81%), mainly located in the Zuckerkandl organ, the bladder, the renal hilum, the urethra or the prostate gland[14].
b) **Thoracic** (11%) **and cranial sympathetic** (3%) **paraganglia**, mainly located at the median region of the thorax or the base of the heart.
c) **Head and neck parasympathetic paraganglia** (5%), mostly occurring at the carotid bifurcation, the jugular bulb or the tympanic plexus on the promontory and the vagal nerve.

Both, PCCs and PGLs can present as single, bilateral or multiple tumors distributed across any of the aforementioned anatomical locations. Moreover, their clinical presentation is often associated with the presence of germinal alterations affecting specific susceptibility genes[15].

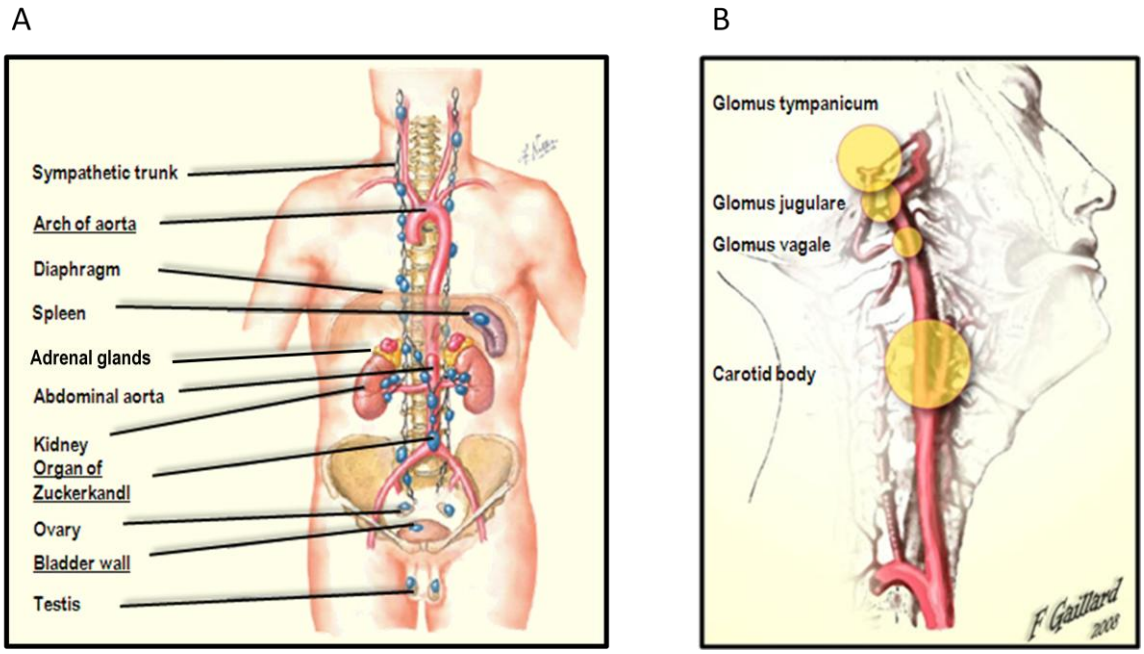

Figure 1. Overview of the main locations for PCC and PGL of the parasympathetic and sympathethic nerve system. **A)** Anatomic distribution of PCC and PGL in the thoraco-abdominal region. **B)** Distribution of the paragangliomas of the head and neck. Ilustration A was published in The Netter Collection of Medical Illustrations - Endocrine System. Image B was created by Frank Gaillard and the original background image by Gray's Anatomy 1918.

1.4 DIAGNOSIS

The vast majority of patients suffering from PCC/PGL presents with the symptoms mentioned previously. However, a small percentage presents with less specific symptoms which makes diagnosis much more complicated. Regardless of the symptoms, the main procedures used to detect the presence of these tumors are biochemical tests and imaging.

1.4.1 Biochemical testing

Catecholamines are hormones mainly synthesized by the adrenal medulla, the sympathetic nerves and the central nervous system (CNS), although other non-neuronal cells located in the digestive tract and the kidneys are also able to produce them in smaller amounts[16]. The diagnosis of PCC and sympathetic PGL is based on biochemical evidence of the hypersecretion of catecholamines[6] since these tumors produce, store, synthesize and metabolize high levels of these hormones. The most abundant catecholamines in the human body are epinephrine (adrenaline), norepinephrine (noradrenaline) and dopamine. In addition, PCC/PGL chromaffin cells have specific catecol-O-methyltransferase (COMT) activity that metabolizes catecholamines (epinephrine, norepinephrine and dopamine) into metanephrines (metanephrine, normetanephrine and methoxytyramine)[17].

The production of catecholamines in tumors is highly fluctuating[13] and may lead to false-negative results, making the diagnosis of PCC/PGL based on measurement of catecholamine levels in plasma or urine unreliable and outdated. In contrast, the release of metanephrines (epinephrine and norepinephrine) by the tumor is very stable in time and is consistently elevated in patients with biochemically active PCC/PGL[6], unless the tumor mass is very small[18]. There is little consensus on the utility of urine or plasma to perform the measurement of metanephrines. While the determination of metanephrines in plasma has greater specificity and sensitivity (98% and 100%, respectively) than that in urine (both 96%), it requires that the patient meet the following conditions in order to minimize the number of false positives: free of stress, 8-12 hours fasting, supine position and extraction after 20-30 minutes following insertion of the venous cannula (reviewed in[19]). In general, when a level more than four-times greater than the upper limit of the normal range is observed, the chance of finding PCC/PGL is high and further analysis to determine the tumor location is indicated. When a smaller increase is observed or when the result is unclear, checks should be carried out for technical errors, inadequate sample extraction and other clinical conditions that could elevate catecholamines. Results can be confirmed in plasma if originally determined in urine, or vice versa. Finally, in rare cases PCCs/PGLs can secrete dopamine only, and the diagnosis of these tumors can be overlooked by the metanephrine measurement tests. Recent studies have demonstrated that methoxytyramine, a metabolite of dopamine, can be used to detect these particular secreting PCCs/PGLs[20].

1.4.2 Imaging-based determination of tumor location

Studies to determine tumor location should only be carried out following a positive biochemical diagnosis, except for non-secreting parasympathetic PGLs (mainly located in the head and neck region). Computed tomography (CT) or magnetic resonance imaging (MRI) are the imaging techniques most widely used to detect PCC/PGL; they have sensitivity and specificity of 90-100% and 70-80%, respectively[21]. CT scans can visualize adrenal tumors larger than 1cm and extra-adrenal tumors larger than 2cm[9]. MRI is more expensive but has three key advantages: 1) intravenous contrast is not required; 2) it is better than CT at detecting extra-adrenal tumors; 3) it does not emit ionizing radiation[22]. Thus, MRI is preferred in patients with extra-adrenal tumors, CT-contrast allergies, in pregnant or pediatric patients and in patients in whom radiation exposure should be limited[13].

Functional tests may be carried out to determine PCC/PGL location when other methods fail or require confirmation, or in order to identify metastatic disease overlooked by the anatomic techniques explained above. In these tests, detection of the tumors is based on their *in vivo* metabolic activity. ^{123}I- or ^{131}I-metaiodobenzylguanidine (MIBG) scintigraphy is usually the functional test of choice since the molecular structure of MIBG resembles norepinephrine and it may enter tumor cells via the same

transporters. ^{131}I-MIGB is most widely used because of its high sensitivity, better detection rate, higher possible doses, and shorter required intervals between injection and image acquisition[23]. MIBG has some limitations in detecting metastases, extra-adrenal tumors or tumors harboring *SDHB* mutations[24]. More recently, positron emission tomography (PET) has come to be considered a better functional test because of its high sensitivity, shorter image acquisition times and higher image resolution[23,25]. This technique uses radiotracers such as ^{18}F-fluorodeoxyglucose (FDG), which are taken up by the glucose transporter[25]. Other radiotracers used include ^{18}F-fluorodopamine (FDA) and ^{18}F-fluorodopa (FDOPA), the latter of which is highly specific for head and neck PGL[26]. Techniques involving radiotracers FDOPA and FDG are especially effective in detecting metastasis in patients carrying mutations in *SDHB*[6,9,22,27,28]. Additional imaging techniques include OctreoScan® and ^{68}-Ga-DOTA peptides[23,29,30].

1.5 TREATMENT

Surgery is currently the only option to treat PCC/PGL with the possibility of curing the disease. Biochemically active tumors, once localized, should be treated immediately with antihypertensive medications (α- and β-blockers) to control symptoms and reduce the risk of hypertensive crises. Treatment is preferentially initiated with α-blockers, and after this β- blockers should be introduced if tachyarrhythmia appears[31,32]; these may not eliminate the possibility of hypertensive crisis during surgery, but reduce the severity should one occur[33]. Laparoscopic intervention has lower associated morbidity and mortality than open procedures, and thus is preferred, when possible, both for PCC and sympathetic PGL[33], and also for large, multiple, bilateral or recurrent tumors. If metastases are suspected, open resection is recommended in order to remove as much malignant tissue as possible[34]. Bilateral adrenalectomy is an option for cases of hereditary PCC, but bilateral partial adrenalectomy can be a better option because it preserves partial function of the organ[6]. The choice of surgery or chemotherapy treatment for patients with head and neck PGLs depends on the accessibility of the tumor, the size, and possible secondary effects of its location and vascularisation. If surgery cannot be performed, is critical to closely follow-up the patient in order to avoid damage (local vessel and nerve compression) triggered by the tumor.

The therapeutic options for malignant cases are limited and rarely curative. For unresectable tumors detected by ^{123}I-MIBG scintigraphy, radiotherapy with ^{131}I is recommended. When the tumor is negative for ^{123}I-MIBG scintigraphy or is fast-growing, chemotherapy (cyclophosphamide, vincristine or dacarbazine) alone, or in combination with radiotherapy, may be a feasible option[35]. Our increasing knowledge of the molecular biology of these tumors is helping to extend the therapeutic options applicable to unresectable tumors. There are currently two types:

a) **Pro-apoptotic agents**: somatostatin analogues, histone deacetylase (HDAC) inhibitors, eicosapentaenoic acid, triptolide/capsaicin, gamitrinib and camptothecin[36-41].
b) **Anti-proliferative agents**: everolimus (a mammalian target of rapamycin [mTOR] pathway 1 inhibitor), AEZS-131 (ERK inhibitor), AZD-8055 (mTOR1 and mTOR2 inhibitor), sunitinib[42,43] and other tyrosine kinase inhibitors[44], LB1 (inhibitor of serine/threonine protein phosphatase 2A) combined with temozolomide and inhibitors of carboxypeptidase E[35].

There are several treatment options to alleviate pain or symptoms due to local compression, including radiotherapy (especially for bone metastases) and local treatments such as cryo- and radiofrequency ablation, radionucleotides and or/embolization[6,28]

1.6 GENETICS

Many years ago, PCC was dubbed the "10 percent tumor" since it was thought that 10% of tumors were bilateral, 10% ocurred in childhood, 10% were extra-adrenal, 10% were hereditary and 10% were malignant[14]. However, studies published since 2000 have shown that some of these percentages are quite different to 10%. Thus, nowadays we know that more than 30% of patients develop extra-adrenal tumors[45,46], that malignancy depends on the location of the primary tumor and/or the gene mutated (e.g. more than 30% of tumors harboring mutations in the *SDHB* gene are malignant)[47], and that approximately 40% of cases carry a germline mutation in one the known susceptibility genes[15], which means that PCC/PGL has the highest heritability of all human tumors. This figure is even higher for pediatric disease since up to 80% of children with PCC harbor mutations, regardless of their family history[10,26].

Despite being rare tumor entities, PCC and PGL are the common phenotypes across the major hereditary endocrine cancer syndromes: neurofibromatosis type 1 (NF1), MEN types 1, 2A and 2B, and von Hippel-Lindau (VHL) syndrome. Moreover, PCC and PGL susceptibility can be inherited, with or without the presence of other tumors that form part of these paraganglionic syndromes (PGL1-5). They can be also found associated with gastrointestinal tumors (GIST) in Carney-Stratakis syndrome (OMIM: #606864) or with GIST and pulmonary chondromas in the Carney Tryad (OMIM: #604287). Finally, PCC and PGL susceptibility can be inherited alone via germline mutations in transmembrane protein 127 (*TMEM127*)[48,], MYC associated factor X (*MAX*)[49], the fumarate hydratase (*FH*)[50] gene, or the malate dehydrogenase (MDH) 2 gene (in press). Overall, 16 different susceptibility genes[15,51] (in press) have been shown to be mutated in the germline of patients with PCC/PGL. In addition, around 25-30% of PCCs/PGLs are caused by somatic mutations affecting the same susceptibility genes involved in hereditary cases.

Ten yeas ago, Eisenhofer *et al*. (2004)[52] performed the first transcriptional profiling study of PCC. In this study, the authors compared tumors harboring mutations in *VHL* (norepinephrine secreting tumors) *versus* tumors carrying mutations in the *RET* proto-oncogene (epinephrine secreting tumors) with the aim of identifying differences in gene expression patterns. Thus, they observed for the first time an enrichment of the hypoxia-driven angiogenic pathways in *VHL*-mutated tumors. A second transcriptional profiling study performed by Dahia *et al*. (2005)[53] described a functional link between tumors with *VHL* mutations and those with disruption of the genes encoding succinate dehydrogenase (SDH) subunits B (SDHB) and D (SDHD). Moreover, they proposed that PCCs and PGLs can be segregated into two clusters based on their genetic background: **Cluster 1**, enriched with tumors carrying alterations in genes related to the hypoxic response (*VHL* and the SDH genes), and **Cluster 2**, containing tumors that activate kinase signaling (via mutations in *RET* and *NF1*). Subsequently, studies performed by Favier *et al*[54] and our group[55] replicated the two characteristic transcriptional clusters, and demonstrated that tumors belonging to Cluster 1 can be further distinguished into two sub-clusters (*VHL*- and SDH gene-related) based on the activation of distinct pseudo-hypoxic pathways. Studies since then have demonstrated the utility of "omics"-based classification tools in the discovery of hidden alterations in PCC/PGL patients without mutations in the known susceptibility genes[49,50].

The known susceptibility genes (Figure 2) can be described in the context of this transcriptional classification of PCCs/PGLs into two clusters:

a) **Cluster 1**: the hypoxia-driven angiogenesis cluster enriched with tumors carrying alterations in genes implicated in the hypoxic response, including *VHL*, the SDH genes (*SDHA, SDHB, SDHC, SDHD* and *SDHAF2*), *FH*, *MDH2*, and hypoxia-inducible factor (HIF)-2α (also known as endothelial PAS domain protein 1, *EPAS1*).
b) **Cluster 2**: the RAS/mTOR cluster composed of tumors harboring mutations in genes involved in the activation of kinase signaling, such as *RET*, *NF1*, *MAX*, *TMEM127* and the Harvey rat sarcoma viral oncogene (*HRAS*).

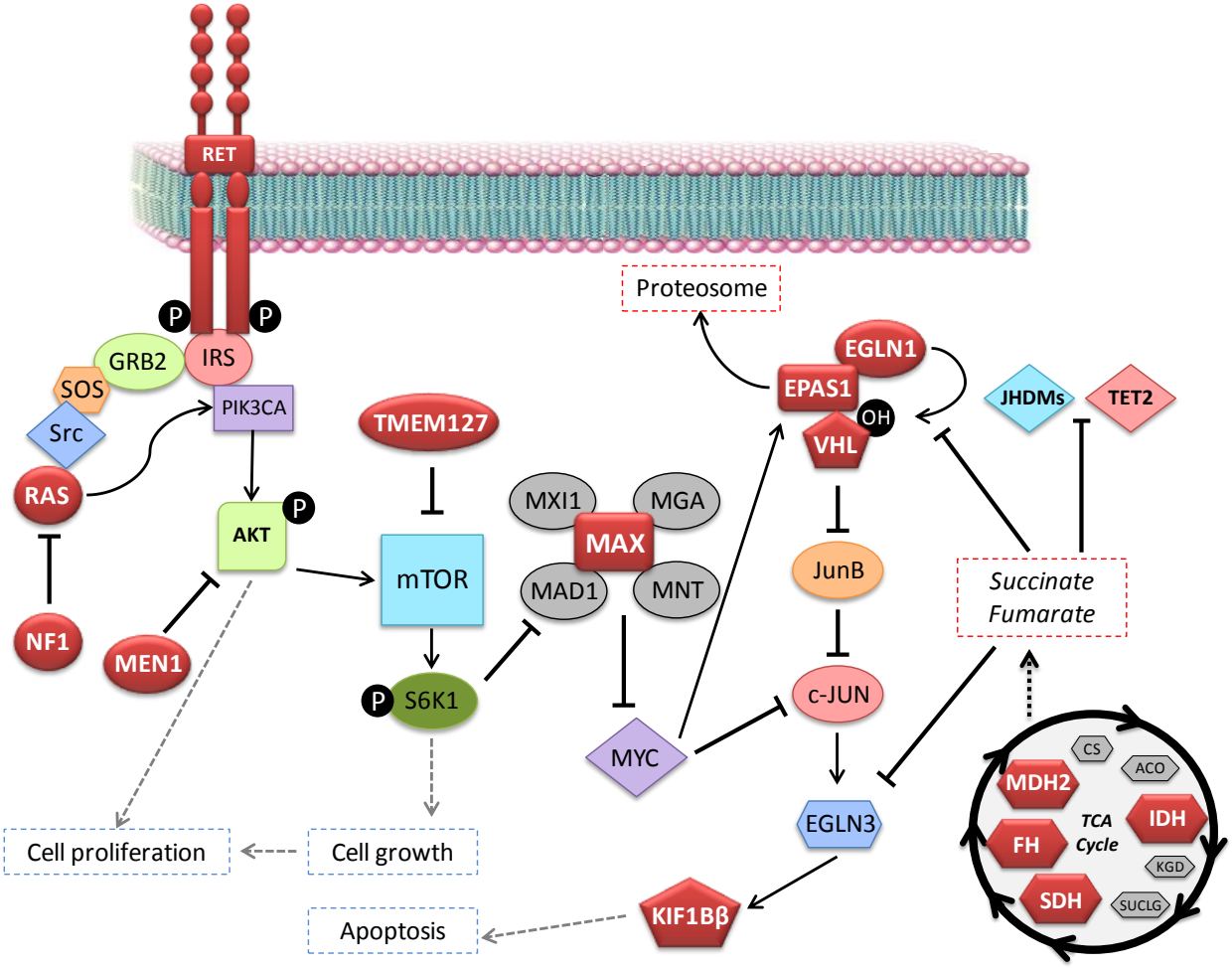

Figure 2. Schematic representation of the canonical pathways for PCC/PGL susceptibility genes (filled in red).

Cluster 1 genes: *VHL*, the SDH genes, *EPAS1*, *FH* and *MDH2*

Under normal conditions, the hypoxic response is activated to adapt the organism to a lack of oxygen[56]. However, this pathway can be activated regardless of oxygen levels as a consequence of mutations in one of several genes; this process is called pseudo-hypoxia[57].

- *VHL*

The VHL protein is the substrate recognition component of a very important E3 ubiquitin ligase complex that plays a central role in the ubiquitination and posterior degradation of the transcription factors HIF-1, HIF-2 and HIF-3α by the proteosome, preventing the subsequent activation of genes implicated in the hypoxic response[58]. The inactivation of VHL triggers the stabilization of the HIF family of transcription factors (pseudo-hypoxia) and the consequent expression of HIF-target genes involved in

transformation, angiogenesis and glucose uptake. It also triggers an increase in expression of growth factors such as vascular endothelial growth factor (VEGF), platelet-derived growth factor (PDGFB), transforming growth factor (TGF) and erythropoietin (EPO)[59].

VHL (OMIM: #193300) is an autosomal dominant syndrome with a prevalence of 1 in 36,000, and variable clinical manifestation. The syndrome is caused by germline mutations affecting the tumor suppressor gene *VHL*[60]. Besides the development of PCC, and more rarely PGL, VHL patients are at high risk of developing hemangioblastoma (HB) of the retina and CNS, clear cell renal cell carcinoma (ccRCC), renal and pancreatic cysts, neuroendocrine pancreatic tumors, endolympathic sac tumors, pancreatic serous cystadenomas and papillary cystadenomas of the epididymis in men and of the broad ligament in women[61].

VHL families are categorised into two main types based on the risk of developing PCC[62]:

VHL type 1: the most common form of the disease. Patients can present with all the conditions described above, have a low risk of PCC, and can be classified in two subtypes depending on ccRCC risk:

i. Subtype 1A: high risk of ccRCC.
ii. Subtype 2B: low risk of ccRCC.

VHL type 2: patients have high risk of PCC and HB and can be classified in three subtypes depending on ccRCC risk:

i. Subtype 2A**:** low risk of ccRCC.
ii. Subtype 2B: high risk of ccRCC.
iii. Subtype 2C: PCC is the unique sign in the disease.

Approximately 20% of patients with VHL develop PCC. *VHL* has a high mutation rate (20-21%)[19], and so mutation testing of this gene is specifically recommended for detecting *de novo* cases amongst apparently sporadic and non-syndromic patients. In fact, somatic mutations affecting *VHL* are frequent in sporadic PCCs, being the second most prevalent somatic alteration found in PCC/PGL after *NF1* mutations[15]. Other clinical and molecular characteristics associated with *VHL*-mutated PCCs/PGLs, as well as with mutations affecting the susceptibily genes, are described in Table 1.

Table 1. Summary of phenotypic and genetic features associated with the described PCC/PGL predisposing genes

Gene	Secretory phenotype	Mean age at diagnosis (years)	Inheritance (proportion of mutation carriers)	Predominant tumor location	Number of tumors	Frequency of somatic mutations	Risk of Malignancy	Hereditary syndrome: PCC-associated pathologies
VHL	NA	30	Autosomal dominant (9%)	Adrenal>>TA, H&N	Bilateral	Frequent	Low	**VHL**: ccRCC and CNS hemangioblastomas
EPAS1	NA	33	Somatic mosaicism	TA>Adrenal	Multiple	Frequent	Unknown	**Hereditary polycythemia**: somatostatinoma polycythemia
SDHA	Unknown	40	Autosomal dominant (<1%)	Adrenal, TA	Single	Unknown	Unknown	**PGL5**: Leigh syndrome (homozygous mutations), ccRCC, GIST, PA
SDHB	NA/DA	30	Autosomal dominant (8%)	TA>H&N>Adrenal	Single and multiple	Very rare	High	**PGL4**: ccRCC, GIST, PA, neuroblastoma
SDHC	NS or NA/DA	40-50	Autosomal dominant (1%)	H&N>>TA, Adrenal	Multiple	Very rare	Low	**PGL3**: ccRCC, GIST, PA
SDHD	NS or NA/DA	35	Autosomal dominant with maternal imprinting (5%)	H&N>>TA, Adrenal	Multiple	Very rare	Low	**PGL1**: ccRCC, GIST, PA
SDHAF2	NS	30-40	Autosomal dominant with maternal imprinting (<1%)	H&N	Multiple	Unknown	Low	**PGL2**: none
FH	NA	46	Autosomal dominant (0.8%)	TA>Adrenal>>H&N	Multiple	Unknown	High	**HLRCC syndrome**: none
MDH2	Unknown	Unknown	Autosomal dominant (Unknown)	TA	Multiple	Unknown	Unknown	**Hereditary PCC/PGL**
RET	A	30-40	Autosomal dominant (5%)	Adrenal	Bilateral	Frequent	Low	**MEN2**: MTC, PHPT, marfanoid habitus and mucosal ganglioneuroma
NF1	A	42	Autosomal dominant (3%)	Adrenal>>TA	Single	Frequent	Moderate	**NF1**: neurofibromas, *cafe au lait* spots, axillary freckling, optic gliomas, pigmented harmatomas of the iris
TMEM127	NA/A	43	Autosomal dominant (<2%)	Adrenal	Bilateral	Unknown	Low	**Hereditary PCC/PGL**
MAX	NA/A	32	Autosomal dominant with paternal transmission (1,6%)	Adrenal	Bilateral	Frequent	Moderate	**Hereditary PCC/PGL**
HRAS	NA/A	59	-	Adrenal>>TA	Single	Frequent	Low	**Costello syndrome**: none
KIF1B	Unknown	Unknown	Autosomal dominant (unknown)	Adrenal	Bilateral	Unknown	Unknown	**Hereditary cancer**: neural and non-neural tumors
EGLN1/2	Unknown	Unknown	Autosomal dominant (unknown)	TA>>Adrenal	Multiple	Unknown	Unknown	**Hereditary polycythemia**: polycythemia
MEN1	Unknown	Unknown	Autosomal dominant (unknown)	Adrenal	Single	Unknown	Unknown	**MEN1**: PHPT, PA, neuroendocrine gastroenteropancreatic tumors
IDH1	Unknown	Unknown	-	H&N	Single	Very rare	Unknown	-

NA: noradrenergic; DA: dopaminergic; NS: non-secretory; A: adrenergic; H&N: head and neck; TA: thoracic-abdominal; >: more frequent than; >>: much more frequent than; PCC: pheochromocytoma; ccRCC: clear cell renal cell carcinoma; CNS: central nervous system; PGL1-5: paraganglionic syndromes 1-5; GIST: gastrointestinal tumor; PA: pituitary adenoma; HLRCC: hereditary leiomyomatosis and renal cell cancer; MEN2: multiple endocrine neoplasia type 2; MTC: medullary thyroid cancer; PHPT: primary hyperparathyroidism; NF1: neurofibromatosis type 1; MEN1: multiple endocrine neoplasia type 1. The colour of the rows, purple, green and white, represents Cluster 1, Cluster 2 and other genes respectively.

- *EPAS1*

As mentioned previously, the HIF family of transcription factors (HIF-1α, HIF-2α [EPAS1] and HIF-3α) plays a key role in the regulation of hypoxia response to counteract the lack of oxygen in normal homeostasis. HIF-1α has been suggested to preferentially drive genes implicated in apoptosis and glycolisis, while HIF-2α is involved in cell proliferation and angiogenesis[56,57]. Recently, a new and direct link between HIF proteins and PCC/PGL development has been found[63]; post-zygotic somatic mutations in *EPAS1* were found in two unrelated patients with multiple PGLs, somatostatinomas and polycythemia. The mutations were found in the residues located close to the prolyl hydroxylation site of the protein (proline 531) which was shown to disrupt the recognition of EPAS1 by the PHD (EGLN) family members, its hydroxylation and the consequent degradation by VHL[64,65]. Thus, mutations affecting the *EPAS1* gene stabilize the protein, causing the aforementioned pseudohypoxia, indicating that *EPAS1* behaves as an oncogene. A germline alteration affecting *EPAS1* has been recently found in a patient with multiple PGLs and polycythemia. Although it has been demonstrated that the variant stabilizes the protein, its location outside the prolyl hydroxylation sites and the absence of segregation with the disease in the family of the variant carrier makes this result somewhat controversial[66].

A detailed description of our findings on the involvement of *EPAS1* in the pathogenesis of PCC/PGL[67] will be provided and discussed throughout this thesis.

- The SDH genes

The SDH enzyme is a heteroligomer located in the mitochondrial inner membrane and is composed of four subunits: SDHA, SDHB, SDHC and SDHD. Two additional enzymes, SDHAF1 and SDHAF2, are implicated in the flavinization of the SDHA component, thus making possible the assembly of the complex[68]. SDH, also called complex II, is a part of the mitochondrial respiratory chain, which reduces ubiquinone during ATP synthesis. In addition, SDH catalyzes a pivotal step in the Krebs Cycle, converting succinate into fumarate by means of an oxidative dehydrogenation process[68]. In 2000 mutations in the *SDHD* gene were linked for the first time with the development of PGL[69]. Since then, all the genes encoding the subunits of the complex, as well as the gene encoding the related enzyme SDHAF2, have been implicated in the development of PCC and/or PGL within the five paraganglionic syndromes: PGL1 (OMIM: #168000), PGL2 (OMIM: #601650), PGL3 (OMIM: #605373), PGL4 (OMIM: #115310) and PGL5 (OMIM: #614165) (Table 1)[69-73].

As mentioned previously, based on gene expression profiling, tumors harboring mutations in the SDH genes cluster together with tumors presenting with activation of the pseudohypoxic pathway (i.e

VHL-mutated tumors)[52,55]. The regulation of the HIF family of transcription factors depends on the activity of a family of prolyl hydroxylases (PDHs 1-3)[74,75], which hydroxylates HIF, promoting its degradation by the VHL protein[76]. Succinate accumulation due to SDH impairment triggers the inhibition of the PDHs in the cytosol because of the competitive inhibition that this oncometabolite exerts due to its similarity to α-ketoglutarate (αKG), the normal substrate of the PHD family members. This inhibition leads to HIF stabilization and the subsequent expression of its hypoxic-response target genes[53,55,77,78].

Recently, genome-wide hypermethylation associated with SDH impairment has been demonstrated in SDH gene-mutated tumors[50]. This hypermethylation, and the resulting CpG island methylator phenotype (CIMP), are due to the accumulation of succinate which leads to the inhibition of two types of αKG-dependent dioxygenases: the histone demethylases of the Jumonji (JMJ) demethylase family and the TET family of 5-methycytosine (5-mC) hydroxylases. This hypermethylation has been demonstrated *in vitro*, *in vivo* and in a subset of PCCs/PGLs affected by mutations in the SDH genes[50,79]. In addition, a similar CIMP has been observed for one tumor carrying a mutation affecting *FH*[50], as well as in glioblastomas and other CNS tumors carrying mutations in the isocitrate dehydrogenase (IDH) genes 1 and 2[80] .

- *FH*

FH is the Krebs cycle enzyme involved in the reversible hydration/dehydration of fumarate to malate. It is known that germline mutations in *FH* predispose to leiomyomas and ccRCC in an autosomal-dominant hereditary syndrome named hereditary leiomyomatosis and renal cell cancer (HLRCC)[81]. Loss-of-function mutations of *FH* lead to the accumulation of fumarate in the tumors which, like succinate, promotes the inhibition of the αKG-dependent dioxygenases[79]. Very recently, Letouze *et al*.[50] identified a germline mutation in *FH* by whole-exome sequencing applied to blood and tumor DNA obtained from a 63 year-old female presenting with one PCC. The patient was selected to be sequenced because the tumor showed a methylome- and transcriptome-based profile very similar to that found in tumors carrying mutations in the SDH genes. The subsequent screening of almost 600 patients with PCC/PGL but no mutations in the major susceptibility genes revealed that five carried pathogenic germline *FH* mutations, providing further evidence of the involvement of this gene in the development of PCC/PGL[82].

- *MDH2*

The *MDH2* gene encodes mitochondrial malate dehydrogenase 2, a key Krebs cycle enzyme implicated in the reversible conversion of malate to oxaloacetate with the concurrent reduction of NAD to NADH. The discovery of *MDH2* as a new tumor susceptibility gene involved in PCC/PGL development (in press) will be described throughout this thesis.

Cluster 2 genes: *RET*, *NF1*, *TMEM127*, *MAX* and *HRAS*

Tumors belonging to this cluster carry mutations affecting genes involved in apparently different processes, however disruption of the PIK3CA-AKT1-mTOR axis appears to be a common characteristic, by RET-mediated cell transformation[82], inactivation of the tumor suppressor *NF1*[83], oncogenic activation of *HRAS*[84], loss of the mTOR negative regulator *TMEM127*[48], or by deregulation of the proto-oncogene MYC caused by *MAX* mutations[49].

- *RET*

The *RET* gene encodes a tyrosine-kinase receptor mainly expressed in cells derived from the neural crest (C cells, parafollicular thyroid cells, adrenal medulla cells and others) and in urogenital system precursor cells[85]. Ligand-induced activation of RET (via glial cell line-derived neurotrophic factor, GDNF) involves dimerization and autophosphorylation of the receptor[86], and the subsequent stimulation of multiple signal transduction pathways, including the MAPK/ERK and the PIK3CA-AKT1 pathways[87]. Germline gain-of-function mutations in *RET* cause MEN2, an autosomal dominant hereditary syndrome characterized by the presence of medullary thyroid cancer (MTC), PCC and/or primary hyperparathyroidism (PHPT)[88]. MEN2 can be classified into 3 sub-types:

MEN2A (OMIM: #171400): the most common form of the disease (90%), characterized by a 95% risk of developing MTC, a 50% risk of PCC, and a 15%-30% risk of developing hyperparathyroidism.

MEN2B (OMIM: #162300): representing approximately 5% of all cases. Patients typically present with MTC, PCC, marphanoid body habitus and multiple neuromas in mucosal tissue.

FMTC (OMIM: #155240): characterized by MTC only.

Mutations in the intracytoplasmic region of the receptor lead to constitutive activation of the protein without dimerization, triggering the activation of the aforementioned downstream pathways

involved in cellular proliferation and apoptosis[89]. *RET* mutations have variable clinical expression and penetrance that depends on their transformative capacity, giving rise to a genotype-phenotype relationship which is used to classify the aggressiveness of the disease[90]. In MEN2A patients the specific altered codon influences the level of mutant RET expression at the cell surface, contributing to signal variability[91]. On the other hand, MEN2B patients harbor alterations in codons localized in the catalytic site of the kinase, leading to loss of substrate specificity and more aggressive disease[92].

Approximately 50% of patients harboring *RET* pathogenic mutations develop PCC and, as occurs with *VHL*, *de novo* mutations are relatively common. In addition, somatic *RET* mutations are detected in approximately 5% of sporadic PCC/PGL[77].

- *NF1*

NF1 (neurofibromin) is a GTPase-activating protein that negatively regulates the RAS family of oncogenes, suppressing cell proliferation[93]. Germline mutations affecting the *NF1* gene cause NF1 (OMIM: #162200), an autosomal dominant disorder characterized by the presence of neurofibromas, *cafe au lait* spots, axillary freckling, optic gliomas, pigmented hamartomas of the iris, carcinoid tumors, parathyroid tumors, PCC, peripheral nerves tumors, long-term myeloid leukemia and other conditions[27,93]. Genetic testing of *NF1* is challenging because the gene is very large, and diagnosis is usually based on clinical criteria (i.e. *cafe au lait* spots or neurofibromas). Of note, *NF1* has one of the highest rates of spontaneous mutation of any known gene[94], and therefore the percentage of patients harboring *de novo* mutations is very high (between 30-50%). An estimated 0.1-5.7% of NF1 patients develop PCC.

In 2012, two independent studies found that mutations in *NF1*, and a concomitant chromosomal loss of the wild-type allele, are the most frequent somatic alterations found in sporadic PCCs (Table 1)[95,96].

- *TMEM127*

The *TMEM127* gene encodes a transmembrane protein, associated with the endomembrane and the vacuolar network, that negatively regulates the mTOR pathway. In 2010, Qin *et al*. used linkage analysis, gene expression profiling and mapping of chromosomal gains and losses to identify the first germline mutations in *TMEM127* in patients with PCC[48]. Alterations of the TMEM127 protein lead to the activation of phosphorylation of mTOR targets (for example, 4EBP1 and S6K), triggering cell growth and

proliferation[48]. A subsequent study of a large series of patients revealed a modest role of the gene in hereditary susceptibility to PCC (Table 1)[97].

- *MAX*

MAX is a ubiquitously expressed basic helix-loop-helix leucine zipper (bHLHZip) protein that plays a central role in the regulation of the transforming protein MYC. MYC, via heterodimerization with MAX, activates the transcription at thousands of target promoters binding hexameric DNA consensus sequences "CANNTG" (E-boxes), and promoting the expression of genes involved in cell proliferation, differentiation and apoptosis[98]. In addition, MAX antagonizes MYC-dependent cell transformation through its interaction with several negative regulators (MNT, MXD proteins, and MGA)[99], competing for the same E-boxes[100]. The discovery of *MAX* mutations in PCCs[49], the genetic characterization of *MAX* VUS, and the genetic screening for mutations in a large and well-characterized series of PCC/PGL patients will be extensively discussed throughout this thesis.

- *HRAS*

The members of the RAS family of oncoproteins (e.g. *HRAS*, *NRAS*, and *KRAS*) are small GTP-binding proteins that affect multiple downstream pathways related to cell growth and homeostasis. They were first linked to cancer in 1982[84], and nowadays it is known that together they represent around 30% of the total oncogenic activating mutations distributed across many different cancers[84,101]. Mutations in *KRAS* appear in 21.6% of human cancers, *NRAS* is mutated in 8.0% of tumors and *HRAS* mutations are found in 3.3% of cancers (www.sanger.ac.uk/genetics/CGP/cosmic/)[102]. A mutation affecting *HRAS* was first described in one PCC by Yoshimoto *et al*.[103]. Crona *et al*.[104] recently applied whole-exome sequencing to 58 PCCs and found that four harbored somatic mutations in the gene. The subsequent study of a large series of tumors determined that 10% of sporadic PCCs have mutations in *HRAS*, and ruled out the involvement of *NRAS* and *KRAS* in the disease[105]. The presence of mutations in one of the isoforms of RAS is not a new issue in the development of endocrine tumors since they are present in around 10-20% of follicular cell-derived thyroid cancers and in 18% of *RET*-negative sporadic MTCs[106-108]. Although the gene expression profile of *HRAS*-mutated tumors has not been studied to date, the pivotal role of RAS genes in the PIK3CA-AKT1-mTOR pathway suggests that they would group within the so-called transcriptional Cluster 2. Unpublished data from our laboratory have confirmed that this is indeed the case.

OTHER GENES

Besides the major susceptibility genes described above, there are other genes anecdotally implicated in the disease. One of these is kinesin family member 1B (*KIF1B)*, a gene involved in apoptosis, that has been found mutated in one sporadic PCC, and in the germline of one apparently sporadic patient and a single family affected by PCC and neuroblastoma[109-111]. Of note, it has been suggested that this gene could have a more relevant role in PCC development than expected, but the large size of its coding sequence makes screening for additional deleterious mutations a difficult task (commented at the 2014 *International Symposium on Pheochromocytoma and Paraganglioma*, Kyoto, Japan). Moreover, *EGLN1* (*PHD2*) and *EGLN2* (*PHD1*) have been found mutated in one and two patients, respectively, suffering from multiple PGLs and congenital polycythemia[51,112]. While it is known that, apart from tumors in the parathyroid glands, pancreatic islet cells and anterior pituitary gland, MEN1 patients can develop PCC[113,114], little is known about which patients are at highest risk. Finally *IDH1*, another Krebs cycle-related gene, was found to be somatically mutated in one sporadic tumor amongst 365 PCCs/PGLs[115]. It is known that the two PCCs carrying *KIF1B* mutations group within the transcriptional PIK3CA-AKT1-mTOR Cluster 2[110] and, considering their respective alterations, we suppose that tumors carrying *IDH1* or *EGLN1/2* mutations would be grouped with tumors belonging to the pseudohypoxic Cluster 1.

2. NEXT GENERATION SEQUENCING

One of the central goals of human genetics is to identify genetic variants responsible for complex (common, multigenic) and for Mendelian (rare, monogenic) diseases. Geneticists have attempted over the last 30 years to identify cancer predisposition genes, rare mutations in which confer high or moderate risks of cancer. Thus, at least one new cancer predisposition gene has been identified each year since 1990, the majority of them responsible for Mendelian diseases[116]. Genome-wide linkage analyses have been successfully performed to identify high-penetrance alterations in families in which multiple cases of a particular disease have occurred. These mutations are typically rare in the population. Genome-wide association studies (GWAS) are another methodology used to identify cancer predisposition genes. Genetic variants identified by GWAS typically are common in the population and have low effect sizes associated with cancer risk. In addition, many other genes have been identified through various candidate-based strategies: candidate genes that have been chosen because they act in pathways similar to those of known cancer genes or genes found to be somatically mutated in other cancers. However, for rare Mendelian disorders, several factors including rarity of the disease, locus heterogeneity and low penetrance, make linkage and GWAS suboptimal for the discovery of susceptibility genes[117].

In the early 2000's the first draft of the human genome was published, and this finding was the turning point for human genetics and the starting point for human genomics, something that completely changed the approaches adopted for the identification of cancer predisposition genes. The Human Genome Project (HGP) was an international scientific research project with the goals of determining the sequence of chemical base pairs that make up human DNA, and of identifying and mapping all of the genes in the human genome. The HGP, funded by the US government, started in 1990 and required 3.4 billion USD, 13 years, and collaboration of hundreds of international laboratories. In 2003, the human genome assembly representing 99% of the euchromatic sequence was almost finalized[118,119]. The human reference genome generated was a haploid consensus mosaic sequence derived from multiple individuals, which includes variations such as single nucleotide polymorphisms (SNPs), segmental duplications, deletions (INDELs) and low-copy repeats. Nowadays, this information is freely available in the dbSNP database (http://www.ncbi.nlm.nih.gov/projects/SNP/), created with the collaboration of the National Human Genome Research Institute and The National Center for Biotechnology Information (NCBI). This database contains information of more than 10 million well-characterized common variants in different world populations.

In the last 10 years through the availability of the HGP data we have witnessed a revolution in the development of massively parallel next-generation sequencing (NGS). The technical development of whole-genome sequencing (WGS) began with a series of experiments which demonstrated the utility of NGS in the generation of complete diploid sequences of human genomes. These included the sequencing of James D. Watson's[120] (first human genome sequenced by NGS) and J. Craig Venter's[121] genomes. Later, the genomes of people from different ethnical origins were also sequenced[122-127]. The first application of WGS to discover cancer-initiating mutations was published in 2008 by Ley et al., and was based in sequencing the genome of a cytogenetically normal acute myeloid leukemia[128].

Rapid advances in the NGS field enabled the development of what is currently one of the most frequently used human genetics technologies worldwide: whole-exome sequencing (WES). The term exome refers to the protein-coding regions of the genome (i.e. the ~180,000 exons of the ~19,000 human genes), and represents a very small portion of the genome, around 1%. WES is possible by means of a first capture step followed by massive parallel sequencing[129], that makes this technique cheaper, reducing the cost by a third to a tenth compared to WGS, and more easily managed from a bioinformatic point of view. Ng *et al*. published the first WES in 2009 after sequencing eight HapMap individuals as well as four additional exomes of previously genetically diagnosed Freeman-Sheldon syndrome patients (OMIM #193700) in order to demonstrate the sensitivity and specificity of the technique in the identification of rare and common variants[130]. Subsequent use of WES has demonstrated the utility of the technique to

discover the genetic causes of Mendelian genetic traits[131-134]. Despite biases introduced during the exome capture and amplification steps, the fact that most alleles underlying Mendelian disorders disrupt protein-coding sequences[135] has meant that WES and targeted-WES (using commercial or home-made gene panels) have become standard tools for analyzing cancer-prone families showing monogenic modes of disease inheritance.

Two crucial considerations before starting a NGS project are the adequate selection of patients and the choice of the inheritance model to be considered. To select patients for study, and in order to avoid genetic heterogeneity, finding specific molecular or clinical markers may be essential to find a common causal gene. Moreover, the inheritance model assumed can determine not only the sampling but also the filtering process. On average, exome sequencing performed in one individual identifies ~20,000 variants. More than 95% of these variations are polymorphisms present in the general population. In the case of very rare Mendelian diseases, such as hereditary PCC/PGL, filtering the list of candidate variants by ruling out those alterations found in in-house exomes or described in data bases such as dbSNP, 1000 genomes (http://www.1000genomes.org/) or ESP data server (http://evs.gs.washington.edu/EVS/) makes the identification of the causal gene more likely[132]. Further to these and other quality-based filtering steps, several approaches can be adopted in order to maximise the chances of finding the causal variant of a rare monogenic disorder by NGS[136]:

a) Sequence multiple unrelated affected individuals and consider only those variants affecting the same gene in all or a subset of the sequenced patients. The more affected individuals sequenced, the greater the power to identify the causal mutation. This requires a reliable method to select the patients for inclusion in NGS studies, such as a common molecular or clinical marker or the presence of very specific clinical features.
b) Sequence multiple affected and unaffected individuals from the same pedigree, in order to identify the altered gene (or genes) segregating with the disease.
c) Sequence one or more trios (an affected individual and each of their biological parents) sharing similar clinical characteristics. This approach is suitable if the hypothetical inheritance model is a recessive or a *de novo* mutation is the cause.
d) Analyze and compare matched tumor and normal genomes/exomes of the same patient, in the case of cancer-prone syndromes. The main advantage of this approach is to identify and assess germline and somatic alterations at the same time (for example, a germline mutation in a given gene and somatic loss of the corresponding wild-type allele).

When the final list of candidate variants is obtained, stratification based on the effect of the change (e.g. truncating or missense variants) is usually applied. For instance, variants leading to a premature stop codon (truncating mutations caused by nonsense, splice site or frameshift variants) are usually considered the best candidates for study since the effect of the variant on encoded protein is more obvious. In the case of missense variants causing the substitution of one amino acid for another, the predicted functional impact obtained from *in silico* prediction programs such as SIFT (http://sift.jcvi.org/) or PolyPhen-2 (http://genetics.bwh.harvard.edu/pph2/) can be considered. In addition, the presence of the candidate variant in databases of proven disease-causing alterations (e.g. The Catalogue of Somatic Mutations in Cancer, COSMIC; http://cancer.sanger.ac.uk/cancergenome/projects/cosmic/, in the case of cancer) and the biological meaning of a given alteration in the context of the disease of interest are usually taken into account in the assessment of potentially causal variants.

OBJECTIVES

NGS, and more specifically WES, has become a very useful tool in the discovery of new susceptibility genes involved in genetic diseases showing a Mendelian pattern of inheritance. Thus, the main objective of this thesis was:

1) To identify using WES new susceptibility genes involved in PCC/PGL development in patients with clinical characteristics of heritability and without mutations in the main susceptibility genes. Once a new PCC/PGL susceptibility gene (s) was identified we aimed:

    a) To develop adequate cellular models in order to demonstrate the impact of mutations in the gene;

    b) To assess the prevalence of mutations in new gene in a large series of PCC/PGL patients, and establish the associated clinical presentation.

ARTICLES

ARTICLE 1: Exome sequencing identifies *MAX* mutations as a cause of hereditary pheochromocytoma.

Authors: **Iñaki Comino-Méndez**, Francisco J Gracia-Aznárez, Francesca Schiavi, Iñigo Landa, Luis J Leandro-García, Rocío Letón, Emiliano Honrado, Rocío Ramos-Medina, Daniela Caronia, Guillermo Pita, Álvaro Gómez-Graña, Aguirre A de Cubas, Lucía Inglada-Pérez, Agnieszka Maliszewska, Elisa Taschin, Sara Bobisse, Giuseppe Pica, Paola Loli, Rafael Hernández-Lavado, José A Díaz, Mercedes Gómez-Morales, Anna González-Neira, Giovanna Roncador, Cristina Rodríguez-Antona, Javier Benítez, Massimo Mannelli, Giuseppe Opocher, Mercedes Robledo, Alberto Cascón.

Published in Nature Genetics 2011 Jun 19;43(7):663-7

ABSTRACT

Around 40% of PCC cases are due to germline mutations affecting one of the major susceptibility genes described so far, however there are some cases (<10%) that present with clinical characteristics of heritability but aren't found to carry mutations in the known genes. In this study, we took advantage of an expression profiling analysis performed in a large series of PCCs/PGLs to select for NGS three independent hereditary cases without germline mutations in the known susceptibility genes. The patients were selected because their tumors showed a very homogeneous transcriptional profile, suggesting a possible genetic alteration affecting the same gene in the three cases.

For the exome analysis, a bioinformatic pipeline was developed that enabled the identification of germline mutations affecting the same gene in the three individuals. We also sequenced and used as quality and filtering controls seven Hap Map individuals. We focused on heterozygous SNSs and indels, discarding variants present in the Hap Map controls or reported in the dbSNP130, 132 or 1000 Genomes Project databases, as well as variants in intergenic or intronic regions, and synonymous amino acid changes. Only variants affecting the same gene in the three samples were considered.

A variant affecting the *MYC associated factor X* (*MAX*) gene was validated by Sanger Sequencing and segregated with the disease. The absence of MAX protein in all tumors carrying mutations, and loss of heterozygosity (LOH) caused by paternal uniparental disomy (UPD), provided evidence of the involvement of *MAX* alterations in the disease, playing a role as tumor suppressor gene.

Further analysis of 59 cases with PCC/PGL selected because they had clinical features of heritability such as familial history of the disease, early age at onset (less than 30 years) and/or

multiplicity, identified five additional *MAX* mutations (two truncating and three missense). The clinical characteristics of *MAX* mutation-carriers suggested preferential paternal transmission of *MAX* mutations and initially an association with malignant outcome. Further evidence of the involvement of the MYC-MAX-MXD1 network in the development and progression of neural crest cell tumors is provided by the lack of functional MAX in rat PCC (PC12) cells and by the amplification of *MYCN* observed in neuroblastoma, a tumor closely related to PCC.

Personal contribution: I participated in the analysis of the raw NGS data and in the subsequent filtering process. Further, I participated in the identification of the LOH and the paternal origin of the UPD demonstrated by SNP-array and methylation-specific PCR, the western blot analyses, and the screening for *MAX* mutations in the additional selected series of patients. I also participated in the drafting of the paper.

nature genetics

Exome sequencing identifies *MAX* mutations as a cause of hereditary pheochromocytoma

Iñaki Comino-Méndez[1,2,15], Francisco J Gracia-Aznárez[2,3,15], Francesca Schiavi[4,15], Iñigo Landa[1], Luis J Leandro-García[1], Rocío Letón[1], Emiliano Honrado[5], Rocío Ramos-Medina[6], Daniela Caronia[7], Guillermo Pita[7], Álvaro Gómez-Graña[1], Aguirre A de Cubas[1], Lucía Inglada-Pérez[1,2], Agnieszka Maliszewska[1], Elisa Taschin[4], Sara Bobisse[4], Giuseppe Pica[8], Paola Loli[9], Rafael Hernández-Lavado[10], José A Díaz[11], Mercedes Gómez-Morales[12], Anna González-Neira[7], Giovanna Roncador[6], Cristina Rodríguez-Antona[1,2], Javier Benítez[2,3], Massimo Mannelli[13], Giuseppe Opocher[4,14], Mercedes Robledo[1,2] & Alberto Cascón[1,2]

Hereditary pheochromocytoma (PCC) is often caused by germline mutations in one of nine susceptibility genes described to date[1–4], but there are familial cases without mutations in these known genes. We sequenced the exomes of three unrelated individuals with hereditary PCC (cases) and identified mutations in *MAX*, the MYC associated factor X gene. Absence of MAX protein in the tumors and loss of heterozygosity caused by uniparental disomy supported the involvement of *MAX* alterations in the disease. A follow-up study of a selected series of 59 cases with PCC identified five additional *MAX* mutations and suggested an association with malignant outcome and preferential paternal transmission of *MAX* mutations. The involvement of the MYC-MAX-MXD1 network in the development and progression of neural crest cell tumors is further supported by the lack of functional MAX in rat PCC (PC12) cells[5] and by the amplification of *MYCN* in neuroblastoma[6] and suggests that loss of MAX function is correlated with metastatic potential.

PCC is a rare neural crest cell tumor mainly localized within the adrenal medulla that usually causes secondary hypertension by oversecretion of catecholamines and which rarely metastasizes. Around 30–40% of individuals with PCC are familial cases[7,8] who show dominant autosomal inheritance caused by germline mutations affecting one of nine susceptibility genes: *RET*, *VHL*, *SDHA*, *SDHB*, *SDHC*, *SDHD*, *SDHAF2*, *NF1* or *TMEM127*. However, there are some hereditary cases (<10%)[7,8] not explained by mutations in these genes. Recent gene expression analyses have identified a common transcriptional profile for tumors carrying germline mutations altering the same gene[9,10]. Moreover, we showed that a subset of tumors from familial cases with PCC without germline alterations in the susceptibility genes identified to date showed a homogeneous expression profile (GEO accession number GSE19422)[11], suggesting that mutations in the same as yet unidentified gene could be responsible for these cases.

Here we used next-generation sequencing to analyze the exomes of three independent familial cases with PCC without any known predisposing germline alteration and whose tumors had a common transcriptional profile[11]. We also included seven HapMap individuals (three males and four females) as quality and filtering controls. As it is very unlikely that homozygous variants can act as founder mutations, we focused on studying single nucleotide substitutions (SNSs) and small insertions and deletions (indels) in heterozygosity. We selected the heterozygous SNSs and consecutively filtered them by discarding (i) variants present in the sequenced HapMap controls or in the dbSNP130 database and (ii) variants in intergenic or intronic regions (**Table 1** and **Supplementary Table 1**). Next, we selected only those variants within coding regions not predicted to produce synonymous amino acid changes, affecting the same gene in all three samples and presenting sufficient depth and quality. After that, we checked candidate variants against the last version of dbSNP (dbSNP132) and the 1000 Genomes Project data (see URLs). This resulted in only five SNSs, corresponding to two genes (*MAX* and *ADCY6*), that passed the filtering process. We performed filtering for indels in a similar manner, but no variant passed the filtering criteria.

After validation by Sanger sequencing, we discarded *ADCY6* as a PCC susceptibility gene because one of the variants (p.Arg1065Gln; **Supplementary Table 1**) did not segregate with the disease in the

[1]Hereditary Endocrine Cancer Group, Spanish National Cancer Research Centre (CNIO), Madrid, Spain. [2]Centro de Investigación Biomédica en Red de Enfermedades Raras (CIBERER), Madrid, Spain. [3]Human Genetics Group, Spanish National Cancer Research Centre, Madrid, Spain. [4]Familial Cancer Clinic, Veneto Institute of Oncology, Padova, Italy. [5]Anatomical Pathology Service, Hospital de León, León, Spain. [6]Monoclonal Antibodies Unit, Biotechnology Programme, Spanish National Cancer Research Centre, Madrid, Spain. [7]Human Genotyping Unit-CeGen, Human Cancer Genetics Programme, Spanish National Cancer Centre, Madrid, Spain. [8]Endocrinology and Metabolic Diseases, University of Foggia, Foggia, Italy. [9]Department of Endocrinology, Ospedale Niguarda Ca' Granda, Milan, Italy. [10]Endocrinology Section, Hospital Infanta Cristina, Badajoz, Spain. [11]Department of Endocrinology, Hospital Universitario Clínico San Carlos, Madrid, Spain. [12]Department of Pathology, University Hospital, University of Granada, Granada, Spain. [13]Department of Clinical Pathophysiology, University of Florence and Istituto Toscano Tumori, Florence, Italy. [14]Department of Medical and Surgical Sciences, University of Padova, Padova, Italy. [15]These authors contributed equally to this work. Correspondence should be addressed to A.C. (acascon@cnio.es) or M.R. (mrobledo@cnio.es).

Received 16 March; accepted 18 May; published online 19 June 2011; doi:10.1038/ng.861

Table 1 Single nucleotide substitution filtering steps

Sample number	Total number of SNSs	Heterozygous SNSs	SNSs after HapMap control filtering	SNSs after dbSNP130 filtering	SNSs after removing intronic and intergenic variants	SNSs affecting the same gene in the three samples	SNSs in coding regions (not in UTR)	SNSs after removing synonymous, deep<7, and Phred_qual<20	SNSs after removing entries in additional databases[a]
924	95,100	28,292	9,088	2,911	763	41[b]	17	9	5
3037	92,855	26,859	7,884	3,066	789				
3121	89,784	26,232	8,292	3,676	743				
Average	92,580	27,128	8,421	3,218	765	41	17	9	5
Percent of SNSs remaining[c]	100	29.30	9.10	3.48	0.83	0.04	0.02	0.01	0.005

[a]1000 Genomes and dbSNP132. [b]A complete list of these variants is shown in **Supplementary Table 1**. [c]Percentage of single nucleotide substitutions (SNSs) after each filtering step.

affected relatives of the family. On the other hand, we observed segregation of *MAX* c.1A>G (p.Met1Val) and c.223C>T (p.Arg75X) variants with disease in the two families for which DNA from affected relatives was available (**Supplementary Fig. 1**). We did not detect these variants in more than 750 population-matched control chromosomes. The three mutations found in *MAX* (**Supplementary Fig. 2a**) were predicted to alter the initiation ATG codon (c.1A>G), introduce a premature stop signal (c.223C>T) and cause exon 4 skipping (c.295+1G>A) (**Supplementary Fig. 2b**). Immunohistochemical analysis of the three PCCs carrying *MAX* mutations showed a lack of full-length MAX protein (**Fig. 1**). Next, we analyzed the tumor DNA and found loss of the wild-type *MAX* allele in all three cases, indicating loss of heterozygosity (LOH) (**Fig. 2a**). By array CGH analysis, we had previously ruled out the presence of chromosomal losses affecting the *MAX* locus in the same tumors (I.C.-M., F.S., G.O., A.C. & M.R., data not shown). Thus, to decipher the mechanism responsible for the LOH, we carried out a genome-wide SNP array analysis for one of the tumors and found copy-neutral homozygosity caused by uniparental disomy (UPD) affecting almost the entire chromosome 14q (**Fig. 2b**). Multiplex PCR microsatellite analysis confirmed that the LOH found in the remaining *MAX* PCCs was also caused by UPD (**Fig. 2c**). The paternal origin of the UPD was clear for one of the hereditary cases because of his familial antecedents (**Supplementary Fig. 1a**). To investigate the origin of the UPD in the other two cases, we studied the methylation status of *MEG3* (the maternally expressed gene 3), an imprinted gene within the disomy region. We detected only the silenced paternal allele in the tumors of these individuals (**Supplementary Fig. 3**), showing that loss of the maternal allele accounted for the LOH in the three cases. Taken together, these data suggest that *MAX* germline mutations are associated with PCC susceptibility and that *MAX* behaves as a classic tumor suppressor gene.

MAX is the most conserved dimerization component of the MYC-MAX-MXD1 network of basic helix-loop-helix leucine zipper (bHLHZip) transcription factors that regulate cell proliferation, differentiation and apoptosis[12]. In this network, MAX plays an essential role, as it is the common interaction partner for both MYC and MXD1 proteins. Whereas heterodimerization of the MYC family of proteins with MAX mediates their function as transcription factors, heterodimers of MAX with MXD1 family members (MXD1, MXI1, MXD3 and MXD4), MNT and MGA antagonize MYC-dependent cell transformation by transcriptional repression of the same E-box target DNA sequences[13]. The conservation of the MAX sequence is particularly high in the bHLHZip domain, which is involved in protein-protein interactions and DNA binding. In addition, it has been reported that phosphorylation of N- or C-terminal consensus signals for casein kinase II modulates MAX DNA binding properties[14,15]. With respect to PCC, it is well known that PC12 cells, derived from rat adrenal PCC, express a mutant form of MAX lacking the carboxyl terminus of the protein that is incapable of repressing transcription from E-box sequences[5,16]. Reintroduction of MAX in these cells results in transcriptional repression and reduction in growth rate. These findings suggest that MAX disruption leads to increased cell proliferation and that MYC functions as a transcriptional regulator despite the lack of normally functioning MAX protein in PCC cells. In addition, the NRAS-PIK3CA-AKT1-mTOR axis is essential for the development of PCCs related to oncogenic c-RET–mediated cell transformation[17], inactivation of the tumor suppressor *NF1* (ref. 18) and mutation of the mTOR regulator *TMEM127* (ref. 19). Because crosstalk between the NRAS-PIK3CA-AKT1-mTOR and MYC-MAX-MXD1 pathways has been reported[20,21], it is not surprising that alterations in the central regulating protein of the MYC network could also lead to PCC development. In agreement with this, it has been reported that MYC inhibits NRAS-mediated neuronal differentiation of PC12 cells by blocking c-Jun upregulation[22]. In addition, amplification and overexpression of MYCN is a genetic hallmark in neuroblastoma[6], another neural crest cell tumor mainly originating in the adrenal gland. Thus, *MAX* mutations in PCCs could avoid transcriptional repression by MAX of E-box target DNA sequences, leading to oncogenic MYCN deregulation as in neuroblastoma.

We decided to extend our screening for *MAX* mutations to a selected series of 59 cases with PCC without germline alterations in

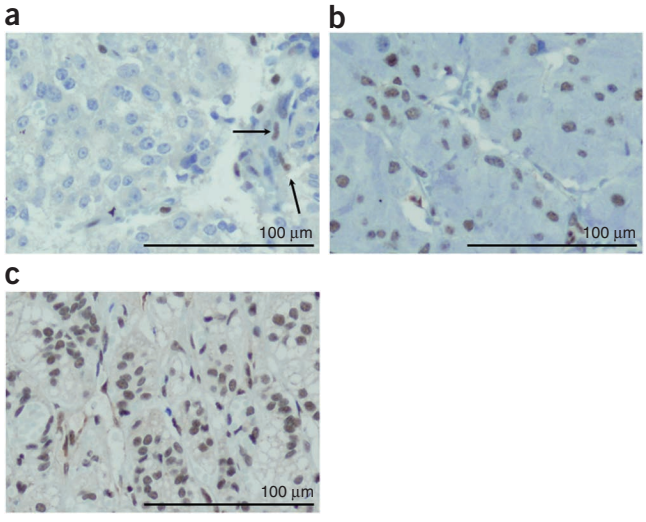

Figure 1 Detection of MAX by immunohistochemistry with a MAX C-terminus–specific antibody. (**a**) Negative staining of tumor cells in a *MAX*-mutation–positive PCC compared to positive stromal cells (indicated with arrows). (**b**) Positive staining of a *RET*-mutated PCC. (**c**) Normal adrenal tissue showing MAX-positive staining.

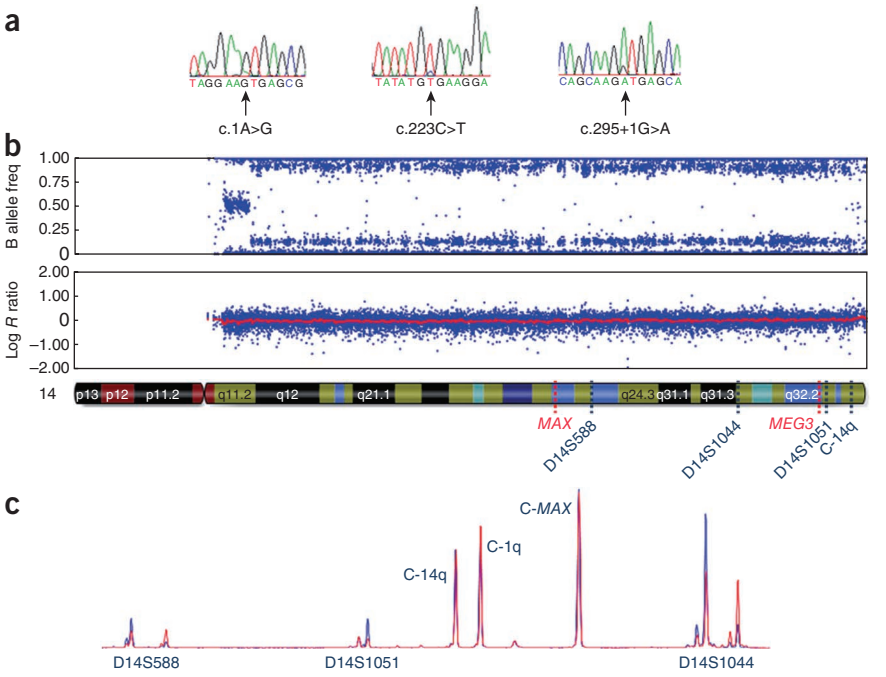

Figure 2 Loss of heterozygosity (LOH) analysis of three tumors with *MAX* mutations. (**a**) Tumor DNA sequence chromatograms of the three *MAX* mutations showing, in each case, loss of the wild-type allele. (**b**) SNP array analysis of chromosome 14 performed with tumor DNA from the individual carrying the c.1A>G mutation shows uniparental disomy (UPD). The lower panel shows the genomic plots of the log *R* ratio (log2 $R_{case}/R_{reference}$) indicating the presence of two alleles, and the upper panel shows the allele frequency parameters along chromosome 14, indicating LOH. Chromosomal locations of *MAX*, *MEG3*, C-14q control and microsatellites are indicated. (**c**) Multiplex PCR microsatellite analysis performed in blood (red) and tumor (blue) DNA from the individual carrying the c.223C>T mutation shows biallelic chromosome 14 amplification and LOH of the three informative microsatellites caused by UPD. C-14q, control amplicon from chromosome 14q; C-1q, control amplicon from chromosome 1q; C-*MAX*, control amplicon from the *MAX* locus.

the known susceptibility genes and who were highly suspected of having hereditary tumors because of the presence of bilateral adrenal PCC, age of onset below 30 years and/or familial antecedents of the disease (**Supplementary Table 2**). We detected two additional truncating *MAX* mutations affecting exon 3 (c.97C>T) and 4 (c.185_186delA) and three missense variants (c.67G>A, c.281T>C and c.425C>T) located in exons 3, 4 and 5, respectively (**Table 2**). Immunohistochemical analysis confirmed the lack of full-length MAX in the tumors with truncating variants. The c.67G>A and the c.425C>T variants affect two highly conserved amino acids (aspartic acid and serine) within two different casein kinase II recognition sites (**Fig. 3**), which suggests that these mutations alter MAX function by modifying its DNA binding abilities. The c.281T>C mutation changed one of the conserved leucines located in the leucine zipper motif of the protein, which is necessary for MAX protein-protein interactions and oligomerization[23,24]. However, further functional studies are needed to provide direct evidence of the pathogenic character of these three *MAX* missense variants. We found none of the five new variants in controls, and we confirmed chromosome 14q LOH caused by either chromosomal loss or UPD in three more tumors (**Table 2**), which is consistent with a pathogenic role of these *MAX* germline variants. The paternal transmission of the mutation was known in the two hereditary cases and was confirmed by *MEG3* methylation analysis in another case for which tumor material was available. Acquired segmental UPD is being increasingly recognized as one of the mechanisms of LOH, and it therefore constitutes the somatic second hit of Knudson's hypothesis for tumor suppressor genes in a wide variety of neoplasms[25–27]. Moreover, paternal and maternal chromosome 14 UPD are known to contribute to the development of several malformation syndromes[28], and interestingly, bilateral PCC was recently found in an individual with mosaicism for genome-wide paternal UPD[29]. Taking all these findings into account, it seems that *MAX* is mainly inactivated by this mechanism in the tumors. In addition, the paternal origin of the mutated allele detected in six families suggests a preferentially paternal transmission of the disease ($P = 0.031$). Regarding this, we confirmed both the absence of methylation in various CpG islands of the *MAX* promoter in normal lymphocytes and the biallelic expression of *MAX* mutations in the mRNA of four cases (I.C.-M., A.C. & M.R., data not shown), which ruled out that the expression of this gene is affected

Table 2 Clinical features of individuals with *MAX* mutations

Family	ID	Sex	Age at onset	Familial antecedents	Tumor	Malignant	cDNA mutation[a]	Protein alteration[a]	Tumor 2nd hit	p*MEG3*
a	**3121**	M	29	Yes[b]	bPCC	No	c.223C>T	p.Arg75X	UPD	Yes
a	3119	M	35	–	bPCC	No	c.223C>T	p.Arg75X	n.a.	n.a.
a	1090	F	34	–	bPCC	No	c.223C>T	p.Arg75X	n.a.	n.a.
a	3122	F	28	–	bPCC	No	c.223C>T	p.Arg75X	n.a.	n.a.
b	**3037**	M	32	Yes[c]	bPCC	Yes	c.295+1G>A	p.?	UPD	Yes
c	**924**[d]	F	46	Yes[c]	bPCC	Yes	c.1A>G	p.Met1?	UPD	Yes
c	922	M	29	–	PCC	No	c.1A>G	p.Met1?	n.a.	n.a.
d	190	M	17, 20	No	bPCC	No	c.97C>T	p.Arg33X	14q loss	Yes
e	1016	F	47	Yes[b]	bPCC	No	c.185_186delA	p.Gln62Asn*fs*X23	14q loss	Yes
f	368	F	26	No	PCC	Yes	c.67G>A	p.Asp23Asn	n.a.	n.a.
g	1075	F	22	No	PCC	No	c.425C>T	p.Ser142Leu	n.a.	n.a.
h	F31S	F	41	Yes[b]	PCC	No	c.281T>C	p.Leu94Pro	UPD	Yes

The three cases whose exomes were sequenced are shown in bold.
[a]All cDNA and protein nomenclature is based on reference sequence ENST00000358664. [b]Paternal familial antecedents. [c]Unknown. [d]Deceased. bPCC, bilateral adrenal pheochromocytoma. UPD, uniparental disomy; n.a., not available; p*MEG3*, exclusive paternal *MEG3* allele detection; cDNA, complementary DNA.

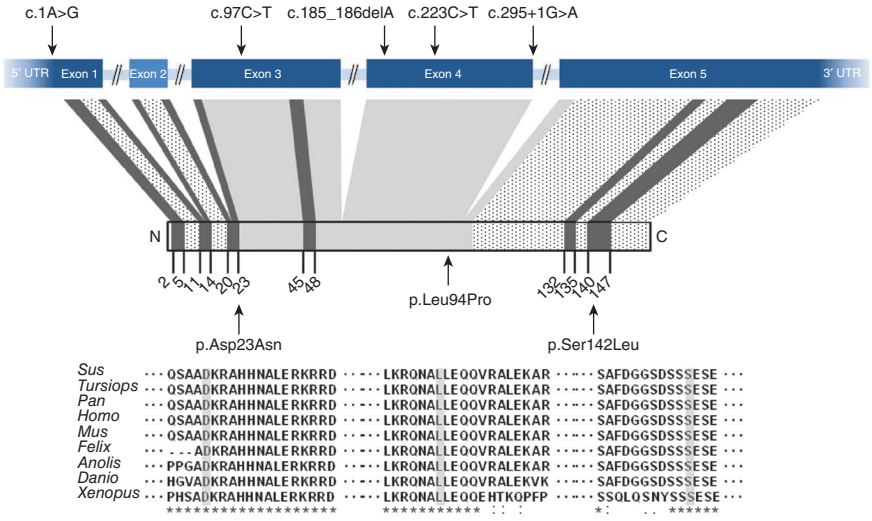

Figure 3 Schematic representation of *MAX* mutations found in individuals with PCC. *MAX* transcript 2 (ENST00000358664) contains five exons that encode 160 amino acids, including the bHLHZip domain (denoted with a light gray bar; amino acids 22 to 102) and the casein kinase II phosphorylation sites (denoted with dark gray bars; numbers indicate the first and the last amino acid of each site). Truncating and missense mutations are marked with vertical arrows above the gene schematic and below the protein schematic, respectively. The bottom panel shows the conservation of the three amino acids altered by missense substitutions in individuals with PCC (marked with a vertical gray bar). UTR, untranslated region.

by imprinting. This model of inheritance, if confirmed, would constitute the third example of sex-linked transmission in hereditary PCC, in addition to inheritance of mutated *SDHAF2* and *SDHD* (refs. 2,30). The absence of PCC in two children who inherited the mutation from their mother and in two obligate carriers of a different family further supports this theory (**Supplementary Fig. 1a**,**c**). The absence of familial antecedents in three of the eight *MAX*-mutation–positive cases with germline mutations is not unusual and could be caused by the suggested preferential paternal transmission. In fact, a substantial proportion of cases with PCC with apparently sporadic tumors harbor a germline mutation in one of the susceptibility genes described so far[8]. The appearance of bilateral adrenal PCC in eight of the twelve cases studied (**Table 2**) is in agreement with the association between bilaterality and the presence of germline alterations in cases with PCC[8] and underscores the importance of selecting cases with multiple tumors in screening for PCC susceptibility genes. In addition, malignant adrenal PCC is a rare condition, with the exception of cases carrying *SDHB* germline mutations. Notably, three out of eight probands showed metastases at diagnosis and another had familial antecedents of PCC-related malignancy, suggesting the association of *MAX* mutations with PCC aggressiveness.

Next-generation sequencing is steadily attracting interest as one of the most important tools for discovering genes responsible for genetically heterogeneous diseases. Moreover, exome sequencing represents the best option in this type of agnostic causal variant identification study over other strategies such as whole-genome sequencing. In the present study, next-generation sequencing allowed us to identify *MAX* as a new PCC tumor suppressor gene. The discovery of *MAX* germline mutations in individuals with hereditary adrenal tumors supports a key role for the MYC-MAX-MXD1 network in the development and progression of neural crest tumors. Moreover, the malignant behavior of MAX-related PCCs, similar to neuroblastomas with *MYCN* amplification, supports the idea that MAX loss of function is correlated to metastatic potential. The analysis of a larger series of cases will provide further information about the prevalence of *MAX* mutations in PCC and will clarify the phenotype associated with *MAX* mutations, which is of fundamental importance for both genetic counseling and genetic testing algorithms.

URLs. 1000 Genomes Project, http://www.1000genomes.org/; Novoalign, http://www.novocraft.com; R, http://www.r-project.org.

METHODS

Methods and any associated references are available in the online version of the paper at http://www.nature.com/naturegenetics/.

Accession codes. A full listing of the sequencing results have been deposited in the ArrayExpress database under accession number E-MTAB-591.

Note: Supplementary information is available on the Nature Genetics website.

ACKNOWLEDGMENTS

This work was supported in part by the Fondo de Investigaciones Sanitarias (projects PS09/00942 and P1080883 to A.C. and M.R., respectively), Mutua Madrileña (project AP2775/2008 to M.R.), FP7-Grant (ENS@T-CANCER; HEALTH-F2-2010-259735) and Innovation project INTRA-706-2 ISCIII CIBER-ER (Center for Biomedical Research on Rare Diseases). I.C.-M. holds a shuttle CIBER-ER fellowship.

AUTHOR CONTRIBUTIONS

A.C., M.R., F.S. and G.O. conceived the project. G. Pica, P.L., R.H.-L., J.A.D., M.G.-M. and M.M. collected tumor samples. F.J.G.-A., I.C.-M. and A.C. performed next-generation sequencing analysis and filtering. I.C.-M., F.J.G.-A., F.S., I.L., L.J.L.-G., R.L., R.R.-M., D.C., A.G.-G., A.A.d.C., L.I.-P., E.T., S.B., A.M., A.G.-N. and G.R. performed additional experiments. A.C., I.C.-M., E.H. and G. Pita performed additional data analysis. A.C., I.C.-M., F.J.G.-A., M.R., C.R.-A. and J.B. wrote the manuscript. All authors approved the final draft.

COMPETING FINANCIAL INTERESTS

The authors declare no competing financial interests.

Published online at http://www.nature.com/naturegenetics/.
Reprints and permissions information is available online at http://www.nature.com/reprints/index.html.

1. Neumann, H.P. *et al.* Germ-line mutations in nonsyndromic pheochromocytoma. *N. Engl. J. Med.* **346**, 1459–1466 (2002).
2. Hao, H.X. *et al. SDH5*, a gene required for flavination of succinate dehydrogenase, is mutated in paraganglioma. *Science* **325**, 1139–1142 (2009).
3. Yao, L. *et al.* Spectrum and prevalence of *FP/TMEM127* gene mutations in pheochromocytomas and paragangliomas. *J. Am. Med. Assoc.* **304**, 2611–2619 (2010).
4. Burnichon, N. *et al. SDHA* is a tumor suppressor gene causing paraganglioma. *Hum. Mol. Genet.* **19**, 3011–3020 (2010).
5. Hopewell, R. & Ziff, E.B. The nerve growth factor-responsive PC12 cell line does not express the Myc dimerization partner Max. *Mol. Cell. Biol.* **15**, 3470–3478 (1995).
6. Kohl, N.E. *et al.* Transposition and amplification of oncogene-related sequences in human neuroblastomas. *Cell* **35**, 359–367 (1983).
7. Mannelli, M. *et al.* Clinically guided genetic screening in a large cohort of Italian patients with pheochromocytomas and/or functional or nonfunctional paragangliomas. *J. Clin. Endocrinol. Metab.* **94**, 1541–1547 (2009).
8. Cascón, A. *et al.* Genetics of pheochromocytoma and paraganglioma in Spanish patients. *J. Clin. Endocrinol. Metab.* **94**, 1701–1705 (2009).
9. Favier, J. *et al.* The Warburg effect is genetically determined in inherited pheochromocytomas. *PLoS ONE* **4**, e7094 (2009).
10. Dahia, P.L. *et al.* A HIF1α regulatory loop links hypoxia and mitochondrial signals in pheochromocytomas. *PLoS Genet.* **1**, 72–80 (2005).

11. López-Jiménez, E. *et al.* Research resource: transcriptional profiling reveals different pseudohypoxic signatures in *SDHB* and *VHL*-related pheochromocytomas. *Mol. Endocrinol.* **24**, 2382–2391 (2010).
12. Atchley, W.R. & Fitch, W.M. Myc and Max: molecular evolution of a family of proto-oncogene products and their dimerization partner. *Proc. Natl. Acad. Sci. USA* **92**, 10217–10221 (1995).
13. Grandori, C., Cowley, S.M., James, L.P. & Eisenman, R.N. The Myc/Max/Mad network and the transcriptional control of cell behavior. *Annu. Rev. Cell Dev. Biol.* **16**, 653–699 (2000).
14. Bousset, K., Henriksson, M., Luscher-Firzlaff, J.M., Litchfield, D.W. & Luscher, B. Identification of casein kinase II phosphorylation sites in Max: effects on DNA-binding kinetics of Max homo- and Myc/Max heterodimers. *Oncogene* **8**, 3211–3220 (1993).
15. Prendergast, G.C., Hopewell, R., Gorham, B.J. & Ziff, E.B. Biphasic effect of Max on Myc cotransformation activity and dependence on amino- and carboxy-terminal Max functions. *Genes Dev.* **6**, 2429–2439 (1992).
16. Ribon, V., Leff, T. & Saltiel, A.R. c-Myc does not require max for transcriptional activity in PC-12 cells. *Mol. Cell. Neurosci.* **5**, 277–282 (1994).
17. Segouffin-Cariou, C. & Billaud, M. Transforming ability of MEN2A-RET requires activation of the phosphatidylinositol 3-kinase/AKT signaling pathway. *J. Biol. Chem.* **275**, 3568–3576 (2000).
18. Johannessen, C.M. *et al.* The *NF1* tumor suppressor critically regulates TSC2 and mTOR. *Proc. Natl. Acad. Sci. USA* **102**, 8573–8578 (2005).
19. Qin, Y. *et al.* Germline mutations in *TMEM127* confer susceptibility to pheochromocytoma. *Nat. Genet.* **42**, 229–233 (2010).
20. Zhu, J., Blenis, J. & Yuan, J. Activation of PI3K/Akt and MAPK pathways regulates Myc-mediated transcription by phosphorylating and promoting the degradation of Mad1. *Proc. Natl. Acad. Sci. USA* **105**, 6584–6589 (2008).
21. Jimenez, R.H. *et al.* Regulation of gene expression in hepatic cells by the mammalian Target of Rapamycin (mTOR). *PLoS ONE* **5**, e9084 (2010).
22. Vaqué, J.P. *et al.* c-Myc inhibits Ras-mediated differentiation of pheochromocytoma cells by blocking c-Jun up-regulation. *Mol. Cancer Res.* **6**, 325–339 (2008).
23. Nair, S.K. & Burley, S.K. X-ray structures of Myc-Max and Mad-Max recognizing DNA. Molecular bases of regulation by proto-oncogenic transcription factors. *Cell* **112**, 193–205 (2003).
24. Dang, C.V., McGuire, M., Buckmire, M. & Lee, W.M. Involvement of the 'leucine zipper' region in the oligomerization and transforming activity of human c-myc protein. *Nature* **337**, 664–666 (1989).
25. Teh, M.T. *et al.* Genomewide single nucleotide polymorphism microarray mapping in basal cell carcinomas unveils uniparental disomy as a key somatic event. *Cancer Res.* **65**, 8597–8603 (2005).
26. Murthy, S.K., DiFrancesco, L.M., Ogilvie, R.T. & Demetrick, D.J. Loss of heterozygosity associated with uniparental disomy in breast carcinoma. *Mod. Pathol.* **15**, 1241–1250 (2002).
27. Tiu, R.V. *et al.* New lesions detected by single nucleotide polymorphism array-based chromosomal analysis have important clinical impact in acute myeloid leukemia. *J. Clin. Oncol.* **27**, 5219–5226 (2009).
28. Kurosawa, K. *et al.* Paternal UPD14 is responsible for a distinctive malformation complex. *Am. J. Med. Genet.* **110**, 268–272 (2002).
29. Wilson, M. *et al.* The clinical phenotype of mosaicism for genome-wide paternal uniparental disomy: two new reports. *Am. J. Med. Genet. A.* **146A**, 137–148 (2008).
30. Baysal, B.E. *et al.* Mutations in *SDHD*, a mitochondrial complex II gene, in hereditary paraganglioma. *Science* **287**, 848–851 (2000).

ONLINE METHODS

Cases and controls. Cases were clinically diagnosed with functioning or non-functioning adrenal PCC in Spanish and Italian public hospitals. All cases tested negative for mutations in the seven major PCC susceptibility genes: *VHL*, *RET*, *SDHB*, *SDHC*, *SDHD*, *SDHAF2* and *TMEM127*. Genomic DNA was extracted from blood following a standard method[31]. Tumor DNA from frozen and paraffin-embedded tissues was obtained using the DNeasy kit (QIAGEN) following the manufacturer's instructions. Informed consent was obtained from all subjects. DNA samples from at least 375 unrelated, unaffected individuals were analyzed as controls. HapMap DNA samples used as quality and filtering controls for next-generation sequencing were extracted from the cell lines of seven individuals of European-American ancestry (NA11881, NA12144, NA12750, NA12761, NA12763, NA12813 and NA12892) originally sourced from Coriell Cell Repositories.

Exome enrichment and next-generation sequencing. DNA samples from cases and controls were enriched for exomic regions according to Agilent's SureSelect Human All Exon Kit protocol (Agilent Technologies). Resulting DNA libraries were sequenced using 78-bp paired-end technology on an Illumina Genome Analyzer II following the manufacturer's protocol. Two sequencing lanes per sample were used in order to obtain sufficient sequencing depth for the final variant analysis. Real-time image analysis and base calling was performed using Illumina's Real Time Analysis software version 1.6 using standard parameters.

Next-generation sequencing data analysis. Unaligned data from each of the four sequence files generated per individual (two files per sequencing lane, one for each of the pair ends) were merged into two files, one containing the information for the first sequencing pair for both lanes and the other containing the corresponding information for the other pair. Both files were then filtered coordinately to remove low-quality reads (containing six or more undefined bases), homopolymers and dinucleotide repetitions using an in-house–developed Perl script (Quality-Control-1). Filtered files were aligned against the whole human genome (hg18 assembly) using Novoalign version 2.06.09 (see URLs). Standard alignment settings were used, except for the gap extension penalty (set to five) and the option of reporting up to three alignment locations for those reads matching more than one region on the genome. Aligned SAM files were sorted by chromosome and coordinate and then analyzed with the Perl script Read_selection in order to select on-target reads with sufficient quality for subsequent analysis. SAMtools version 0.1.8 (ref. 32) was used to remove PCR duplicates (rmdup option) and for variant calling (pileup option). SNS and indel data was extracted from pileup files using a Perl script (Pileup4annotation), which also calculated two scores: deep score and quality score (**Supplementary Table 1**). These scores represent a ratio between the read depth (deep) or the Phred-scaled quality score for the variant allele (Xv) and the reference allele (Xr):

$$\text{Deep score (or quality score)} = \left(\frac{\text{Xv}}{\text{Xr}}\right) \times 100$$

Variant selection. SNS and indel data were analyzed separately. Using a series of newly developed Perl scripts, they were first confronted against two sets of variants (SNSs and indels, respectively) obtained from the seven HapMap controls using specific thresholds (see above) (**Table 1**). This comparison was performed with Perl scripts (Comp_against_controls-SNSs, Comp_against_controls-INDELs). Next, both variant types were filtered against the information in dbSNP130 and annotated using the Ensembl database in Annovar[33]. Variants in intergenic or intronic regions were subsequently discarded, and high-quality variants (deep > 7 and Phred quality > 20) affecting the same gene in all three samples and not producing synonymous amino acid changes in the resulting protein were selected.

***MAX* Sanger sequencing.** Primers spanning the five exons of the major *MAX* transcript (ENST00000358664) were used to amplify germline DNA from the selected cases with PCC. The purified products were subsequently sequenced using the automatic sequencer ABI 3730xl (Applied Biosystems). Primer sequences and PCR conditions are available upon request.

RT-PCR. Total RNA was isolated from frozen tumor tissue carrying the mutation c.295+1G>A using the TRI Reagent kit (MRC) following the manufacturer's instructions. First-strand complementary DNA was synthesized from 2 μg of total RNA by oligo(dT)14 primer reverse transcription with Superscript II Reverse Transcriptase (Invitrogen) following the manufacturer's instructions. PCR was then performed to generate a fragment spanning exons 1–5 of *MAX* transcript 2 (ENST00000358664) using the primers shown in **Supplementary Table 3**. The PCR products were analyzed by electrophoresis on a 2% agarose gel. Complementary DNA from peripheral blood lymphocytes of a healthy volunteer was used as control.

Loss of heterozygosity (LOH) and uniparental disomy (UPD) analyses. LOH analysis of the *MAX* locus was performed on seven tumors for which blood and tumor DNA were available. We first performed direct sequencing of tumor DNA using the same PCR conditions as we applied for germline DNA. To investigate the origin of the LOH found in the tumors, we performed high-density SNP-array analysis in one of the tumors. A genome-wide scan of 616,795 markers was conducted on 250 ng of tumor DNA using the Illumina Human610-Quad BeadChip according to the manufacturer's specifications. Image data was analyzed using the Chromosome Viewer tool contained in GenomeStudio 2010.2 (Illumina). The metric used was the log *R* ratio, which is the log ratio of the observed normalized *R* value for a SNP divided by the expected normalized *R* value[34]. In addition, an allele frequency analysis was applied for all SNPs. UPD or chromosomal loss was assessed in the other *MAX*-mutation–positive tumors by microsatellite analysis. Three polymorphic markers spanning chromosome 14 from the *MAX* locus to the telomere were selected (**Supplementary Table 3**) and analyzed by multiplex amplification. We first designed and labeled (5′ 6-FAM) a pair of primers for each marker. We used labeled control fragments from *MAX* and from chromosomes 1q and 14q as internal controls. We amplified genomic and tumor DNA separately by means of a multiplex PCR kit (QIAGEN, GmbH), as previously described[35]. Purified PCR amplification products were used for fragment analysis on an ABI PRISM 310 capillary sequencer (Applied Biosystems) and analyzed using Peak Scanner Software v1.0 (Applied Biosystems). Normalization was performed by overlapping each germline DNA sample with the corresponding tumor sample, determining the peak surface of all fragments and calculating the normal peak fractions. A second multiplex PCR that included control peaks from three different regions (chromosomes 5, 12 and 15), as well as one *MAX* amplicon and two 14q fragments, was performed to determine the loss of chromosome 14q. Finally, we genotyped various subtelomeric SNPs (**Supplementary Table 3**) both in blood and tumor DNA to assess the extension of the LOH.

Methylation of *MEG3*. To show the paternal origin of the mutated allele, we analyzed the methylation status of the *MEG3* promoter in six cases for which tissue was available by conventional methylation-specific PCR using previously described primers and conditions[36]. Bisulphite treatment of tumor DNA was performed using the EZ DNA methylation kit (Zymo Research) according to the manufacturer's instructions. DNA from normal lymphocytes and from a *RET*-mutation–positive PCC were used as controls. PCR products were visualized by ethidium bromide staining after 2.5% agarose gel electrophoresis. A 160-bp PCR product represented the methylated state, and a 120-bp PCR product corresponded to the unmethylated maternal allele of *MEG3*. Statistical evidence for paternally transmission was assessed by a two-tailed binomial test using R version 2.9.0 (see URLs).

MAX protein analyses. Prior to showing the absence of full-length MAX in tumors carrying *MAX* truncating mutations, we evaluated the specificity of the sc-197 antibody (Santa Cruz Biotechnology) by protein blot in HeLa, Jurkat and PC12 cells (**Supplementary Fig. 4**). This is a commercial polyclonal antibody raised against the C terminus of the human MAX protein that specifically recognizes translated *MAX* transcripts 1 (ENST00000358402) and 2 (ENST00000358664). Proteins were separated by 4–12% SDS-PAGE and transferred to a polyvinylidene fluoride membrane as previously described[37]. The membrane was blocked and then incubated with a 1:200 dilution of the antibody following the manufacturer's instructions. Equal protein loading was assessed using a 1:12,000 dilution of β actin antibody (A5441, Sigma).

doi:10.1038/ng.861

Immunohistochemical staining was performed using 3 μm formalin-fixed paraffin-embedded tumor sections from the five PCCs carrying truncating *MAX* mutations. Two normal adrenal sections and ten tumors carrying mutations in other PCC susceptibility genes (*RET*, *NF1*, *SDHB*, *SDHD* and *TMEM127*) were used as controls. After drying the sections in a 60 °C oven overnight, they were placed in a Bond MAX Automated Immunohistochemistry Vision Biosystem (Leica Microsystems GmbH) according to the following protocol: first, tissues were deparaffinized and pretreated with Epitope Retrieval Solution 2 (EDTA-buffer pH 8.8) at 98 °C for 20 min. After several washing steps, peroxidase blocking was carried out for 10 min using the Bond Polymer Refine Detection Kit DC9800 (Leica Microsystems GmbH). Tissues were again washed and then incubated with sc-197 MAX primary antibody (1:1600) for 30 min. Subsequently, tissues were incubated with polymer for 15 min and developed with DAB-Chromogen for 10 min. Only cases showing nuclear staining of stromal cells were considered scorable.

31. Sambrook, J., Maniatis, T. & Fritsch, E.F. *Molecular Cloning: A Laboratory Manual*, 3 v. (Cold Spring Harbor Laboratory, Cold Spring Harbor, New York, 1989).
32. Li, H. *et al.* The Sequence Alignment/Map format and SAMtools. *Bioinformatics* **25**, 2078–2079 (2009).
33. Wang, K., Li, M. & Hakonarson, H. ANNOVAR: functional annotation of genetic variants from high-throughput sequencing data. *Nucleic Acids Res.* **38**, e164 (2010).
34. Simon-Sanchez, J. *et al.* Genome-wide SNP assay reveals structural genomic variation, extended homozygosity and cell-line induced alterations in normal individuals. *Hum. Mol. Genet.* **16**, 1–14 (2007).
35. Cascón, A. *et al.* Gross *SDHB* deletions in patients with paraganglioma detected by multiplex PCR: a possible hot spot? *Genes Chromosom. Cancer* **45**, 213–219 (2006).
36. Astuti, D. *et al.* Epigenetic alteration at the *DLK1–GTL2* imprinted domain in human neoplasia: analysis of neuroblastoma, phaeochromocytoma and Wilms' tumour. *Br. J. Cancer* **92**, 1574–1580 (2005).
37. Landa, I. *et al.* Allelic variant at -79 (C>T) in *CDKN1B* (p27Kip1) confers an increased risk of thyroid cancer and alters mRNA levels. *Endocr. Relat. Cancer* **17**, 317–328 (2010).

SUPPLEMENTARY MATERIAL

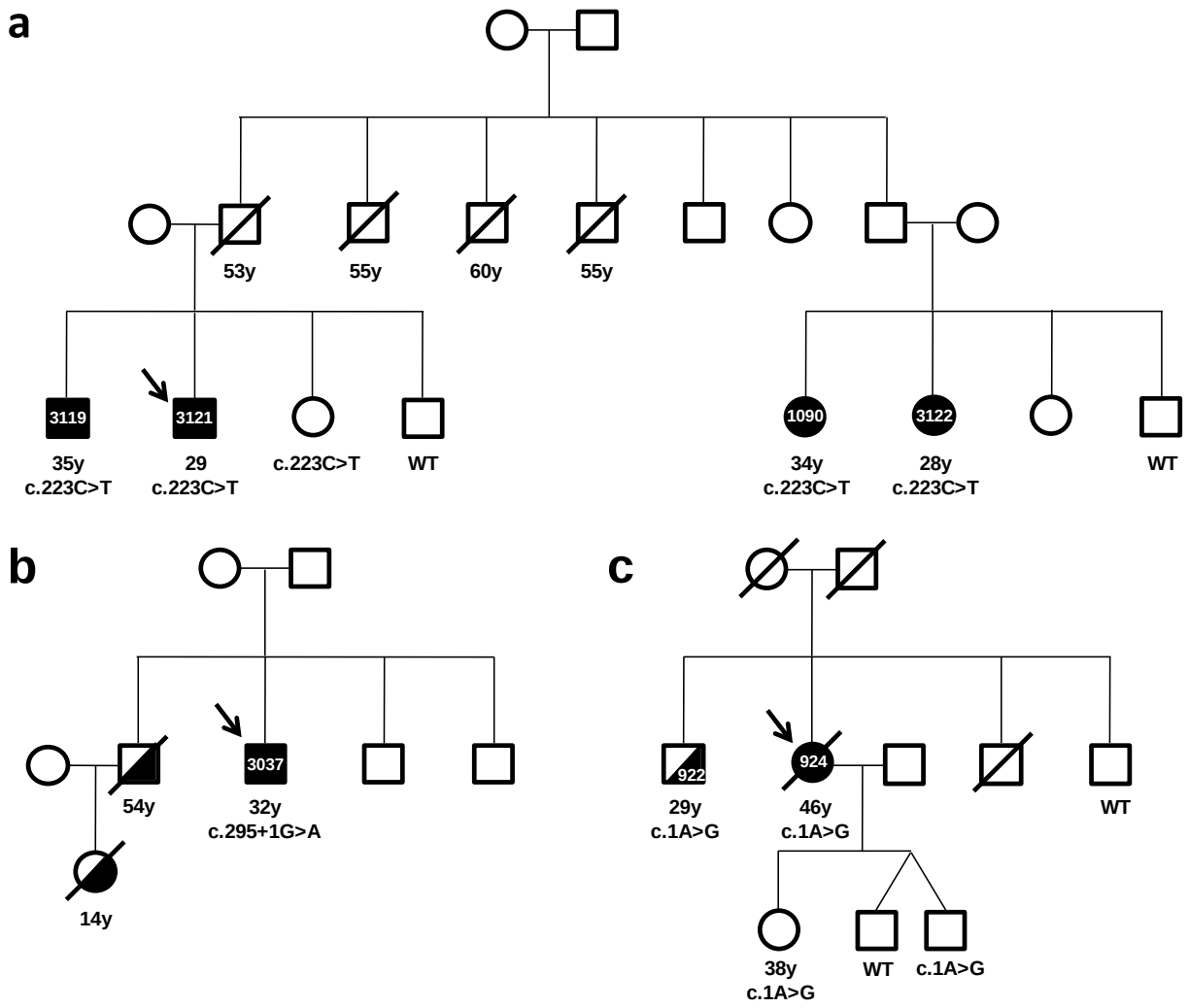

Supplementary Figure 1. Pedigrees (**a**, **b**, and **c**) of the three patients (3121, 3037, and 924, respectively) used for NGS analysis (marked with an arrow). Studied carriers and non-carriers of the corresponding *MAX* mutation are indicated by the mutated and the wild type (WT) allele, respectively. Complete and partial filled symbols represent individuals with bilateral and unilateral PCC, respectively.

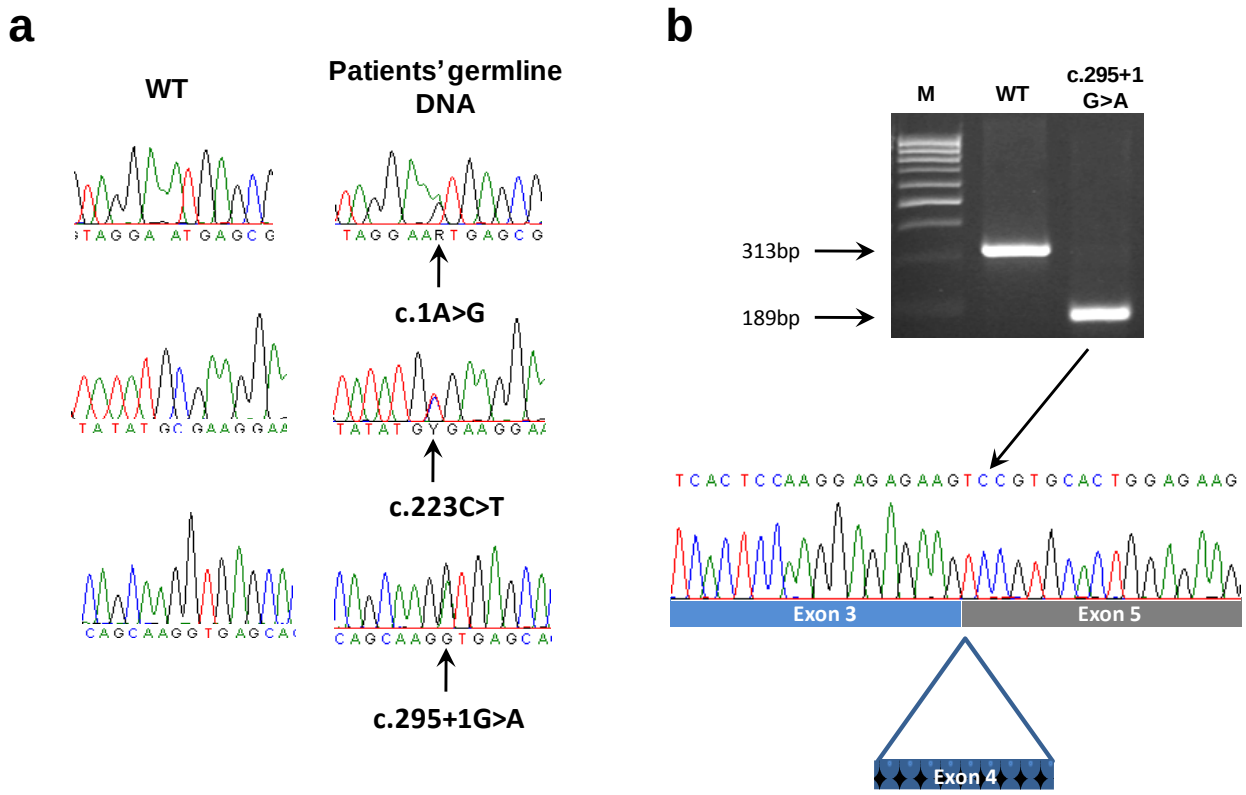

Supplementary Figure 2. *MAX* germline mutations identified by exome sequencing. **a,** DNA sequence chromatograms of the three *MAX* mutations. The left panels show the wild type (WT) alleles, and the right panels show the corresponding heterozygous germline mutation (indicated by an arrow); **b,** RT-PCR amplification, encompassing exons 1–5, of *MAX* wild type (WT) and c.295+1G>A tumor cDNAs. The arrows indicate the size of the WT (313bp) and the mutant (189bp) cDNAs. The lower part of the figure shows complete exon 4 skipping by direct sequencing of the mutated transcript. M: molecular size marker.

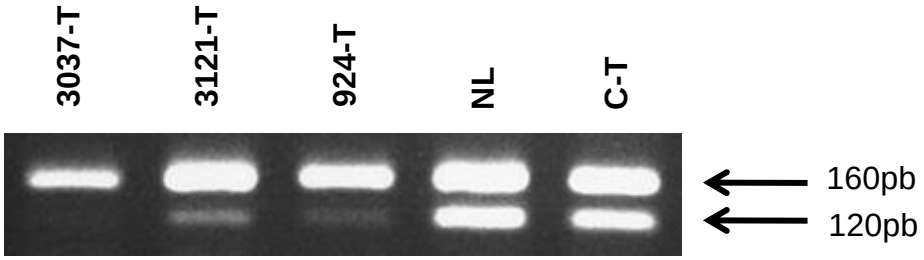

Supplementary Figure 3. *MEG3* methylation-specific PCR analysis. The study was performed in the tumor with known paternal transmission of the mutated allele (3121-T), and the two tumors with unknown origin of the mutated *MAX* allele (924-T and 3037-T). The methylated (160pb) and the unmethylated (120pb) alleles are denoted by arrows. NL: normal lymphocytes; C-T: RET PCC used as control.

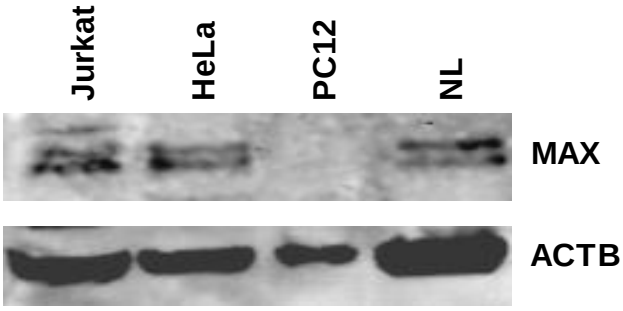

Supplementary Figure 4. Immunoblot experiment performed to assess the specificity of the C-terminus specific sc-197 MAX antibody. Band corresponding to MAX protein is absent in extracts from rat PC12 cells, which express a defective protein lacking the C-terminus. ACTB: beta actin; NL: normal lymphocytes.

Supplementary Table 1. List of variants that passed the first six filtering steps

Sample	Consequence	Ensembl gene	Chr.	Chromosomal position	Reference	Variant	QUAL	SNP_QUAL	DEEP	DS	QS
924	UTR3	ENSG00000006634	7	87375469	T	C	127	116	33	94,12	86,37
3037	UTR3	ENSG00000006634	7	87375469	T	C	114	114	55	111,54	111,17
3121	UTR3	ENSG00000006634	7	87375469	T	C	89	69	51	142,86	145,94
924	nonsynonymous SNV	ENSG00000093010:	22	18330164	A	G	36	36	25	200	73,86
3037	nonsynonymous SNV	ENSG00000093010:	22	18330164	A	G	18	18	16	166,67	51,18
3121	UTR3	ENSG00000093010	22	18336270	G	C	36	36	27	28,57	25,93
924	nonsynonymous SNV	ENSG00000106665:	7	73409685	C	A	17	17	18	157,14	82,07
3037	nonsynonymous SNV	ENSG00000106665:	7	73412498	C	T	3	3	11	22,22	32,64
3121	nonsynonymous SNV	ENSG00000106665:	7	73409685	C	A	24	24	29	145,45	85,32
924	nonsynonymous SNV	ENSG00000125952:	14	64638810	T	C	49	49	19	58,33	45,12
3037	splicing	ENSG00000125952:	14	64614383	C	T	185	144	65	156	131,11
3121	stopgain SNV	ENSG00000125952:	14	64614456	G	A	97	97	139	76,92	79,72
924	UTR5	ENSG00000128059	4	56996426	A	C	7	7	44	90,91	57,3
3037	synonymous SNV	ENSG00000128059:	4	56963085	T	C	130	130	129	98,46	99,08
3121	synonymous SNV	ENSG00000128059:	4	56963085	T	C	27	15	178	113,25	114,44
924	downstream	ENSG00000163060	2	94906374	G	A	34	34	16	33,33	35,03
3037	nonsynonymous SNV	ENSG00000163060:	2	94901320	C	G	19	19	36	25	20,98
3121	nonsynonymous SNV	ENSG00000163060:	2	94901320	C	G	53	53	33	37,5	35,96
924	nonsynonymous SNV	ENSG00000169876:	7	100466086	A	G	23	23	644	96,64	96,85
3037	nonsynonymous SNV	ENSG00000169876:	7	100468685	A	C	61	61	857	89,33	90,93
3121	nonsynonymous SNV	ENSG00000169876:	7	100464350	C	T	228	228	1605	77,61	76,6
924	nonsynonymous SNV	ENSG00000174233:	12	47463072	C	T	61	61	16	128,57	114,22
3037	nonsynonymous SNV	ENSG00000174233:	12	47463072	C	T	21	21	12	50	51,34
3121	nonsynonymous SNV	ENSG00000174233:	12	47450878	C	T	191	165	108	118,37	118,45
924	nonsynonymous SNV	ENSG00000178209:	8	145064257	G	A	88	32	14	333,33	245,61
3037	nonsynonymous SNV	ENSG00000178209:	8	145096771	C	T	76	73	12	100	82,7
3121	synonymous SNV	ENSG00000178209:	8	145074058	G	A	68	23	11	120	182,65
924	nonsynonymous SNV	ENSG00000178401:	12	48029409	G	A	228	191	56	143,48	155,48
3037	nonsynonymous SNV	ENSG00000178401:	12	48029409	G	A	195	195	76	92,31	109,36
3121	UTR3	ENSG00000178401	12	48031596	G	A	67	67	71	62,79	64,09

924	nonsynonymous SNV	ENSG00000184185:	17	21260453	C	A	22	16	97	96,67	77,72
3037	nonsynonymous SNV	ENSG00000184185:	17	21260360	C	G	9	9	243	77,91	74,92
3121	UTR3	ENSG00000184185	17	21260582	C	A	42	18	22	125	145,61
924	nonsynonymous SNV	ENSG00000184584:	5	138838109	C	G	212	212	68	71,79	79,05
3037	nonsynonymous SNV	ENSG00000184584:	5	138838109	C	G	183	183	63	65,79	70,77
3121	nonsynonymous SNV	ENSG00000184584:	5	138838109	C	G	200	200	72	84,62	74,7
924	synonymous SNV	ENSG00000187634:	1	856285	C	T	100	100	23	53,33	54,63
3037	nonsynonymous SNV	ENSG00000187634:	1	868971	A	C	9	9	12	125	61,11
3121	nonsynonymous SNV	ENSG00000187634:	1	867426	A	G	9	9	10	28,57	26,25
924	nonsynonymous SNV	ENSG00000198502:	6	32597822	C	T	96	65	17	183,33	112,02
3037	UTR5	ENSG00000198502	6	32606012	G	C	44	38	14	140	145,51
3121	nonsynonymous SNV	ENSG00000198502:	6	32597744	A	G	15	15	14	62,5	31,95
924	downstream	ENSG00000200434	16	33873213	T	C	6	6	14	100	79,66
3037	downstream	ENSG00000200434	16	33873128	T	C	44	5	85	175	174,31
3121	downstream	ENSG00000200434	16	33873188	C	T	57	57	12	50	49,34
924	nonsynonymous SNV	ENSG00000204525:	6	31432910	A	C	51	51	14	55,56	60,28
3037	upstream	ENSG00000204525	6	31432975	G	A	19	19	7	40	43,37
3121	nonsynonymous SNV	ENSG00000204525:	6	31432003	C	A	133	68	36	176,92	170,54
924	nonsynonymous SNV	ENSG00000206503:	6	30020321	G	A	65	65	136	56,98	59,5
3037	UTR5	ENSG00000206503	6	30018244	G	T	61	61	9	80	82,78
3121	UTR3	ENSG00000206503	6	30021323	G	C	36	11	103	43,48	43,64

QUAL: Phred-scaled consensus quality for the site.
SNP_QUAL: Phred-scaled probability of the consensus being identical to the reference.
DEEP: Number of reads covering a given position. Also known as read depth.
DS: Deep Score
QS: Quality Score

Supplementary Table 2. Clinical features of selected patients screened for *MAX* mutations

ID	Sex	Age at onset	Tumor	Malignant	Familal antecedents
100	M	11	bPCC*	No	No
475	M	16	bPCC	No	No
249	M	19	bPCC	No	No
1694	M	19	bPCC	No	No
190	M	22	bPCC	No	No
554	F	34	bPCC	No	No
60	M	36	bPCC	No	No
83	M	37	bPCC	No	No
416	F	38	bPCC	No	No
974	M	38	bPCC	No	No
329	F	40	bPCC	Yes	No
3468	F	43	bPCC	No	No
183	M	44	bPCC	No	No
525	F	46	bPCC	No	No
796	F	46	bPCC	No	No
1016	F	47	bPCC	No	Yes
874	M	48	bPCC	No	No
3514	F	56	bPCC	No	No
1049	M	59	bPCC	No	No
F004	F	62	bPCC	No	No
1299	M	74	bPCC	No	No
912	M	75	bPCC	Yes	No
490	M	80	bPCC	No	No
960	M	5	PCC	No	No
754	F	9	PCC	No	No
115	M	11	PCC	No	No
92	F	11	PCC	No	No
F084	F	13	PCC	No	No
F132	F	13	PCC	No	No
3406	M	14	PCC	No	No
555	M	15	PCC	No	No
F088	F	15	PCC	No	No
3558	M	17	PCC	No	No
424	F	19	PCC	No	No
908	M	21	PCC	No	No
1078	F	22	PCC	No	No
650	F	22	PCC	No	No
1075	F	22	PCC	No	No
S190	M	23	PCC	No	No
285	F	23	PCC	No	No
473	F	23	PCC	Yes	No
3245	M	23	PCC	No	No

1746	M	24	PCC	No	No
1048	M	25	PCC	Yes	No
368	F	26	PCC	Yes	No
717	F	26	PCC	No	No
F011	M	26	PCC	No	No
F021	F	26	PCC	No	No
258	M	26	PCC	Yes	No
671	F	27	PCC	No	No
F015K	F	27	PCC	No	No
246	F	28	PCC	No	No
3388	M	28	PCC	No	No
565	M	29	PCC	No	No
1079	F	29	PCC	No	No
1351	M	42	PCC	No	Yes
3030	F	48	PCC	No	Yes
612	F	50	PCC	No	Yes
3510	M	50	PCC	No	Yes

*bPCC, bilateral adrenal pheochromocytoma

Supplementary Table 3. Primers used for amplification of cDNA and polymorphic markers

	Name	Primer sequence 5'-3'
cDNA	MAX-F	AGAGCGACGAAGAGCAACCGA
	MAX-R	TTGGTCTGCAGTTGGGCACT
Microsatellites	D14S588-F	GCCGAAAGAAAGAAAAAAGG
	D14S588-R	CGAATGCATACTTGCTGTTG
	D14S1044-F	AAGTCCTTGCTTTGCAGGTT
	D14S1044-R	ATTGTTTTCACTGGTTGTTGTTCAT
	D14S1051-F	TCAATGAGGCCAAAGC
	D14S1051-R	TGTTGACGGTCCCTTG
SNPs	rs17101145-rs13379319-F	TATCATCAGGGGCTGACCTC
	rs17101145-rs13379319-R	CGTTACAGCATGGTTTGGAG
	rs3783398-F	TTAAAAGACAGGGCCCATTG
	rs3783398-R	TGCCGAAGAAGTCATCTGTG
	rs56729078-rs60916402-F	CAGGCTGGTCCTGTCTCCT
	rs56729078-rs60916402-R	GGGACCATTAGCAGAGAAAGC
	rs3730358-rs2494737-F	AGTCTGCCTTCCCGTTGAC
	rs3730358-rs2494737-R	CAGCCAGTGCTTGTTGCTT

ARTICLE 2: ***MAX* mutations cause hereditary and sporadic pheochromocytoma and paraganglioma.**

Authors: Nelly Burnichon, Alberto Cascón, Francesca Schiavi, Nicole Paes Morales, **Iñaki Comino-Méndez**, Nassèra Abermil, Lucía Inglada-Pérez, Aguirre A. de Cubas, Laurence Amar, Marta Barontini, Sandra Bernaldo de Quirós, Jérôme Bertherat, Yves-Jean Bignon, Marinus J. Blok, Sara Bobisse, Salud Borrego, Maurizio Castellano, Philippe Chanson, María-Dolores Chiara, Eleonora P.M. Corssmit, Mara Giacchè, Ronald R. de Krijger, Tonino Ercolino, Xavier Girerd, Encarna B. Gómez-García, Álvaro Gómez-Graña, Isabelle Guilhem, Frederik J. Hes, Emiliano Honrado, Esther Korpershoek, Jacques W.M. Lenders, Rocío Letón, Arjen R. Mensenkamp, Anna Merlo, Luigi Mori, Arnaud Murat, Peggy Pierre, Pierre-François Plouin, Tamara Prodanov, Miguel Quesada-Charneco, Nan Qin, Elena Rapizzi, Victoria Raymond, Nicole Reisch, Giovanna Roncador, Macarena Ruiz-Ferrer, Frank Schillo, Alexander P.A. Stegmann, Carlos Suarez, Elisa Taschin, Henri J.L.M. Timmers, Carli M.J. Tops, Miguel Urioste, Felix Beuschlein, Karel Pacak, Massimo Mannelli, Patricia L. M. Dahia, Giuseppe Opocher, Graeme Eisenhofer, Anne-Paule Gimenez-Roqueplo, and Mercedes Robledo.

Published in Clinical Cancer Research 2012 May 15; 18 (10).

ABSTRACT

In the first NGS-based project we discovered the involvement of the *MAX* gene in susceptibility to develop PCC/PGL. How this gene contributes to tumor development and the associated phenotype remains unclear. The second aim of this thesis was to study the prevalence of *MAX* mutations in PCC/PGL patients and the associated phenotypic features of *MAX*-mutated patients.

We first sequenced *MAX* in 1,694 patients with PCC or PGL, without mutations in other major susceptibility genes, from 17 independent referral centers. We also screened for large deletions/duplications in 1,535 patients using a multiplex PCR-based method. We screened the tumors from an additional 245 patients for somatic mutations.

Sixteen pathogenic *MAX* mutations were identified in 23 index patients. All had adrenal tumors, 13 were bilateral or multiple PCCs within the same gland and 3 developed additional tumors at thoraco-abdominal sites. This latter finding extends the implication of *MAX* to extradrenal tumors. Moreover, it was found that 37% of mutation carriers had familial antecedents appearing in the paternal branch of their pedigree, with more than one generation of affected members. The age at diagnosis was significantly lower for *MAX* mutation carriers than for non-carrier cases. Besides, only 10.5% of patients

developed metastatic disease, so we reconsidered our initial hypothesis about the metastatic potential of *MAX*-related tumors. Five tumors carried mutations in *MAX*, four of them confirmed as somatic (1.6%) pointing the importance of the *MAX* gene in this disease. Regarding catecholamines secretion, *MAX* tumors were characterized by substantial increases in normetanephrine, associated with normal or minor increases in metanephrine.

In summary, we determined that germline mutations in *MAX* are responsible for 1.1% of PCC/PGL in patients without evidence of other known mutations and should be considered in the genetic work-up of these patients.

Personal contribution: I participated in the conception and design of the study and the acquisition of the data. I was actively involved in the screening for the large insertions/deletions using a multiplex PCR-based method and in the posterior computational analysis. Finally, I contributed to the discussion of the results and the drafting of the paper.

Published OnlineFirst on March 27, 2012; DOI:10.1158/1078-0432.CCR-12-0160

Human Cancer Biology

Clinical Cancer Research

MAX Mutations Cause Hereditary and Sporadic Pheochromocytoma and Paraganglioma

Nelly Burnichon[1,2,3], Alberto Cascón[8,11], Francesca Schiavi[12], Nicole Paes Morales[14], Iñaki Comino-Méndez[8], Nasséra Abermil[1,2,3], Lucía Inglada-Pérez[8,11], Aguirre A. de Cubas[8], Laurence Amar[2,3,4], Marta Barontini[16], Sandra Bernaldo de Quirós[17], Jérôme Bertherat[2,5], Yves-Jean Bignon[18], Marinus J. Blok[19], Sara Bobisse[12], Salud Borrego[11,20], Maurizio Castellano[21], Philippe Chanson[6], María-Dolores Chiara[17], Eleonora P.M. Corssmit[22], Mara Giacchè[21], Ronald R. de Krijger[24], Tonino Ercolino[25], Xavier Girerd[7], Encarna B. Gómez-García[19], Álvaro Gómez-Graña[8], Isabelle Guilhem[28], Frederik J. Hes[23], Emiliano Honrado[29], Esther Korpershoek[24], Jacques W.M. Lenders[30], Rocío Letón[8], Arjen R. Mensenkamp[31], Anna Merlo[17], Luigi Mori[21], Arnaud Murat[33], Peggy Pierre[34], Pierre-François Plouin[2,3,4], Tamara Prodanov[36], Miguel Quesada-Charneco[37], Nan Qin[38], Elena Rapizzi[26], Victoria Raymond[39], Nicole Reisch[40], Giovanna Roncador[9], Macarena Ruiz-Ferrer[11,20], Frank Schillo[41], Alexander P.A. Stegmann[19], Carlos Suarez[17], Elisa Taschin[12], Henri J.L.M. Timmers[32], Carli M.J. Tops[23], Miguel Urioste[10,11], Felix Beuschlein[40], Karel Pacak[35], Massimo Mannelli[26,27], Patricia L. M. Dahia[14,15], Giuseppe Opocher[13], Graeme Eisenhofer[38], Anne-Paule Gimenez-Roqueplo[1,2,3], and Mercedes Robledo[8,11]

Abstract

Purpose: Pheochromocytomas (PCC) and paragangliomas (PGL) are genetically heterogeneous neural crest–derived neoplasms. Recently we identified germline mutations in a new tumor suppressor susceptibility gene, *MAX* (MYC-associated factor X), which predisposes carriers to PCC. How *MAX* mutations contribute to PCC/PGL and associated phenotypes remain unclear. This study aimed to examine the prevalence and associated phenotypic features of germline and somatic *MAX* mutations in PCC/PGL.

Design: We sequenced *MAX* in 1,694 patients with PCC or PGL (without mutations in other major susceptibility genes) from 17 independent referral centers. We screened for large deletions/duplications in 1,535 patients using a multiplex PCR-based method. Somatic mutations were searched for in tumors from an additional 245 patients. The frequency and type of *MAX* mutation was assessed overall and by clinical characteristics.

Results: Sixteen *MAX* pathogenic mutations were identified in 23 index patients. All had adrenal tumors, including 13 bilateral or multiple PCCs within the same gland ($P < 0.001$), 15.8% developed additional tumors at thoracoabdominal sites, and 37% had familial antecedents. Age at diagnosis was lower ($P = 0.001$) in *MAX* mutation carriers compared with nonmutated cases. Two patients (10.5%) developed metastatic disease. A mutation affecting *MAX* was found in five tumors, four of them confirmed as somatic (1.65%). MAX tumors were characterized by substantial increases in normetanephrine, associated with normal or minor increases in metanephrine.

Conclusions: Germline mutations in *MAX* are responsible for 1.12% of PCC/PGL in patients without evidence of other known mutations and should be considered in the genetic work-up of these patients. *Clin Cancer Res; 18(10); 1–10. ©2012 AACR.*

Authors' Affiliations: [1]Assistance Publique-Hôpitaux de Paris, Hôpital Européen Georges Pompidou, Service de Génétique; [2]Université Paris Descartes, Sorbonne Paris Cité, Faculté de Médecine; [3]INSERM, UMR970, Paris Cardiovascular Research Center; [4]Assistance Publique-Hôpitaux de Paris, Hôpital Européen Georges Pompidou, Service de Médecine vasculaire et d'Hypertension artérielle; [5]INSERM U1016, CNRS UMR 8104, Institut Cochin; [6]Assistance Publique Hôpitaux de Paris, Hôpital de Bicêtre Endocrinology Unit, Le Kremlin-Bicêtre; [7]Assistance Publique Hôpitaux de Paris, Groupe Hospitalier Pitié-Salpêtrière, Unité de Prévention Cardiovasculaire, Pôle Endocrinologie, Paris, France; [8]Hereditary Endocrine Cancer Group, [9]Monoclonal Antibodies Unit, [10]Human Genetics Cancer Group, Spanish National Cancer Research Centre (CNIO), Madrid; [11]Centro de Investigación Biomédica en Red de Enfermedades Raras (CIBERER), Spain; [12]Familial Cancer Clinic and Oncoendocrinology, Veneto Institute of Oncology, IRCCS; [13]Department of Medical and Surgical Sciences, University of Padova, Padua, Italy; [14]Department of Medicine, [15]Cancer Therapy and Research Center, University of Texas Health Science Center, San Antonio, Texas; [16]Center for Endocrinological Investigations-CEDIE, Hospital de Ninos Dr. Ricardo Gutierrez, Buenos Aires, Argentina; [17]Othorhinolaryngology Service, Hospital Universitario Central de Asturias, Instituto Universitario de Oncología del Principado de Asturias, Oviedo, Spain; [18]Oncogenetic Department, Centre Jean Perrin, Clermont-Ferrand, France; [19]Department of Clinical Genetics, Maastricht University Medical Center, Maastricht, The Netherlands; [20]Unidad de Gestión Clínica de Genética, Reproducción y Medicina Fetal, Instituto de Biomedicina de Sevilla, Hospital Universitario Virgen del Rocío/CSIC/Universidad de Sevilla, Spain; [21]Clinica Medica, Endocrine and Metabolic Disease Unit and Molecular Medicine Laboratory, University of Brescia, Spedali Civili of Brescia, Brescia, Italy; Departments of [22]Endocrinology and [23]Clinical Genetics, Leiden University Medical Center, Leiden, The Netherlands; [24]Department of Pathology, Erasmus

Published OnlineFirst on March 27, 2012; DOI:10.1158/1078-0432.CCR-12-0160

Translational Relevance

MAX has been recently identified as the tenth susceptibility gene for pheochromocytoma (PCC). However, its clinical relevance was not addressed. This international study, based on an outstanding series of 1,694 unrelated patients with PCC or paraganglioma (PGL), has been able to ascertain the prevalence of *MAX* mutations in PCC patients, extended the spectrum of MAX-related tumors to PGL, uncovered contributions of somatic *MAX* mutations to sporadic disease, and defined an intermediate catecholamine phenotype, which may guide testing of *MAX* gene in patients with PCC/PGLs. This study also confirms a preferential paternal mode of transmission with important consequences for genetic counseling. We establish here that *MAX* germline mutations are responsible for the disease in 1.12% of cases, similarly to the genes recently described, such as *TMEM127*, *SDHAF2*, or *SDHA*, and now *MAX* should be considered in the genetic work-up of affected patients.

Introduction

Pheochromocytoma (PCC) has been referred to as "the 10 percent" tumor due in part to the belief that 10% are hereditary and usually associated with 3 well-known cancer syndromes: von Hippel–Lindau disease, multiple endocrine neoplasia type 2, and neurofibromatosis type 1 due to mutations in *VHL* (1), *RET* (2), and *NF1* (3), respectively. The 10 percent rule was challenged after identification of germline mutations in *SDHD*, *SDHB*, and *SDHC* as important causes of familial paraganglioma (PGL; refs. 4–6) that led Neumann and colleagues to establish that up to a quarter of affected patients carried a PCC/PGL susceptibility gene mutation (7). Since then 3 additional susceptibility genes (*SDHAF2*, *SDHA*, and *TMEM127*) (8–10) have been identified. Thus, the proportion of hereditary PCC/PGLs may exceed estimates of 30% to 40% (11, 12), rendering PCC/PGL one of the most inherited tumor entities in existence.

Findings of other patients with a clinical presentation of PCC/PGL that includes a positive family history, early age of presentation, and bilateral adrenal or multiple tumors, but without known mutations, has suggested the presence of further susceptibility genes. With this observation in mind, we recently identified *MAX* (MYC-associated factor X) as a new PCC tumor suppressor susceptibility gene in 3 independent patients with familial antecedents of the disease (13). Further analysis of 59 patients, selected because they had bilateral PCC and/or an early age of disease presentation, allowed detection of 5 additional cases with *MAX* mutations (13). Preliminary genotype–phenotype associations suggested *MAX* mutations were associated with bilateral PCC and an apparent paternal transmission of the disease (13).

Although little is known about genetic alterations in sporadic tumors, it has been proposed that mutations in PCC/PGL susceptibility genes are detrimental for neuronal precursor cells, explaining the apparent rarity of somatic mutations in these genes in apparently sporadic PCC/PGL (14, 15). Guided by transcriptome classification and LOH profiles of a large series of 202 PCC/PGL, we nevertheless recently established that 14% of sporadic tumors harbored somatic mutations in *VHL* or *RET* genes (16). Because deregulation of MYC is a prominent hallmark in numerous forms of cancer (17), with activation of *MYC* genes commonly detected in solid human tumors (18), it is plausible that *MAX* somatic mutations may also occur in sporadic PCC/PGL.

Establishing the above associations and the prevalence of *MAX* mutations among patients with PCC/PGL requires analysis of a larger cohort of patients. In a large international collaborative effort, we therefore screened for the presence of germline mutations affecting *MAX* in 1,694 patients without mutations in major PCC/PGL susceptibility genes. Somatic mutations were searched for in tumors from an additional 245 patients.

Materials and Methods

Patients

The study population consisted of 1,694 apparently unrelated index cases with PCC or PGL, from whom blood-leukocyte DNA samples were available and in whom familial antecedents, presence of metastasis, and number of primary tumors are shown in Table 1. Clinical variables collected for this study were the following: gender, number

MC, University Medical Center Rotterdam, Rotterdam, The Netherlands; [25]Endocrinology Unit, Azienda Ospedaliera Universitaria Careggi; [26]Department of Clinical Pathophysiology, University of Florence; [27]Istituto Toscano Tumori, Florence, Italy; [28]Endocrinology Unit, Centre Hospitalier de Rennes, Rennes, France; [29]Anatomical Pathology Service, Hospital de León, León, Spain; [30]Internal Medicine, [31]Human Genetics, [32]Endocrinology, Radboud University Nijmegen Medical Centre, Nijmegen, The Netherlands; [33]Endocrinology Unit, Hôpital Laënnec, Nantes, France; [34]Endocrinology Unit, Centre Hospitalier Régional Universitaire Bretonneau, Tours, France; [35]Section on Medical Neuroendocrinology, [36]Program in Reproductive and Adult Endocrinology, National Institute of Child Health and Human Development, NIH, Bethesda, Maryland; [37]Endocrinology Service, Hospital Clínico Universitario San Cecilio, Granada, Spain; [38]Institute of Clinical Chemistry and Laboratory Medicine and Department of Medicine, University Hospital Dresden, Dresden, Germany; [39]Division of Molecular Medicine & Genetics, University of Michigan, Ann Arbor, Michigan; [40]Endocrine Research Unit, Medizinische Klinik Campus Innenstadt, Klinikum der LMU, Munich, Germany; and [41]Endocrinology Unit, Centre Hospitalier Universitaire de Besançon, Besançon, France

Note: Supplementary data for this article are available at Clinical Cancer Research Online (http://clincancerres.aacrjournals.org/).

The following 3 groups of authors contributed equally to the article: N. Burnichon and A. Cascón; F. Schiavi, N. Paes Morales, I. Comino-Méndez, N. Abermil, and L. Inglada-Pérez; and G. Eisenhofer, A.-P. Gimenez-Roqueplo, and M. Robledo.

Corresponding Author: Mercedes Robledo, Hereditary Endocrine Cancer Group, Human Cancer Genetics Programme, Centro Nacional de Investigaciones Oncológicas, CNIO, Melchor Fernández Almagro 3, 28029 Madrid, Spain. Phone: 34-91-224-69-47; Fax: 34-91-224-69-23; E-mail: mrobledo@cnio.es

doi: 10.1158/1078-0432.CCR-12-0160

Published OnlineFirst on March 27, 2012; DOI:10.1158/1078-0432.CCR-12-0160

Table 1. Clinical features of the entire pheochromocytoma and paraganglioma cohort

Analysis	Clinical features	*n*	Single PCC	Single PGL H&N/TA	mPGL H&N/TA/both	PCC&PGL H&N/TA/both	bPCC/mPCC
	Total	**1,694**[a]	**1,252**	**315**	**29**	**35**	**63**
				110/205	**1/23/5**	**1/34/0**	
Index cases	With familial antecedents[b] (%)	37 (2.18%)	24 (1.91%)	5 (1.58%)	0	2 (5.71%)	6 (9.52%)
	Malignant[c] (%)	129 (7.61%)	79 (6.30%)	27 (8.57%)	2 (6.89%)	15 (42.85%)	6 (9.52%)
	Gender (female/male/unknown)	1,003/682/9					
	Median age first tumor (range)	48 (3–88)					
Tumors	**Total**	**245**[d]	**216**	**29**			
	Gender (female/male)	150/95					
	Median age (range)	52 (11–83)					

Abbreviations: PCC, adrenal pheochromocytoma; PGL, paraganglioma; mPGL, multiple paragangliomas; bPCC, bilateral adrenal pheochromocytoma; mPCC, multiple pheochromocytomas within the same gland; H&N, Head and Neck; TA, thoracoabdominal; Both – H&N and TA PGL.

[a]Index cases origin (n): France (664), Italy (428), Spain (245), The Netherlands (166), United States (152), Germany (39).

[b]A hereditary cause of PCC/PGL was considered likely when disease affected at least two family members.

[c]Malignancy was defined as the presence of metastases in which chromaffin cells are normally absent.

[d]Tumor origin (*n*): France (106), United States (75), The Netherlands (39), Spain (17), Germany (8).

of PCC/PGLs, tumor location, age of diagnosis for each tumor (in patients with multiple tumors), the biochemical secretion when available, as well as other malignancies developed by probands. These clinical variables were collected electronically into preformatted forms provided to all contributors, and statistically analyzed in a single center. More detailed assessment of clinical data was further obtained for *MAX* mutation carriers. Mutations in *RET*, *VHL*, *SDHB*, *SDHC*, *SDHD*, and *TMEM127* were excluded, and there were no clinical features of neurofibromatosis type 1. Patients were referred from 15 participating centers of the European Network for the Study of Adrenal Tumours (ENS@T) consortium [Madrid, Oviedo, and Seville in Spain (12), Paris, Marseille and Angers in France (19, 20), Leiden, Rotterdam, Nijmegen, and Maastricht in The Netherlands, Padua, Florence, and Brescia in Italy (11), Munich and Dresden in Germany] and 2 centers in the United States (San Antonio and Bethesda). Diagnosis of PCC and/or PGL, including tumors of both sympathetic (thoracic or abdominal) and parasympathetic (head and neck) origin, was established following conventional procedures (including clinical, biochemical, and imaging tests).

Written informed consent to collect phenotypic and genotypic data was obtained from all participants in accordance with institution review board–approved protocols for each center. DNA from 400 unrelated and unaffected individuals was analyzed as controls.

Tumors

Frozen tumors obtained from a total of 245 apparently unrelated patients without known mutations in the mentioned susceptibility genes were collected through the Spanish National Tumor Bank Network in Madrid (Spain; ref. 21), the Erasmus MC Tissue Bank in Rotterdam (Netherlands), Munich (Germany), the International Familial Pheochromocytoma Consortium of San Antonio and Bethesda (22), Nijmegen Pheochromocytoma Tissue Bank, and the COMETE network in Paris, France (Table 1; refs. 16, 23). From these 245 samples, 106 belonged to patients included in the germline screening. The remaining 139 tumors represented independent cohort. For samples with identified *MAX* mutations, the corresponding mutation was assessed in constitutive DNA when available to classify them as germline or somatic.

Molecular genetic analyses

Complete genetic characterization of *MAX* included both point mutation and gross deletion/duplication analyses, the latter done in 1,535 cases with good DNA quality. Primers spanning the 5 exons and intron–exon boundaries of the *MAX* transcript 2 (ENST00000358664, NM_002382.3) were used as previously described (13). To assess for rearrangements, a semiquantitative multiplex-PCR method using labeled primers was designed as previously described for other genes (24). PCR conditions and primers are available upon request. To assess the pathogenicity of variants we used Alamut mutation interpretation software (http://www.interactive-biosoftware.com/software.html).

LOH was estimated by direct sequencing when tumor DNA was available. Uniparental disomy or chromosomal loss was assessed by microsatellite analysis as previously described (13).

Immunohistochemistry

Immunohistochemical staining was done using 3-μm formalin-fixed paraffin-embedded tumor sections from

Published OnlineFirst on March 27, 2012; DOI:10.1158/1078-0432.CCR-12-0160

tumors carrying *MAX* mutations, as previously described (13). Normal adrenal sections and tumors carrying mutations in other PCC susceptibility genes were used as controls. Only cases showing nuclear staining of stromal cells were considered as evaluable.

Biochemical test results and biologic features

Biochemical test results available in patients with *MAX* mutations included urinary fractionated metanephrines in 16 patients measured as part of the routine diagnostic work-up at participating centers, either by liquid chromatography with electrochemical detection (LC-EC) or tandem mass spectrometry. Concentrations of catecholamines (epinephrine, norepinephrine, and dopamine) in tumor tissue available from 7 patients with *MAX* mutations were quantified in frozen specimens by LC-EC as described elsewhere (25). Results were compared with historical data from 57 patients in one group with mutations of *VHL* ($n = 44$), *SDHB* ($n = 10$), and *SDHD* ($n = 3$) and 36 patients in the other group with *RET* ($n = 31$) and *NF1* ($n = 5$) mutations, in all of whom tumor tissue catecholamine results were available (26). Transcriptomic data, involving 2 different microarray platforms (Affymetrix for the French series and Agilent for Spanish series; refs. 27, 28), were further used to determine the expression of mRNA for phenylethanolamine *N*-methyltransferase (*PNMT*).

Statistical analysis

Statistical analyses were carried out using SPSS software package version 17.0 (SPSS, Inc.). The 4 patients carrying variants of unknown significance (VUS) and a subject in whom it was not possible to establish the germline status were not considered for statistical purposes. Thus, only patients with mutations leading to truncated proteins or affecting conserved amino acids were included in the final analysis. Differences between mutation carriers and non-mutation carriers for gender, adrenal multiple tumors, familial history, and malignancy were assessed using a χ^2 test or Fisher exact test, where appropriate. Because age, biochemical, and gene expression data could not be established to be normally distributed, nonparametric analysis by Mann–Whitney and Kruskal–Wallis tests were used to assess statistical significance of differences in these variables among the different groups examined.

Results

Germline and somatic *MAX* variants

Among the 1,694 patients with PCC and/or PGL and no evident germline mutations in *RET*, *VHL*, *SDHB*, *SDHC*, *SDHD*, and *TMEM127* genes (Table 1), we identified 16 different heterozygous variants affecting 23 subjects that spanned all 5 exons of the *MAX* gene (Fig. 1; Table 2). In addition, we analyzed *MAX* in 245 tumors (Table 1) and

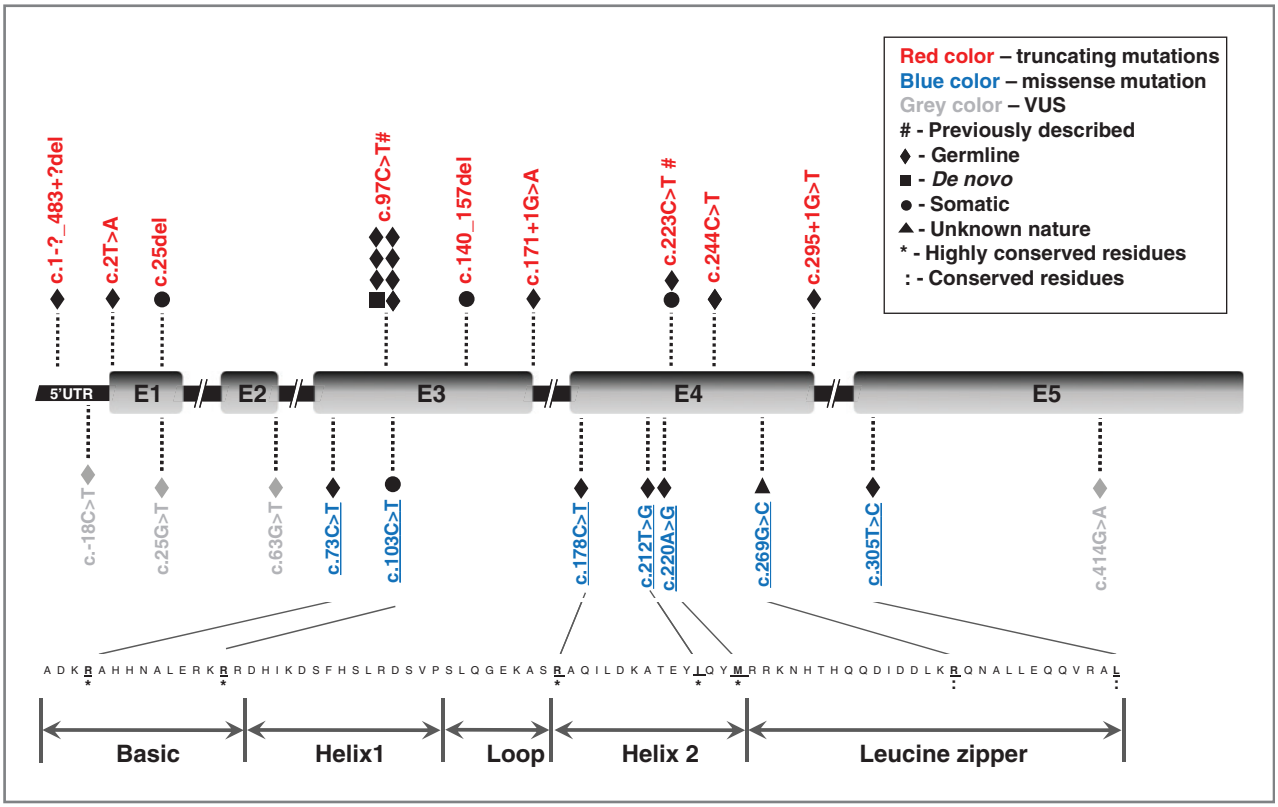

Figure 1. Schematic representation of *MAX* [transcript ENST00000358664] mutations identified in this study. The bottom panel shows the conservation of the amino acids altered by pathogenic missense changes (underlined). Double arrows delimit protein domains between the first and the last missense mutation.

Published OnlineFirst on March 27, 2012; DOI:10.1158/1078-0432.CCR-12-0160

found 4 cases (1.65%) carrying a mutation that was confirmed as somatic by the finding of no mutation in the germline DNA (Table 2). A fifth tumor with a *MAX* mutation (case 24, Table 2) was not considered in further analysis because it was not possible to establish its germline status. None of the variants were found in at least 400 controls, or in public databases (dbSNP132 and 1000 Genomes Project; www.1000genomes.org/).

Table 2. Genetic and clinical features of the 28 *MAX* positive patients[a] and tumors[6]

ID	Gender/ age	Fam	PCC	PGL	Mets	Other disease[d]	cDNA mutation[b]/ Protein alteration[b]	Predicted Pathogenicity[c]	LOH	IHC
1	M/27	No	PCC	No	No	No	c.1-?_483+?del/p.?	n.a.	Yes	Neg
2	F/46	No	bPCC	1 TA	No	No	c.2T>A/p.?	n.a.	Yes[UPD]	Neg
3	F/43	No	bPCC	4 TA	No	BrC, RO	c.73C>T/p.(Arg25Trp)	Y	—	—
4	M/23	Yes	bPCC	No	No	No	c.97C>T/p.(Arg33*)	n.a.	—	—
5	M/27	Yes[p]	bPCC & mPCC	No	No	No	c.97C>T/p.(Arg33*)	n.a.	Yes	—
6	M/34	No[dn]	bPCC	No	No	No	c.97C>T/p.(Arg33*)	n.a.	Yes	Neg
7	F/58	Yes	mPCC	No	No	No	c.97C>T/p.(Arg33*)	n.a.	Yes	Neg
8	F/26	Yes[p]	PCC	No	No	No	c.97C>T/p.(Arg33*)	n.a.	Yes	Neg
9	M/38	No	PCC	No	No	SCCT	c.97C>T/p.(Arg33*)	n.a.	—	—
10	M/24	Yes	bPCC	No	No	CCH	c.97C>T/p.(Arg33*)	n.a.	—	—
11	F/43	No	PCC	1TA	No	No	c.97C>T/p.(Arg33*)	n.a.	Yes	—
12	F/18	No	bPCC	No	No	No	c.171+1G>A/p.?	n.a.	Yes	—
13	F/55	No	bPCC	No	No	No	c.178C>T/p.(Arg60Trp)	Y	—	—
14	F/34	No	bPCC	No	No	No	c.212T>G/p.(Ile71Ser)	Y	Yes[UPD]	Pos
15	M/57	No	mPCC	No	No	PA	c.220A>G/p.(Met74Val)	Y	Yes	Pos
16	M/18	No	bPCC	No	No	1ºHPT	c.223C>T/p.(Arg75*)	n.a.	—	—
17	F/18	Yes	PCC	No	Yes	No	c.244C>T/p.(Gln82*)	n.a.	—	—
18	F/40	No	bPCC	1 TA	Yes	No	c.295+1G>T/p.?	n.a.	Yes	Neg
19	M/13	Yes[p]	PCC	No	No	No	c.305T>C/p.(Leu102Pro)	Y	—	—
20[e]	F/48	No	—	1 H&N	No	No	c.-18C>T/p.(=)	N	—	—
21[e]	M/13	No	PCC	1 TA	No	No	c.25G>T/p.(Val9Leu)	N	No	Pos
22[e]	M/22	No	PCC	No	No	No	c.63G>T/p.(=)	N	No	—
23[e]	F/80	No	PCC	No	No	No	c.414G>A/p.(=)	N	—	—
24[6g]	F/29	No	PCC	No	No	No	c.269G>C/p.(Arg90Pro)	Y	Yes	—
25[6f]	M/39	No	PCC	No	No	No	c.223C>T/p.(Arg75*)	n.a.	Yes	Neg
26[6f]	F/57	No	PCC	No	No	RC	c.103C>T/p.(Arg35Cys)	Y	Yes	Pos
27[6f]	M/24	No	PCC	No	No	No	c.140_157del/p.(Arg47_Ser52del)	n.a.	Yes	Neg
28[6f]	F/56	No	PCC	No	No	No	c.25del/p.(Val9Trpfs*56)	n.a.	Yes[UPD]	Neg

Abbreviations. Gender: F, female; M, male. Fam: familial antecedents; PCC, adrenal pheochromocytoma; bPCC, bilateral adrenal pheochromocytoma; mPCC, multiple pheochromocytomas within the same gland; PGL, paraganglioma; H&N, Head and Neck; TA, thoracoabdominal; Mets, presence of metastases in which chromaffin cells are normally absent; Other disease: BrC, breast Cancer; RO, renal oncocytoma; SCCT, squamous cell carcinoma of the tongue; CCH, C-cell hyperplasia; PA, pituitary adenoma; 1ºHPT, primary hyperparathyroidism; RC, renal carcinoma; n.a., not applicable;—, not available; UPD, uniparental disomy; IHC, immunohistochemistry: Pos, positive; Neg, negative.

[a]Only data from probands are shown in the table.

[b]All cDNA and protein nomenclature is based on reference sequence ENST00000358664. All MAX variants were named following Human Genome Variation Society and checked using Mutalyzer Name Checker (www.mutalyzer.nl).

[c]Pathogenicity potential of missense variants was examined by Alamut mutation interpretation software (version 2.5), which provides variant interpretation according to several prediction methods (AlignGVGD, Polyphen, SIFT, ESEfinder, GeneSplicer, RESCUE-ESE).

[d]Other tumors in the proband.

[p]Paternal familial antecedents.

[dn]*de novo* case.

[e]VUS, not considered for examination of phenotypic associations.

[f]Somatic mutation.

[g]This tumor was not considered in further analysis because it was not possible to establish its germline status.

Published OnlineFirst on March 27, 2012; DOI:10.1158/1078-0432.CCR-12-0160

Overall, taking into account the germline and the somatic findings, we identified 18 novel variants affecting *MAX* and 2 previously reported mutations, c.97C>T and c.223C>T (13). Seven mutations disrupted the MAX protein because they affected the initial methionine (c.2T>A), created a premature stop codon (c.25del, c.97C>T, c.223C>T, and c.244C>T) or affected a donor/acceptor splice site (c.171 + 1G>A and c.295 + 1G>T; Fig. 1). In addition, 2 deletions were identified: the first caused an in-frame loss of 6 highly conserved amino acids within the first helix of the protein (c.140_157del), and the second, detected by multiplex-PCR (Supplementary Fig. S1), spanned the whole gene (c.1-?_483+?del). Immunohistochemical detection of MAX in tumor-embedded paraffin slides showed complete loss of the protein in all analyzed tumors that carried truncating mutations (Supplementary Fig. S2).

Among the 11 nontruncating variants, 7 mutations (c.73C>T, c.103C>T, c.178C>T, c.212T>G, c.220A>G, c.269G>C, and c.305T>C) changed conserved or highly conserved amino acids located within the basic helix-loop-helix leucine zipper (bHLH-Zip) domain of the MAX protein (Fig. 1) and were classified as deleterious by the Alamut software. The remaining 4 nontruncating variants (c.25G>T, c.63G>T, c.414G>A, and c.-18C>T) were classified as VUS because these were predicted as benign through bioinformatic tools; it was also not possible to show their pathogenicity with further analyses (Table 2). Positive immunohistochemistry staining was observed in all nontruncating variants assessed (Supplementary Fig. S2).

LOH of the *MAX* wild-type allele was found in 16 of 18 tumors analyzed (Table 2). *MAX* wild-type allele was present in 2 tumor associated with the variants c.25G > T/p.(Val9Leu), and c.63G>T/p.(=), both considered as VUS.

In summary, we found pathogenic germline *MAX* variants in the 1.12% of the 1,694 index cases included in this analysis. All mutations, except one gross deletion, consisted of a single nucleotide substitution.

Clinical presentation of *MAX* carriers

Only those 19 patients who harbored a germline variant defined as pathogenic were considered for examination of phenotypic associations (Table 2). The presence of familial antecedents of disease was found in 7 of the 19 patients (37%) and appeared in the paternal branch in the 3 pedigrees with more than one generation of affected members (Supplementary Fig. S3). These 19 patients developed at least one PCC, with 13 (68.4%) showing either bilateral PCC or multiple PCCs within the same gland, a 48-fold higher rate ($P < 0.001$) than in *MAX*-negative cases (4.28%). Age at diagnosis was lower ($P < 0.001$) in mutation carriers than in cases without mutations (median 34, range 13–58 years vs. 48 range 3–88 years). Three of the 19 patients (15.8%) developed additional tumors at thoracoabdominal sites at a median age of 48 years (range 44–64 years). Importantly, these tumors presented as PGLs, distinct from recurrences of the earlier adrenal tumors. Two patients (10.5%) developed metastatic disease.

Among 4 sporadic cases with *MAX* somatic mutations, the median age at diagnosis was 47.5 years (range 24–57 years), which was not significantly different from those with *MAX*-negative sporadic tumors (median 52, range 11–83 years; Table 1).

Biochemical test results and biologic features

All patients with *MAX* mutations showed increased urinary outputs of normetanephrine that did not differ from patients in the group with *VHL* and *SDHB/D* mutations or the other with *RET* and *NF1* mutations (Fig. 2A). In contrast, urinary outputs of metanephrine were either normal or moderately increased in patients with *MAX* mutations and showed an intermediate distribution, significantly ($P < 0.001$) higher than in the VHL/SDH group, but lower than in the RET/NF1 group (Fig. 2B). Similarly, tumor tissue concentrations of epinephrine also showed an intermediate distribution, representing 8.4% of total catecholamine contents in *MAX* tumors, a proportion 5.6-fold higher ($P < 0.001$) than in VHL/SDH tumors, but a sixth ($P = 0.003$) that in *RET/NF1* tumors (Fig. 2C). Furthermore, levels of PNMT expression in *MAX* tumors were 14-fold higher ($P < 0.001$) than in *VHL/SDH* tumors and a little under a half ($P = 0.05$) than in *RET/NF1/TMEM127* tumors (Fig. 2D).

Discussion

It is widely accepted that MYC deregulation is not restricted to translocations and amplifications at the MYC locus, which suggests that the impact of its deregulation on human cancer incidence is higher than previously thought (18). We recently found *MAX* germline mutations in patients with PCC (13), suggesting that alterations in this most important regulator of the MYC/MAX/MXD1 network promote hereditary susceptibility to neoplasias. This study followed up on these observations, taking advantage of a large international collaborative network to determine the prevalence and the genotype–phenotype correlations of *MAX* mutations in 1,694 PCC/PGL patients previously negative for 6 major PCC/PGL susceptibility genes. We establish here that *MAX* germline mutations are responsible for the disease in 1.12% of cases, a similar contribution to that of the recently reported *TMEM127* mutation (29). Furthermore, our findings reveal the presence of *MAX* somatic mutations in sporadic tumors, extend the spectrum of *MAX*-related tumors to PGLs, ascertain that *MAX* tumors are not particularly prone to malignancy, and show that *MAX* tumors produce predominantly norepinephrine, but with some capacity to also produce epinephrine.

Though it has been reported that somatic mutations in the known PCC susceptibility genes constitute an extremely rare event, we recently found 14% of sporadic PCC/PGL carrying somatic mutations in *VHL* or *RET* (16). The presence of somatic *MAX* mutations in 1.65% of sporadic tumors described here is in agreement with this latter

Published OnlineFirst on March 27, 2012; DOI:10.1158/1078-0432.CCR-12-0160

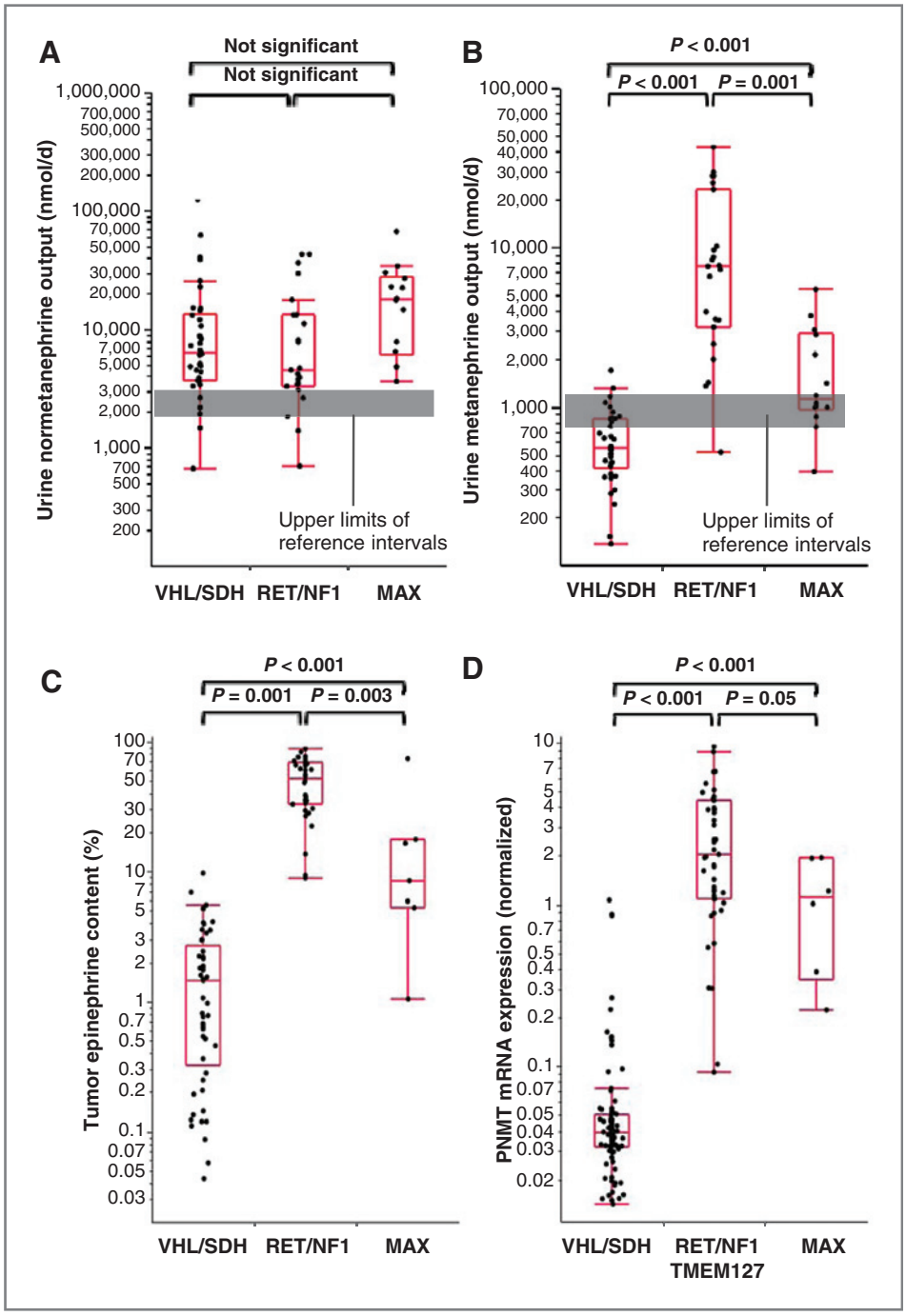

Figure 2. Dot-box plots illustrating urinary outputs of normetanephrine (A) and metanephrine (B), tumor tissue contents of epinephrine (C), and expression of PNMT mRNA (D) for patients with *MAX* mutations compared with those with *VHL* and *SDHB/D* mutations or *RET*, *NF1*, and *TMEM127* mutations.

finding and highlights the importance of the MYC/MAX/MXD1 network in the development of neural crest tumors. It is well known that somatic amplification and overexpression of MYCN is a genetic hallmark in neuroblastoma (30), so ablation of *MAX* transcriptional repression of MYC in PCC could lead to the same oncogenic MYC dysregulation that occurs in neuroblastoma. Nevertheless, no meaningful trend for a contribution of *MAX* mutations to other neoplasms, including neuroblastoma, was found in the current series.

The identified variants were distributed along the gene but were especially frequent in exons 3 and 4, matching some of the most important residues within the conserved bHLH-Zip domain of MAX. The majority of mutations lead to truncated proteins, and the expected LOH affecting the remaining wild-type allele of the *MAX* tumor suppressor gene was further supported by the absence of the protein by immunohistochemistry.

The most frequently found mutation was the previously described c.97C > T variant (13) discovered in 8 unrelated

Published OnlineFirst on March 27, 2012; DOI:10.1158/1078-0432.CCR-12-0160

patients from 5 nations (Italy, Spain, United States, France, and The Netherlands). This recurrent mutation affects a CpG dinucleotide located contiguous to Glu32, the crucial residue for DNA binding, and represents the first hotspot mutation affecting *MAX*. In agreement with this, one of the c.97C > T mutation carriers was a *de novo* case, further suggesting the high mutability of this dinucleotide. The 6 missense variants that altered conserved MAX residues were predicted as deleterious by the Alamut software (Table 2) and have been reported as critical for dimerization and DNA binding of HLH proteins or for interactions within the protein structure (31, 32). Mutations affecting highly conserved amino acids within the bHLH-Zip domain of MAX, involved in protein–protein interactions and DNA binding, can be expected to destroy the ability of MAX to antagonize MYC-dependent cell transformation leading to tumor development.

The absence of familial antecedents in more than 65% of individuals, as well as the paternal transmission identified in 3 pedigrees, further supports previous suggestions of a paternal mode of transmission (13). This mode of inheritance, with its consequence of generation skipping, complicates identification of candidate mutation carriers. In general, the phenotypic characteristics of *MAX* mutant patients overlap with clinical features observed for other PCC/PGL-related hereditary disorders. For example, the presence of a significant proportion of bilateral/multiple PCC cases among *MAX* germline mutation carriers, representing 21% (13 of 63) of patients included in this cohort (Table 1), is in agreement with the high percentage (35%–60%) of bilateral tumors found in patients with mutations in *VHL*, *RET*, or *TMEM127* (7, 29, 33, 34). The age at diagnosis of PCCs in *MAX* mutation carriers (34 years) was clearly lower than in negative cases (48 years), also lower than the reported on average in patients with *TMEM127*, *RET*, and *NF1* mutations (38–42 years), but higher to that for *VHL* and *SDH* mutation carriers (27–32 years; refs. 19, 20, 29, 33–35).

Extraadrenal thoracoabdominal PGL are relatively common compared with adrenal tumors in patients with *SDHB* and *SDHD* mutations, less common in *TMEM127* and *VHL* mutation carriers, and rarely associated with *RET* and *NF1* germline mutations (12, 33, 36). Interestingly, in all *MAX* patients with PGL, the extraadrenal tumor was diagnosed after the adrenal tumor. This contrasts with VHL patients with head and neck PGLs, 50% of whom showed no adrenal tumors (34). In this study, only 2 patients developed metastasis, suggesting that unlike *SDHB* mutations, mutations of *MAX* are not associated with a high risk of malignancy.

The catecholamine-related information available from patients with *MAX* mutations indicated a biochemical phenotype intermediate between the established phenotypes of epinephrine producing tumors due to *NF1* and *RET* mutations and the predominantly norepinephrine producing tumors due to *VHL* or *SDHB/D* mutations (26). This intermediate diagnostic phenotype, manifested by at least 3-fold larger tumor-associated increases in urinary outputs of normetanephrine than of metanephrine, was explained by a significant but limited capacity to produce epinephrine. This latter finding is supported by the intermediate tissue concentrations of epinephrine and expression of mRNA for PNMT, the enzyme responsible for conversion of norepinephrine to epinephrine. The intermediate biochemical phenotype associated with *MAX* mutations, together with lack of MAX immunohistochemical staining of tumor tissue, may prove useful for guiding testing of the *MAX* gene in patients with PCC/PGLs.

In summary, this study involving an unprecedented international effort to genotype and phenotype a substantial number of patients with PCC/PGLs reveals the importance of the MYC/MAX/MXD1 network in the development of both hereditary and sporadic forms of these tumors. *MAX* is the tenth PCC/PGL susceptibility gene described to date, which now should be considered in the genetic work-up of affected patients.

Disclosure of Potential Conflicts of Interest

The authors have no potential conflicts of interest to declare.

Authors' Contributions

Conception and design: N. Burnichon, A. Cascon, M. Castellano, T. Prodanov, M. Mannelli, G. Opocher, A.-P. Gimenez-Roqueplo, M. Robledo

Development of methodology: N. Burnichon, A. Cascon, I. Comino-Méndez, M. Abermil, L. Inglada-Pérez, A.A. de Cubas, P.-F. Plouin, M. Qin, A.-P. Gimenez-Roqueplo

Acquisition of data (provided animals, acquired and managed patients, provided facilities, etc.): N. Burnichon, F. Schiavi, I. Comino-Méndez, M. Abermil, L. Inglada-Pérez, A.A. de Cubas, L. Amar, M.B. Barontini, S.B. de Quirós, J. Bertherat, Y.-V. Bignon, M.J. Blok, S. Borrego, M. Castellano, P. Chanson, M.-D. Chiara, E.P.M. Corssmit, M. Giacché, R.R. de Krijger, X. Girerd, E.B. Gómez-García, I. Guilhem, F. Hes, E. Honrado, J.W.M. Lenders, A.R. Mensenkamp, A. Merlo, A. Murat, P. Pierre, P.-F. Plouin, T. Prodanov, M. Quesada-Charneco, V. Raymond, N. Reisch, M. Ruiz-Ferrer, F. Schillo, A.P.A. Stegmann, C. Suarez, E. Taschin, H.J.L.M. Timmers, C. Tops, M. Urioste, F. Beuschlein, K. Pacak, M. Mannelli, P.L. Dahia, G. Opocher, G. Eisenhofer, A.-P. Gimenez-Roqueplo, M. Robledo

Analysis and interpretation of data (e.g., statistical analysis, biostatistics, computational analysis): N. Burnichon, N.P. Morales, I. Comino-Méndez, M. Abermil, L. Inglada-Pérez, A.A. de Cubas, M. Castellano, M.-D. Chiara, F. Hes, A.R. Mensenkamp, L. Mori, T. Prodanov, M. Qin, A.P.A. Stegmann, H.J.L.M. Timmers, P.L. Dahia, G. Eisenhofer, A.-P. Gimenez-Roqueplo, M. Robledo

Writing, review, and/or revision of the manuscript: N. Burnichon, A. Cascon, L. Inglada-Pérez, L. Amar, J. Bertherat, Y.-V. Bignon, M. Castellano, P. Chanson, R.R. de Krijger, E.B. Gómez-García, F. Hes, E. Korpershoek, J.W. M. Lenders, A.R. Mensenkamp, P.-F. Plouin, N. Reisch, M. Ruiz-Ferrer, H.J.L. M. Timmers, F. Beuschlein, K. Pacak, M. Mannelli, P.L. Dahia, G. Opocher, G. Eisenhofer, A.-P. Gimenez-Roqueplo, M. Robledo

Administrative, technical, or material support (i.e., reporting or organizing data, constructing databases): N. Burnichon, F. Schiavi, N.P. Morales, M. Abermil, S. Bobisse, M. Castellano, T. Ercolino, F. Hes, E. Korpershoek, R. Letón, P.-F. Plouin, T. Prodanov, E. Rapizzi, N. Reisch, G. Roncador, K. Pacak, P.L. Dahia, G. Eisenhofer, A.-P. Gimenez-Roqueplo, M. Robledo

Study supervision: P.L. Dahia, A.-P. Gimenez-Roqueplo, M. Robledo

Mutation analysis: L. Mori

Experimental High Resolution Array running & subsequent analysis: A.P.A. Stegmann

Acknowledgments

The authors thank Franco Veglio, MD and Paolo Mulatero, MD, University of Turin, Luigi Bartalena, MD, University of Insubria Varese, Ermanno Rossi, MD, Reggio Emilia Hospital, Pietro Nicolai, MD, and Fabio Facchetti, MD, University of Brescia, who contributed to the recruitment of patients; Alessandra Panarotto for excellent technical assistance; Enrico Agabiti Rosei for continued support and encouragement (Brescia); Roland Därr who contributed to patient enrollment and evaluation (Dresden); Annabelle Vénisse, Christophe Simian, Céline Loriot and Judith Favier (AP-HP, Hôpital européen Georges Pompidou,

Published OnlineFirst on March 27, 2012; DOI:10.1158/1078-0432.CCR-12-0160

Genetics department and INSERM U970, Paris France) for technical assistance and the members of the COMETE (Cortico and Medullar Endocrine Tumors) and PGL.NET networks, of the GTE (Groupe des Tumeurs Endocrines) and of the INCA-COMETE and INCA-RENATEN reference centers, particularly Frédéric Illouz, Vincent Rohmer, Delphine Prunier-Mirebeau (CHU d'Angers Endocrinology and biochemical departments), Anne Barlier, Morgane Pertuit (CHU de Marseille, Molecular Biological department), Catherine Genestie, Julie Rigabert, Charlotte Lepoutre (APHP-Hôpital de la PItié Salpétrière, Endocrinology and nuclear medicine departments); Serge Guyetant (CHU de Tours, Pathological department,); Nathalie Rioux-Leclercq, Elisabeth Tarasco, Catherine Dugast (CHU de Rennes, Endocrinology and Genetics departments); Jihad Samrani, Philippe Thieblot, Igor Tauveron (CHU de Clermont Ferrand, Endocrinology department); Sylvette Helbert-Davidson (APHP Hôpital Henri Mondor, Nuclear Medicine department); Séverine Valmary-Degano, Bernadette Kantelip (Tumorothèque régionale de Franche-Comté), Bruno Heyd, Gabriel Viennet, Franck Monnien, Alfred Penfornis (CHU de Besançon, Surgical, pathological and endocrinology departments); Xavier Bertagna, Rossella Libé, Frédérique Tissier (APHP, Hôpital Cochin, Endocrinology and pathological departments); Annick Rossi, Thierry Frébourg (CHU de Rouen, Genetic department); Michel Krempf, Anne Moreau, Maelle Lebras (CHU de Nantes, Endocrinology department); Cécile Badoual, Claudia de Toma, Plateforme de ressources biologiques de l'HEGP (APHP, Hôpital européen Georges Pompidou, Pathological department), Sophie Ferlicot, Annonciade Biaggi (CHU de Bicêtre, Pathological department) for their helpful assistance in this study (France); Karen Adams who contributed to the patient enrollment and evaluation (NIH, Bethesda); Neeltje Arts and Erik Jansen for excellent technical assistance (Nijmegen); the following colleagues who contributed to the recruitment of patients and/or clinical information: Adele Nardecchia, MD, Domenico Meringolo, MD, Giuseppe Picca, MD, Paola Loli, MD, Erika Grossrubatscher, MD, Maurizio Iacobone, MD, Antonio Toniato, MD, Ambrogio Fassina, MD, Isabella Negro, MD, GianPaolo Rossi, MD, Massimo Terzolo, MD, Serena Demattè, MD, Maria Vittoria Davì, MD, Giorgio Bertola, MD, Luca Persani, MD, Uberta Verga, MD, Iacopo Chiodini, MD, Gilberta Giacchetti, MD, Giorgio Arnaldi, MD (Padova); the members of the Familial Pheochromocytoma Consortium for their support and earlier contributions; the following colleagues who contributed to the recruitment of patients and/or clinical information: Elizabeth King, MD, Jan Bruder, MD, Neil Aronin, MD, Kathy Schneider, MPH, and Stephen Gruber, MD (San Antonio). Finally, the authors thank Sara Cristina Hernández for excellent technical assistance, Cristina Álvarez-Escolá, MD, Carmen Bernal, MD, Amparo Meoro, MD, José Ángel Díaz, MD, María Teresa Calvo, MD, José María de Campos, MD, María García-Barcina, MD, Sharona Azriel, MD, Marcos Lahera, MD, who contributed to the recruitment of patients and clinical information, María Jesús Artiga, PhD, and Manuel Morente, MD, for contributing to the recruitment of tumor samples, as well as Biobanco del Sistema Sanitario Público de Andalucía and the Tumor Bank Network coordinated by CNIO (Spain).

Grant Support

The ENS@T consortium received funding from the European Union Seventh Framework Programme (ENS@T-CANCER; HEALTH-F2-2010-259735). The ENS@T registry is supported by a grant of the European Science Foundation (ESF-ENS@T).

This work was supported in part by the Fondo de Investigaciones Sanitarias (projects PI11/01359, PS09/00942, PI10/01290, PI08/0531 and P108/0883), Mutua Madrileña (AP2775/2008), Consejería de Innovación Ciencia y Empresa de la Junta de Andalucía (CTS-2590), Red Temática de Investigación Cooperativa en Cáncer (RD06/0020/0034).

The French COMETE network is supported in part by the Programme Hospitalier de Recherche Clinique grant COMETE 3 (AOM 06 179), by grants from INSERM and Ministère Délégué à la Recherche et des Nouvelles Technologies and by the Institut National du Cancer.

This work was also funded by grants from the Agence Nationale de la Recherche (ANR 08 GENOPATH 029 MitOxy) and by the national program "Cartes d'Identité des Tumeurs" funded and developed by the "Ligue Nationale contre le Cancer" (http://cit.ligue-cancer.net).

This research was supported, in part, by the Intramural Research Program of the NIH, NICHD.

This work received funding support from the Voelcker Fund to P.L.M. Dahia.

This work was also supported in part by grants from the Fondazione Comunità Bresciana and the Fondazione Guido Berlucchi.

The costs of publication of this article were defrayed in part by the payment of page charges. This article must therefore be hereby marked *advertisement* in accordance with 18 U.S.C. Section 1734 solely to indicate this fact.

Received January 18, 2012; revised March 2, 2012; accepted March 8, 2012; published OnlineFirst March 27, 2012.

References

1. Latif F, Tory K, Gnarra J, Yao M, Duh FM, Orcutt ML, et al. Identification of the von Hippel-Lindau disease tumor suppressor gene. Science 1993;260:1317–20.
2. Mulligan LM, Kwok JB, Healey CS, Elsdon MJ, Eng C, Gardner E, et al. Germ-line mutations of the RET proto-oncogene in multiple endocrine neoplasia type 2A. Nature 1993;363:458–60.
3. Wallace MR, Andersen LB, Saulino AM, Gregory PE, Glover TW, Collins FS. A *de novo* Alu insertion results in neurofibromatosis type 1. Nature 1991;353:864–6.
4. Baysal BE, Ferrell RE, Willett-Brozick JE, Lawrence EC, Myssiorek D, Bosch A, et al. Mutations in SDHD, a mitochondrial complex II gene, in hereditary paraganglioma. Science 2000;287:848–51.
5. Astuti D, Latif F, Dallol A, Dahia PL, Douglas F, George E, et al. Gene mutations in the succinate dehydrogenase subunit SDHB cause susceptibility to familial pheochromocytoma and to familial paraganglioma. Am J Hum Genet 2001;69:49–54.
6. Niemann S, Muller U. Mutations in SDHC cause autosomal dominant paraganglioma, type 3. Nat Genet 2000;26:268–70.
7. Neumann HP, Bausch B, McWhinney SR, Bender BU, Gimm O, Franke G, et al. Germ-line mutations in nonsyndromic pheochromocytoma. N Engl J Med 2002;346:1459–66.
8. Hao HX, Khalimonchuk O, Schraders M, Dephoure N, Bayley JP, Kunst H, et al. SDH5, a gene required for flavination of succinate dehydrogenase, is mutated in paraganglioma. Science 2009;325:1139–42.
9. Burnichon N, Briere JJ, Libe R, Vescovo L, Riviere J, Tissier F, et al. SDHA is a tumor suppressor gene causing paraganglioma. Hum Mol Genet 2010;19:3011–20.
10. Qin Y, Yao L, King EE, Buddavarapu K, Lenci RE, Chocron ES, et al. Germline mutations in TMEM127 confer susceptibility to pheochromocytoma. Nat Genet 2010;42:229–33.
11. Mannelli M, Castellano M, Schiavi F, Filetti S, Giacche M, Mori L, et al. Clinically guided genetic screening in a large cohort of Italian patients with pheochromocytomas and/or functional or nonfunctional paragangliomas. J Clin Endocrinol Metab 2009;94:1541–7.
12. Cascon A, Pita G, Burnichon N, Landa I, Lopez-Jimenez E, Montero-Conde C, et al. Genetics of pheochromocytoma and paraganglioma in Spanish patients. J Clin Endocrinol Metab 2009;94:1701–5.
13. Comino-Mendez I, Gracia-Aznarez FJ, Schiavi F, Landa I, Leandro-Garcia LJ, Leton R, et al. Exome sequencing identifies MAX mutations as a cause of hereditary pheochromocytoma. Nat Genet 2011;43:663–7.
14. Lee S, Nakamura E, Yang H, Wei W, Linggi MS, Sajan MP, et al. Neuronal apoptosis linked to EglN3 prolyl hydroxylase and familial pheochromocytoma genes: developmental culling and cancer. Cancer Cell 2005;8:155–67.
15. Maher ER, Eng C. The pressure rises: update on the genetics of phaeochromocytoma. Hum Mol Genet 2002;11:2347–54.
16. Burnichon N, Vescovo L, Amar L, Libe R, de Reynies A, Venisse A, et al. Integrative genomic analysis reveals somatic mutations in pheochromocytoma and paraganglioma. Hum Mol Genet 2011;20:3974–85.
17. Hanahan D, Weinberg RA. Hallmarks of cancer: the next generation. Cell 2011;144:646–74.
18. Meyer N, Penn LZ. Reflecting on 25 years with MYC. Nat Rev Cancer 2008;8:976–90.
19. Amar L, Bertherat J, Baudin E, Ajzenberg C, Bressac-de Paillerets B, Chabre O, et al. Genetic testing in pheochromocytoma or functional paraganglioma. J Clin Oncol 2005;23:8812–8.
20. Burnichon N, Rohmer V, Amar L, Herman P, Leboulleux S, Darrouzet V, et al. The succinate dehydrogenase genetic testing in a large prospective series of patients with paragangliomas. J Clin Endocrinol Metab 2009;94:2817–27.

Published OnlineFirst on March 27, 2012; DOI:10.1158/1078-0432.CCR-12-0160

21. Rodriguez-Antona C, Pallares J, Montero-Conde C, Inglada-Perez L, Castelblanco E, Landa I, et al. Overexpression and activation of EGFR and VEGFR2 in medullary thyroid carcinomas is related to metastasis. Endocr Relat Cancer 2010;17:7–16.
22. Dahia PL, Ross KN, Wright ME, Hayashida CY, Santagata S, Barontini M, et al. A HIF1alpha regulatory loop links hypoxia and mitochondrial signals in pheochromocytomas. PLoS Genet 2005;1:72–80.
23. Favier J, Gimenez-Roqueplo AP. Pheochromocytomas: the (pseudo)-hypoxia hypothesis. Best Pract Res Clin Endocrinol Metab 2010; 24:957–68.
24. Cascon A, Montero-Conde C, Ruiz-Llorente S, Mercadillo F, Leton R, Rodriguez-Antona C, et al. Gross SDHB deletions in patients with paraganglioma detected by multiplex PCR: a possible hot spot? Genes Chromosomes Cancer 2006;45:213–9.
25. Eisenhofer G, Lenders JW, Timmers H, Mannelli M, Grebe SK, Hofbauer LC, et al. Measurements of plasma methoxytyramine, normetanephrine, and metanephrine as discriminators of different hereditary forms of pheochromocytoma. Clin Chem 2011;57:411–20.
26. Eisenhofer G, Pacak K, Huynh TT, Qin N, Bratslavsky G, Linehan WM, et al. Catecholamine metabolomic and secretory phenotypes in phaeochromocytoma. Endocr Relat Cancer 2011;18:97–111.
27. Favier J, Briere JJ, Burnichon N, Riviere J, Vescovo L, Benit P, et al. The Warburg effect is genetically determined in inherited pheochromocytomas. PLoS One 2009;4:e7094.
28. Lopez-Jimenez E, Gomez-Lopez G, Leandro-Garcia LJ, Munoz I, Schiavi F, Montero-Conde C, et al. Research resource: Transcriptional profiling reveals different pseudohypoxic signatures in SDHB and VHL-related pheochromocytomas. Mol Endocrinol 2010;24:2382–91.
29. Yao L, Schiavi F, Cascon A, Qin Y, Inglada-Perez L, King EE, et al. Spectrum and prevalence of FP/TMEM127 gene mutations in pheochromocytomas and paragangliomas. JAMA 2010;304:2611–9.
30. Kohl NE, Kanda N, Schreck RR, Bruns G, Latt SA, Gilbert F, et al. Transposition and amplification of oncogene-related sequences in human neuroblastomas. Cell 1983;35:359–67.
31. Ferre-D'Amare AR, Prendergast GC, Ziff EB, Burley SK. Recognition by Max of its cognate DNA through a dimeric b/HLH/Z domain. Nature 1993;363:38–45.
32. Voronova A, Baltimore D. Mutations that disrupt DNA binding and dimer formation in the E47 helix-loop-helix protein map to distinct domains. Proc Natl Acad Sci U S A 1990;87:4722–6.
33. Mannelli M, Castellano M, Schiavi F, Filetti S, Giacche M, Mori L, et al. Clinically guided genetic screening in a large cohort of Italian patients with pheochromocytomas and/or functional or non-functional paragangliomas. J Clin Endocrinol Metab 2009;94:1541–7.
34. Cascon A, Pita G, Burnichon N, Landa I, Lopez-Jimenez E, Montero-Conde C, et al. Genetics of pheochromocytoma and paraganglioma in Spanish patients. J Clin Endocrinol Metab 2009;94: 1701–5.
35. Eisenhofer G, Timmers HJ, Lenders JW, Bornstein SR, Tiebel O, Mannelli M, et al. Age at diagnosis of pheochromocytoma differs according to catecholamine phenotype and tumor location. J Clin Endocrinol Metab 2011;96:375–84.
36. Boedeker CC, Erlic Z, Richard S, Kontny U, Gimenez-Roqueplo AP, Cascon A, et al. Head and neck paragangliomas in von Hippel-Lindau disease and multiple endocrine neoplasia type 2. J Clin Endocrinol Metab 2009;94:1938–44.

Supplementary material:

Supplementary figure S1. Gross *MAX* deletion analysis

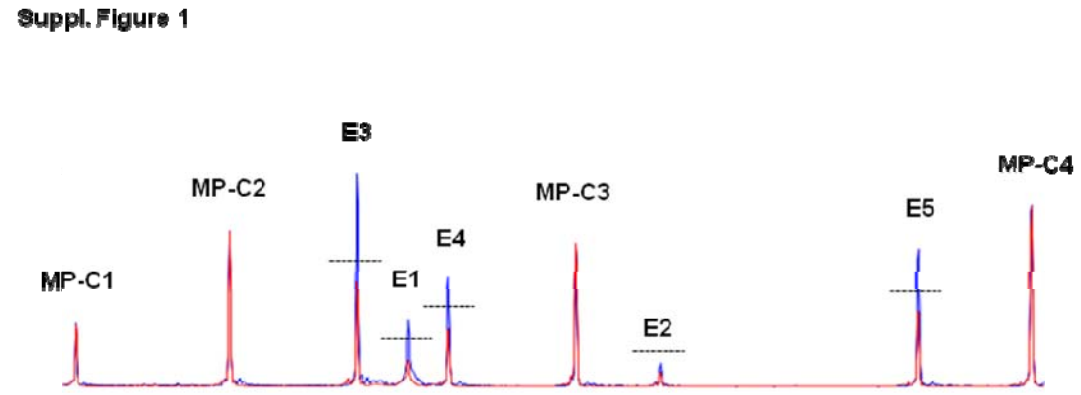

Peak Scanner analysis of amplified PCR fragments using MAX multiplex assay (including all exons) of a control sample (blue) overlapped with the proband's sample (red). Fragments MP-C1, MP-C2, MP-C3, and MP-C4 were used as internal controls of the assay. 50% of amplification (indicating the presence of only one allele) is denoted by a horizontal dotted line.

Supplementary figure S2. Immunohistochemical assesment.

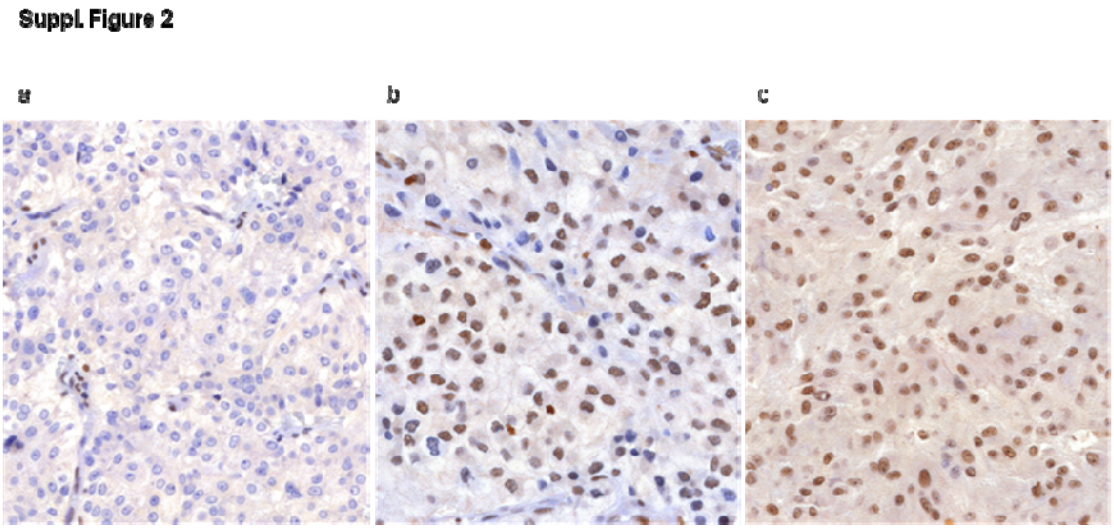

Detection of MAX by immunohistochemistry with a MAX C-terminus–specific antibody. (a) Negative staining of tumor cells in a PCC of a patient carrying a MAX truncating mutation, compared to positive stromal cells (indicated with arrows). (b) Positive staining of PCC tumor cells in a case with a MAX missense mutation. (c) Positive staining of a RET-mutated PCC.

Supplementary figure S3. Pedigree of 3 families with affected relatives in more than one generation.

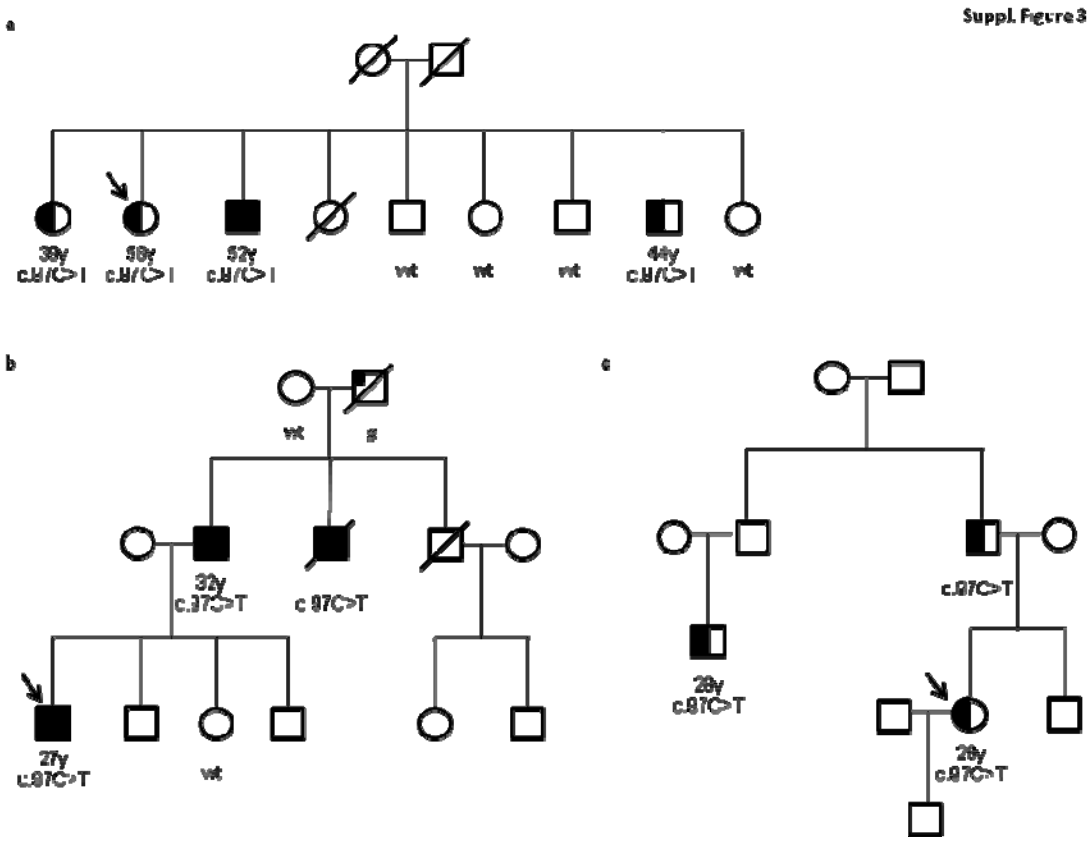

Probands are denoted by arrows. Unilateral PCC are represented by black semi-circles or semi-squares and bilateral PCC are represented by black squares. #denotes an obligate carrier, affected with a lymphoma, and lung cancer, represented by a black upper left segment.

ARTICLE 3: Functional and *in-silico* assessment of *MAX* variants of unknown significance.

Authors: Iñaki Comino-Méndez, Luis J Leandro-García, Guillermo Montoya, Lucía Inglada-Pérez, Aguirre A de Cubas, María Currás-Freixes, Carolyn Tysoe, Louise Izatt, Rocío Letón, Álvaro Gómez-Graña, Veronika Mancikova, María Apellániz-Ruiz, Massimo Mannelli, Francesca Schiavi, Judith Favier, Anne-Paule Gimenez-Roqueplo, Henri J L M Timmers, Giovanna Roncador, Juan F Garcia, Cristina Rodríguez-Antona, Mercedes Robledo, and Alberto Cascón.

Sent to peer-review

ABSTRACT

Besides clearly pathogenic mutations, the two previous studies included in this thesis, identified an appreciable number of variants of unknown significance (VUS) affecting *MAX*. In order to establish the potential role of *MAX* VUS in the disease and help in the clinical management of carriers of these variants, we constructed a PC12-based functional model. In addition, we proposed a consensus computational prediction method based on five "state of the art" algorithms, combined with relevant clinical data. For all but two of the twelve VUS considered, the functional assay and the consensus computational prediction gave consistent results; seven variants were classified as pathogenic and three as non-pathogenic. The introduction of wild-type *MAX* cDNA into PC12 cells significantly decreased MYC's ability to bind to canonical E-boxes, while pathogenic MAX proteins were not able to fully repress MYC activity. This latter result further suggested that, at least in PCC/PGL, MAX exerted a predominant role as a negative regulator of the MYC/MAX/MXD1. Further clinical and molecular evaluation of variant carriers corroborated the results obtained with our functional assessment.

In summary, in the absence of clear heritability, a combination of clinical and molecular data, with consensus computational prediction and a reliable functional model, are able to correctly classify VUS in *MAX*.

Personal contribution: I participated in the conception and design of the study as well as in the acquisition of the data. I carried out the cloning and site-directed mutagenesis assays, the luciferase experiments, the consensus *in silico* prediction and other experiments. Finally, I contributed to the discussion of the results and the drafting of the paper.

TITLE: Functional and *in-silico* assessment of *MAX* variants of unknown significance

Iñaki Comino-Méndez[1], Luis J Leandro-García[1], Guillermo Montoya[2,3], Lucía Inglada-Pérez[1,4], Aguirre A de Cubas[1], María Currás-Freixes[1], Carolyn Tysoe[5], Louise Izatt[6], Rocío Letón[1], Álvaro Gómez-Graña[1], Veronika Mancikova[1], María Apellániz-Ruiz[1], Massimo Mannelli[7], Francesca Schiavi[8], Judith Favier[9], Anne-Paule Gimenez-Roqueplo[9], Henri J L M Timmers[10], Giovanna Roncador[11], Juan F Garcia[12], Cristina Rodríguez-Antona[1,4], Mercedes Robledo[1,4], and Alberto Cascón[1,4]*

Affiliations:

[1]Hereditary Endocrine Cancer Group and [2]Macromolecular Crystallography Group, Spanish National Cancer Research Centre (CNIO), Madrid, Spain

[3]Structural Biology Group, Novo Nordisk Foundation Center for Protein Research, Faculty of Health and Medical Sciences, University of Copenhagen, Denmark

[4]ISCIII Center for Biomedical Research on Rare Diseases (CIBERER), Spain

[5]Department of Molecular Genetics, Royal Devon & Exeter NHS Foundation Trust, Exeter, UK

[6]Department of Clinical Genetics, Guy's and St Thomas' Foundation Trust, Guy's Hospital, London, UK

[7]Department of Experimental and Clinical Biomedical Sciences, University of Florence, Florence, Italy

[8]Familial Cancer Clinic and Oncoendocrinology, Veneto Institute of Oncology IRCCS, Padova, Italy

[9]INSERM, UMR970, Paris-Cardiovascular Research Center, and Université Paris Descartes, Sorbonne Paris Cité, Faculté de Médecine, Paris, France

[10]Department of Medicine, Division of Endocrinology, Radboud University Nijmegen Medical Centre, Nijmegen,The Netherlands

[11]Monoclonal Antibodies Unit, Biotechnology Programme, Spanish National Cancer Research Centre (CNIO), Madrid, Spain

[12]Department of Pathology, M D Anderson Cancer Center Madrid, Madrid, Spain

***Address correspondence to**: Alberto Cascón,

Hereditary Endocrine Cancer Group, Human Cancer Genetics Programme, Spanish National Cancer Research Centre (CNIO), Melchor Fernández Almagro 3, 28029 Madrid, Spain

Phone: +34 91 224 69 47

Fax: +34 91 224 69 23

e-mail: acascon@cnio.es

ABSTRACT

The presence of germline mutations affecting the *MAX* gene has recently been identified as one of the now eleven major genetic predisposition factors for the development of hereditary pheochromocytoma and/or paraganglioma. Little is known regarding how missense variants of unknown significance (VUS) in *MAX* affect its pivotal role in the regulation of the MYC/MAX/MXD axis. In the present study, we propose a consensus computational prediction based on five "state of the art" algorithms. We also describe a PC12-based functional assay to assess the effects that twelve *MAX* VUS may have on MYC's E-box transcriptional activation. For all but two of these twelve VUS, the functional assay and the consensus computational prediction gave consistent results; we classified seven variants as pathogenic and three as non-pathogenic. The introduction of wild-type *MAX* cDNA into PC12 cells significantly decreased MYC's ability to bind to canonical E-boxes, while pathogenic MAX proteins were not able to fully repress MYC activity. Further clinical and molecular evaluation of variant carriers corroborated the results obtained with our functional assessment. In the absence of clear heritability, clinical information and molecular data, consensus computational predictions and functional models are able to correctly classify VUS affecting *MAX*.

KEY WORDS: Pheochromocytoma; paraganglioma; PC12 cells; variants of unknown significance; MAX.

INTRODUCTION

Pheochromocytomas (PCC) and paragangliomas (PGL) are rare neuroendocrine tumors; PCC are localized in the adrenal medulla and PGL in the intra-abdominal, thoracic or head and neck paraganglia. Around 30–40% of individuals with PCC/PGL are familial cases [1-4] due to germline mutations affecting one of five succinate dehydrogenase genes (*SDHA, SDHB, SDHC, SDHD* and *SDHAF2*), the *RET* oncogene, or the tumor suppressor genes (TSG) *VHL*, *NF1*, *FH*, *TMEM127* and *KIF1B beta* [5-17]. Recently, we identified MYC-associated protein X (*MAX)* as new PCC susceptibility gene by sequencing the exomes of three patients with shared clinical features of hereditary disease [18]. The subsequent analysis of an independent series of patients with PCC/PGL showed that around one percent of cases negative for mutations in the other known susceptibility genes carried a germline mutation affecting *MAX* [19]. This result confirmed that *MAX* is a new TSG associated with the development of hereditary PCC/PGL and highlighted the importance of including *MAX* in the algorithms used in the genetic diagnosis of the disease. Also consistent with *MAX* acting as a TSG in cancers with neuroendocrinal features is the recent finding of tumor-specific inactivation of *MAX* in small cell lung cancer [20].

MAX is a ubiquitously expressed and highly conserved transcription factor, which plays a central role in the regulation of the MYC/MAX/MXD network of basic helix-loop-helix leucine zipper (bHLHZip) transcription factors involved in cell proliferation, differentiation and apoptosis [21]. MYC, via heterodimerization with MAX, activates the transcription at target promoters by binding hexameric DNA consensus sequences “CANNTG” (E-boxes) [22]. In addition, MAX antagonizes MYC-dependent cell transformation by transcriptional repression of the same E-boxes through its interaction with several repressors (MXD, MNT, and MGA) [23]. The repression of MYC's transforming ability depends on the balance between MYC–MAX and MXD/MNT/MGA–MAX complexes [23]. Moreover, MAX homodimers can also repress the transcription of genes activated by MYC-MAX heterodimers by reducing the population of free MAX monomers and by binding to E-box DNA sequences [24]. The fact that MYC can maintain its function in the absence of normally functioning MAX protein [25] suggests that the pivotal role of MAX in the network can be related more to repression than to activation [26].

To date, twenty-six *MAX* variants have been reported to be associated with PCC/PGL, and almost half of these are missense alterations [18, 19, 27]. While truncating mutations in TSGs are usually considered deleterious, establishing the pathogenicity of a missense variant requires further analysis (e.g. identifying the presence of a second hit or loss of heterozygosity). *In silico* algorithms are widely used to predict the biological consequences of variants of unknown significance (VUS); however, in the absence of other biological evidence they are insufficient to conclude whether a variant is causal. Therefore, in order to improve the genetic counseling and clinical follow-up of variant carriers it is necessary to develop functional systems to clarify the role that an individual VUS may have in tumor development. The

characterization of *MAX* VUS described herein is based on three consecutive approaches: (i) modeling the affected residue in the protein structure in order to predict the effect of the alterations at the molecular level (ii) using five algorithms (SIFT, Polyphen, MutPred, SNPs&GO and PON-P2) to obtain a consensus prediction of plausible functional effects caused by the variants and (iii) implementing a luciferase-reporter assay in PC12 cells to assess disruptions in MYC regulation.

MATERIALS AND METHODS

Variants

Twelve non-truncating missense variants in *MAX,* eleven of which had been previously reported [18, 19] were included in the present analyses: p.V9L, p.D14N, p.R16W, p.R26C, p.R51W, p.I62S, p.M65V, p.R81P, p.L85P, p.L93P, p.N105T and p.S133L (Table 1). The numbering of variants was based upon the *MAX* transcript of 151 amino acids (NM_145112.1), though to avoid confusion with the previously reported numbering of *MAX* mutations (based on the transcript of 160 amino acids, NM_002382.3) we provide the correspondence of the variants in Table 1. None of the variants assessed were found in controls or reported in public databases of SNPs (http://www.1000genomes.org/ and http://evs.gs.washington.edu/EVS/), with the exception of p.V9L which appears in 1 of 470 exomes from the ClinSeq project (http://www.genome.gov/20519355). Three somatic missense variants affecting amino acids R26, R51 and M65 were reported in the COSMIC (http://cancer.sanger.ac.uk/cancergenome/projects/cosmic/) database, but the changes were different from those considered in the present study.

In silico prediction

We used the SIFT algorithm [28] and the programs PolyPhen-2 [29], MutPred [30], SNPs&GO [31] and PON-P2 (http://structure.bmc.lu.se/PON-P2/) to predict the impact of each of the twelve *MAX* VUS on protein structure/function. SIFT uses multiple alignment information to predict tolerated and not tolerated (deleterious) substitutions for every position of a given query sequence. PolyPhen-2 categorizes variants as benign, possibly damaging, or probably damaging based on a sequence-based characterization of the substitution site, profile analysis of homologous sequences, and mapping of the substitution site to a known protein's 3-dimentional structure. MutPred uses multiple alignment information, but also includes information on the gain/loss of 14 different structural and functional properties to assign a pathogenicity score; we considered scores greater than 0.5 to define pathogenicity. SNPs&GO predicts whether a variant is disease-related or neutral by exploiting the functional annotation of the protein. Finally, PON-P2 predicts the pathogenicity of amino acid substitutions based on amino acid features, Gene Ontology (GO) annotations, evolutionary conservation, and if available, annotations of functional sites. PON-P2 estimates the reliability of predictions and groups variants into pathogenic, neutral and unknown classes. In addition, we used the metaservers PredictSNP [32] and Meta-SNP [33] to validate the results obtained by our consensus prediction. These programs use a compendium of *in silico* algorithms to establish a consensus prediction. The consensus prediction given by PredictSNP is based on MAPP, PhD-SNP, PolyPhen-1, Polyphen-2, SIFT, SNAP nsSNPAnalyzer and PANTHER. Meta-SNP consensus prediction is based on PANTHER, PhD-SNP, SIFT and SNAP.

To assess for the concordance between the *in silico* predictions and the results of the functional assays, a one-sided binomial test was applied.

Structural mapping

The coordinates of the MAX-MAX-DNA (1HLO) and MAX-MYC-DNA (1NKP) crystal structures were downloaded from the Protein Data Bank and superimposed using the secondary structure alignment algorithm implemented in Coot [34]. The variations were then modeled using the "mutate replace" routine in the same program. Figures were generated using PyMol (The PyMOL Molecular Graphics System, Version 1.2r3pre, Schrödinger, LLC.)

cDNA cloning and mutagenesis

A full length sequence of the *MAX* transcript of 151 amino acids (NM_145112.1) was amplified from human peripheral lymphocyte cDNA and cloned into the expression vector pcDNA3.1 (+) (Invitrogen, Eugene, OR). The twelve *MAX* missense variants were generated by mutagenesis using the QuikChange II Site-Directed Mutagenesis Kit (Stratagene, La Jolla, CA, USA), according to the manufacturer's instructions. The designed primers used to generate all mutated alleles are described in the Online Resource (Online Resource, Table S1). Both wild-type and mutagenized inserts were verified by sequencing both strands.

Cell culture and luciferase assays

PC12 cells were cultured in Dulbecco's modified Eagle medium Gluta MAX (DMEM; Invitrogen), supplemented with 10% (v/v) foetal bovine serum (FBS, PAA laboratories, Westborough, MA, USA), 5% horse serum (Gibco, Grand Island, NY, USA), 1% (v/v) penicillin/streptomycin and 0.6% (v/v) Fungizone (Gibco). Cells were routinely tested for mycoplasma and transfected with Lipofectamine 2000 (Invitrogen), following the manufacturer's instructions. PC12 cells were seeded at 200,000 cells per well on 24-well plates for 72h before transfection. pBV-Luc wt MBS1-4 (luciferase reporter; Addgene, Cambridge, MA, USA), containing four tandem DNA binding sites for the MYC/MAX heterodimer was used as a reporter plasmid. Each well of a 24-well plate was transfected with 0.3 µg of pcDNA3.1 (EV), pcDNA3.1-MAXwt or pcDNA3.1-MAXmut constructs, pRL-SV40 (Renilla reporter; Promega, Madison, WI, USA) (10ng) and pBV-Luc wt MBS1-4 (0.6µg). After 48h, cells were washed and lysed in 100µl of Passive Lysis Buffer (Promega) and luminescence recorded using the Dual-Luciferase assay system (Promega), according to manufacturer's instructions. The plate was read on a Turner Biosystems Veritas Microplate Luminometer (Promega). We present as results the mean and standard error of at least three independent transfections. To explore potential dominant negative mechanisms occurring variants for

which LOH was not or could not be observed, we transfected PC12 cells with equal amounts (0.3 µg) of MAX-wt and each of these variants, as well as MAX-wt and a nonsense truncating mutation used as control (p.R24X), (Online Resource, Fig S2). We expected that if a dominant negative effect were present, the mutant MAX proteins would interfere with the wt MAX, leading to differences in the functional assay, compared with a truncated (null) MAX protein or the wt MAX alone.

RESULTS

VUS introduce structural alterations in the MAX protein

The twelve non-truncating missense variants in *MAX* described so far were included in the present analyses: p.V9L, p.D14N, p.R16W, p.R26C, p.R51W, p.I62S, p.M65V, p.R81P, p.L85P, p.L93P, p.N105T and p.S133L. Nine of the twelve VUS affect conserved or highly conserved amino acids located within the basic helix-loop-helix leucine zipper (bHLH-Zip) domain of the MAX protein (Online Resource, Fig S1). The other three variants, p.V9L, p.N105T and p.S133L, are also conserved but are located outside this region. Table 1 summarizes their predicted structural effects. Four variants (p.D14N, p.R16W, p.R26C and p.R51W) were predicted to affect DNA-binding, based on the interaction of each of these residues with DNA in the wild-type protein (Figure 1). Two variants (p.I62S and p.M65V) probably affect the homodimerization of MAX and its heterodimerization with MYC, and three variants (p.R81P, p.L85P and p.L93P) introduce proline, a residue that produces substantial kinks in α-helices affecting the structure of the protein. The amino acids V9, N105 and S133 are not observed in the reported protein structures [35, 36], probably due to the intrinsic disorder of these regions, located in the N- and C-termini of the protein.

In-silico prediction algorithms show high discrepancy in predicting the pathogenicity of *MAX* VUS

Only four variants (p.R16W, p.R26C, p.R51W and p.I62S) were classified as pathogenic by the five prediction algorithms considered. Three variants were considered disease-causing by four programs (p.R81P, p.L85P and p.L93P), one by two (p.M65V), and two variants by just one program (p.D14N and p.S133L). Only two variants were predicted to be non-pathogenic by all the prediction methods (p.V9L and p.N105T). Thus, a consensus prediction based on the agreement of at least three programs was available for 11 of the twelve VUS analyzed. These results are shown in Table 1. Furthermore, the four *MAX* polymorphic missense variants present in the Exome Variant Server (EVS) database (p.D5G, p.D12E, p.Y115H and p.G136R) were classified as non-pathogenic by this consensus prediction (data not shown). To assess the reliability of our consensus prediction, all variants were tested using two different online available metasevers, PredictSNP and Meta-SNP. The consensus established by each of these for the twelve variants studied were in agreement with the consensus prediction proposed herein except for the variant p.S133L, which was classified as pathogenic by the two metaservers. On the other hand, the unique variant unclassified by our consensus prediction (p.M65V) was classified as non pathogenic. The four *MAX* polymorphic missense variants described in the EVS database were also predicted to be non pathogenic.

Pathogenic *MAX* variants repress to a lesser extent MYC's E-box binding ability

PC12 cells carry a homozygous chromosomal alteration involving the MAX gene which gives rise to a protein incapable of repressing MYC–dependent transcription from E-box elements [26]. To determine whether each non-truncating variant had an effect on the regulation of MYC by MAX, we co-transfected PC12 cells with a reporter plasmid containing four E-boxes and expression vectors containing either *MAX* wild-type cDNA, the empty vector (EV) or the VUS in question. Significantly higher luciferase activity relative to wild-type MAX ($p<0.05$) was observed for all variants, with the exception of p.D14N, p.N105T and p.S133L (Figure 2). The concordance of the results of the functional assays with the consensus prediction was highly statistically significant ($p=1.1x10^{-19}$), and higher than the concordance with each of the *in silico* prediction algorithms. Thus, all the variants predicted by at least three *in silico* algorithms as deleterious were found to significantly alter the ability of MAX to regulate MYC. Furthermore, three of the four missense variants predicted to be non-pathogenic, p.D14N, p.N105T and p.S133L, showed luciferase activities similar to wild-type MAX, while cells transfected with the p.M65V variant (the only unclassified change in the consensus prediction), exhibited significant differences compared to the control. The p.V9L alteration, predicted by all the methods to be benign and tolerated, was found to substantially affect MYC's E-box transcriptional activation.

As expected, transfection of PC12 cells with EV led to significantly higher luciferase levels than transfection with wild-type MAX (Figure 2). The absence of LOH in the tumor carrying the p.V9L variation suggested that a dominant negative mechanism could be acting in this particular case. Moreover, three additional variations (p.R25W, p.R60W, and p.L102P) were not analyzed for LOH. To explore possible dominant negative mechanims we transfected PC12 cells with wild-type MAX alone and in combination with: a nonsense truncating mutation (p.R24X) and the p.V9L, p.R25W, p.R60W, and p.L102P variations (Online Resource, Fig S2). There was no difference in luciferase levels, compared to the control, associated with either the p.V9L or the other three variations tested, which suggests that a dominant negative effect does not occur for these alterations.

DISCUSSION

In the absence of informative pedigrees to assess the co-segregation of a novel amino acid substitution with a hereditary disease, other indicators, such as the presence of the variant in other patients, its absence in controls, and/or the finding of other distinctive syndromic clinical features in the patient are widely used to classify its pathogenicity. When all the above methods fail to classify VUS, prediction algorithms can be used. Many of these *in silico* methods have been specifically created to evaluate whether a given alteration may have a biological consequence. However, the different algorithms often give discrepant results, and this makes the establishment of the clinical relevance of a new variant a challenge. *MAX* is one of the major susceptibility genes that have most recently incorporated into the picture of hereditary predisposition to PCC/PGL. Half of all reported *MAX* variants are missense alterations, each found only once (with the exception of p.S133L) [27] and mostly in patients without familial antecedents (probably due to a paternal transmission effect) [18, 19], so the development of a reliable method to determine their role in the disease is especially important. In the present study, we proposed a PC12-based model for classifying non-truncating *MAX* variants according to their potential functional effect. The proposed functional approach showed high concordance with the results from a consensus *in silico* prediction obtained from five "state of the art" prediction algorithms.

No prediction of changes in MAX protein structural properties could be made for the variants p.V9L, p.N105T and p.S133L since they were not observed in the crystal structures. However, we were able to classify the other nine variants into three groups. The first comprised residues that are involved in protein-DNA interactions. Three of these missense variants consist of a change from arginine to hydrophobic tryptophan or cysteine. These variants alter the DNA binding properties of the protein to a different extent depending on each protein-DNA interaction, but all imply the loss of a residue commonly found in specific protein-DNA interactions. The p.D14N variant is an exception, involving the exchange of an acidic side chain for a polar one, which is also able to interact with the nucleic acid, indicating, as suggested by our data (Figure 2; Table 1), that this variation may not produce drastic consequences in the protein-DNA interaction. The second group of variants involved changes in the dimerization region of the protein. These variants strongly affect the MAX homodimer and therefore the assembly of monomers. The lack of MAX homodimers may make accessible for the transcription machinery the promoter regions of certain genes, which are normally repressed by MAX, thus facilitating their expression. The third group of variants involved the change from the wild-type residue to proline, a residue that alters the helical structure and may again lead to alterations in the hetero- or homo-dimerization capabilities of the mutated protein.

When we classified variants according to the consensus of different combinations of five *in silico* predictors, the result differed from the functional classification for at least two variants (range: 2-5). This

improved on considering the consensus of at least three algorithms, and was further supported by the prediction specifically obtained for the four polymorphic missense *MAX* variants present in the EVS database. Though most computational methods used to investigate the disease association of coding variants take into consideration the protein sequence, structure, and conservation across species, recent studies have demonstrated that they give discrepant results [37]. It has previously been suggested that more reliable results may be obtained by integrating the predictions of several algorithms [38, 39]. The consistent results obtained in the present study between the consensus prediction and the functional assay further supports the validity of this approach.

The presence of germline-inactivating *MAX* mutations in patients with hereditary PCC was the definitive evidence of the predominant role of MAX as a negative regulator of the MYC/MAX/MXD1 network [26]. The luciferase-reporter assay described herein further supports this pivotal role of MAX in MYC regulation. Thus, transient expression of wild-type MAX protein in PC12 cells significantly decreases MYC's ability to bind to canonical E-boxes (Figure 2). On the other hand, MAX mutant proteins less extensively repress MYC activity, thereby increasing luciferase activity, compared to wild-type MAX. Of note, the only variant that could not be classified by the consensus prediction (p.M65V) had an effect according to the assay. A different somatic change in the amino acid position 65 (to isoleucine) has been found in a prostate carcinoma, supporting its potential role in tumor development. Interestingly, the p.I62S variation that showed the most significant difference in the luciferase-reporter assay relative to the wild-type MAX, was the only variant predicted by MutPred to cause a gain of disorder in the MAX protein (p=0.0051).

For the nine variants predicted to be pathogenic via our functional assays, other features corroborated these results. These included the presence of familial antecedents, segregation with disease in the pedigree, the development of multiple or bilateral tumors in the carrier, and the presence of the previously described *MAX*-associated secretion phenotype (norepinephrine and epinephrine) [19] and/or the detection of LOH in the tumor (Table 1). On the other hand, the three VUS with no functional effect on MYC regulation (p.D14N, p.N105T and p.S133L) were found in patients with isolated tumors and no clinical features of hereditary disease. Two additional variants (p.R26C and p.R81P) were also found in patients with unilateral PCC but the first was somatic, and in both cases LOH affecting the wild-type allele was detected in the tumor. The only contradictory result between the consensus prediction and the functional assays occurred for variant p.V9L, a controversial change found both in a patient (1/1,694 cases) [19] who developed two sympathoadrenal tumors, and in 1/470 unaffected individuals (ClinSeq project). It has been recently suggested that even in the context of rare Mendelian disorders, the potential pathogenicity of variants reported by public databases should not be overlooked [40]. Although LOH was not observed in the tumor from the p.V9L variant carrier, the presence of both adrenal and

extra-adrenal tumors in this patient, as well as the intermediate norepinephrine/epinephrine secretion phenotype observed, suggest that this variation may be pathogenic. Overall, while this patient does not carry any other pathogenic variation in the known susceptibility PCC genes, the inconsistent data available do not allow us to reach a conclusion regarding the pathogenicity of this variant.

The appropriate management of relevant clinical information is one of the most effective tools used to decipher whether a germline VUS is causative. Nevertheless, the absence of clinical signs suggestive of heritability does not necessarily rule out that the variant is involved in the disease. In fact, *MAX*-associated tumor susceptibility exhibits paternal transmission of unknown origin, which makes the characterization of VUS even more complicated. In the present study, results from the clinical revision of cases and further molecular evaluation of both pathogenic and non-pathogenic alterations were consistent with the results obtained with our functional assays.

Understanding the possible effects of VUS and elucidating a disease association is a pivotal research challenge. The assay proposed in the present study efficiently categorizes the vast majority of *MAX* VUS as pathogenic or non-pathogenic, based on the function disruption of the protein. In addition, the consensus prediction obtained from proven computational methods offers a useful tool that complements more direct functional tests.

ACKNOWLEDGMENTS

This work was supported in part by the *Fondo de Investigaciones Sanitarias* (projects PI12/00236 and PI11/01359 to A.C. and M.R., respectively), the *Fundación Mutua Madrileña* (project AP2775/2008 to M.R.), and a grant from the European Community´s Seventh Framework Programme (ENS@T-CANCER; HEALTH-F2-2010-259735). Aguirre A de Cubas and Veronika Mancikova are predoctoral fellows in "la Caixa"/CNIO International PhD Programme. Lucía Inglada-Pérez and Iñaki Comino-Méndez are predoctoral fellows with the CIBERER, and the Fundacion Ferrer, respectively.

Disclosure Statement:

The authors have nothing to disclose.

References

1. Mannelli M, Castellano M, Schiavi F, Filetti S, Giacche M, Mori L, Pignataro V, Bernini G, Giache V, Bacca A, Biondi B, Corona G, Di Trapani G, Grossrubatscher E, Reimondo G, Arnaldi G, Giacchetti G, Veglio F, Loli P, Colao A, Ambrosio MR, Terzolo M, Letizia C, Ercolino T, Opocher G (2009) Clinically guided genetic screening in a large cohort of italian patients with pheochromocytomas and/or functional or nonfunctional paragangliomas. J Clin Endocrinol Metab 94: 1541-1547. DOI jc.2008-2419 [pii] 10.1210/jc.2008-2419
2. Cascon A, Pita G, Burnichon N, Landa I, Lopez-Jimenez E, Montero-Conde C, Leskela S, Leandro-Garcia LJ, Leton R, Rodriguez-Antona C, Diaz JA, Lopez-Vidriero E, Gonzalez-Neira A, Velasco A, Matias-Guiu X, Gimenez-Roqueplo AP, Robledo M (2009) Genetics of pheochromocytoma and paraganglioma in Spanish patients. J Clin Endocrinol Metab 94: 1701-1705. DOI jc.2008-2756 [pii] 10.1210/jc.2008-2756
3. Welander J, Soderkvist P, Gimm O (2011) Genetics and clinical characteristics of hereditary pheochromocytomas and paragangliomas. Endocr Relat Cancer 18: R253-276. DOI ERC-11-0170 [pii] 10.1530/ERC-11-0170
4. Burnichon N, Buffet A, Parfait B, Letouze E, Laurendeau I, Loriot C, Pasmant E, Abermil N, Valeyrie-Allanore L, Bertherat J, Amar L, Vidaud D, Favier J, Gimenez-Roqueplo AP (2012) Somatic NF1 Inactivation is a Frequent Event in Sporadic Pheochromocytoma. Hum Mol Genet. DOI dds374 [pii] 10.1093/hmg/dds374
5. Astuti D, Latif F, Dallol A, Dahia PL, Douglas F, George E, Skoldberg F, Husebye ES, Eng C, Maher ER (2001) Gene mutations in the succinate dehydrogenase subunit SDHB cause susceptibility to familial pheochromocytoma and to familial paraganglioma. Am J Hum Genet 69: 49-54
6. Burnichon N, Briere JJ, Libe R, Vescovo L, Riviere J, Tissier F, Jouanno E, Jeunemaitre X, Benit P, Tzagoloff A, Rustin P, Bertherat J, Favier J, Gimenez-Roqueplo AP (2010) SDHA is a tumor suppressor gene causing paraganglioma. Hum Mol Genet 19: 3011-3020. DOI ddq206 [pii] 10.1093/hmg/ddq206
7. Baysal BE, Ferrell RE, Willett-Brozick JE, Lawrence EC, Myssiorek D, Bosch A, van der Mey A, Taschner PE, Rubinstein WS, Myers EN, Richard CW, 3rd, Cornelisse CJ, Devilee P, Devlin B (2000) Mutations in SDHD, a mitochondrial complex II gene, in hereditary paraganglioma. Science 287: 848-851
8. Latif F, Tory K, Gnarra J, Yao M, Duh FM, Orcutt ML, Stackhouse T, Kuzmin I, Modi W, Geil L, et al. (1993) Identification of the von Hippel-Lindau disease tumor suppressor gene. Science 260: 1317-1320
9. Mulligan LM, Kwok JB, Healey CS, Elsdon MJ, Eng C, Gardner E, Love DR, Mole SE, Moore JK, Papi L, et al. (1993) Germ-line mutations of the RET proto-oncogene in multiple endocrine neoplasia type 2A. Nature 363: 458-460
10. Qin Y, Yao L, King EE, Buddavarapu K, Lenci RE, Chocron ES, Lechleiter JD, Sass M, Aronin N, Schiavi F, Boaretto F, Opocher G, Toledo RA, Toledo SP, Stiles C, Aguiar RC, Dahia PL (2010) Germline mutations in TMEM127 confer susceptibility to pheochromocytoma. Nat Genet 42: 229-233. DOI ng.533 [pii] 10.1038/ng.533
11. Niemann S, Muller U (2000) Mutations in SDHC cause autosomal dominant paraganglioma, type 3. Nat Genet 26: 268-270
12. Wallace MR, Marchuk DA, Andersen LB, Letcher R, Odeh HM, Saulino AM, Fountain JW, Brereton A, Nicholson J, Mitchell AL, et al. (1990) Type 1 neurofibromatosis gene: identification of a large transcript disrupted in three NF1 patients. Science 249: 181-186
13. Hao HX, Khalimonchuk O, Schraders M, Dephoure N, Bayley JP, Kunst H, Devilee P, Cremers CW, Schiffman JD, Bentz BG, Gygi SP, Winge DR, Kremer H, Rutter J (2009) SDH5, a gene required for flavination of succinate dehydrogenase, is mutated in paraganglioma. Science 325: 1139-1142. DOI 1175689 [pii]

10.1126/science.1175689
14. Castro-Vega LJ, Buffet A, De Cubas AA, Cascon A, Menara M, Khalifa E, Amar L, Azriel S, Bourdeau I, Chabre O, Curras-Freixes M, Franco-Vidal V, Guillaud-Bataille M, Simian C, Morin A, Leton R, Gomez-Grana A, Pollard PJ, Rustin P, Robledo M, Favier J, Gimenez-Roqueplo AP (2014) Germline mutations in FH confer predisposition to malignant pheochromocytomas and paragangliomas. Hum Mol Genet 23: 2440-2446. DOI ddt639 [pii]
10.1093/hmg/ddt639
15. Schlisio S, Kenchappa RS, Vredeveld LC, George RE, Stewart R, Greulich H, Shahriari K, Nguyen NV, Pigny P, Dahia PL, Pomeroy SL, Maris JM, Look AT, Meyerson M, Peeper DS, Carter BD, Kaelin WG, Jr. (2008) The kinesin KIF1Bbeta acts downstream from EglN3 to induce apoptosis and is a potential 1p36 tumor suppressor. Genes Dev 22: 884-893. DOI gad.1648608 [pii]
10.1101/gad.1648608
16. Yeh IT, Lenci RE, Qin Y, Buddavarapu K, Ligon AH, Leteurtre E, Do Cao C, Cardot-Bauters C, Pigny P, Dahia PL (2008) A germline mutation of the KIF1B beta gene on 1p36 in a family with neural and nonneural tumors. Hum Genet 124: 279-285. DOI 10.1007/s00439-008-0553-1
17. Welander J, Andreasson A, Juhlin CC, Wiseman RW, Backdahl M, Hoog A, Larsson C, Gimm O, Soderkvist P (2014) Rare germline mutations identified by targeted next-generation sequencing of susceptibility genes in pheochromocytoma and paraganglioma. J Clin Endocrinol Metab 99: E1352-1360. DOI 10.1210/jc.2013-4375
18. Comino-Mendez I, Gracia-Aznarez FJ, Schiavi F, Landa I, Leandro-Garcia LJ, Leton R, Honrado E, Ramos-Medina R, Caronia D, Pita G, Gomez-Grana A, de Cubas AA, Inglada-Perez L, Maliszewska A, Taschin E, Bobisse S, Pica G, Loli P, Hernandez-Lavado R, Diaz JA, Gomez-Morales M, Gonzalez-Neira A, Roncador G, Rodriguez-Antona C, Benitez J, Mannelli M, Opocher G, Robledo M, Cascon A (2011) Exome sequencing identifies MAX mutations as a cause of hereditary pheochromocytoma. Nat Genet 43: 663-667. DOI ng.861 [pii]
10.1038/ng.861
19. Burnichon N, Cascon A, Schiavi F, Morales NP, Comino-Mendez I, Abermil N, Inglada-Perez L, de Cubas AA, Amar L, Barontini M, de Quiros SB, Bertherat J, Bignon YJ, Blok MJ, Bobisse S, Borrego S, Castellano M, Chanson P, Chiara MD, Corssmit EP, Giacche M, de Krijger RR, Ercolino T, Girerd X, Gomez-Garcia EB, Gomez-Grana A, Guilhem I, Hes FJ, Honrado E, Korpershoek E, Lenders JW, Leton R, Mensenkamp AR, Merlo A, Mori L, Murat A, Pierre P, Plouin PF, Prodanov T, Quesada-Charneco M, Qin N, Rapizzi E, Raymond V, Reisch N, Roncador G, Ruiz-Ferrer M, Schillo F, Stegmann AP, Suarez C, Taschin E, Timmers HJ, Tops CM, Urioste M, Beuschlein F, Pacak K, Mannelli M, Dahia PL, Opocher G, Eisenhofer G, Gimenez-Roqueplo AP, Robledo M (2012) MAX mutations cause hereditary and sporadic pheochromocytoma and paraganglioma. Clin Cancer Res 18: 2828-2837. DOI 1078-0432.CCR-12-0160 [pii]
10.1158/1078-0432.CCR-12-0160
20. Romero OA, Torres-Diz M, Pros E, Savola S, Gomez A, Moran S, Saez C, Iwakawa R, Villanueva A, Montuenga LM, Kohno T, Yokota J, Sanchez-Cespedes M (2013) MAX inactivation in small-cell lung cancer disrupts the MYC-SWI/SNF programs and is synthetic lethal with BRG1. Cancer Discov. DOI 2159-8290.CD-13-0799 [pii]
10.1158/2159-8290.CD-13-0799
21. Atchley WR, Fitch WM (1995) Myc and Max: molecular evolution of a family of proto-oncogene products and their dimerization partner. Proc Natl Acad Sci U S A 92: 10217-10221
22. Vervoorts J, Luscher B (1999) DNA binding of Myc/Max/Mad network complexes to oligonucleotides containing two E box elements: c-Myc/Max heterodimers do not bind DNA cooperatively. Biol Chem 380: 1121-1126. DOI 10.1515/BC.1999.140
23. Grandori C, Cowley SM, James LP, Eisenman RN (2000) The Myc/Max/Mad network and the transcriptional control of cell behavior. Annu Rev Cell Dev Biol 16: 653-699. DOI
10.1146/annurev.cellbio.16.1.653
16/1/653 [pii]

24. Beaulieu ME, McDuff FO, Frappier V, Montagne M, Naud JF, Lavigne P (2012) New structural determinants for c-Myc specific heterodimerization with Max and development of a novel homodimeric c-Myc b-HLH-LZ. J Mol Recognit 25: 414-426. DOI 10.1002/jmr.2203
25. Gallant P, Steiger D (2009) Myc's secret life without Max. Cell Cycle 8: 3848-3853. DOI 10088 [pii]
26. Cascon A, Robledo M (2012) MAX and MYC: A Heritable Breakup. Cancer Res 72: 3119-3124. DOI 0008-5472.CAN-11-3891 [pii]
10.1158/0008-5472.CAN-11-3891
27. Rattenberry E, Vialard L, Yeung A, Bair H, McKay K, Jafri M, Canham N, Cole TR, Denes J, Hodgson SV, Irving R, Izatt L, Korbonits M, Kumar AV, Lalloo F, Morrison PJ, Woodward ER, Macdonald F, Wallis Y, Maher ER (2013) A comprehensive next generation sequencing-based genetic testing strategy to improve diagnosis of inherited pheochromocytoma and paraganglioma. J Clin Endocrinol Metab 98: E1248-1256. DOI jc.2013-1319 [pii]
10.1210/jc.2013-1319
28. Kumar P, Henikoff S, Ng PC (2009) Predicting the effects of coding non-synonymous variants on protein function using the SIFT algorithm. Nat Protoc 4: 1073-1081. DOI nprot.2009.86 [pii]
10.1038/nprot.2009.86
29. Adzhubei IA, Schmidt S, Peshkin L, Ramensky VE, Gerasimova A, Bork P, Kondrashov AS, Sunyaev SR (2010) A method and server for predicting damaging missense mutations. Nat Methods 7: 248-249. DOI nmeth0410-248 [pii]
10.1038/nmeth0410-248
30. Li B, Krishnan VG, Mort ME, Xin F, Kamati KK, Cooper DN, Mooney SD, Radivojac P (2009) Automated inference of molecular mechanisms of disease from amino acid substitutions. Bioinformatics 25: 2744-2750. DOI btp528 [pii]
10.1093/bioinformatics/btp528
31. Calabrese R, Capriotti E, Fariselli P, Martelli PL, Casadio R (2009) Functional annotations improve the predictive score of human disease-related mutations in proteins. Hum Mutat 30: 1237-1244. DOI 10.1002/humu.21047
32. Bendl J, Stourac J, Salanda O, Pavelka A, Wieben ED, Zendulka J, Brezovsky J, Damborsky J (2014) PredictSNP: robust and accurate consensus classifier for prediction of disease-related mutations. PLoS Comput Biol 10: e1003440. DOI 10.1371/journal.pcbi.1003440
PCOMPBIOL-D-13-01477 [pii]
33. Capriotti E, Altman RB, Bromberg Y (2013) Collective judgment predicts disease-associated single nucleotide variants. BMC Genomics 14 Suppl 3: S2. DOI 1471-2164-14-S3-S2 [pii]
10.1186/1471-2164-14-S3-S2
34. Emsley P, Lohkamp B, Scott WG, Cowtan K (2010) Features and development of Coot. Acta Crystallogr D Biol Crystallogr 66: 486-501. DOI S0907444910007493 [pii]
10.1107/S0907444910007493
35. Brownlie P, Ceska T, Lamers M, Romier C, Stier G, Teo H, Suck D (1997) The crystal structure of an intact human Max-DNA complex: new insights into mechanisms of transcriptional control. Structure 5: 509-520
36. Nair SK, Burley SK (2003) X-ray structures of Myc-Max and Mad-Max recognizing DNA. Molecular bases of regulation by proto-oncogenic transcription factors. Cell 112: 193-205. DOI S0092867402012849 [pii]
37. Thusberg J, Olatubosun A, Vihinen M (2011) Performance of mutation pathogenicity prediction methods on missense variants. Hum Mutat 32: 358-368. DOI 10.1002/humu.21445
38. Olatubosun A, Valiaho J, Harkonen J, Thusberg J, Vihinen M (2012) PON-P: integrated predictor for pathogenicity of missense variants. Hum Mutat 33: 1166-1174. DOI 10.1002/humu.22102
39. Gonzalez-Perez A, Lopez-Bigas N (2011) Improving the assessment of the outcome of nonsynonymous SNVs with a consensus deleteriousness score, Condel. Am J Hum Genet 88: 440-449. DOI S0002-9297(11)00096-6 [pii]
10.1016/j.ajhg.2011.03.004

40. Kenna KP, McLaughlin RL, Hardiman O, Bradley DG (2013) Using Reference Databases of Genetic Variation to Evaluate the Potential Pathogenicity of Candidate Disease Variants. Hum Mutat. DOI 10.1002/humu.22303
41. Gouet P, Courcelle E, Stuart DI, Metoz F (1999) ESPript: analysis of multiple sequence alignments in PostScript. Bioinformatics 15: 305-308. DOI btc028 [pii]

Table 1. Missense variants of unknown significance (VUS) investigated and results obtained from the analyses performed

Protein variant[a] (original notation)	Predicted structural alteration	Polyphen-2 prediction	SIFT prediction	MutPred prediction[¥]	SNPs&GO prediction	PON-P2 prediction	Consensus prediction[#]	Functional testing result	Relevant clinical and/or molecular data
p.V9L	None observed[c]	Benign	Tolerated	Non pathogenic	Neutral	Neutral	Non pathogenic	Alteration	U, P, no LOH, NE+E
p.D14N (p.D23N)	DNA-binding	Benign	**Not tolerated**	Non pathogenic	Neutral	Unknown	Non pathogenic	No effect	U, LOH n.a.
p.R16W (p.R25W)	DNA-binding	**Probably damaging**	**Not tolerated**	**Pathogenic**	**Disease-related**	**Pathogenic**	**Pathogenic**	Alteration	B, M [4], LOH n.a., NE
p.R26C (p.R35C*[b])	DNA-binding	**Probably damaging**	**Not tolerated**	**Pathogenic**	**Disease-related**	**Pathogenic**	**Pathogenic**	Alteration	U, LOH, NE+E
p.R51W (p.R60W[b])	DNA-binding	**Probably damaging**	**Not tolerated**	**Pathogenic**	**Disease-related**	**Pathogenic**	**Pathogenic**	Alteration	B, LOH n.a., NE+E
p.I62S (p.I71S)	Heterodimerization	**Probably damaging**	**Not tolerated**	**Pathogenic**	**Disease-related**	**Pathogenic**	**Pathogenic**	Alteration	B, LOH, NE+E
p.M65V (p.M74V[b])	Heterodimerization	Benign	**Not tolerated**	**Pathogenic**	Neutral	Unknown	Unclassified	Alteration	B, LOH, NE+E
p.R81P (p.R90P)	Helical properties affected	**Possibly damaging**	**Not tolerated**	Non pathogenic	**Disease-related**	**Pathogenic**	**Pathogenic**	Alteration	U, LOH
p.L85P (p.L94P)	Helical properties affected	**Possibly damaging**	**Not tolerated**	Non pathogenic	**Disease-related**	**Pathogenic**	**Pathogenic**	Alteration	U, FA, LOH
p.L93P (p.L102P)	Helical properties affected	**Probably damaging**	**Not tolerated**	**Pathogenic**	Neutral	**Pathogenic**	**Pathogenic**	Alteration	U, FA, LOH n.a.
p.N105T (p.N114T)[§]	None observed[c]	Benign	Tolerated	Non pathogenic	Neutral	Unknown	Non pathogenic	No effect	P, LOH n.a.
p.S133L (p.S142L)	None observed[c]	**Possibly damaging**	Tolerated	Non pathogenic	Neutral	Unknown	Non pathogenic	No effect	U, LOH n.a., NE+E

[a]: numbering of variants is based on *MAX* transcript NM_145112.1; *: somatic mutation; [b]: amino acid mutated in other tumors and reported in the COSMIC database (http://cancer.sanger.ac.uk/cancergenome/projects/cosmic/); [§]: variant not reported; [c]: amino acid not observed in the reported protein structures; [¥]: variants with MutPred scores over 0.5 were considered probably pathogenic; [#]: the consensus prediction is based on the agreement of at least three predictors; U: unilateral PCC; P: paraganglioma; LOH: loss of heterozygosity detected in the tumor; n.a.: data not available; B: bilateral PCC; M: multiple PGLs, number of tumors is specified in parenthesis; FA: familial antecedents of PCC; NE: norepinephrine secretion; E: epinephrine secretion. Variants for which a likely pathogenic effect was predicted by each *in silico* algorithm are denoted in bold type.

FIGURES

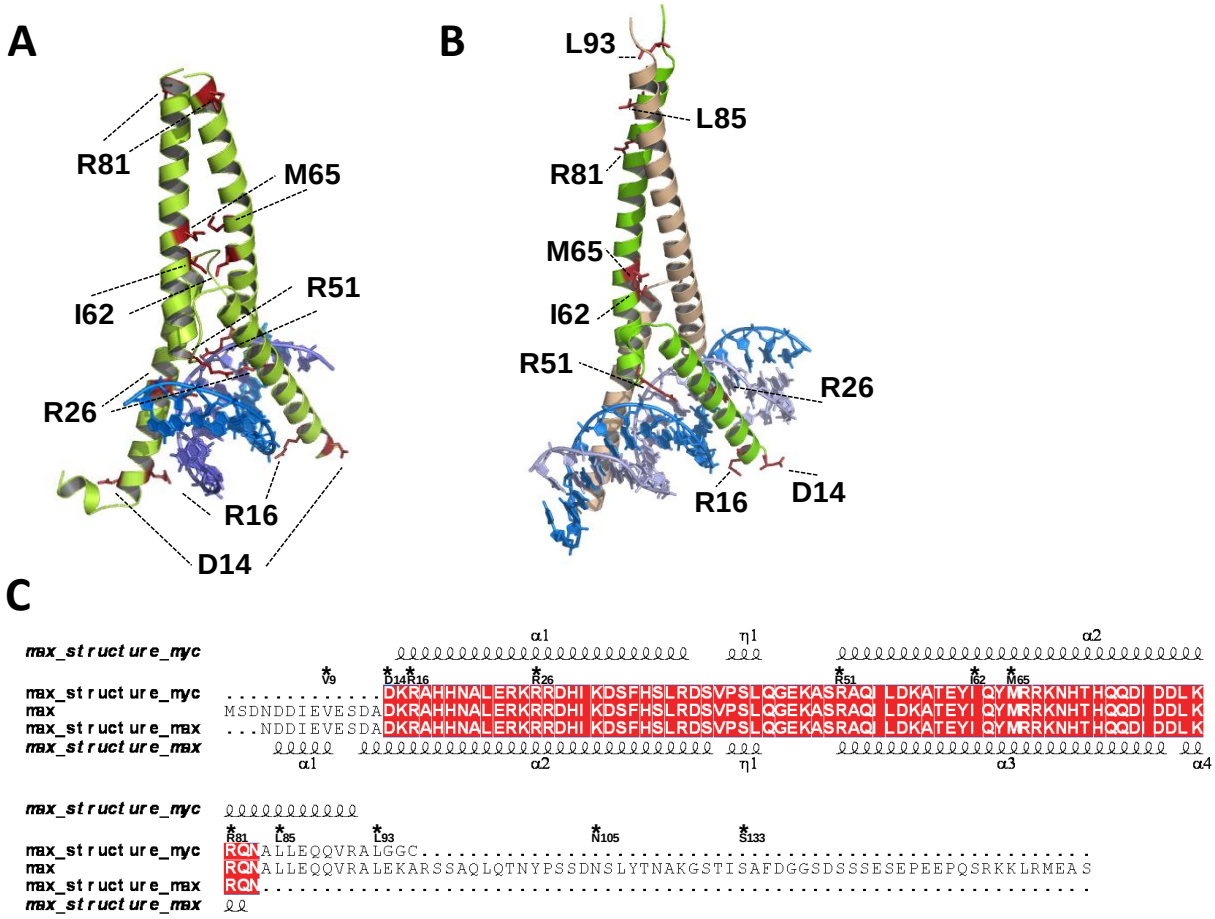

Figure 1. Mapping of the twelve variants in the MAX-MAX-DNA (PDB file 1HLO) and MYC-MAX-DNA (PDB file 1NKP) crystallographic structures: A) Ribbon diagram of the MAX homodimer; B) Ribbon diagram of the MAX (green-colored chain)-MYC (flesh-colored chain) heterodimer bound to DNA (blue-colored chains); C) Structure guided sequence alignment of MAX. In A and B, the side chains of the amino acids in the mutated positions are colored in red. In C, the sequence common to both structures and the full-length protein is shown with a red background, the positions of the mutations are depicted with an asterisk and the upper and lower lines of the alignment display the secondary structure of MAX in each PDB file; the alignment was generated with ESPRIPT.[41]

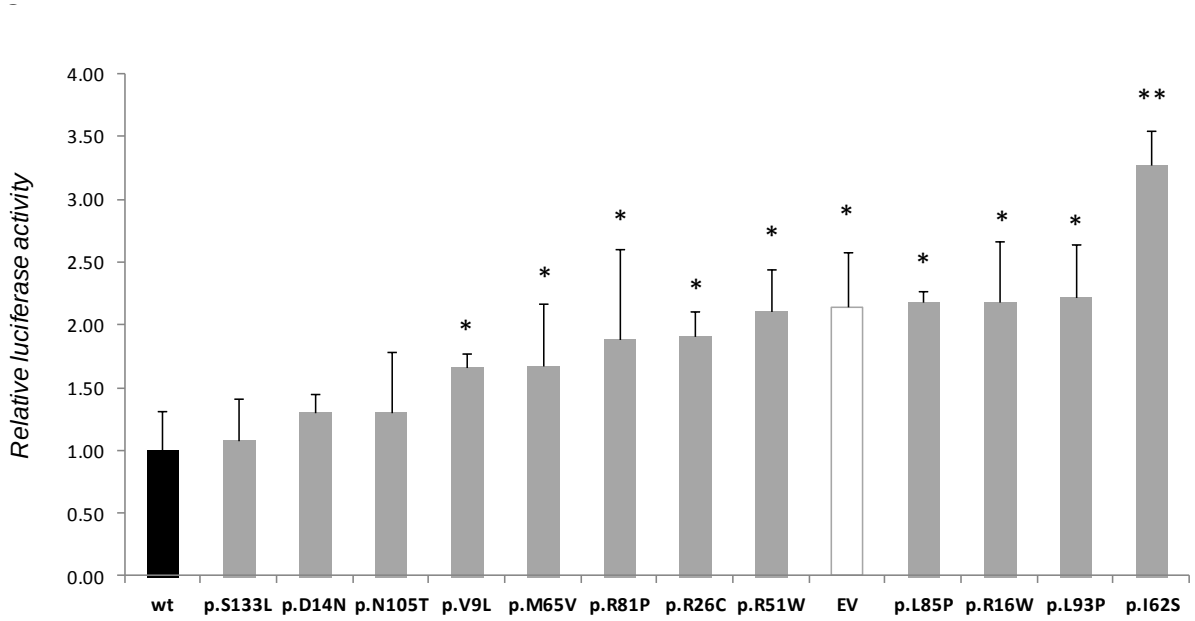

Figure 2. Luciferase-reporter assays performed in PC12 cells. pBV-Luc wt MBS1-4 luciferase construct was co-transfected in PC12 cells with pcDNA3.1 including either the wild-type *MAX* cDNA or one of the *MAX* VUS . The relative luciferase activity was calculated as the ratio of the firefly luciferase activity to the Renilla luciferase activity and expressed as mean±s.d. (n≥3). *: p-value <0.05; **: p-value <0.0001 (compared in each case to the luciferase relative activity detected for the wild-type *MAX* cDNA).

Supplementary Materials for

Functional and in-silico assessment of MAX variants of unknown significance

Iñaki Comino-Méndez, Luis J Leandro-García, Guillermo Montoya, Lucía Inglada-Pérez, Aguirre A de Cubas, María Currás-Freixes, Carolyn Tysoe, Louise Izatt, Rocío Letón, Álvaro Gómez-Graña, Veronika Mancikova, María Apellániz-Ruiz, Massimo Mannelli, Francesca Schiavi, Judith Favier, Anne-Paule Gimenez-Roqueplo, Henri J L M Timmers, Giovanna Roncador, Juan F Garcia, Cristina Rodríguez-Antona, Mercedes Robledo, and Alberto Cascón*

*Address correspondence to: Alberto Cascón,

Hereditary Endocrine Cancer Group, Human Cancer Genetics Programme, Spanish National Cancer Research Centre (CNIO), Melchor Fernández Almagro 3, 28029 Madrid, Spain

Phone: +34 91 224 69 47

Fax: +34 91 224 69 23

e-mail: acascon@cnio.es

The PDF file includes:

Fig. S1. Sequence alignment of multiple amino acids from MAX proteins across various species. The conservation of the studied amino acids (marked with a vertical red bar) is shown at the bottom of the alignment. Conserved and similar residues are indicated with asterisks and dots below the alignment, respectively. Protein sequences were aligned using Clustal Omega (http://www.ebi.ac.uk/Tools/msa/clustalo/). The following protein accession numbers were used in the alignment: *Homo sapiens* (GI:21704263), *Macaca mulatta* (GI:386780834), *Rattus norvegicus* (GI:485399), *Mus musculus* (GI:226051848), *Sus scrofa* (F2Z5K0), *Felis catus* (GI:57619109), *Monodelphis domestica* (GI:126282606), *Danio rerio* (GI:56207613), *Tetraodon nigroviridis* (H3BWK6), and *Takifugu rubripes* (GI:410898003).

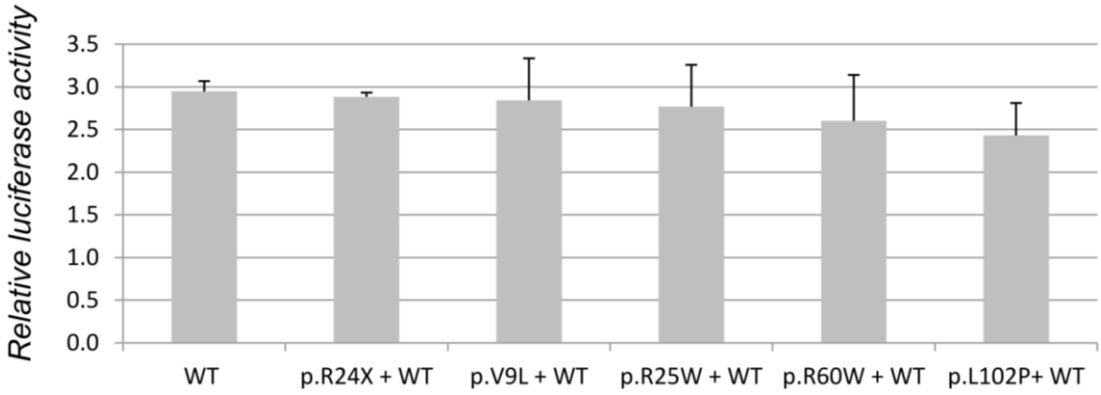

Fig. S2. Luciferase-reporter assays performed to explore dominant negative effects of *MAX* VUS. pBV-Luc wt MBS1-4 luciferase construct was co-transfected in PC12 cells with pcDNA3.1 including either the wild-type *MAX* cDNA, a control truncating mutation (p.R24X) or the four *MAX* VUS without demonstrated LOH . The relative luciferase activity was calculated as the ratio of the firefly luciferase activity to the Renilla luciferase activity and expressed as mean±s.d. (n≥3).

Table S1. Primer sequences used in the mutagenesis experiments

Variant	Primer name	Sequence (5' to 3')
p.V9L	p.V9L _S	5'-aacgatgacatcgagttggagagcgacgctg-3'
	p.V9L _AS	5'-cagcgtcgctctccaactcgatgtcatcgtt-3'
p.D14N	p.D14N_S	5'-ggtggagagcgacgctaacaaacgggctc-3'
	p.D14N_AS	5'-ggtggagagcgacgctaacaaacgggctc-3'
p.R16W	p.R16W_S	5'-ggagagcgacgctgacaaatgggctcatca-3'
	p.R16W_AS	5'-tgatgagcccatttgtcagcgtcgctctcc-3'
p.R24X	p.R24X_S	5'-catcataatgcactggaatgaaaacgtagggaccaca-3'
	p.R24X_AS	5'-tgtggtccctacgttttcattccagtgcattatgatg-3'
p.R26C	p.R26C_S	5'-tcatcataatgcactggaacgaaaatgtagggaccacatc-3'
	p.R26C_AS	5'-gatgtggtccctacattttcgttccagtgcattatgatga-3'
p.R51W	p.R51W_S	5'-ggagagaaggcatcctgggcccaaatcctag-3'
	p.R51W_AS	5'-ctaggatttgggcccaggatgccttctctcc-3'
p.I62S	p.I62S_S	5'-cctagacaaagccacagaatatagccagtatatgcgaag-3'
	p.I62S_AS	5'-cttcgcatatactggctatattctgtggctttgtctagg-3'
p.M65V	p.M65V_S	5'-agacaaagccacagaatatatccagtatgtgcgaaggaaaaacc-3'
	p.M65V_AS	5'-ggtttttccttcgcacatactggatatattctgtggctttgtct-3'
p.R81P	p.R81P_S	5'-attgacgacctcaagccgcagaatgctcttctg-3'
	p.R81P_AS	5'-cagaagagcattctgcggcttgaggtcgtcaat-3'
p.L85P	p.L85P_S	5'-tcaagcggcagaatgctcctctggagcag–3’
	p.L85P_AS	5’-gagcattctgccgcttgagcagcagttatag-3’
p.L93P	p.L93P_S	5'-caagtccgtgcaccggagaaggcgagg-3'
	p.L93P_AS	5'-cctcgccttctccggtgcacggacttg-3'
p.N105T	p.N105t_S	5'-ccaactgcagaccacctacccctcctcag-3'
	p.N105t_AS	5'-ctgaggaggggtaggtggtctgcagttgg-3'
p.S129S	p.S129L_S	5'-cgatgggggctcagactccagctcg-3'
	p.S129L_AS	5'-cgagctggagtctgagcccccatcg-3'
p.S133L	p.S133L_S	5'-ctcggactccagcttggagtctgagcc-3'
	p.S133L_AS	5'-ggctcagactccaagctggagtccgag-3'

ARTICLE 4: Tumoral *EPAS1* (*HIF2A*) mutations explain sporadic pheochromocytoma and paraganglioma in the absence of erythrocytosis.

Authors: Iñaki Comino-Méndez, Aguirre A. de Cubas, Carmen Bernal, Cristina Álvarez-Escolá, Carolina Sánchez-Malo, César L. Ramírez-Tortosa, Susana Pedrinaci, Elena Rapizzi, Tonino Ercolino, Giampaolo Bernini, Alessandra Bacca, Rocío Letón, Guillermo Pita, María R. Alonso, Luis J. Leandro-García, Álvaro Gómez-Graña, Lucía Inglada-Pérez, Veronika Mancikova, Cristina Rodríguez-Antona, Massimo Mannelli, Mercedes Robledo and Alberto Cascón.

Published in Human Molecular Genetics 2013 February 14; 22 (11): 2169-2176.

ABSTRACT

As previously mentioned, sequencing multiple trios (a patient and their unaffected parents) in which affected individuals share similar clinical characteristics is a suitable approach to find a causal gene, especially for genes harboring *de novo* mutations or following a recessive inheritance model.

In a second NGS project we applied WES to the germline DNA of three trios selected because the probands showed a very unusual clinical presentation: idiopathic polycythemia and multiple PCCs/PGLs. During the analysis of the WES data, Pacak's group in USA (Zhuang et al., 2012) published their discovery of somatic post-zygotic *HIF2A* gain-of-function mutations in patients with PGLs and congenital polycythemia. Subsequent analysis of *HIF2A* in our three selected probands revealed that all of them carried somatic post-zygotic mutations in the gene. The inheritance model underlying *HIF2A* mutations in PCC/PGL, despite being very uncommon, presents a challenge to non-agnostic approaches, and highlights the importance of performing WES in tumor-blood matched samples in order to cover as many genetic models as possible.

In this study we assessed 41 PCCs/ PGLs for mutations in *HIF2A* and described the clinical, molecular and genetic characteristics of the seven patients found to carry somatic *HIF2A* mutations; four presented with multiple PGLs (three of them were the initially sequenced tumors and also had congenital polycythemia), whereas three were single sporadic PCC/PGL cases. After excluding the three probands with multiple tumors and polycythemia, somatic mutations affecting *HIF2A* accounted for 10% of the tumors analyzed in this series, suggesting that this alteration is a relevant somatic oncogenic event in PCC/PGL development. All the tumors were also screened for *HIF1A* mutations, however none were found. The gene expression analysis of *HIF2A*-mutated tumors revealed similar mRNA *HIF2A* levels to

those found in *SDH*-gene- and *VHL*-mutated cases and a significant up-regulation of two hypoxia-induced genes (*PCSK6* and *GNA14*). Interestingly, single nucleotide polymorphism (SNP) array analysis revealed an exclusive gain of chromosome 2p in three *HIF2A*-mutated tumors. Furthermore, multiplex-PCR screening for small rearrangements detected a specific *HIF2A* gain in another *HIF2A*-mutated tumor and in three non-mutated cases suggesting that the gain of the gene is an important oncogenic event in the development of the disease.

The finding that *HIF2A* is involved in the sporadic presentation of the disease not only increases the percentage of PCCs/PGLs with known driver mutations, but also highlights the relevance of studying other hypoxia-related genes in apparently sporadic tumors. Finally, the detection of a specific copy number alteration affecting chromosome 2p in *HIF2A*-mutated tumors may guide the genetic diagnosis of patients with this disease.

Personal contribution: I participated in the conception and design of the study and the acquisition of the samples and data. Besides, I was actively involved in the genetic screening for mutations in *HIF2A* and *HIF1A* in our selected series of tumors by means of Denaturing High-Performance Liquid Chromatography (dHPLC) and Sanger sequencing. I also participated in the analysis of the tumors, testing for gains in the gene using a multiplex PCR-based method and SNP array. Finally I was involved in the analysis of the expression data, the discussion of the results and the drafting of the paper.

Human Molecular Genetics, 2013, Vol. 22, No. 11 **2169–2176**
doi:10.1093/hmg/ddt069
Advance Access published on February 14, 2013

Tumoral *EPAS1* (*HIF2A*) mutations explain sporadic pheochromocytoma and paraganglioma in the absence of erythrocytosis

Iñaki Comino-Méndez[1], Aguirre A. de Cubas[1], Carmen Bernal[2], Cristina Álvarez-Escolá[3], Carolina Sánchez-Malo[4], César L. Ramírez-Tortosa[5], Susana Pedrinaci[6], Elena Rapizzi[7,8], Tonino Ercolino[9], Giampaolo Bernini[10], Alessandra Bacca[10], Rocío Letón[1], Guillermoó Pita[11], María R. Alonso[11], Luis J. Leandro-García[1], Álvaro Gómez-Graña[1], Lucía Inglada-Pérez[1,12], Veronika Mancikova[1], Cristina Rodríguez-Antona[1,12], Massimo Mannelli[7,8], Mercedes Robledo[1,12] and Alberto Cascón[1,12,*]

[1]Hereditary Endocrine Cancer Group, Spanish National Cancer Research Centre (CNIO), Madrid, Spain, [2]Endocrinology Service, Hospital 12 de Octubre, Madrid, Spain, [3]Department of Endocrinology, Hospital La Paz, Madrid, Spain, [4]Endocrinology Service, [5]Pathology Service, Complejo Hospitalario de Jaén, Jaén, Spain, [6]Servicio de Análisis Clínicos, Hospital Universitario Virgen de las Nieves, Universidad de Granada, Granada, Spain, [7]Department of Clinical Pathophysiology, University of Florence, Florence, Italy, [8]Istituto Toscano Tumori, Florence, Italy, [9]Endocrinology Unit, Careggi Hospital, Florence, Italy, [10]Department of Internal Medicine, University of Pisa, Pisa, Italy, [11]Human Genotyping Unit-CeGen, Human Cancer Genetics Programme, Spanish National Cancer Centre, Madrid, Spain and [12]ISCIII Center for Biomedical Research on Rare Diseases (CIBERER), Valencia, Spain

Received November 29, 2012; Revised January 22, 2013; Accepted February 8, 2013

Pheochromocytomas (PCCs) and paragangliomas (PGLs) are chromaffin-cell tumors that arise from the adrenal medulla and extra-adrenal paraganglia, respectively. The dysfunction of genes involved in the cellular response to hypoxia, such as *VHL*, EGL nine homolog 1, and the succinate dehydrogenase (*SDH*) genes, leads to a direct abrogation of hypoxia inducible factor (HIF) degradation, resulting in a pseudo-hypoxic state implicated in PCC/PGL development. Recently, somatic post-zygotic mutations in *EPAS1* (*HIF2A*) have been found in patients with multiple PGLs and congenital erythrocytosis. We assessed 41 PCCs/PGLs for mutations in *EPAS1* and herein describe the clinical, molecular and genetic characteristics of the 7 patients found to carry somatic *EPAS1* mutations; 4 presented with multiple PGLs (3 of them also had congenital erythrocytosis), whereas 3 were single sporadic PCC/PGL cases. Gene expression analysis of *EPAS1*-mutated tumors revealed similar mRNA *EPAS1* levels to those found in *SDH*-gene- and *VHL*-mutated cases and a significant up-regulation of two hypoxia-induced genes (*PCSK6* and *GNA14*). Interestingly, single nucleotide polymorphism array analysis revealed an exclusive gain of chromosome 2p in three *EPAS1*-mutated tumors. Furthermore, multiplex-PCR screening for small rearrangements detected a specific *EPAS1* gain in another *EPAS1*-mutated tumor and in three non-*EPAS1*-mutated cases. The finding that *EPAS1* is involved in the sporadic presentation of the disease not only increases the percentage of PCCs/PGLs with known driver mutations, but also highlights the relevance of studying other hypoxia-related genes in apparently sporadic tumors. Finally, the detection of a specific copy number alteration affecting chromosome 2p in *EPAS1*-mutated tumors may guide the genetic diagnosis of patients with this disease.

*To whom correspondence should be addressed at: Hereditary Endocrine Cancer Group, Human Cancer Genetics Programme, Centro Nacional de Investigaciones Oncológicas (CNIO), Melchor Fernández Almagro 3, Madrid 28029, Spain. Tel: +34 912246947; Fax: +34 912246923; Email: acascon@cnio.es

INTRODUCTION

Pheochromocytomas (PCCs) and paragangliomas (PGLs) are rare neural crest tumors that arise from the adrenal medulla and from the extra-adrenal sympathetic and parasympathetic paraganglia, respectively. The genetics of PCCs/PGLs is extremely puzzling, with up to 40% of patients carrying a germline mutation that affects 1 of 10 major susceptibility genes (1–10). Depending to a great extent on the gene mutated, the clinical phenotype of mutation carriers can vary dramatically (e.g. patients carrying germline mutations in *VHL* versus *RET*) as can risk of malignancy or age-related penetrance (e.g. patients carrying germline mutations in *SDHB* versus *SDHD*). Furthermore, some of the genes (i.e. *SDHD*, *SDHAF2* and *MAX*) are affected by maternal *imprinting* or paternal transmission. In addition to this high and heterogeneous genetic predisposition, there is also a substantive percentage of hereditary cases, either with familial antecedents of PCC/PGL or with other clinical characteristics suggestive of hereditary disease, that do not harbor mutations in any of the susceptibility genes mentioned above. The sporadic presentation of the disease appears to also have a complex genetic etiology; *NF1* that, of the known susceptibility genes, has one of the lowest associated incidences of PCC/PGL has recently been found to play a very important role in the sporadic presentation of the disease (11). For all these reasons, the genetic diagnosis, genetic counseling and clinical follow-up of patients with PCC/PGL syndromes are major challenges.

The most recent addition to the growing list of PCC/PGL-associated genes is endothelial PAS domain-containing protein 1 (*EPAS1*) (12). *EPAS1*, also known as *HIF2A*, encodes one of the members of the hypoxia inducible factor (HIF) family of transcriptional regulators involved in hypoxic response (13). Zhuang *et al.* (12) described somatic mutations in *EPAS1* in two unrelated patients presenting with multiple PGLs. The mutations seemed to occur during early embryogenesis because both patients also had congenital erythrocytosis and one of them developed multiple somatostatinomas. Despite the fact that germline gain-of-function mutations affecting this gene are associated with increased erythropoietin and familial erythrocytosis (14–16), and unlike what happens with mutations in other polycythemia-related genes such as *VHL* and EGL nine homolog 1 (17), none of *EPAS1* mutation carriers developed cancer. The discovery of somatic mutations affecting *EPAS1* in PCC/PGL not only once again links polycythemia and cancer, but it also adds further weight to the hypothesis that the stabilization of HIF-alpha is important in chromaffin tumor development. This process, known as pseudo-hypoxia, has been described in PCC/PGL harboring mutations in *VHL* or in the succinate dehydrogenase (SDH) genes (18). Like *EPAS1* mutations, pseudo-hypoxia prolongs the half-life of HIF-alpha and triggers the activation of the cellular adaptation to hypoxia in *VHL*- and *SDH*-related tumors (19), which seems to be of pivotal importance in the development of other neural crest tumors (20).

In the present study, we tested for *EPAS1* mutations in three patients with multiple PCC/PGLs and erythrocytosis, as well as an additional series of 38 PCCs/PGLs, and described the clinical, molecular and genetic features of seven patients carrying somatic *EPAS1* mutations. Of note, only three of these seven patients with EPAS1-mutated tumors presented with congenital erythrocytosis and three had a single sporadic PCC/PGL.

RESULTS

Somatic *EPAS1* mutations are frequently found in PCC/PGL

We first genotyped exon 12 of *EPAS1* in three tumors from three unrelated individuals who had developed multiple PCC/PGLs and congenital erythrocytosis. Three missense mutations, p.Ala530Thr, p.Pro531Ser and p.Pro531Leu, were found in three tumors (Table 1). To assess the involvement of *EPAS1* mutations in PCC/PGL development, genotyping of exon 12 was also performed in 38 apparently sporadic tumors. Four non-truncating mutations were identified in four independent tumors: two were missense variants (p.Ala530Val and p.Asp539Tyr) and two were in-frame deletions (p.Ile533_Pro534del and p.Pro534_Asp536del) (Table 1). The p.Pro531Ser and pPro531Leu mutations affect the primary prolyl hydroxylation site, Pro-531, in *EPAS1*, whereas the remaining variants affect amino acids in proximity to this site. The two mutations involving Ala-530 had been previously reported (12); the other five were novel variants. None of the mutations were found in the corresponding patients' germline DNA. The subsequent analysis of additional tumors developed by cases 1, 3 and 4 (Table 1) confirmed the presence of the same mutations (p.Ala530Thr, p.Pro531Ser and p.Pro531Leu, respectively), suggesting that the mutations occurred in a chromaffin precursor cell in these three cases. Moreover, the mutations found in tumors were neither present in extra-adrenal normal tissue (cases 2 and 3) nor in a non-neural-crest tumor obtained from case 2, supporting that a genetic mosaicism occurred in these patients. The analysis of normal adrenal tissue adjacent to the tumor obtained from one of the patients who developed a single tumor (case 7, Table 1) revealed the absence of the mutated allele, demonstrating that, at least in this case, the somatic mutation occurred only in the tumor.

The screening for mutations in exon 12 of the *EPAS1* gene carried out in germline DNA from 186 patients without mutations in the known susceptibility genes revealed a missense variant (c.1700T > C; p.Met567Thr) in two apparently sporadic cases (Table 1). Alamut software predicts that the variant is not deleterious because it affects a moderately conserved residue, and the change to threonine is not physicochemically relevant. Furthermore, this variant was found in 1 of 4300 European individuals in the NHLBI Exome Sequencing Project and in 3 of 254 Spanish controls included in the present study. Based on these findings and the mild phenotype of the corresponding patients, we concluded that this variant is not disease causing.

Gain of 2p is an alteration exclusive to tumors harboring *EPAS1* mutations

High-density single nucleotide polymorphism (SNP) genotyping performed in four *EPAS1*-mutated tumors revealed that three carried a gain of the short arm of chromosome 2 that

Table 1. Clinical presentation and genetic data for patients carrying variants in exon 12 of *EPAS1*

ID	Age at onset	Sex	Tumor (*n*)	Congenital erythrocytosis (age at onset)	Secretion	Other tumors (age at onset)	Tumor variant cDNA	Protein	Germline variant	2p gain[a]	*EPAS1* gain[b]
1	18, 22, 26	F	PCC, TA PGLs (6)	Yes (1 year)	EPO, NE, DA	No	c.1588G > A	p.Ala530Thr	No	Yes	–
2	40	F	bPCC, TA PGLs (3)	No	E, NE	Basal cell carcinoma (75 years)	c.1589C > T	p.Ala530Val	No	ND	ND
3	13, 22, 23	M	PCC, TA PGL (3)	Yes (7 years)	EPO	Parotid adenoma (21 years)	c.1591C > T	p.Pro531Ser	No	ND	ND
4	18, 20	F	PCC, TA PGLs (5)	Yes (1 year)	EPO	No	c.1592C > T	p.Pro531Leu	No	ND	ND
5	46	F	PCC	No	n.a.	No	c.1599_1604del	p.Ile533_Pro534del	No	Yes	–
6	43	F	PCC	No	E, NE	Uterine myoma (41 years)	c.1600_1608del	p.Pro534_Asp536del	No	Yes	–
7	78	F	TA PGL	No	n.a.	No	c.1615G > T	p.Asp539Tyr	No	No	Yes
8	73	F	PCC	No	n.a.	No	–	–	c.1700T > C	–	–
9	46	F	PCC	No	NE, DA	No	–	–	c.1700T > C	–	–

F, female; M, male; PCC, pheochromocytoma; PGL, paraganglioma; bPCC, bilateral PCC; TA, thoracic-abdominal; NE, norepinephrine; E, epinephrine, EPO, erythropoietin; DA, dopamine; n.a., not available; ND, not done due to poor DNA quality.
[a]Gain detected by SNP-array analysis.
[b]Gain detected by multiplex-PCR analysis.

includes *EPAS1* (Fig. 1A; Table 1). To investigate whether this somatic mechanism could be exclusive to tumors carrying *EPAS1* mutations, we interrogated SNP array data from a further 94 PCC/PGLs with or without mutations in other PCC/PGL susceptibility genes (Data not shown), 34 of which had no somatic mutations in *EPAS1*, and found that none presented a gain of chromosome 2p ($P = 4.7 \times 10^{-4}$). We found by allele-specific PCR that the duplication of 2p detected in the *EPAS1*-mutated cases affected the mutated allele in one tumor and the non-mutated allele in the other two (Supplementary Material, Fig. S1A and B). Using a multiplex-PCR assay for the detection of chromosomal rearrangements under SNP-array detection limits, we identified the specific gain of *EPAS1* in one of the *EPAS1*-mutated cases and in three additional *EPAS1*-mutation-negative tumors (Supplementary Material, Fig. S1C). Genotyping of the two additional *EPAS1* prolyl hydroxylation sites (Pro-405 and Asn-847) revealed no mutations in the three tumors with specific *EPAS1* gain, or in the remaining 31 *EPAS1*-mutation-negative tumors. The same negative result was obtained when exon 12 of both *HIF1A* and *HIF3A* was analyzed in the 34 *EPAS1*-mutation-negative tumors.

EPAS1-mutated tumors showed overexpression of several hypoxia-induced genes

It has been reported that gain-of-function mutations in *EPAS1* lead to the up-regulation of hypoxia-related genes (12). To assess whether the tumors carrying *EPAS1* mutations exhibited a characteristic pseudo-hypoxic transcriptional profile, we used previously reported gene expression data from four of the seven *EPAS1*-mutated tumors (21). A previous hierarchical cluster analysis had grouped one of the *EPAS1*-mutated tumors in 'cluster 1', composed primarily of pseudo-hypoxic PCCs, whereas the remaining three cases were spread across the Ras/PI3K/mammalian target of rapamycin cluster ('cluster 2') (21). To decipher the particular hypoxic profile of *EPAS1*-mutated tumors, we carried out a supervised cluster analysis of the 4 altered tumors when compared with 22 sporadic tumors negative for mutations in *EPAS1* included in the original expression profile study. This analysis revealed 12 probes (corresponding to 11 genes) significantly up-regulated in *EPAS1* tumors (Fig. 1B) and 3 of these (*TMEM45A*, *PCSK6* and *LMO4*) were known hypoxia-induced genes (22–24). After excluding 6 tumors suspected to carry *NF1* somatic mutations (because they exhibited known chromosome 17 losses), the up-regulation of 4 of the 11 genes remained significant: *PCSK6*, *GNA14*, *AMZ1* and *THC2316750* (denoted in red in Fig. 1B). Furthermore, we found significantly higher levels of *EPAS1* mRNA expression in the *EPAS1*-mutated tumors when compared with 'cluster 2' cases ($P = 0.002$, Supplementary Material, Fig. S2); no differences in expression were found when we compared *EPAS1*-mutated tumors with pseudo-hypoxic cases ('cluster 1', *SDH* and *VHL*). Finally, the sporadic tumor group, which included cases belonging to both PCC transcriptional clusters, showed an intermediate level of expression, suggesting that it includes both pseudo-hypoxic and non-pseudo-hypoxic cases. When we subclassified these cases depending on the transcriptional cluster they belonged to, we found significant differences with the *EPAS1*-mutated tumors within each subgroup, confirming that 'cluster 1' sporadic cases are even more pseudo-

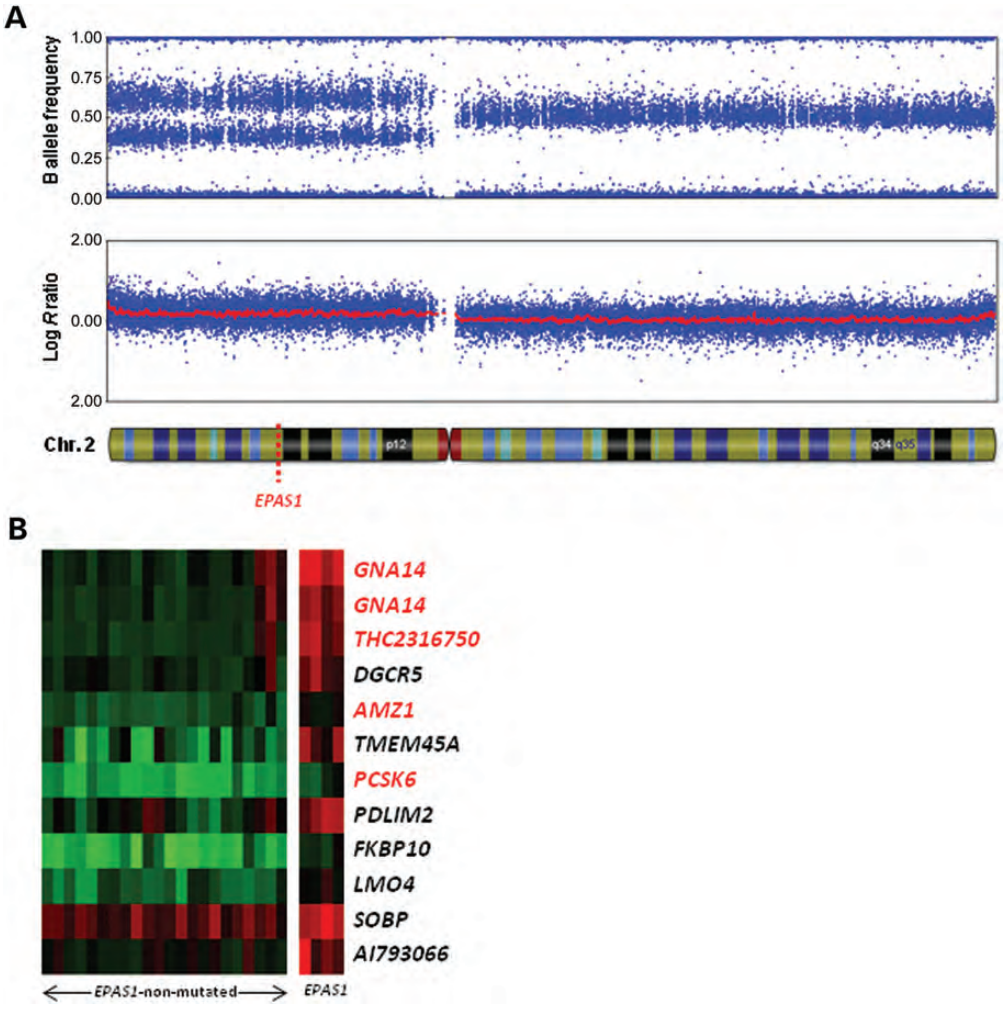

Figure 1. (**A**) SNP-array analysis of chromosome 2 performed with tumor DNA from the patient carrying the p.Ile533_Pro534del mutation reveals a gain of the short arm. The lower panel shows the genomic plots of the log R ratio [$\log_2$(Rpatient/Rreference)], indicating the presence of three alleles along the short arm. The upper panel gives the allele frequency parameters along chromosome 2, showing that the heterozygous state splits into two clusters. The chromosomal location of *EPAS1* is also indicated; (**B**) Heat map showing the 11 genes (represented in the rows) differentially up-regulated (FDR < 0.15) in the supervised cluster analysis of *EPAS1*-mutated and *EPAS1*-non-mutated tumors (represented in the columns). Significantly up-regulated genes after ruling out tumors potentially NF1 mutated are highlighted in red. Color bar: green and red colors represent $\geq$2-fold relative under- and over-expression, respectively.

hypoxic and that 'cluster 2' sporadic tumors exhibit a non-hypoxic expression profile similar to the mutated tumors from this cluster ($P = 0.038$ and $P = 0.029$, respectively).

DISCUSSION

The presence of known germline mutations in almost 40% of patients means that PCC/PGL is one of the human tumor entities with the highest explained heritability worldwide. In addition, the demonstrated relevance of somatic mutations affecting some of the susceptibility genes (especially *NF1*) in the sporadic forms of the disease has rapidly increased during recent years to 24–35% of cases (11,25). The discovery of somatic post-zygotic *EPAS1* mutations in patients developing multiple PCC/PGLs represents a new twist in the genetics of the disease and means that some patients who apparently exhibit a familial phenotype are really non-hereditary. In the present study, we found somatic *EPAS1* mutations not only in three additional patients with multiple PCC/PGLs, but also in three cases presenting with single tumors, the latter result revealing *EPAS1* as a new gene involved in the sporadic presentation of the disease. Overall, after excluding the three selected cases with multiple tumors and erythrocytosis, mutations affecting the *EPAS1* gene accounted for 10% of the consecutive tumors analyzed in this study which suggests that this somatic oncogenic event is one of the most relevant in the development of sporadic PCC/PGL, together with *NF1*, *VHL* and *RET* alterations.

The Pro-531 mutations constitute the first example of variants causing the direct abrogation of prolyl hydroxylation in *EPAS1*. In addition, as occurs with mutations found in patients with familial erythrocytosis, the remaining *EPAS1* variants identified in the present study affect amino acids in proximity to the primary prolyl hydroxylation site (Fig. 2) and could, therefore, affect the conformation of the hydroxylation domain interfering with prolyl hydroxylase recognition, as

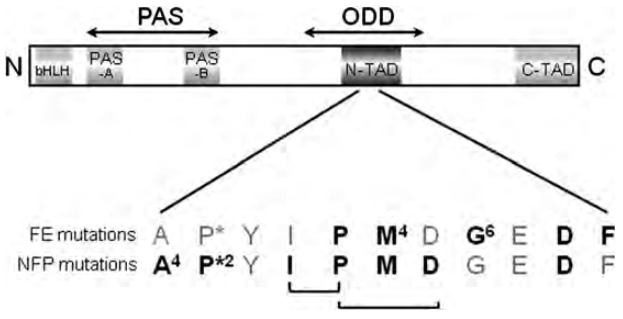

Figure 2. Schematic representation of *EPAS1* domains and the location of mutations (in bold letters) along the N-TAD. N-TAD, N-terminal transcriptional activation domain; bHLH, basic helix-loop-helix domain; PAS, per-ARNT-Sim domains; ODD, oxygen-dependent degradation domain; C-TAD, C-terminal transcriptional activation domain; FE, familial erythrocytosis; NFP, non-familial paraganglioma/PCC; *: primary site of prolyl hydroxylation. In square brackets are the residues affected by the two in-frame deletions. Numbers denote more than one case found carrying a mutation in the specified amino acid.

demonstrated for the Ala-530 substitutions (12). The identification of two new cases harboring mutations in Ala-530, and another one involving Asp-539, a residue mutated in a patient with erythrocytosis (26), suggests that these two amino acids could be hotspots for both erythrocytosis and PCC/PGL. On the other hand, the absence of PCCs and PGLs in the reported cases of familial erythrocytosis carrying *EPAS1* germline mutations suggests that, as occurs with mutations in the *VHL* gene, different mutations in *EPAS1* predispose to different diseases. Nevertheless, we cannot rule out that additional genetic factors modulate the clinical phenotype of *EPAS1* mutation carriers. In the case of the patient with multiple tumors found to carry one of the Ala-530 mutations (previously reported in a patient with erythrocytosis and PGLs) (12), the absence of erythrocytosis could be related to the time at which the mutation occurs. Studying a larger number of patients with erythrocytosis and/or PCC/PGL who carry *EPAS1* mutations could help to solve this new phenotypic puzzle.

As recently reported for PCCs carrying somatic mutations in *NF1*, the detection of a specific copy number alteration may guide the genetic diagnosis of the disease. Indeed, it is nowadays accepted that negative immunostaining for SDHB, partially due to the somatic loss of chromosome 1p, almost guarantees the detection of a mutation in one of the SDH genes (27). The exclusive gain of chromosome 2p identified in three of the four *EPAS1*-mutated tumors analyzed, and the specific gain of the gene detected in another mutated case, could, therefore, be used to select candidate tumors to be analyzed for mutations in this particular gene, avoiding unnecessary expenses. Unexpectedly, we found that the chromosomal gain of 2p affected both the wild-type and the mutated alleles alike (Supplementary Material, Fig. S1A and B). There are three well-known genetic mechanisms to activate oncogenes in human neoplasm: activating mutations, gene amplifications and chromosomal rearrangements. Although it is widely accepted that a single altered copy of an oncogene is sufficient to cause alterations in cell growth, it has been reported that PCCs in patients carrying germline activating mutations in *RET* may harbor either somatic duplications of the mutated allele or loss of the wild-type *RET* allele (28). Although duplication of the mutated allele would lead to higher amount of stabilized EPAS1 protein, somatic gain of an extra copy of the wild-type allele can also activate the hypoxic response in the tumor. This is because, in the case of a monomeric protein such as EPAS1, a dominant negative effect is not required. Finally, the detection of the specific gain of the gene in three *EPAS1*-mutation-negative cases strongly suggests that somatic gain of *EPAS1* could be a driving oncogenic event in some PCCs/PGLs.

A hierarchical cluster analysis suggested that *EPAS1*-mutated tumors do not exhibit the classical pseudo-hypoxic profile of VHL and SDH cases. Nevertheless, we found two hypoxia-related genes that were up-regulated in *EPAS1*-mutated cases when compared with sporadic tumors without *EPAS1* mutations: *PCSK6* and *GNA14*. Although the latter has not been reported as a hypoxia-related gene, it seems that it has an oxygen concentration-dependent expression and may play an important role in placental and fetal vascular endothelial functions, especially under chronic hypoxia (http://www.erp.wisc.edu/symposium/2012_abstracts.pdf). In addition, it has been reported that activation of the GNA14 protein can lead to STAT3 stimulation that plays a critical role in the development and function of normal hematopoietic cells (29). On the other hand, it is known that *PCSK6* overexpression resulted in enhanced susceptibility to carcinogenesis and tumor progression (30), and it has been proposed as an invasion-associated gene in malignant gliomas (31). The low number of hypoxia-related genes significantly up-regulated in *EPAS1*-mutated cases suggested that some of the sporadic tumors could harbor alterations in other hypoxia-related genes. That we found high *EPAS1* mRNA levels in 'cluster 1' sporadic tumors (Supplementary Material, Fig. S2) is consistent with this hypothesis. Interestingly, for two of these samples, the high mRNA expression of *EPAS1* was associated with the gain of the specific gene. Further studies are needed to assess the involvement of still unknown pseudo-hypoxic alterations in the development of sporadic tumors. Whereas *HIF1A* is ubiquitously expressed, *EPAS1* is encountered only in a limited number of cell types, with particularly elevated mRNA levels found in catecholamine-producing cells of the sympathetic nervous system (32). Interestingly, it has been proposed that the pattern of EPAS1 abundance may be responsible for the observed organ specificity of the VHL syndrome (33). Thus, considering that other organs affected in this syndrome, such as the retina, the kidney and the pancreas, also have high *EPAS1* expression levels, it is plausible that *EPAS1* driver mutations would be found in non-VHL hemangioblastomas, clear cell renal cell carcinomas or pancreatic neuroendocrine tumors. Indeed, the *EPAS1 locus* has been recently identified as a new genomic region associated with renal cell carcinoma risk (34).

In summary, the finding of somatic post-zygotic mutations affecting *EPAS1* in PCC/PGL patients suggests an alternative genetic explanation for the etiology of the disease in patients with multiple tumors, but not germline mutations. In addition, the discovery of the involvement of this gene in the sporadic presentation of the disease (i.e. one single tumor) not only increases the percentage of tumors with known driver mutations, but also highlights the relevance of studying other

hypoxia-related genes in apparently sporadic PCC/PGLs. Finally, the detection of a specific copy number alteration affecting *EPAS1* may guide the genetic diagnosis of the disease in these patients.

MATERIALS AND METHODS

Tumors and patients

Three tumors, one frozen and two formalin-fixed paraffin-embedded (FFPE), were obtained from patients with multiple PGLs/PCCs and congenital erythrocytosis. In addition, frozen tumors were obtained through the Spanish National Tumor Bank Network in Madrid (Spain) for a total of 38 unrelated consecutive patients with PCC/PGL who were tested negative for germline and somatic mutations in the major susceptibility genes *VHL*, *RET*, *SDHB*, *SDHC*, *SDHD*, *TMEM127* and *MAX*. Additional FFPE PCCs/PGLs were obtained from three of the four cases with somatic *EPAS1* mutations who developed multiple tumors (a second tumor from cases 1 and 3 and the five additional tumors from case 4; Table 1); other tissue specimens were obtained from case 2 (bone and basal cell carcinoma), case 4 (lymphatic ganglia and intestine) and case 7 (normal adrenal medulla). A further 186 consecutive non-related index patients without germline mutations in *VHL*, *RET*, *SDHA*, *SDHB*, *SDHC*, *SDHD*, *SDHAF2*, *TMEM127* and *MAX* were also included in the study. All patients were clinically diagnosed in public Spanish hospitals with functioning or non-functioning PCC/PGL. Genomic DNA was obtained from tumor tissue using the DNAeasy (Qiagen Inc., Valencia, CA, USA) kit and from blood samples using a standard procedure (35). Clinical data were collected for all patients by means of detailed questionnaires, and written informed consent was obtained from each patient. We used DNA from 254 unrelated unaffected individuals as a control sample for the study of the variant of unknown significance detected in the germline genetic screening.

Mutational and molecular analyses

Analysis of point mutations affecting exon 12 of *EPAS1* (ENST00000263734, NM_001430.4), which contains the primary hydroxylation site of the protein, was performed both in tumor and germline DNA, as well as in the non-paraganglionic tissue samples, using a standard PCR amplification protocol. Additional analysis of the 2 remaining *EPAS1* hydroxylation sites (i.e. Pro-405 and Asn-847 located in exons 9 and 16, respectively), and exon 12 of *HIF1A* (ENST00000337138, NM_001530.3) and *HIF3A* (ENST00000377670, NM_152795.3), was performed in the 34 frozen tumors without mutations at the primary site. PCR conditions and primers are available on request. The Alamut® mutation interpretation software (http://www.interactivebiosoftware.com/software.html) was used to assess the pathogenicity of the germline variants identified.

SNP-array and multiplex-PCR analyses

To investigate the presence of chromosomal rearrangements in the tumors, we performed high-density SNP-array analysis in four *EPAS1*-mutated cases (three of the tumors were not analyzed due to poor DNA quality). A genome-wide scan of 616 795 markers was conducted on 250 ng of tumor DNA, using the Illumina Human610-Quad BeadChip according to the manufacturer's specifications. Image data were analyzed using the Chromosome Viewer tool contained in GenomeStudio 2010.2 (Illumina). The metric used was the log-R ratio that is the binary logarithm of the ratio of the observed to expected normalized *R* values for a given SNP (36). The allele frequency was also estimated for all SNPs. *EPAS1* genomic gains were assessed in the 40 tumors by multiplex-PCR, including 2 pairs of primers for exons 12 and 14, as previously described for other genes (37). A similar semi-quantitative multiplex-PCR method was used to investigate which allele was duplicated in the three tumors exhibiting chromosome 2p gain in the array-SNP analysis. Briefly, we first designed and labeled (5′ 6-FAM) two pairs of primers for each mutation that discriminated the wild-type allele from the mutated allele. Following that, three cocktails containing each specific pair of primers mixed with three control-labeled pairs of primers for chromosomes 5 and 16 (as internal controls) were prepared and used to amplify the corresponding tumor DNA by multiplex-PCR. The subsequent normalization was performed for each PCR product by overlapping each tumor sample with a control sample using the Peak Scanner™ software (Applied Biosystems, Foster City, CA, USA), as previously described for other genes (37).

Gene expression analysis

To identify specific transcripts related to EPAS1 deregulation, we used gene expression data for four of the 7 mutated tumors and for 22 sporadic cases negative for mutations affecting *EPAS1* exon 12, as deposited in the National Center for Biotechnology Information GEO database under the accession number GSE19422 (21). A *t*-test was applied using POMELOII (http://pomelo2.bioinfo.cnio.es/) to compare the expression of individual genes between the two groups (38). Benjamini's false discovery rate (FDR) correction was used to account for multiple testing (39); genes up-regulated in the mutated tumors with an FDR < 0.15 were selected as differentially expressed. In addition, we assessed the mRNA expression of *EPAS1* in the whole series of PCC/PGLs (21), by the gene mutated. Considering that some of the sporadic cases included in the present study could have *NF1*-mutated tumors, we performed a second analysis excluding the six that exhibited chromosome 17 losses, based on the report that 84–90% of tumors with these losses harbor mutations in *NF1* (11,25).

Statistical analysis

Difference in frequency of 2p gain between *EPAS1*-mutation-positive and -negative cases was assessed by Fisher's exact test, using the SPSS software, version 17.0 (SPSS Inc., Chicago, IL, USA).

SUPPLEMENTARY MATERIAL

Supplementary Material is available at *HMG* online.

Conflict of Interest statement. A.A.d.C. and V.M. are predoctoral fellows of 'la Caixa'/CNIO International PhD Programme. L.I.-P. and I.C.-M. are predoctoral fellows of the CIBERER and the Fundacion Ferrer, respectively.

FUNDING

This work was supported in part by the Fondo de Investigaciones Sanitarias (projects PI12/00236 and PI11/01359 to A.C. and M.R., respectively), the Fundación Mutua Madrileña (project AP2775/2008 to M.R.) and a grant from the European Community's Seventh Framework Programme (ENS@T-CANCER; HEALTH-F2-2010-259735).

REFERENCES

1. Latif, F., Tory, K., Gnarra, J., Yao, M., Duh, F.M., Orcutt, M.L., Stackhouse, T., Kuzmin, I., Modi, W., Geil, L. *et al.* (1993) Identification of the von Hippel-Lindau disease tumor suppressor gene. *Science*, **260**, 1317–1320.
2. Mulligan, L.M., Kwok, J.B., Healey, C.S., Elsdon, M.J., Eng, C., Gardner, E., Love, D.R., Mole, S.E., Moore, J.K., Papi, L. *et al.* (1993) Germ-line mutations of the RET proto-oncogene in multiple endocrine neoplasia type 2A. *Nature*, **363**, 458–460.
3. Wallace, M.R., Andersen, L.B., Saulino, A.M., Gregory, P.E., Glover, T.W. and Collins, F.S. (1991) A de novo Alu insertion results in neurofibromatosis type 1. *Nature*, **353**, 864–866.
4. Hao, H.X., Khalimonchuk, O., Schraders, M., Dephoure, N., Bayley, J.P., Kunst, H., Devilee, P., Cremers, C.W., Schiffman, J.D., Bentz, B.G. *et al.* (2009) SDH5, a gene required for flavination of succinate dehydrogenase, is mutated in paraganglioma. *Science*, **325**, 1139–1142.
5. Burnichon, N., Briere, J.J., Libe, R., Vescovo, L., Riviere, J., Tissier, F., Jouanno, E., Jeunemaitre, X., Benit, P., Tzagoloff, A. *et al.* (2010) SDHA is a tumor suppressor gene causing paraganglioma. *Hum. Mol. Genet.*, **19**, 3011–3020.
6. Comino-Mendez, I., Gracia-Aznarez, F.J., Schiavi, F., Landa, I., Leandro-Garcia, L.J., Leton, R., Honrado, E., Ramos-Medina, R., Caronia, D., Pita, G. *et al.* (2011) Exome sequencing identifies MAX mutations as a cause of hereditary pheochromocytoma. *Nat. Genet.*, **43**, 663–667.
7. Qin, Y., Yao, L., King, E.E., Buddavarapu, K., Lenci, R.E., Chocron, E.S., Lechleiter, J.D., Sass, M., Aronin, N., Schiavi, F. *et al.* (2010) Germline mutations in TMEM127 confer susceptibility to pheochromocytoma. *Nat. Genet.*, **42**, 229–233.
8. Baysal, B.E., Ferrell, R.E., Willett-Brozick, J.E., Lawrence, E.C., Myssiorek, D., Bosch, A., van der Mey, A., Taschner, P.E., Rubinstein, W.S., Myers, E.N. *et al.* (2000) Mutations in SDHD, a mitochondrial complex II gene, in hereditary paraganglioma. *Science*, **287**, 848–851.
9. Astuti, D., Latif, F., Dallol, A., Dahia, P.L., Douglas, F., George, E., Skoldberg, F., Husebye, E.S., Eng, C. and Maher, E.R. (2001) Gene mutations in the succinate dehydrogenase subunit SDHB cause susceptibility to familial pheochromocytoma and to familial paraganglioma. *Am. J. Hum. Genet.*, **69**, 49–54.
10. Niemann, S. and Muller, U. (2000) Mutations in SDHC cause autosomal dominant paraganglioma, type 3. *Nat. Genet.*, **26**, 268–270.
11. Burnichon, N., Buffet, A., Parfait, B., Letouze, E., Laurendeau, I., Loriot, C., Pasmant, E., Abermil, N., Valeyrie-Allanore, L., Bertherat, J. *et al.* (2012) Somatic NF1 inactivation is a frequent event in sporadic pheochromocytoma. *Hum. Mol. Genet*, **21**, 5397–5405
12. Zhuang, Z., Yang, C., Lorenzo, F., Merino, M., Fojo, T., Kebebew, E., Popovic, V., Stratakis, C.A., Prchal, J.T. and Pacak, K. (2012) Somatic HIF2A gain-of-function mutations in paraganglioma with polycythemia. *N. Engl. J. Med.*, **367**, 922–930.
13. Tian, H., McKnight, S.L. and Russell, D.W. (1997) Endothelial PAS domain protein 1 (EPAS1), a transcription factor selectively expressed in endothelial cells. *Genes Dev.*, **11**, 72–82.
14. Percy, M.J., Furlow, P.W., Lucas, G.S., Li, X., Lappin, T.R., McMullin, M.F. and Lee, F.S. (2008) A gain-of-function mutation in the HIF2A gene in familial erythrocytosis. *N. Engl. J. Med.*, **358**, 162–168.
15. Percy, M.J., Chung, Y.J., Harrison, C., Mercieca, J., Hoffbrand, A.V., Dinardo, C.L., Santos, P.C., Fonseca, G.H., Gualandro, S.F., Pereira, A.C. *et al.* (2012) Two new mutations in the HIF2A gene associated with erythrocytosis. *Am. J. Hematol.*, **87**, 439–442.
16. Percy, M.J., Beer, P.A., Campbell, G., Dekker, A.W., Green, A.R., Oscier, D., Rainey, M.G., van Wijk, R., Wood, M., Lappin, T.R. *et al.* (2008) Novel exon 12 mutations in the HIF2A gene associated with erythrocytosis. *Blood*, **111**, 5400–5402.
17. Lee, F.S. and Percy, M.J. (2011) The HIF pathway and erythrocytosis. *Annu. Rev. Pathol.*, **6**, 165–192.
18. Dahia, P.L., Ross, K.N., Wright, M.E., Hayashida, C.Y., Santagata, S., Barontini, M., Kung, A.L., Sanso, G., Powers, J.F., Tischler, A.S. *et al.* (2005) A HIF1alpha regulatory loop links hypoxia and mitochondrial signals in pheochromocytomas. *PLoS Genet.*, **1**, 72–80.
19. Maxwell, P.H. (2005) A common pathway for genetic events leading to pheochromocytoma. *Cancer Cell*, **8**, 91–93.
20. Holmquist-Mengelbier, L., Fredlund, E., Lofstedt, T., Noguera, R., Navarro, S., Nilsson, H., Pietras, A., Vallon-Christersson, J., Borg, A., Gradin, K. *et al.* (2006) Recruitment of HIF-1alpha and HIF-2alpha to common target genes is differentially regulated in neuroblastoma: HIF-2alpha promotes an aggressive phenotype. *Cancer Cell*, **10**, 413–423.
21. Lopez-Jimenez, E., Gomez-Lopez, G., Leandro-Garcia, L.J., Munoz, I., Schiavi, F., Montero-Conde, C., de Cubas, A.A., Ramires, R., Landa, I., Leskela, S. *et al.* (2010) Research resource: transcriptional profiling reveals different pseudohypoxic signatures in SDHB and VHL-related pheochromocytomas. *Mol. Endocrinol.*, **24**, 2382–2391.
22. Martin-Rendon, E., Hale, S.J., Ryan, D., Baban, D., Forde, S.P., Roubelakis, M., Sweeney, D., Moukayed, M., Harris, A.L., Davies, K. *et al.* (2007) Transcriptional profiling of human cord blood CD133+ and cultured bone marrow mesenchymal stem cells in response to hypoxia. *Stem Cells*, **25**, 1003–1012.
23. Egger, M., Schgoer, W., Beer, A.G., Jeschke, J., Leierer, J., Theurl, M., Frauscher, S., Tepper, O.M., Niederwanger, A., Ritsch, A. *et al.* (2007) Hypoxia up-regulates the angiogenic cytokine secretoneurin via an HIF-1alpha- and basic FGF-dependent pathway in muscle cells. *FASEB J.*, **21**, 2906–2917.
24. Chen, H.H., Schock, S.C., Xu, J., Safarpour, F., Thompson, C.S. and Stewart, A.F. (2007) Extracellular ATP-dependent upregulation of the transcription cofactor LMO4 promotes neuron survival from hypoxia. *Exp. Cell. Res.*, **313**, 3106–3116.
25. Welander, J., Larsson, C., Backdahl, M., Hareni, N., Sivler, T., Brauckhoff, M., Soderkvist, P. and Gimm, O. (2012) Integrative genomics reveals frequent somatic NF1 mutations in sporadic pheochromocytomas. *Hum. Mol. Genet*, **21**, 5406–5416
26. van Wijk, R., Sutherland, S., Van Wesel, A.C., Huizinga, E.G., Percy, M.J., Bierings, M. and Lee, F.S. (2010) Erythrocytosis associated with a novel missense mutation in the HIF2A gene. *Haematologica*, **95**, 829–832.
27. van Nederveen, F.H., Gaal, J., Favier, J., Korpershoek, E., Oldenburg, R.A., de Bruyn, E.M., Sleddens, H.F., Derkx, P., Riviere, J., Dannenberg, H. *et al.* (2009) An immunohistochemical procedure to detect patients with paraganglioma and phaeochromocytoma with germline SDHB, SDHC, or SDHD gene mutations: a retrospective and prospective analysis. *Lancet Oncol.*, **10**, 764–771.
28. Huang, S.C., Koch, C.A., Vortmeyer, A.O., Pack, S.D., Lichtenauer, U.D., Mannan, P., Lubensky, I.A., Chrousos, G.P., Gagel, R.F., Pacak, K. *et al.* (2000) Duplication of the mutant RET allele in trisomy 10 or loss of the wild-type allele in multiple endocrine neoplasia type 2-associated pheochromocytomas. *Cancer Res.*, **60**, 6223–6226.
29. Lo, R.K. and Wong, Y.H. (2004) Signal transducer and activator of transcription 3 activation by the delta-opioid receptor via Galpha14 involves multiple intermediates. *Mol. Pharmacol.*, **65**, 1427–1439.
30. Bassi, D.E., Lopez De Cicco, R., Cenna, J., Litwin, S., Cukierman, E. and Klein-Szanto, A.J. (2005) PACE4 expression in mouse basal keratinocytes results in basement membrane disruption and acceleration of tumor progression. *Cancer Res.*, **65**, 7310–7319.
31. Delic, S., Lottmann, N., Jetschke, K., Reifenberger, G. and Riemenschneider, M.J. (2012) Identification and functional validation of CDH11, PCSK6 and SH3GL3 as novel glioma invasion-associated candidate genes. *Neuropathol. Appl. Neurobiol.*, **38**, 201–212.

32. Favier, J., Kempf, H., Corvol, P. and Gasc, J.M. (1999) Cloning and expression pattern of EPAS1 in the chicken embryo. Colocalization with tyrosine hydroxylase. *FEBS Lett.*, **462**, 19–24.
33. Maranchie, J.K., Vasselli, J.R., Riss, J., Bonifacino, J.S., Linehan, W.M. and Klausner, R.D. (2002) The contribution of VHL substrate binding and HIF1-alpha to the phenotype of VHL loss in renal cell carcinoma. *Cancer Cell*, **1**, 247–255.
34. Purdue, M.P., Johansson, M., Zelenika, D., Toro, J.R., Scelo, G., Moore, L.E., Prokhortchouk, E., Wu, X., Kiemeney, L.A., Gaborieau, V. *et al.* (2011) Genome-wide association study of renal cell carcinoma identifies two susceptibility loci on 2p21 and 11q13.3. *Nat. Genet.*, **43**, 60–65.
35. Sambrook, J., Maniatis, T. and Fritsch, E.F. (1989) *Molecular Cloning: A Laboratory Manual*. Cold Spring Harbor Laboratory, Cold Spring Harbor, NY.
36. Simon-Sanchez, J., Scholz, S., Fung, H.C., Matarin, M., Hernandez, D., Gibbs, J.R., Britton, A., de Vrieze, F.W., Peckham, E., Gwinn-Hardy, K. *et al.* (2007) Genome-wide SNP assay reveals structural genomic variation, extended homozygosity and cell-line induced alterations in normal individuals. *Hum. Mol. Genet.*, **16**, 1–14.
37. Cascon, A., Montero-Conde, C., Ruiz-Llorente, S., Mercadillo, F., Leton, R., Rodriguez-Antona, C., Martinez-Delgado, B., Delgado, M., Diez, A., Rovira, A. *et al.* (2006) Gross SDHB deletions in patients with paraganglioma detected by multiplex PCR: a possible hot spot? *Genes Chromosomes Cancer*, **45**, 213–219.
38. Morrissey, E.R. and Diaz-Uriarte, R. (2009) Pomelo II: finding differentially expressed genes. *Nucleic Acids Res*, **37**, W581–W586.
39. Benjamini, Y., Drai, D., Elmer, G., Kafkafi, N. and Golani, I. (2001) Controlling the false discovery rate in behavior genetics research. *Behav. Brain Res.*, **125**, 279–284.

SUPPLEMENTARY MATERIAL

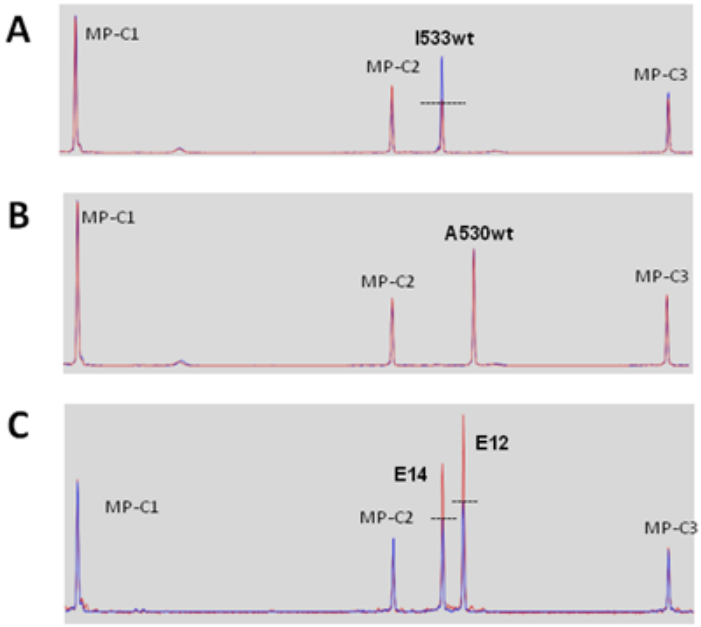

Supplementary Figure 1. Peak Scanner analysis of amplified PCR fragments, using wild-type allele-specific primers, of a control tumor sample (blue) overlapped with patient tumor samples (red): **A**, tumor sample carrying the mutation p.Ile533_Pro534del; **B**, tumor sample carrying the mutation p.Ala530Thr; **C**, tumor sample (red) negative for chromosome 2p gain by SNParray exhibiting specific *EPAS1* gain affecting exons 12 and 14, compared with a control sample (blue). Fragments MP-C1, MP-C2, and MP-C3 were used as internal controls for these assays.

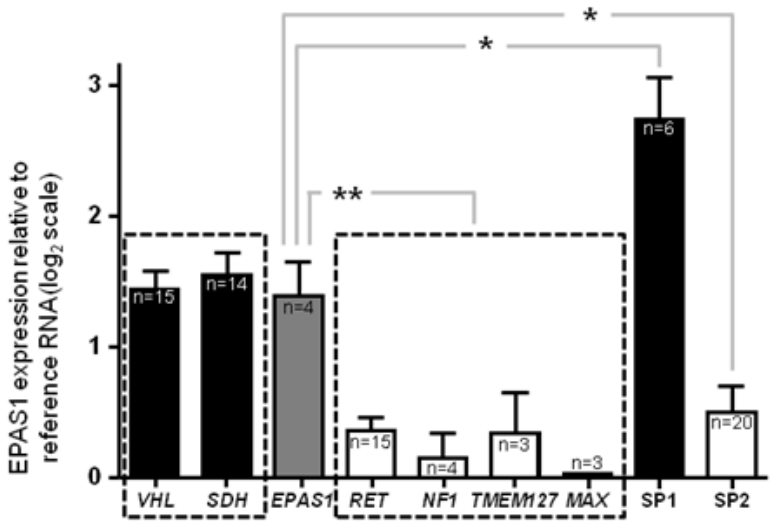

Supplementary Figure 2. n-fold *EPAS1* mRNA expression relative to reference RNA. Black rectangles represent "cluster 1" tumors, white rectangles, "cluster 2" tumors and grey rectangles mixed cluster 1 and 2 tumors; VHL, SDH, EPAS1, RET, NF1, TMEM127, and MAX: tumors carrying mutations in the corresponding pheochromocytoma/paraganglioma susceptibility gene; SP1: sporadic tumors belonging to cluster 1; SP2: sporadic tumors belonging to cluster 2.

ARTICLE 5: Whole-exome sequencing identifies *MDH2* as a new familial paraganglioma gene.

Authors: Alberto Cascón*, **Iñaki Comino-Méndez***, María Currás-Freixes, Aguirre A de Cubas, Laura Contreras, Susan Richter, Veronika Mancikova, Andrés Pérez- Barrios, María Calatayud, Sharona Azriel, Rosa Villar-Vicente, Javier Aller, Fernando Setién, Juan F Garcia, Ana Río-Machín, Rocío Letón, Álvaro Gómez-Graña, Lucía Inglada-Pérez, María Apellániz-Ruiz, Giovanna Roncador, Manel Esteller, Cristina Rodríguez-Antona, Jorgina Satrústegui, Graeme Eisenhofer, Miguel Urioste, and Mercedes Robledo.

In press in the Journal of the National Cancer Institute, 2015

ABSTRACT

This study started with the design of a WES project focused on patients presenting with multiple tumors and therefore candidates to be hereditary. After filtering known polymorphisms and variants causing low or moderate impact in the protein, we found a variant affecting the donor splice-site of *MDH2* in tumor DNA from one of the selected patients. *MDH2* encodes the mitochondrial malate dehydrogenase enzyme involved in the Krebs cycle. Disruption of Krebs cycle is a hallmark of cancer, and especially of PCC/PGL in which mutations affecting the *SDH*- or *FH* genes are involved in the susceptibility to the disease.

We first demonstrated the deleterious effect of the splice-site mutation, the presence of LOH in some tumors, and the absence of the protein in all available tumors. MDH2 enzymatic activity was almost abolished in the mutant tumors, and a high fumarate:succinate ratio suggested the accumulation of fumarate. Depletion of MDH2 in HeLa cells showed an accumulation of both fumarate and malate, that was partially restored upon reintroduction of wild-type MDH2. Gene expression analysis, as well as 5-hmC and H3K27me3 immunohistochemistry, of *MDH2*-mutated tumors showed a CpG island methylator phenotype typical of tumors harboring Krebs cycle alterations. Finally, segregation of the variant with the disease in the family further demonstrated the implication of the *MDH2* mutation in the disease, and suggested that it behaves as a classical tumor suppressor gene.

Overall, our finding of a novel PCC/PGL susceptibility gene once again links the disruption of the Krebs cycle with tumor development, and also suggests that alterations in other Krebs cycle genes may be involved in PCC/PGL susceptibility.

Personal contribution: I actively participated in the conception of the project, the preparation of the samples, the WES data analysis, the validation, and the mRNA and protein expression studies. I carried out the silencing of the gene in HeLa cells, and performed additional experiments and statistical analyses. Finally, I participated in the discussion and writing of the manuscript.

TITLE: Whole-exome sequencing identifies *MDH2* as a new familial paraganglioma gene

Alberto Cascón[1,2*†], Iñaki Comino-Méndez[1*], María Currás-Freixes[1], Aguirre A de Cubas[1], Laura Contreras[2,3], Susan Richter[4], Mirko Peitzsch[4], Veronika Mancikova[1], Lucía Inglada-Pérez[1,2], Andrés Pérez-Barrios[5], María Calatayud[6], Sharona Azriel[7], Rosa Villar-Vicente[8], Javier Aller[9], Fernando Setién[10], Sebastian Moran[10], Juan F Garcia[11], Ana Río-Machín[12], Rocío Letón[1], Álvaro Gómez-Graña[1], María Apellániz-Ruiz[1], Giovanna Roncador[13], Manel Esteller[10], Cristina Rodríguez-Antona[1,2], Jorgina Satrústegui[2,3], Graeme Eisenhofer[4], Miguel Urioste[2,14], and Mercedes Robledo[1,2†]

[1]Hereditary Endocrine Cancer Group, Spanish National Cancer Research Centre (CNIO), Melchor Fernández Almagro 3, Madrid, E-28029, Spain.

[2]Centro de Investigación Biomédica en Red de Enfermedades Raras (CIBERER), Madrid, Spain

[3]Departamento de Biología Molecular, Centro de Biología Molecular Severo Ochoa UAM-CSIC, Universidad Autónoma de Madrid and Instituto de Investigación Sanitaria Fundación Jiménez Díaz (IIS-FJD), Madrid, Spain

[4]Institute of Clinical Chemistry and Laboratory Medicine, University Hospital Carl Gustav Carus, Medical Faculty Carl Gustav Carus, Technische Universität Dresden, Dresden, Germany

[5]Department of Pathology, and [6]Endocrinology and Nutrition Service, Hospital 12 de Octubre, Madrid, Spain

[7]Endocrinology Service, Hospital Infanta Sofía, San Sebastián de los Reyes, Spain

[8]Department of Endocrinology and Nutrition Service, Hospital de Fuenlabrada, Madrid, Spain

[9]Endocrinology Service, Hospital Puerta de Hierro, Majadahonda, Madrid, Spain

[10]Cancer Epigenetics and Biology Program (PEBC), Bellvitge Biomedical Research Institute (IDIBELL), L'Hospitalet, Barcelona, Spain.

[11]Department of Pathology, M D Anderson Cancer Center Madrid, Madrid, Spain

[12]Molecular Cytogenetics Group, Spanish National Cancer Research Centre (CNIO), Madrid, Spain

[13]Monoclonal Antibodies Unit, Biotechnology Programme, Spanish National Cancer Research Centre (CNIO), Madrid, Spain

[14]Familial Cancer Clinical Unit, Spanish National Cancer Research Centre (CNIO), Madrid, Spain

*These two authors contributed equally to this article.

†Address correspondence to: Alberto Cascón or Mercedes Robledo

Hereditary Endocrine Cancer Group, Human Cancer Genetics Programme, Spanish National Cancer Research Centre (CNIO), Melchor Fernández Almagro 3, 28029 Madrid, Spain

Phone: +34 91 224 69 47; Fax: +34 91 224 69 23

e-mail: acascon@cnio.es; mrobledo@cnio.es

ABSTRACT

Disruption of the Krebs cycle is a hallmark of cancer. *IDH1* and *IDH2* mutations are found in many neoplasms, and germline alterations in SDH genes and *FH* predispose to pheochromocytoma/paraganglioma and other cancers. We describe a paraganglioma family carrying a germline mutation in *MDH2*, which encodes a Krebs cycle enzyme. Whole-exome sequencing was applied to tumor DNA obtained from a 55 year-old man diagnosed with multiple malignant paragangliomas. Data were analyzed with the Student t and two-sided Mann-Whitney U tests with Bonferroni correction for multiple comparisons. Between 6- and 14-fold lower levels of MDH2 expression was observed in *MDH2*-mutated tumors compared to controls. Knockdown (KD) of MDH2 in HeLa cells by shRNA triggered the accumulation of both malate (mean±SD: 1±0.18 [WT] vs 2.24±0.17 [KD]; *P*=.043) and fumarate (1±0.06 [WT] vs 2.6±0.25 [KD]; *P*=.033), which was reverted by transient introduction of WT MDH2 cDNA. Segregation of the mutation with disease and absence of MDH2 in mutated tumors reveal *MDH2* as a novel pheochromocytoma/paraganglioma susceptibility gene.

Pheochromocytomas and paragangliomas are tumors that mainly arise from the adrenal medulla and the sympathetic nervous system paraganglia, respectively. Since 1990, eleven major susceptibility genes have been identified: *NF1*, *RET*, *VHL*, *SDHA*, *SDHB*, *SDHC*, *SDHD*, *SDHAF2*, *TMEM127, MAX* and *FH*[1]. However, there are still some patients with clinical indicators of hereditary disease (i.e. family history, multiple tumors and/or young age) that are not explained by mutations in these genes.

Whole-exome sequencing was applied to tumor DNA obtained from a 55 year-old man diagnosed with multiple malignant paragangliomas. Five single nucleotide substitutions and eleven INDELs (insertions or deletions) passed the filtering process (**Supplementary Table 1, available online**). These included a heterozygous variant, c.429+1G>T, affecting a canonical donor splice site on exon 4 of *MDH2*, the gene that encodes the mitochondrial malate dehydrogenase enzyme involved in the Krebs cycle. After confirming the presence of the variant in the sequenced tumor and in peripheral blood lymphocytes from the patient, Sanger sequencing of the available primary tumors from the patient (n=4) revealed loss of the *MDH2* wild type allele in 2 tumors, indicating loss of heterozygosity (**Figure 1A**). Direct sequencing of the cDNA regions flanking the mutation demonstrated that c.429+1G>T gave rise to an altered transcript that incorporated 20 additional amino-acids into the exon as well as to a premature stop codon. Since the stop codon is followed by more than 50 nucleotides, it was considered potentially involved in nonsense-mediated decay[2] (**Figure 1B**). MDH2 mRNA expression analysis revealed 6- to 14-fold lower levels of MDH2 expression in the four tumors carrying the c.429+1G>T mutation, compared to controls (**Figure 1C**). In addition, substantially lower levels of MDH2 protein were detected in the *MDH2*-related tumors compared to controls (**Figure 1D**), suggesting that nonsense-mediated decay was occurring and confirming loss of expression of the wild-type allele in all mutated tumors. The *MDH2*-mutated tumor displayed statistically significantly lower MDH2 activity than that of control tumors (median [range]: 275.78 [181.69-882.43] vs 966.64 [221.07 - 3551.0]; *P*=.006) (**Figure 1E**), suggesting severe malate dehydrogenase deficiency. Krebs cycle metabolite analysis did not detect accumulation of malate in the *MDH2*-mutated tumor. However, a much higher fumarate:succinate ratio was observed in the *MDH2*-mutated tumor (mean±SD: 0.34±0.02) in comparison to succinate dehydrogenase (SDH) gene-mutated (mean±SD: 0.01±0.02; *P*=.044) and non-mutated (mean±SD: 0.06±0.10; *P*=.006) tumors (**Supplementary Figure 1**), suggesting that fumarate could be accumulated in *MDH2*-mutated cells. Knockdown of MDH2 expression in HeLa cells by shRNA (**Supplementary Figure 2A-C**) triggered the accumulation of both malate (mean±SD: 1±0.18 [WT] vs 2.24±0.17 [KD]; *P*=.043) and fumarate (mean±SD:1±0.06 [WT] vs 2.6±0.25 [KD]; *P*=.033) which was reverted by transient introduction of wild-type MDH2 cDNA (**Figure 1F-H**). Additional malate-utilizing enzymes (MDH1 and malic enzymes 1-3) could be responsible for the absence of malate accumulation in *MDH2*-mutated tumors. However, neither the observed MDH1 activity

(**Supplementary Table 2**) nor the expression of malic enzymes 1-3 (data not shown) in the *MDH2*-mutated tumors explain the absence of malate accumulation, suggesting that an unknown mechanism is accounting for this controversial result.

Several studies have demonstrated that the accumulation of succinate and fumarate, caused by SDH gene mutations and *FH* mutations, respectively, and the production of 2-hydroxyglutarate (2HG), associated with *IDH1* and *IDH2* alterations, lead to the enzymatic inhibition of multiple α-KG-dependent dioxygenases[5, 6]. This inhibition causes impaired histone demethylation and 5-mC hydroxylation (5-hmC), and, consequently, genome-wide histone and DNA methylation alterations. This in turn leads to a characteristic CpG island methylator phenotype (CIMP)[7], and provides a rationale for tumor development caused by Krebs cycle disruption. Expression profiling analysis based on genes that were hypermethylated and downregulated in SDH gene- and *FH*-mutated tumors and associated with the characteristic CIMP[7], revealed that the *MDH2*-mutated tumor and three apparently sporadic cases all clustered with SDH gene-mutated tumors, suggesting a similar CIMP (CIMP-like) profile (**Figure 2A**). Immunohistochemical evaluation of 5-hmC (**Figure 2B**) and trimethylation of histone H3 lysine 27 (H3K27me3) (**Supplementary Figure 3A**) were also consistent with the *MDH2*-mutated tumor having a CIMP-like profile. In addition, classification by retinol binding protein 1 (*RBP1*) expression, which is an exclusive biomarker for *IDH* mutations in gliomas[8], segregated the *MDH2*- with the SDH-mutated tumors (**Figure 2C** and **Supplementary Figure 3B**), providing further evidence that *MDH2* mutations are associated with a methylator phenotype. Finally, methylation analysis based on pyrosequencing of CpG sites in seven selected genes (including *RBP1*) (**Supplementary Figure 3C**) demonstrated that the genome-wide downregulation observed for the *MDH2*-mutated tumors was due to CpG island methylation.

A genetic study of five asymptomatic relatives of the patient found that two of them carried the *MDH2* c.429+1G>T mutation. MDH2 mRNA and protein expression in blood cells were statistically significantly lower in the two carriers compared to controls (median±SD: 0.33±0.07 [*P*=.0001] and 0.53±0.05 [*P*=.0001] vs 1.08±0.08, respectively), confirming that the splicing mutation has a deleterious effect (**Supplementary Figure 4)**. Subsequent clinical testing detected high levels of normetanephrine for one of the carriers (II-2), thus confirming the presence of the disease. Neither the three apparently sporadic cases with tumors that grouped within the CIMP-like cluster nor a selected series of cases with clinical features of a hereditary disease (**Supplementary Table 3**) had alterations in the *MDH2* gene.

During the last ten years, germline and acquired alterations affecting some of the enzymes involved in the Krebs cycle have been recognized as one of the hallmarks of cancer, and, more specifically, of pheochromocytoma/paraganglioma development. It is well known that germline mutations in the genes encoding the four structural subunits of the Krebs cycle enzyme SDH[9-12], or in the regulatory enzyme SDHAF2[13], predispose to hereditary pheochromocytoma/paraganglioma. In addition, inactivating

mutations in *FH* predispose to hereditary leiomyomatosis and renal cell cancer (HLRCC)[14], and have recently been identified in patients with pheochromocytoma/paraganglioma[7, 15]. Finally, *IDH1* and *IDH2* are frequently mutated in multiple types of human cancer, including one paraganglioma[16]. In the present study, we have demonstrated the deleterious effect of a germline *MDH2* mutation identified by whole-exome sequencing. We have also confirmed the absence of MDH2 protein in tumors carrying the variant, as well as the segregation of the c.429+1G>T mutation with the disease, suggesting that *MDH2* behaves as a classic tumor suppressor gene.

The *MDH2*-mutated tumor had not only a global transcriptional profile similar to SDH gene-mutated tumors, but also a CIMP-like signature consistent with Krebs cycle disruption. *Mdh2* function abrogation in *Drosophila* pupae results in a severe energy deficit and accumulation of late-stage Krebs cycle intermediates such as malate, succinate, and fumarate[17]. A similar mechanism occurs in *Fh1*-deficient cells which accumulate fumarate and succinate[18]. In the present study we have demonstrated that stable silencing of *MDH2* expression in HeLa cells also leads to malate and fumarate accumulation. Like succinate and fumarate, malate inhibits hypoxia inducible factor alpha (HIF-α) prolyl hydroxylation[19, 20]. Though no malate accumulation was found in the *MDH2*-mutated tumor, the high fumarate:succinate ratio detected suggests that fumarate accumulation may have been present, which would explain the CIMP-like profile observed. The finding of three SDH gene-, *FH*- and *MDH2*-negative tumors exhibiting the CIMP-like signature, points to the possibility that other, still hidden, molecular alterations in the Krebs cycle account for these cases, and for an unknown proportion of additional patients. The absence of paraganglioma in one of the three c.429+1G>T carriers suggests that the penetrance of mutations in this gene is incomplete, as is the case for *SDHB* mutations[21]. Interestingly, none of the seven *FH* mutation carriers described so far with pheochromocytoma/paraganglioma has a family history of the disease[22]. Moreover, mutations in the more recently discovered pheochromocytoma/paraganglioma susceptibility genes (*MAX*, *TMEM127* and *FH*) are present in less than 2% of cases without mutations in known genes[1, 15], and in fact none of the 239 Spanish patients screened for mutations was found to be carrier of an *FH* mutation. Finding additional *MDH2* mutation carriers will presumably require genetic screening of large cohorts of patients. Finally, only one truncating mutation (p.E153*) in *MDH2* is recorded in The Catalogue of Somatic Mutations in Cancer (COSMIC; http://cancer.sanger.ac.uk/cancergenome/projects/cosmic/). The mutation was found in a neuroblastoma, a highly metastatic malignancy of the sympathetic nervous system that is genetically related to pheochromocytoma[23] and that also originates primarily in the adrenal gland.

This study is limited by the number of mutation carriers in the pedigree and the incomplete penetrance observed for the *MDH2* alteration. The identification of additional disease-causing mutations in *MDH2* will provide further information about the clinical relevance of this gene. Though we have no

explanation for the absence of malate accumulation in the *MDH2*-mutated tumor, we have demonstrated using HeLa cells that *MDH2* abrogation leads to increased levels of malate and the oncometabolite fumarate.

In summary, whole-exome sequencing has identified a novel tumor suppressor gene, *MDH2*, associated with paraganglioma development. This finding further links the disruption of the Krebs cycle to cancer etiology and highlights that alterations in this major metabolic pathway may explain additional pheochromocytoma/paraganglioma cases.

Accession code. A full listing of the exome sequencing results and microarray results has been deposited in the ArrayExpress database (accession code: E-MTAB-2422) and the National Center for Biotechnology Information GEO database (accession number: GSE56573), respectively.

Funding

This work was supported in part by the *Fondo de Investigaciones Sanitarias* (grants PI12/00236 and PI11/01359 to A.C. and M.R., respectively), FP7 grant HEALTH-F2-2010-259735 (ENS@T-CANCER). S.R. and G.E. were supported by the Deutsche Forschungsgemeinschaft EI855/1/1.

Notes

We thank the patient's relatives for their participation in this study. We also thank CNAG personnel, and especially Raul Tonda, for their support in whole-exome sequencing. M.C.-F. is a predoctoral fellow of the Severo Ochoa Program, V.M. and M.A.-R. are predoctoral fellows of the "la Caixa"/CNIO international PhD programme, and L.I.-P. is a predoctoral fellow of CIBERER. We thank Maria Jesús Artiga and Manuel Morente for their help to obtain tumor samples, collected from Spanish hospitals through the Spanish National Tumor Bank Network (CNIO).

Author contributions

The project was conceived by A.C. and M.R. Samples and clinical information were collected by M.C.-F., M.U., M.C., S.A. and A.P.-B. Clinical screening in mutation carriers was performed by R.V.-V. and J.A. Whole-exome sequencing data analysis and filtering was performed by I.C.-M. and A.C. mRNA and protein expression analyses were performed by A.C., A.R.-M., I.C.-M., A.A.d.C. and V.M. Protein activity analysis was performed by L.C. and J.S. Metabolite analysis was performed by S.R., M.P. and G.E. Methylation analysis was performed by S.M. Additional experiments were performed by I.C.-M., F.S., M.E., J.F.G., G.R. A.G.-G., R.L. M.A.-R. and L.I.-P. Additional data analysis was performed by A.C. and I. C.-M. The manuscript was written and revised by A.C., I.C.-M., C.R.-A., and M.R. All authors approved the final version.

References

1. Dahia PL. Pheochromocytoma and paraganglioma pathogenesis: learning from genetic heterogeneity. *Nat Rev Cancer.* 2014;14(2):108-119.

2. Nagy E, Maquat LE. A rule for termination-codon position within intron-containing genes: when nonsense affects RNA abundance. *Trends Biochem Sci.* 1998;23(6):198-199.

3. Qin Y, Buddavarapu K, Dahia PL. Pheochromocytomas: from genetic diversity to new paradigms. *Horm Metab Res.* 2009;41(9):664-671.

4. Lin CC, Cheng TL, Tsai WH, et al. Loss of the respiratory enzyme citrate synthase directly links the Warburg effect to tumor malignancy. *Sci Rep.* 2012;2:785.

5. Xiao M, Yang H, Xu W, et al. Inhibition of alpha-KG-dependent histone and DNA demethylases by fumarate and succinate that are accumulated in mutations of FH and SDH tumor suppressors. *Genes Dev.* 2012;26(12):1326-1338.

6. Xu W, Yang H, Liu Y, et al. Oncometabolite 2-hydroxyglutarate is a competitive inhibitor of alpha-ketoglutarate-dependent dioxygenases. *Cancer Cell.* 2011;19(1):17-30.

7. Letouze E, Martinelli C, Loriot C, et al. SDH mutations establish a hypermethylator phenotype in paraganglioma. *Cancer Cell.* 2013;23(6):739-752.

8. Chou AP, Chowdhury R, Li S, et al. Identification of retinol binding protein 1 promoter hypermethylation in isocitrate dehydrogenase 1 and 2 mutant gliomas. *J Natl Cancer Inst.* 2012;104(19):1458-1469.

9. Baysal BE, Ferrell RE, Willett-Brozick JE, et al. Mutations in SDHD, a mitochondrial complex II gene, in hereditary paraganglioma. *Science.* 2000;287(5454):848-851.

10. Niemann S, Muller U. Mutations in SDHC cause autosomal dominant paraganglioma, type 3. *Nat Genet.* 2000;26(3):268-270.

11. Astuti D, Latif F, Dallol A, et al. Gene mutations in the succinate dehydrogenase subunit SDHB cause susceptibility to familial pheochromocytoma and to familial paraganglioma. *Am J Hum Genet.* 2001;69(1):49-54.

12. Burnichon N, Briere JJ, Libe R, et al. SDHA is a tumor suppressor gene causing paraganglioma. *Hum Mol Genet.* 2010;19(15):3011-3020.

13. Hao HX, Khalimonchuk O, Schraders M, et al. SDH5, a gene required for flavination of succinate dehydrogenase, is mutated in paraganglioma. *Science.* 2009;325(5944):1139-1142.

14. Tomlinson IP, Alam NA, Rowan AJ, et al. Germline mutations in FH predispose to dominantly inherited uterine fibroids, skin leiomyomata and papillary renal cell cancer. *Nat Genet.* 2002;30(4):406-410.

15. Castro-Vega LJ, Buffet A, De Cubas AA, et al. Germline mutations in FH confer predisposition to malignant pheochromocytomas and paragangliomas. *Hum Mol Genet.* 2014.

16. Gaal J, Burnichon N, Korpershoek E, et al. Isocitrate dehydrogenase mutations are rare in pheochromocytomas and paragangliomas. *J Clin Endocrinol Metab.* 2010;95(3):1274-1278.

17. Wang L, Lam G, Thummel CS. Med24 and Mdh2 are required for Drosophila larval salivary gland cell death. *Dev Dyn.* 2010;239(3):954-964.

18. Frezza C, Zheng L, Folger O, et al. Haem oxygenase is synthetically lethal with the tumour suppressor fumarate hydratase. *Nature.* 2011;477(7363):225-228.

19. Philip B, Ito K, Moreno-Sanchez R, Ralph SJ. HIF expression and the role of hypoxic microenvironments within primary tumours as protective sites driving cancer stem cell renewal and metastatic progression. *Carcinogenesis.* 2013;34(8):1699-1707.

20. Pan Y, Mansfield KD, Bertozzi CC, et al. Multiple factors affecting cellular redox status and energy metabolism modulate hypoxia-inducible factor prolyl hydroxylase activity in vivo and in vitro. *Mol Cell Biol.* 2007;27(3):912-925.

21. Schiavi F, Milne RL, Anda E, et al. Are we overestimating the penetrance of mutations in SDHB? *Hum Mutat.* 2010;31(6):761-762.

22. Clark GR, Sciacovelli M, Gaude E, et al. Germline FH mutations presenting with pheochromocytoma. *J Clin Endocrinol Metab.* 2014:jc20141659.

23. Schimke RN, Collins DL, Stolle CA. Paraganglioma, neuroblastoma, and a SDHB mutation: Resolution of a 30-year-old mystery. *Am J Med Genet A.* 2010;152A(6):1531-1535.

FIGURES

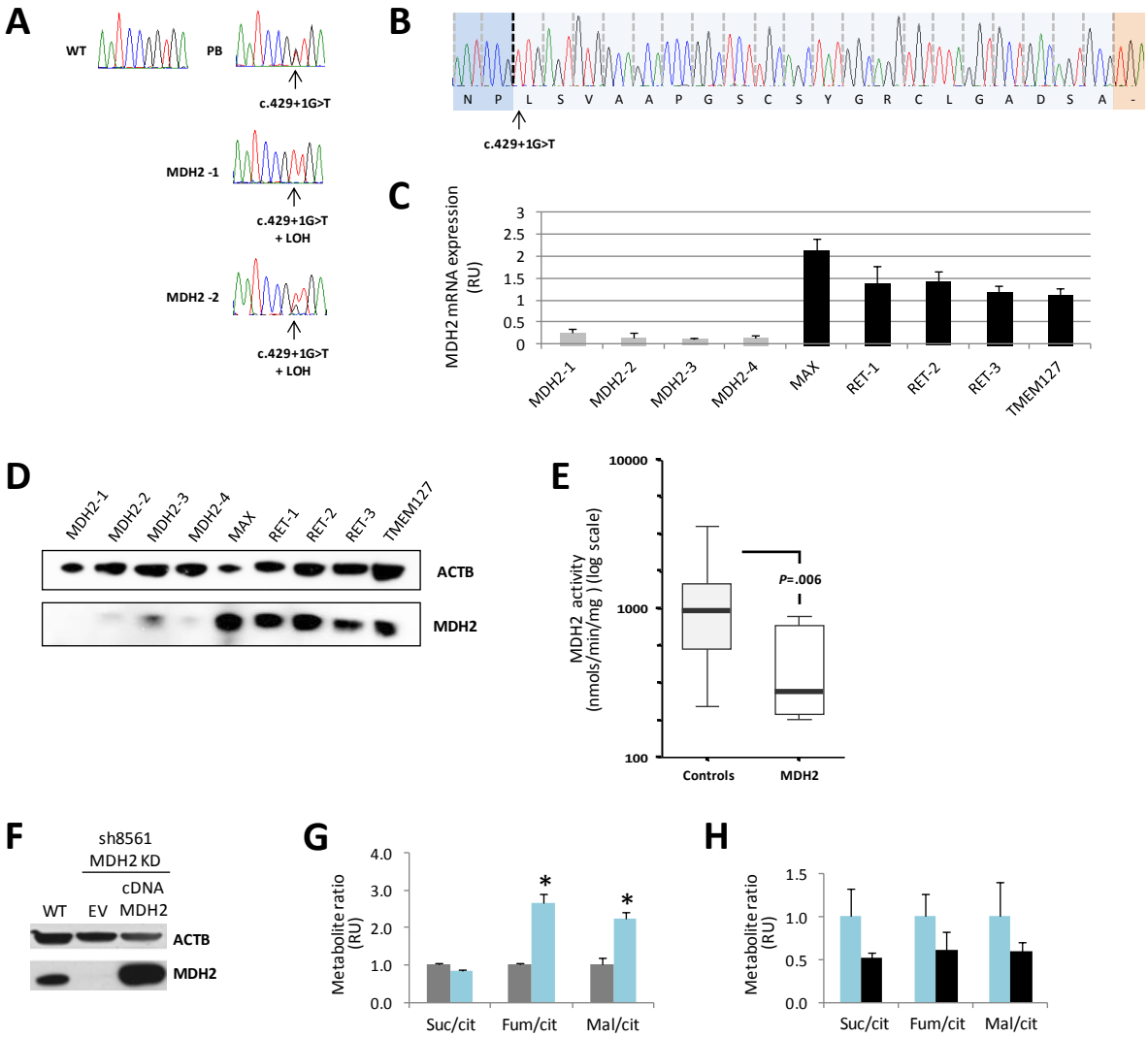

Figure 1. Characterization of *MDH2*-mutated tumors. (**A**) *MDH2* mutation in germline DNA from the patient and loss of the wild-type (WT) allele in two tumors of the patient. (**B**) Sequence of the aberrant transcript caused by the *MDH2* mutation. (**C**) MDH2 mRNA expression in the four *MDH2*-mutated paragangliomas available from the index patient and genetically characterized pheochromocytoma/paraganglioma. Expression level was normalized to β-actin (ACTB) and presented as mean and standard deviation (n≥3). Error bars represent standard deviation. (**D**) MDH2 western blot of mutated tumors and controls. ACTB was used as a loading control. (**E**) Representation of MDH2 activity measured in *MDH2*-mutated and control tumors. The black line at the middle of the box represents the median. Whiskers represent Minimun-Q1, Q3-maximum ranges. P-value based on a two-sided Mann-Whitney U test. (**F**) Western blot of MDH2 KD HeLa cells transfected with a plasmid containing the full cDNA sequence of the human *MDH2* gene (pCMV6-AC-MDH2; Origene), compared to MDH2 KD cells transfected with empty vector (EV), and to untransfected WT HeLa cells. ACTB was used as a loading

control. (**G**) Metabolite ratios assessed by liquid chromatographic tandem-mass spectrometry in MDH2 KD (blue bars) compared to WT (grey bars) HeLa cells. The ratios were normalized relative to WT control values and reported as mean and standard deviation (n=3). A two-sided t-test for independent samples was applied to test for differences. *: $P<.05$. Error bars represent standard deviations. (**H**) Metabolite ratios for MDH2 KD cells transfected with pCMV6-AC-MDH2 (black bars) compared to MDH2 KD cells transfected with EV (blue bars). The ratios were normalized relative to control (EV) values and reported as mean+s.d. (n=3). A two-sided t-test for independent samples was applied to test for differences. Error bars represent standard deviations. *MDH2*: malate dehydrogenase 2.

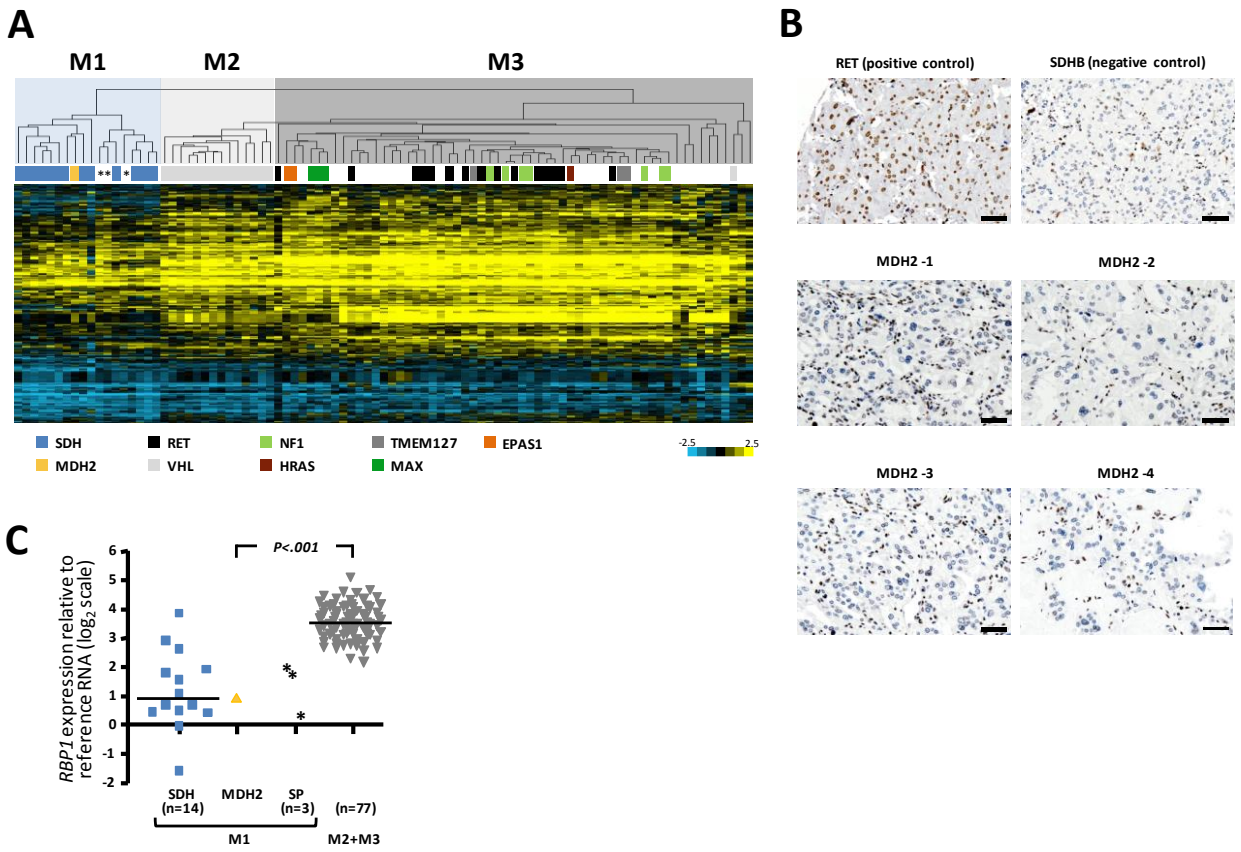

Figure 2. Expression analyses carried out in the *MDH2*-mutated tumors. (**A**) Hierarchical clustering of 91 genetically characterized pheochromocytomas/paragangliomas based on expression data for genes hypermethylated and down-regulated in SDH/*FH*-mutated pheochromocytomas[7]. Three clusters, mimicking those previously obtained using methylation data, were observed and named M1 (CIMP-like), enriched with SDH gene-mutated tumors, M2 with *VHL*-mutated tumors, and M3 with *RET/NF1/MAX/TMEM127*-mutated tumors. Tumors with no color are apparently sporadic cases. Asterisks denote three CIMP-like tumors with no identified mutations in the SDH genes, *FH* or *MDH2*. (**B**) Immunohistochemical staining of 5-hmC in *MDH2*-, *RET*- and *SDHB*-mutated tumors. Nuclear 5-hmC was almost undetectable in *MDH2*- and *SDHB*-mutated tumor cells; it was observed only in sustentacular and some stromal cells. The scale bar represents 50µm. (**C**) mRNA expression of *RBP1* in the *MDH2*-mutated tumor, SDH gene-mutated tumors, the CIMP-like apparently sporadic tumors clustered in M1 (see Panel A) and tumors clustered in the M2 and M3 groups (see Panel A), defined based on gene expression. P-value based on a two-sided exact Mann-Whitney U test. The horizontal black line represents the median. Filled squares and triangles represent individual datapoints. *MDH2*: malate dehydrogenase 2; SDH: succinate dehydrogenase; *FH*: fumarate hydratase; *RET*: ret proto-oncogene; *NF1*: neurofibromin 1; *MAX*: MYC associated factor X; *TMEM127*: transmembrane protein 127; *RBP1*: retinol binding protein 1.

SUPPLEMENTARY MATERIAL

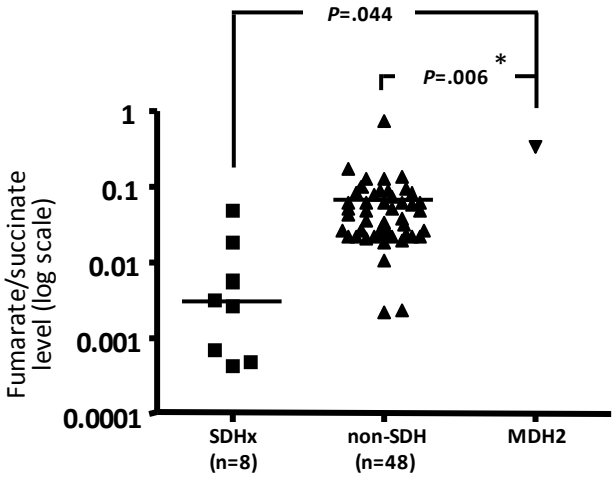

Supplementary Figure 1. Fumarate:succinate ratio for the *MDH2*-mutated tumor (in duplicate), and SDH and non-SDH gene-mutated cases. P-values based on a two-sided exact Mann-Whitney U test.*: statistically significant after applying a Bonferroni correction for multiple testing. The horizontal black line represents the median. Filled squares and triangles represent individual datapoints. MDH2: malate dehydrogenase 2; SDH: succinate dehydrogenase.

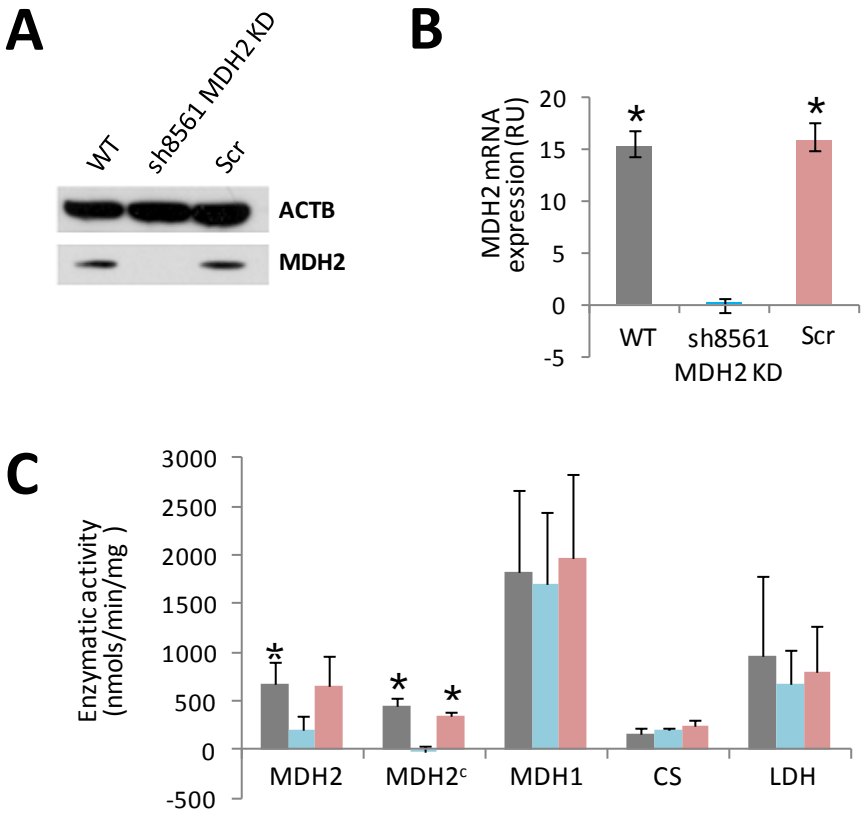

Supplementary Figure 2. Experiments with MDH2-depleted cells. **(A)** MDH2 western blot of HeLa cells stably silenced for MDH2 expression by shRNA transfection (sh8561; Sigma) compared to untransfected wild-type (WT) and non-silenced scrambled (Scr) control cells. β-actin was used as a loading control. **(B)** Quantitative real-time PCR analysis of *MDH2* mRNA performed in MDH2 knock-down (KO) cells, compared to WT and Scr cells. The *MDH2* mRNA level was normalized to *ACTB* and reported as mean+s.d. (n≥3). A two-sided t-test for independent samples was applied to test for differences between MDH2 KO and WT or Scr HeLa cells. *: p<0.01. Error bars represent standard deviation. **(C)** Representation of the enzymatic activities determined in mitochondrial (MDH2, CS) or cytosolic (MDH1, LDH) fractions, as detailed in Methods. Values were expressed in nmols/min/mg and are summarized as mean ± SD of 3 paired independent experiments in HeLa WT (grey bars), Scr (red bars) or MDH2 KO cells (blue bars). MDH2c: MDH2 activity in mitochondrial fractions corrected for residual MDH1. A two-sided t-test for independent samples was applied to test for differences between MDH2 KO and WT or Scr HeLa cells. *: p<0.05. Error bars represent standard deviations. *MDH2*: malate dehydrogenase 2; *ACTB*: β-actin.

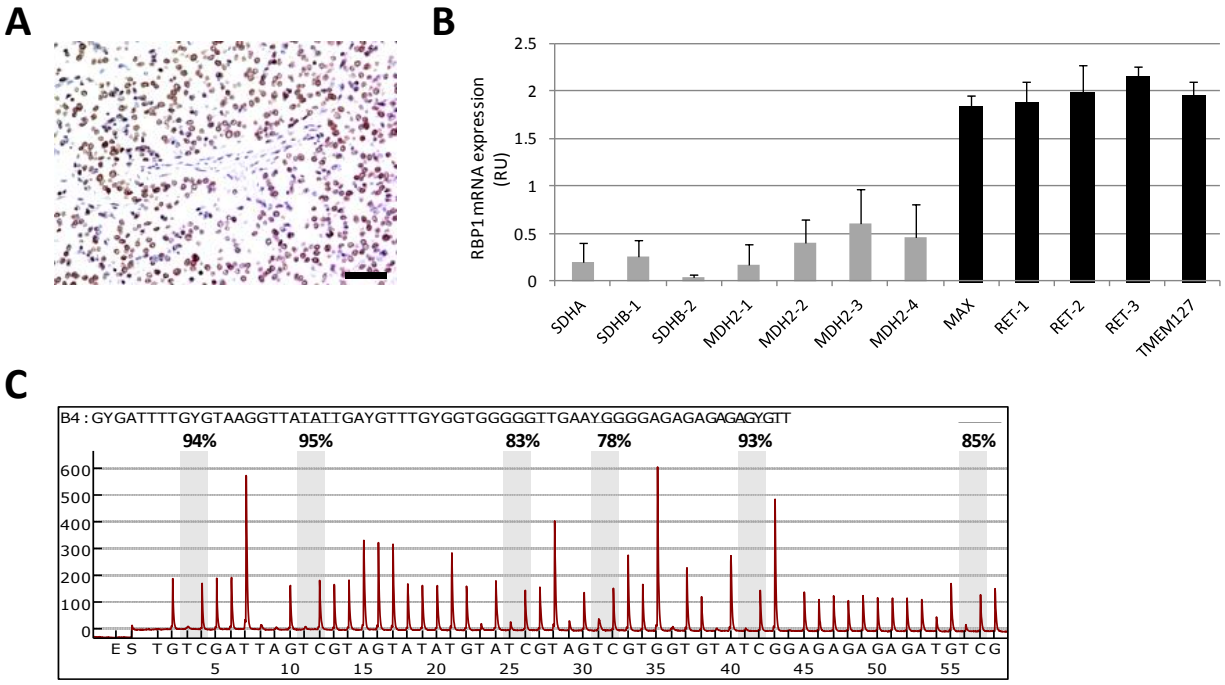

Supplementary Figure 3. *RBP1* and histone methylation analyses. **(A)** Immunohistochemical staining of H3K27me3 in a representative *MDH2*-mutated tumor. Nuclear staining was high in tumor cells and almost undetectable in stromal and endothelial cells. The scale bar represents 50µm. **(B)** *RBP1* mRNA expression in the four *MDH2*-mutated paragangliomas, three SDH-mutated tumors and five pheochromocytoma/paragangliomas without mutations in the Krebs cycle genes. Expression was normalized to *ACTB* and reported as mean+s.d. (n≥3). Error bars represent standard deviations. **(C)** Representative pyrogram from the quantification of the methylation of 6 CpG sites in the *RBP1* promoter of a *MDH2*-mutated tumor. The targeted cytosines are enclosed in gray squares. The percentage methylation at individual CpG positions is shown at the top of the pyrogram. *RBP1*: retinol binding protein 1; *MDH2*: malate dehydrogenase 2; *ACTB*: β-actin.

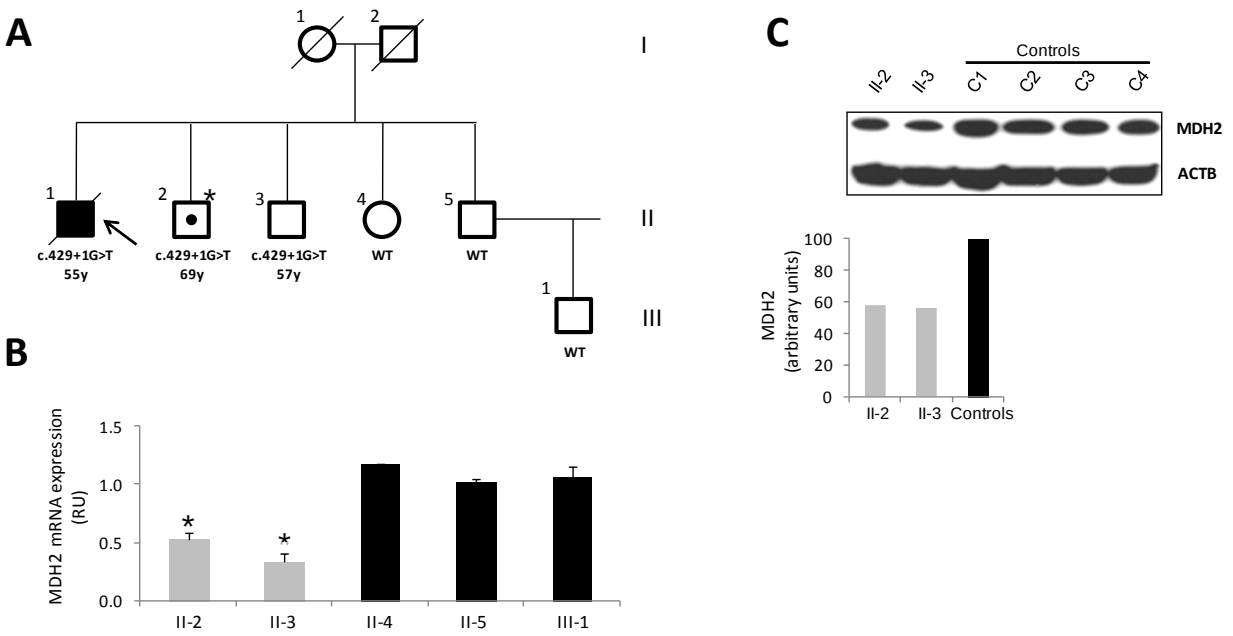

Supplementary Figure 4. Results from genotyping and expression analyses of *MDH2* performed in the patient's relatives. **(A)** Pedigree with the genotype for the c.429+1G>T mutation in *MDH2* for the tested family members. Squares and circles represent male and female family members, respectively, and lines through these indicate deceased individuals. The proband (II-1), diagnosed with multiple paragangliomas, is denoted by an arrow. A black circle in carrier II-2 denotes a positive biochemical diagnosis.*: 123I MIBG scintigraphy and whole-body magnetic resonance imaging gave negative results. The patient refused PET-CT. **(B)** Quantitative real-time PCR analysis of *MDH2* mRNA performed in peripheral blood leukocyte samples (in triplicate) from the patient's relatives who were genotyped for the mutation. A t-test for independent samples was applied to test for differences between carriers (II-2 and II-3) and non-carriers (II-4, II-5, and III-1). *: $p<0.01$. **(C)** MDH2 western blot of lymphoblastic cell lines (LCL) derived from two carriers (II-2 and II-3) of the c.429+1G>T *MDH2* mutation and LCL from unrelated controls (C1-C4). *ACTB* (β-actin) was used as a loading control. *MDH2*: malate dehydrogenase 2.

Patients

A 55 year-old man was diagnosed with asymptomatic paraganglioma by a computed tomography (CT) scan, as part of the clinical staging of a squamous skin cell carcinoma. On hospital admission, the patient reported a history of type-2 diabetes since age 35 years, but no personal or familial antecedents of neural-crest tumors. Continuous monitoring of ambulatory blood pressure revealed nocturnal hypertension. Catecholamine urine testing showed high levels of norepinephrine, and meta-iodobenzylguanidine (MIBG) scintigraphy revealed the presence of two primary retroperitoneal paragangliomas that were surgically removed. Fourteen and fifteen years after the initial diagnosis, MIBG scintigraphy showed an additional retroperitoneal paraganglioma and a thoracic vertebral-invading paraganglioma, respectively; both were extirpated. Two years later, another thoracic paraganglioma, revealed by MIBG scintigraphy and CT scan, was surgically removed, and chemotherapy was initiated, with no clinical response. The patient died 2 years later. Three additional patients, whose tumors exhibited a CIMP-like profile, and a selected series of 29 patients with clinical features of a hereditary disease (i.e. family history and/or multiplicity) (**Supplementary Table 3**) were also tested for *MDH2* mutations. All patients tested negative for mutations in the ten major pheochromocytoma susceptibility genes: *VHL*, *RET*, *SDHA, SDHB*, *SDHC*, *SDHD*, *SDHAF2*, *TMEM127, MAX* and *FH*. Immunohistochemical *SDHB* analysis of formalin-fixed paraffin-embedded (FFPE) tissue from the index case further ruled out the presence of SDH gene mutations[1]. Genomic DNA was extracted from the patients' and relatives' blood following a standard method[2]. Tumor DNA from frozen and FFPE tissue was obtained using the DNeasy kit (Qiagen Inc.), following the manufacturer's instructions. The *Instituto de Salud Carlos III* (ISCIII) ethics committee approved the study, and the patients or their relatives provided written informed consent.

Methods

Whole-exome sequencing analysis

Whole-exome sequencing was carried out in tumor DNA from the index patient at the National Centre for Genomic Analysis (CNAG). Briefly, the covaris S2 System (Covaris) was used for DNA fragmentation and exome capture was performed using the SureSelect XT HumanAllExon 50Mb kit (Agilent Technologies). Exome sequencing at a mean coverage >50x was performed by 75-bp paired-end technology using a HiSeq2000 (Illumina). The GEM and BFAST programs were used to align the reads against the whole human genome (hg19 assembly). To identify single nucleotide substitutions and small insertions and deletions (INDELs) the SAMtools program was used (http://samtools.sourceforge.net). Variants were filtered to rule out those in genome regions with low mappability, with low depth readings, with the alternative allele present in <20% of reads, or with alternative alleles present only in forward or reverse

reads. Single nucleotide substitutions and INDELs were selected and consecutively filtered by excluding: i) variants present in the dbSNP database, the 5400 NHLBI exomes database or in internal exomes; ii) variants in intergenic, intronic or UTR regions; iii) variants with <10 reads and <20 genotype quality; iv) variants affecting transcripts without an annotated consensus coding sequence (CCDS); v) variants with low or moderate impact (i.e. missense or silent variants, respectively). Finally, we used PROVEAN software (http://provean.jcvi.org/index.php), manual curating and additional internal exomes as final steps in the filtering process, thus identifying fifteen variants. We selected for further analysis a variant in *MDH2,* based on the relevant function of this gene in the Krebs cycle, a well-known pheochromocytoma-related pathway.

MDH2 Sanger sequencing and loss of heterozygosity analysis

Primers designed for the amplification of the exon 5 donor site of the *MDH2* gene were used for the validation of the germline variant found by exome sequencing. In addition, primers spanning the nine exons of the most common *MDH2* transcript (ENST00000315758) were used to amplify tumor DNA from the three patients with tumors exhibiting a CIMP-like profile. Loss of heterozygosity of the *MDH2* locus in DNA from the four available tumors developed by the index patient was assessed by direct sequencing using the same PCR conditions as applied for germline DNA. Tumoral cell-enriched FFPE cores were selected to perform the DNA isolation. Primer sequences and PCR conditions are available upon request.

Reverse transcriptase-PCR

Total RNA was isolated from frozen tumor tissue carrying the *MDH2* mutation using the TriReagent kit (MRC), following the manufacturer's instructions. First strand cDNA was synthesized from 0.45 µg of total RNA by oligo (dT)14 primer reverse transcription with Superscript II Reverse Transcriptase (Invitrogen) following the manufacter's instructions. A PCR was then performed using a forward primer designed in the exon1-exon2 junction and a reverse primer located in intron 4, and the PCR product was purified and sequenced.

Quantitative real-time PCR

Total RNA was isolated from peripheral blood lymphocytes, cells and from FFPE tumor tissues using the TriReagent kit (MRC) and the RNeasy FFPE kit (Qiagen), respectively. The quantity and purity of the RNA

were determined using Nanodrop™ 1000 (Thermo Scientific) and cDNA was prepared from 1 µg of total RNA using oligo (dT) primers and SuperScript® III RT (Invitrogen). The *MDH2* and *RBP1* mRNA levels were determined by quantitative PCR on a 7500 fast real-time PCR system (Applied Biosystems) using the Universal ProbeLibrary set (https://www.roche-applied-science.com) as described by the manufacturer. Relative mRNA levels were estimated by the 2-CT method[3] and normalized using β-glucuronidase (*GUS*) and β-actin (*ACTB*) as housekeeping genes. The results are shown as mean+s.d. (n≥3). For the blood *MDH2* mRNA study we used as controls mRNA from three relatives that tested negative for the *MDH2* mutation. mRNA obtained from FFPE tumors carrying mutations in other known pheochromocytoma susceptibility genes were used as controls: three tumors with mutations in *RET*, one with a mutation in *TMEM127*, one with a *MAX* mutation, and three tumors with SDH gene mutations (the latter group only for *RBP1* mRNA assessment).

Western blot

To demonstrate the absence of full-length MDH2 protein in tumors carrying the c.430G>T mutation, we performed western blot analysis using a polyclonal rabbit MDH2 antibody (HPA019716; Sigma-Aldrich) that specifically recognizes translated *MDH2* transcript 1 (ENST00000315758). Proteins were obtained from the four FFPE tissue samples carrying the *MDH2* mutation and from five control tissue samples carrying other known genetic alterations (three tumors carrying mutations in *RET*, one with a *TMEM127* mutation, and one with a *MAX* mutation), using the Qproteome FFPE Tissue kit (Qiagen). Proteins were separated by 10% SDS-PAGE and transferred to a polyvinylidene fluoride membrane. The membrane was blocked and then incubated with a 1:100 dilution of the antibody following the manufacturer's instructions. Equal protein loading was assessed using a 1:12,000 dilution of monoclonal anti- β-actin mouse antibody (A5441, Sigma-Aldrich). Western blot analyses of MDH2 were also performed for proteins obtained from lymphoblastic and HeLa cells using standard procedures.

Immunohistochemistry

Immunohistochemical staining of 5-hmc (Active Motif; 39770) and H3K27me3 (Cell Signaling Technology; 9756) was performed using 3 µm FFPE sections from the four *MDH2*-mutated tumors, following standard procedures. Two tumors carrying mutations in *RET* and *SDHB* were used as controls.

Gene expression analysis

To identify the transcriptional profile associated with alterations in *MDH2* we used gene expression data for the tumor carrying the *MDH2* mutation, for 84 pheochromocytomas and paragangliomas deposited in the National Center for Biotechnology Information GEO database under the accession number GSE19422[4], and for six additional genetically characterized tumors. Tumor sample processing, hybridization on the Agilent Whole Human Genome platform (4x44K) (Agilent Technologies), and data normalization were performed as previously described[4]. Tumor samples were grouped according to their expression profiles by unsupervised clustering using GeneCluster 2.0[5], as previously described[4]. Hierarchical clustering was performed using the 176 genes with expression data available, of the total 191 genes described as hypermethylated and downregulated in SDH gene-mutated and *FH*-mutated pheochromocytomas[6]. We used the clustering average for linkage and uncentered correlation as the distance measure. In addition, we assessed the mRNA expression of *RBP1* in the whole series of pheochromocytoma/paragangliomas, by gene mutated.

Liquid chromatographic tandem-mass spectrometric determination of energy pathway metabolites

Fresh frozen tumor tissue (5-10 mg), from the index case and from eight SDH gene-mutated and 48 non-SDH gene-mutated cases**,** was immersed in 500 µl LC/MS grade methanol containing isotope-labeled internal standards. Homogenization was achieved by vortexing with a metal bead for 2 minutes. Homogenates were then centrifuged at 2000xg for 5 minutes at 4°C to separate insoluble debris. Supernatants were taken to dryness with a speed vac concentrator (Thermo Scientific) and stored at -80°C. Pellets were resuspended in mobile phase and filtered using a centrifugal tube with a pore size of 0.2 µm. Analysis of metabolites was carried out using an API QTRAP 5500 (AB Sciex) mass spectrometer coupled to an Acquity ultra-high performance liquid chromatographic system (Waters). Chromatographic separation was achieved on a Waters Acquity UPLC® HSS T3 column (1.8 µm, 2.1 x 100 mm) with a flow rate of 0.459 ml/min, a mobile phase of 0.2% formic acid in water (A) and 0.2% formic acid in acetonitrile (B), and a gradient of 0.37min 95% A, 4.87min 70% A, 5.37min 100% B, 5.87min 100% B, 6.37min 95% A, 7.5min 95% A. The column was maintained at a temperature of 25°C and the sample manager at 5°C. The mass spectrometer was operated at 550°C in negative ion electrospray mode. Multiple reaction monitoring was used for detection and quantification. For cell line metabolite assessments, the same procedure was applied, using 10^6 cells in each determination.

Enzymatic activity analyses

Cytosolic and mitochondrial fractions were obtained after homogenization of frozen tumor biopsies obtained from the MDH2-patient and from 4 controls, by a standard differential centrifugation procedure[7, 8]. Protein concentration was determined by Bradford with BSA as standard. The cytosolic and mitochondrial fractions were used to determine the enzymatic activity of MDH1 and MDH2, quantified as a decrease in NADH fluorescence, after the addition of OAA, using a BMG plate reader, as previously described.[7] NADH fluorescence was calibrated based on NADH standards. Control and mutant *MDH2* tumor fractions were used at different dilutions in 5-6 paired independent experiments to correct for measurement variability. A similar procedure was carried out for HeLa cell fractions. Lactate dehydrogenase (LDH, measured as the increase in NADH caused by lactate addition) and citrate synthase (CS, measured as the increase in absorbance of 5,5'-dithiobis-2-nitrobenzoic acid after the addition of OAA) were assayed using standard procedures[8, 9]. Contamination of mitochondrial fraction with cytosol (residual LDH activity) was detected in approximately 3% of HeLa extracts, but not in tumor samples. MDH2 activity in HeLA cells was thus corrected by subtracting the estimated cytosolic contamination (% of LDH present) from the activity measured in the mitochondrial fraction. Contamination with broken mitochondria in the cytosolic fraction (residual citrate synthase activity), was approximatley 10% and 50% of tumor and HeLa preparations, respectively.

Cell cultures

Lymphocytes from the two carriers of the c.429+1G>T *MDH2* mutation (II-2 and II-3 in **Supplementary Figure 4**) were immortalized using Epstein-Barr virus, as previously described[10]. HeLa cells were cultured in Dulbecco's modified Eagle medium GlutaMAX (DMEM; Invitrogen), supplemented with 10% (v/v) foetal bovine serum (FBS, PAA laboratories), 1% (v/v) penicillin/streptomycin and 0.6% (v/v) Fungizone (Gibco), and maintained at 37°C in a humidified incubator with 5% CO_2. MISSION® shRNA lentiviral transduction particles (TRCN0000028561; Sigma) were used to specifically knockdown *MDH2*. Stable gene knockdown (KD) was established by cellular resistance to puromycin (3 µg/ml). After one week, selected puromycin-resistant clones were isolated and cloned for further analysis. Scrambled non-target shRNA control vector (Sigma) served as a negative control. To rescue from *MDH2* depletion, HeLa MDH2 KD cells were seeded at 200,000 cells per well on 24-well plates for 24h. Each well was transiently transfected with 0.15 µg of pCMV6-AC-MDH2 (Origene), a plasmid containing the full cDNA sequence (NM_005918) of the human *MDH2* gene, using Lipofectamine 2000 (Invitrogen), according to the manufacturer's recommendations. pCMV6-AC empty vector was used as a control.

Pyrosequencing

Specific sets of primers were designed for PCR amplification and sequencing using a specific software package (PyroMark assay design version 2.0.01.15) to interrogate the methylation status of CpG sites from seven selected genes: *RBP1*, *SPOCK2*, *KRT19*, *ARSG*, *TMEM45B*, *HTATIP2*, and *MAPK13*. Single-stranded DNA templates from the corresponding amplifications of DNA extracted from two *MDH2*-mutated tumors were treated to quantify methylation level using the PyroMark Q24 System, version 2.0.6 (Qiagen), according to the manufacturer's instructions. Whole-genome amplified DNA from normal lymphocytes was used as a control[11].

Statistical methods

The Kolmogorov-Smirnov test was used to assess departure from the normal distribution. When a normal distribution could not be assumed, a two-sided exact Mann-Whitney U test was applied to test for differences. Otherwise a t-test for independent samples was applied. Nominal two-sided P-values less than 0.05 were considered statistically significant. Statistical analyses were performed using SPSS version 17 (SPSS Inc, Chicago, Illinois), R version 3.0.1 and Graphpad Instat version 3.05.

References

1. van Nederveen FH, Gaal J, Favier J, et al. An immunohistochemical procedure to detect patients with paraganglioma and phaeochromocytoma with germline SDHB, SDHC, or SDHD gene mutations: a retrospective and prospective analysis. *Lancet Oncol.* 2009;10(8):764-771.

2. Sambrook J, Maniatis T, Fritsch EF. *Molecular cloning : a laboratory manual*. 2nd ed. Cold Spring Harbor, N.Y.: Cold Spring Harbor Laboratory; 1989.

3. Livak KJ, Schmittgen TD. Analysis of relative gene expression data using real-time quantitative PCR and the 2(-Delta Delta C(T)) Method. *Methods.* 2001;25(4):402-408.

4. Lopez-Jimenez E, Gomez-Lopez G, Leandro-Garcia LJ, et al. Research resource: Transcriptional profiling reveals different pseudohypoxic signatures in SDHB and VHL-related pheochromocytomas. *Mol Endocrinol.* 2010;24(12):2382-2391.

5. Reich M, Ohm K, Angelo M, Tamayo P, Mesirov JP. GeneCluster 2.0: an advanced toolset for bioarray analysis. *Bioinformatics.* 2004;20(11):1797-1798.

6. Letouze E, Martinelli C, Loriot C, et al. SDH mutations establish a hypermethylator phenotype in paraganglioma. *Cancer Cell.* 2013;23(6):739-752.

7. Bergmeyer HU, Bergmeyer J, Grabl M. *Methods of enzymatic analysis. III, Enzymes 1,. Oxireductases, transferases*. 3rd ed ed. Weinheim [etc.]: Verlagchemie; 1983.

8. Bergmeyer HU, Bergmeyer J, Grabl M. *Methods of enzymatic analysis. IV, Enzymes 2,. Esterases, glycosidases, lyases, ligases*. 3rd ed ed. Weinheim [etc.]: Verlagchemie; 1984.

9. Barrientos A. In vivo and in organello assessment of OXPHOS activities. *Methods.* 2002;26(4):307-316.

10. Ausubel FM. Current protocols in molecular biologyNew York: Greene Pub. Associates ; Wiley-Interscience; 1988:v. (loose-leaf).

11. Heyn H, Carmona FJ, Gomez A, et al. DNA methylation profiling in breast cancer discordant identical twins identifies DOK7 as novel epigenetic biomarker. *Carcinogenesis.* 2013;34(1):102-108.

DISCUSSION

PCC/PGL is the most heritable of all cancers, with 40% of cases explained by known genetic factors. Despite this, there are still a substantial number of patients with clinical characteristics suggesting heritability in whom no mutations in PCC/PGL susceptibility genes are found. This clearly suggests the implication of other genes in the predisposition to this already puzzling genetic disease. Linkage analysis and positional cloning have been successfully employed in the past to identify PCC predisposition genes such as *RET*, *NF1*, *VHL*, and *TMEM127*. However, these approaches usually require highly informative pedigrees and therefore are not suitable for patients with no, or limited, family history of disease. In more recent years, NGS, and more specifically WES, has been demonstrated to be a very powerful tool in discovering new genes related to hereditary disorders. Therefore, the purpose of this thesis was to apply WES to identify genes involved in hereditary predisposition to PCC/PGL in patients with clinical characteristics of heritability but no mutations in any of the susceptibility genes known so far. Taking into account the aforementioned genetic heterogeneity of this disease, one of the crucial steps to achieve our objective was the adequate selection of patients to be studied. Thus, we used either molecular or clinical markers to choose sets of patients that were as homogeneous as possible (Figure 3).

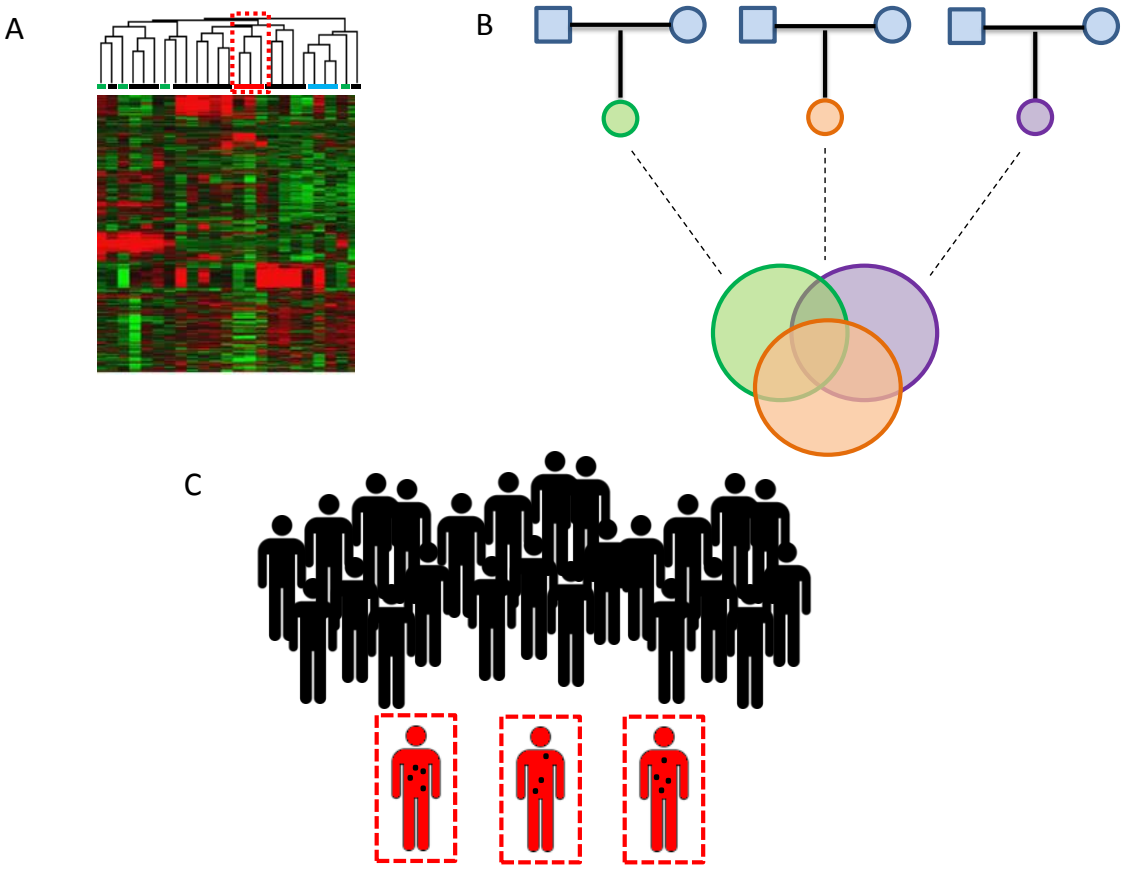

Figure 3. Schematic representation of the three strategies applied for the selection of cases. **A)** Molecular marker: transcriptional profiles of tumors. **B)** Approach based on trios: patient/mother/father. **C)** Clinical marker: tumor multiplicity.

This approach enabled us to identify for the first time two genes (*MAX* and *MDH2*) involved in predisposition to develop PCC/PGL. Although WES performed in blood samples from selected trios (patient-father-mother) did not identify the now-known *EPAS1* somatic mosaic mutations, we were able to provide relevant information about the contribution of *EPAS1* alterations to the disease in our selected series of patients.

• ARTICLE 1: Discovery of germline mutations affecting *MAX* in patients with PCC.

One of the most important applications of genome-wide expression profiling is to classify tumors[182]. Thus, since 2000, several studies have applied hierarchical clustering to identify characteristic patterns of expression for specific tumor phenotypes[183-185]. Especially illustrative of the utility of this approach is the transcriptional classification of breast tumors that distinguishes based on molecular profiles luminal, basal like and ErB2-positive carcinomas[184,186-188]. In the case of PCCs and PGLs, transcriptional profiling has been widely used to cluster tumors according to their genetic background or associated biochemical profile[52-55]. PCCs/PGLs carrying mutations in the same gene have similar expression profiles and can therefore be segregated into well-defined transcriptional clusters. Taking advantage of a hierarchical clustering performed in our laboratory, we selected three unrelated patients, with family history of PCC and no mutations in any of the known susceptibility genes, as candidates for WES since their tumors showed a highly homogeneous expression profile[55].

The bioinformatic pipeline and the filtering steps for WES data that we designed and applied enabled us to identify in all three individuals germline mutations in two genes. The presence of these mutations was confirmed by Sanger sequencing, however only those affecting *MAX* were found to segregate with the disease in the three pedigrees. The truncating effect of the *MAX* variants identified (i.e. alteration of the initiation codon, introduction of a premature stop signal, and frameshift skipping of one complete exon), provided strong evidence that *MAX* loss of function mutations were involved in PCC development in these pedigrees.

Once variants in a gene pass all the filtering steps included in a given WES pipeline, it is highly advisable to assess previous evidence or data that might connect the function of the gene to the disease, in order to inform subsequent work. In the case of MAX, while there was ample knowledge about the role of this protein regulating MYC functions, no association with cancer susceptibility had been reported. However, Ribon *et al.* had demonstrated in 1995 the existence of a homozygous rearrangement affecting *MAX* in PC12 cells, a cell line derived from rat adrenal PCC[189]. The observed alteration led to the inability of the protein to homo- or hetero-dimerized and, therefore, to inefficiency in the repression of the

oncogenic properties of MYC[190]. Further, the authors demonstrated that reintroduction of MAX in PC12 cells resulted in transcriptional repression and a reduction in growth rate. Thus, the presence of *MAX* loss of function mutations in PCCs was consistent with the suggested role of the protein repressing MYC-dependent transcriptional activation in PC12 cells. Moreover, the oncogenic, MAX-independent abilities of MYC, and the role of MAX acting more like repressor than activator of MYC-target genes, had been further demonstrated in *Drosophila* by Gallant *et al*[145].

Subsequently, the loss of the wild type allele (LOH), plus the absence of the protein in the tumors developed by the three sequenced patients, suggested that the mutations found in *MAX* were the cause of the disease in these families. In the genetic models in which a tumor suppressor gene is implicated, the mechanisms producing LOH following the Knudson's two-hit model[191] can be very diverse and sometimes do not affect the coding part of the genome, implying other genetic or epigenetic mechanisms. This can make the establishment of the implication of a gene in a given disease very difficult. In the tumors developed by our three sequenced patients, the LOH was due to paternal uniparental disomy (UPD) affecting chromosome 14, were *MAX* is located.

Taken together, these findings suggested that *MAX* germline mutations were the cause of PCC susceptibility and that *MAX* behaved as a classic tumor suppressor gene. This was endorsed by the identification of two additional truncating mutations and three missense variants by genetic testing of *MAX* mutations in a selected series of PCC/PGL patients suspected to be hereditary. Despite the fact that the missense variants were not found in controls, were predicted to be pathogenic by in-silico prediction algorithms, and affected important regions within the protein, we considered them to be VUS, and developed functional models to determine whether they have a causal role (see project 1.3). Besides the presence of bilateral tumors amongst *MAX* mutation carriers, and an apparent paternal transmission of the disease (a paternal origin of the mutated allele was detected in six families), 25% of cases developed metastases. The malignant behavior of tumors with mutations in *MAX* seemed to be consistent with what was known about neuroblastoma, the other tumor derived from neural crest and developed mainly from the adrenal medulla. Up to 22% of neuroblastomas show *MYC* amplification, strongly associated with advanced disease stages and rapid tumor progression[192], which would support the idea that *MAX* loss of function is related to metastatic potential, since MAX is the main regulator of MYC. Nevertheless, the association of MAX mutations with malignancy was not confirmed in a larger series of MAX mutation carriers (see Project 1.2). Finally, and as previously described[55], tumors carrying mutations in *MAX* were grouped within the PIK3CA-AKT1-mTOR transcriptional cluster 2, along with tumors carrying mutations in *RET*, *NF1* and *TMEM127*. The known crosstalk between the MYC-MAX-MXD1 axis and the PIK3CA-AKT1-

mTOR pathway explains this particular expression profile of MAX tumors and provides further evidence of the implication of the gene in the disease[193,194].

The MYC family of proto-oncogenes is composed of important transcriptional activators implicated in the regulation of normal cell proliferation, differentiation and apoptosis[142]. MAX is a well-known dimerization partner of MYC which plays a central role in the regulation of the cancer-predisposing MYC-MAX-MXD1 network[100]. Deregulation of the MYC-MAX-MXD1 network has been widely linked to cancer, especially neuroblastoma for which the amplification and overexpression of MYCN is a well-known genetic hallmark[195]. Thus, ablation of MAX's transcriptional repression of MYC in PCC could lead to the same oncogenic deregulation of MYC that occurs in neuroblastoma[101]. However, a role of MAX that is independent of MYC cannot be ruled out as the mechanism behind PCC/PGL development. The ubiquitous expression of MAX, plus its central role in the axis, suggests that *MAX* mutations might be implicated in a wider spectrum of neoplasias. Indeed, Romero et al., recently described the implication of *MAX* somatic mutations in small cell lung cancer (SCLC)[196], in which the inactivation of *MAX* occurs in a way that is mutually exclusive of MYC amplifications.

In 2011, *MAX* became the first cancer predisposition gene identified by WES[117], and our next main objective was to establish the prevalence and the associated clinical characteristics of *MAX* mutation carriers.

- **ARTICLE 2: Prevalence of *MAX* mutations in PCC/PGL patients.**

The discovery of a new susceptibility gene should be followed by the screening of a large series of patients in order to elucidate the relative importance of alterations in the gene for the disease. Thus, we combined data from 1,694 unrelated PCC/PGL patients testing negative for mutations in the known susceptibility genes, which were recruited by 17 participating centers from six different countries. An additional series of 245 tumors were also collected[140]. A germline pathogenic mutation in *MAX* was found in 1.12% of the index cases included in this analysis. Thus, the contribution of *MAX* mutations to this disease iss similar to the reported for *TMEM127*[98], and higher than the most recently identified susceptibility genes, *FH* and *MDH2*[82](in press). As a result of this study, the spectrum of patients carrying *MAX* mutations was extended to cases suffering from extra-adrenal tumors (i.e. thoraco-abdominal PGLs). In addition, we established that somatic mutations in *MAX* play a role in the sporadic presentation of the disease. For a long time, somatic driver mutations have been considered rare in PCC/PGL for a long time. However, several recent studies have positioned these mutations as important genetic events in the development of the disease[53,63,67,96,97,106,197]. The presence of *MAX* somatic mutations in 1.65% of tumors further highlights the importance of somatic driver events in the sporadic development of the disease.

Regarding the phenotypic characteristics of *MAX* mutation carriers, the presence of bilateral disease (in the case of PCC) in 21% of patients was consistent with the high percentage of bilateral PCCs observed in patients carrying mutations in other cluster 2 genes such as *RET* or *TMEM127*[45,46,98,198], while the mean age of onset (34 years) was slightly lower than that observed in carriers of mutations in these other genes. It is noteworthy that in all *MAX* mutation carriers developing extra-adrenal tumors, their PGL was diagnosed following the previous development of PCC. None of the patients diagnosed only with PGL carried a *MAX* mutation. Among the patients included in this second study, only two developed metastasis, suggesting that, unlike what typically occurs in *SDHB*-mutated mutated tumors[46], *MAX*-mutated tumors do not have a high risk of malignancy. More than 65% of patients with *MAX* mutations had no family history of the disease, and the finding of three additional cases in which the transmission of the disease was paternal provided further evidence of a parent of origin inheritance. This preferential paternal mode of transmission may provoke generation skipping within pedigrees, with important consequences for genetic counseling. Further, it makes even more difficult the task of establishing the pathogenicity of *MAX* VUS because of the challenges of studying the segregation of variants with disease. It should be noted that, though the overall prevalence of *MAX* mutations in the entire series slightly exceed 1%, this increased to 12% in patients with isolated tumors, and to 66% in cases with bilateral PCC, when we considered only cases with PCC and family history.

The biochemical characteristics of *MAX*-mutated tumors were intermediate, between the predominantly epinephrine secretion of *NF1* and *RET* tumors and the norepinephrine secretion of *VHL* or *SDHB/D* tumors[199]. Consistent with this intermediate phenotype was the observed moderate expression in the tumors of PNMT, the enzyme responsible for converting norepinephrine to epinephrine. Similarly, urinary measures of normetanephrine compared to metanephrine confirmed significant but limited capacity of *MAX* tumors to produce epinephrine.

The majority of the mutations found in this series were located in the conserved exons 3 and 4 of *MAX*, giving rise to truncated proteins. Further, the observed LOH affecting the remaining wild-type allele of *MAX* was corroborated by the absence of the protein according to immunohistochemistry. Interestingly, the c.97C>T variant, which affects a crucial residue within the MAX protein involved in the DNA binding, was found in unrelated patients from 5 countries (Italy, Spain, United States, France, and The Netherlands), suggesting that it represents the first hotspot mutation affecting *MAX*. This was further supported by the finding of a somatic c.97C>T change in a sporadic PCC[112]. Overall, these findings suggest that two phenotypic characteristics may be used to guide the genetic testing of the patients towards *MAX*: 1) lack of nuclear immunohistochemistry staining for MAX (something useful only for variants which

produce the truncation of the protein); 2) intermediate biochemical phenotype (also detectable in fractioned catecholamines tested in blood or urine).

To summarize, this second study elucidated the importance of *MAX* mutations in PCC/PGL susceptibility, pointing to the need for the inclusion of this gene in the genetic work-up of affected patients, particularly those with PCC (bilateral or multifocal), and/or with family history. In addition, the presence of several (n=8) VUS affecting *MAX* made fundamental the development of functional models to guide the prediction of the pathogenicity of this type of variants.

• ARTICLE 3: Functional and *in silico* assessment of *MAX* variants of unknown significance.

While truncating mutations in tumor suppressor genes are usually considered deleterious, to establish the pathogenicity of a new missense variant requires further analysis (e.g. identifying a second hit such as LOH of the wild-type allele). *In silico* algorithms are widely used to predict the biological consequences of VUS; however, in the absence of other clinical evidence (for example, additional affected family members carrying the variant) they are insufficient to conclude whether a variant is deleterious or not. In addition, the prediction given by different algorithms are frequently contradictory, making the *in silico* establishment of pathogenicity a very complex task. Therefore, in order to improve the genetic counseling and clinical follow-up of carriers it is necessary to develop functional systems to clarify the role that a given VUS may have in tumor development. Half of all *MAX* variants identified in patients with PCC to date have been missense changes. In these patients, the frequent absence of family history, probably due to the observed paternal mode of inheritance[49,140], further complicated the assessment of the pathogenicity of the corresponding VUS very complicated. Thus, in order to determine the role of individual *MAX* missense variants in the disease, we developed a reliable PC12-based assay that, combined with the prediction of the effect of each alteration at the molecular level, the consensus prediction of five different *in silico* algorithms and relevant clinical patient information, enabled us to establish the pathogenicity of all except one of the variants considered.

The affected residues (with three exceptions not observed in the crystallized protein) were modeled in the protein structure of MAX. The nine analyzable variants were classified into three groups depending on the function predicted to be affected:

- Variants affecting residues implicated in the interaction with DNA: Three variants altered the DNA binding properties by losing a residue (arginine) commonly found in protein-DNA interactions. Only the p.D14N variant maintained MAX's ability to interact with DNA, consistent with the functional assay, which indicated that this variant was not producing any alteration.

- Variants causing a change affecting the dimerization region of the protein: These variants strongly affected the MAX homodimer and therefore the assembly of monomers. The lack of MAX homodimers may make accessible for the transcription machinery the promoter regions of certain genes that are normally repressed by MAX, thus facilitating their expression.

- Variants causing a change of the wild type amino acid to a destabilizing proline: Proline is a residue that alters the helical structure and may lead to an alteration in the hetero- or homo-dimerization capacity of the mutated protein.

Overall, eight of the nine substitutions considered were predicted to cause an alteration in the properties of the protein, a result that is entirely consistent with those from the proposed PC12-based functional assay.

Classification of the variants according to different combinations of five independent algorithms differed from the result of functional assay for at least two variants (range: 2-5). The prediction improved when we used the agreement of at least three of the algorithms. The reliability of this latter consensus prediction was confirmed by the results obtained assessing the only four *MAX* polymorphic missense variants described in control population databases (ESP data server: http://evs.gs.washington.edu/EVS/). This result is consistent with others from the literature that recommend the combination of different algorithms, rather than just one, to better inform the classification of VUS variants[157,158].

As mentioned previously, MAX plays a key role in cell homeostasis, heterodimerizing with MYC to initiate the expression of hundreds of genes[100]. However, the recent discovery of MAX's involvement in PCC/PGL development, behaving as a classical tumor suppressor gene, suggests that its role in the axis most likely relates to repress the oncogenic activities of MYC, at least in this tissue. The results obtained from our functional assay, which showed high concordance with the results obtained from the proposed consensus *in silico* prediction, further supports this idea. Co-introduction of MYC reporter plasmid containing four E-box sites, together with a plasmid containing wild type *MAX,* decreased the luciferase activity of transfected cells compared to PC12 wild-type, suggesting a regulatory role of the MAX protein. Moreover, MAX mutant proteins less extensively repress MYC activity, thereby increasing luciferase activity. Of note the only variant unclassified by the prediction tools was pathogenic according to our functional assay (p.M65V). The result of the functional assay for this variant was further supported by the presence of other change affecting the same amino acid in prostate cancer (COSMIC database: http://cancer.sanger.ac.uk/cancergenome/projects/cosmic/). Interestingly, the unique mutation predicted by MutPred to provoke a "gain of disorder" within the protein (p=0.0051) was the variant presenting the greatest difference in the luciferase activity, compared to wild type.

The eight individuals carrying *MAX* variants identified as deleterious by our functional assay and by the consensus prediction presented with clinical characteristics of heritability (for example multiplicity/bilaterality or segregation of the variant with the disease). In contrast, the three patients carrying a *MAX* VUS with no apparent effect on MYC regulation presented with isolated tumors and no other clinical features of heritability. Inconsistent results were obtained for the p.V9L variant, classified as pathogenic by the functional assay but non-pathogenic by the consensus *in silico* prediction. The patient harboring this VUS presented with multiple tumors, which suggests pathogenicity. However, the substitution has been observed in 4 of 31,760 unaffected individuals (EXAC server: http://exac.broadinstitute.org) and showed no LOH in the available tumor. Although the patient did not present mutations in other susceptibility genes, the inconsistent data available do not allow us to reach a conclusion regarding the pathogenicity of this variant.

To summarize, in this study we demonstrated how the correct use of clinical information, together with a reliable functional assay and a compendium of computational methods, may inform the clinical management of patients carrying VUS.

• ARTICLE 4: Contributing to the knowledge of *EPAS1* mutations in PCC.

A rare clinical feature, in association with a given pathological condition, can be used to select a homogenous set of patients as candidates to identify causal germline alterations in the same gene. In addition, over the past few years WES has become an efficient means of searching for new molecular defects causing rare diseases transmitted through a recessive or *de novo* inheritance mode[200-203]. Thus, the presence of idiopathic polycythemia (a rare condition) and multiple PCCs/PGLs in three patients from our series without family history of the disease (consistent with a *de novo* or recessive mode of inheritance) led us to conduct a second WES project based on the analysis of blood samples obtained from three trios: affected individuals and each of their biological parents. During the analysis of our WES data, a manuscript was published describing *EPAS1* somatic post-zygotic mutations in two patients with the same candidate clinical features[63]. Somatic post-zygotic variations can occur during mitotic cell division following fertilization and zygote formation, giving rise to individuals that are mosaic: with genetically different populations of somatic cells, only a subset of them harboring the mutation[204]. Somatic post-zygotic models have been described to provoke miscarriage, birth defects, developmental delay and cancer[205-209]. When we analyzed the tumors from our three index cases for the presence of alterations in *EPAS1,* we found mutations affecting either the Proline 531 or the residues located close to this primary hydroxylation site of the protein in all of them. Even though the sampling we carried out for WES was appropriate, we wrongly assumed a germline inheritance model would explain the absence of

family history of the disease. This experience highlights the importance of taking more unlikely genetic models into account in order to cover all contingencies.

Subsequent analysis of a series of frozen PCCs/PGLs uncovered *EPAS1* mutations in one patient with multiple tumors but no polycythemia, and in three additional cases presenting with single adrenal tumors. This latter finding revealed for the first time that *EPAS1* is involved in the sporadic presentation of the disease. Excluding the three index patients who were initially selected for WES, we observed that *EPAS1* mutations accounted for 10% of the frozen tumors analyzed. These results suggested that mutations in *EPAS1* are very frequent in PCC/PGL development, placing *EPAS1* in the group of genes, besides *NF1*, *VHL* and *RET*[15], more frequently involved in the sporadic presentation of the disease.

As mentioned previously, under hypoxic conditions the HIF family of transcription factors (HIF-1α, EPAS1 and HIF-3α) are stabilized leading to the transcription of genes related to the hypoxia response and resulting in the initiation of processes such as angiogenesis, glycolysis, apoptosis, proliferation, and cell growth[210,211]. Mutations in *EPAS1* also stabilize the protein by abrogating its hydroxylation and subsequent proteosomal degradation [63]. Though all reported *EPAS1* mutations, either found in patients with familial erythrocytosis or in patients with multiple PCC/PGL and polycythemia, affect residues located in the proximities of the primary hydroxylation site (proline 531), we found for the first time mutations directly affecting the proline residue[67]. Moreover, with the except of a mutation affecting the Aspartic acid 539[212], all alterations associated with the development of PCC/PGL were different compared to those found in patients with congenital polycythemia[67]. The absence of PCCs and PGLs in the reported cases of familial erythrocytosis carrying *EPAS1* germline mutations suggests that, as occurs with mutations in the *VHL* gene, different mutations in *EPAS1* predispose to different diseases. Nevertheless, we cannot rule out that additional genetic factors could modulate the clinical phenotype of *EPAS1* mutation carriers. On the other hand, the absence of polycythemia in a patient with multiple PGLs from our series carrying a mutation previously found in a patient presenting with polycythemia and PGLs[63], points to the moment during embryogenesis at which the mutation occurs as a crucial factor in the clinical phenotype.

It has been well established that the immunohistochemistry of SDHB can guide the genetic screening for mutations in the PCC/PGL susceptibility genes. Thus, negative staining for SDHB, partly due to the frequent losses of the chromosome 1q, is a good indicator for mutations in the *SDH* genes [173]. Something similar occurs with *NF1*-mutated tumors which usually harbor concomitant chromosome 17 losses. The finding in our series of *EPAS*-mutated tumors of exclusive gain of chromosome 2p, affecting either the mutated or the wild-type allele, could also guide the genetic testing for this gene, avoiding unnecessary expense. While unexpected, it has previously been shown that the gain of an extra copy of

an oncogene may cause alterations in cell growth. Thus, it has been demonstrated that *RET*-mutated PCCs can present with either somatic duplication of the mutated allele or loss of the *wild type RET* allele.[213]. The somatic gain of an extra copy of an *EPAS1*-mutated allele may lead to an increase in the amount of stabilized protein, and the gain of an extra copy of the wild-type allele can also activate the hypoxic response driven by EPAS1. Finally, the observation of tumors without mutations in *EPAS1* presenting a specific gain of chromosome 2p suggests that this event could be an important factor in the development of the disease.

The transcriptional profile of *EPAS1*-mutated tumors did not fit with the typical pseudo-hypoxic profile of tumors harboring *VHL* or SDH gene mutations. In fact, hierarchical clustering of *EPAS1*-mutated tumors and a large series of PCCs/PGLs did not group them within the expected transcriptional Cluster 1 (data not shown). Only two genes, *PCSK6* and *GNA14,* involved in the hypoxic response, were up-regulated in *EPAS1*-mutated tumors. These genes may also play an important role in the development of normal hematopoietic cells [214] and in susceptibility to carcinogenesis, tumor progression [215], apoptosis [216] and tumor malignancy [217].

To summarize, in this second WES project we learned about the risks of applying preconceived inheritance models to the pipeline of a given next generation sequencing experimental design. In addition, we have demonstrated that *EPAS1* mutations are also involved in sporadic presentation of the disease, and found that specific copy number alteration affecting *EPAS1* can be used to guide the genetic screening of patients with PCC/PGL for mutations in the known susceptibility genes.

• ARTICLE 5: Discovery of *MDH2* germline mutations in patients with PCC.

Tumor multiplicity is a relatively common condition in patients affected with PCC/PGL and carrying a germline mutation in one of the major susceptibility genes (for example, in an SDH gene; see Table 1). This phenotypic feature represents one of the most clear clinical signs of disease heritability, and is a major indicator for genetic screening to identify a germline alteration. Of note, tumor multiplicity is sometimes controversial since is difficult to distinguish between the presence of multiple primary tumors in different locations and the local dissemination of an isolated mass. In a third WES project we selected for sequencing tumor DNA (and germline DNA when possible) from three unrelated patients affected with more than three primary PCC/PGLs but no mutations in any of the known susceptibility genes. Preliminary analysis of WES data looking for a common gene mutated in all patients yielded no positive results. Thus, we focused our attention on the analysis of each sample independently, and we present in this thesis the results obtained from the analysis of one of the three sequenced patients. For this

particular case, a patient diagnosed with five tumors and bone metastasis, WES was applied to tumor DNA only because we did not have sufficient germline DNA.

First, a very stringent filtering pipeline was applied in order to obtain a reduced list of candidate variants. In addition to standard filtering steps, we ruled out variants with low or moderate impact (i.e. missense or silent variants, respectively), and used PROVEAN software (http://provean.jcvi.org/index.php), manual curating and additional internal exomes as final steps in the filtering process. After all filtering steps, we identified sixteen high-impact candidate variants (i.e. nonsense or frameshift changes): five single nucleotide substitutions and eleven small insertions and deletions. We selected for further analysis a variant (c.429+1G>T) affecting a donor splice site in *MDH2.* based on the relevant function of this gene in the Krebs cycle, a well-known PCC-related pathway. Disruption of the Krebs cycle is a hallmark of cancer, but this is especially relevant in the case of hereditary PCC/PGL, in which germline mutations affecting the SDH genes are well-known genetic drivers of tumor development[69-72 73]. Moreover, mutations in the *FH* gene have been recently described to be involved in PCC/PGL predisposition[50,82], and at least one PGL has been found to carry a somatic *IDH1* mutation[116].

First, we confirmed by Sanger sequencing the presence of the variant both in the sequenced tumor and in peripheral blood lymphocytes from the patient. The c.429+1G>T variant affected a canonical donor splice site in the exon 4 of *MDH2*, and we demonstrated that it caused a deleterious effect, leading to both an altered transcript that incorporated 20 additional amino-acids into the exon and a premature stop codon. Moreover, the LOH of the wild type allele observed in two of the tumors of the patient, the absence of MDH2 protein and enzymatic activity in all available tumors, and the segregation of the variant with the disease in at least one relative, led us to propose *MDH2* as a classical tumor suppressor gene. In addition, only one truncating mutation in *MDH2* is recorded in COSMIC. The mutation was found in a neuroblastoma, a highly metastatic tumor of the sympathetic nervous system that is genetically related to PCC[172] and that also originates primarily in the adrenal gland.

The study of DNA methylation-associated profiles has led to the identification of characteristic epigenetic subtypes in several cancers[80,218]. Thus, a CIMP profile has been described for colorectal cancers[219], and more recently for gliomas[80], this latter associated with gain-of-function mutations in the *IDH1* and *IDH2* genes. In 2013, Letouze *et al*. described a well-defined CIMP for PCCs and PGLs harboring mutations in genes involved in the Krebs cycle (i.e. *FH* and SDH genes)[50]. To support the implication of the *MDH2* gene in tumor development, we performed hierarchical cluster analysis of a *MDH2*-mutated tumor and a large series of PCCs/PGLs, using data from a subset of genes reported as hypermethylated and downregulated in CIMP-associated PCC/PGL[50]. The transcriptional profiling revealed that the *MDH2*-

mutated tumor clustered together with PCCs/PGLs carrying mutations in the SDH genes, which also suggested a CIMP profile for this tumor. In addition, three apparently sporadic cases (testing negative for mutations in *MDH2* and all other PCC/PGL susceptibility genes) were grouped in this cluster, suggesting that they may harbor a still unknown mutation in a Krebs cycle-related gene. 5-hmC and H3K27me3 immunostaining was consistent with the suggested CIMP profile of all available *MDH2*-mutated tumors from the patient, as occurred with *FH*- and *SDH*-mutated PCCs/PGLs[50]. Amongst the genes found hypermethylated and downregulated in CIMP-tumors, *RBP1* was especially interesting, since its silencing seems to be exclusive for gliomas carrying mutations in the *IDH1* and *2* genes[163]. Our data also confirmed this association for PCCs/PGLs with a CIMP profile, and pyrosequencing analysis revealed that the low *RBP1* expression levels observed in *MDH2*-mutated tumors was actually due to CpG island methylation.

The abrogation of a given enzymatic activity usually provokes the accumulation of its substrates, leading to the absence of the reaction product. In PCC/PGL, the accumulation of substrates is a major feature of tumors affected by mutations in the genes encoding Krebs cycle enzymes. Thus, the accumulation of succinate and fumarate in tumors harboring mutations in *FH* and the SDH genes, respectively, leads to the inhibition of DNA and histone demethylases, *in vitro* and *in vivo*, producing the mentioned CIMP profile[50,79] (Figure 4). A similar effect was observed in *Fh1*-deficient mouse cells[167].

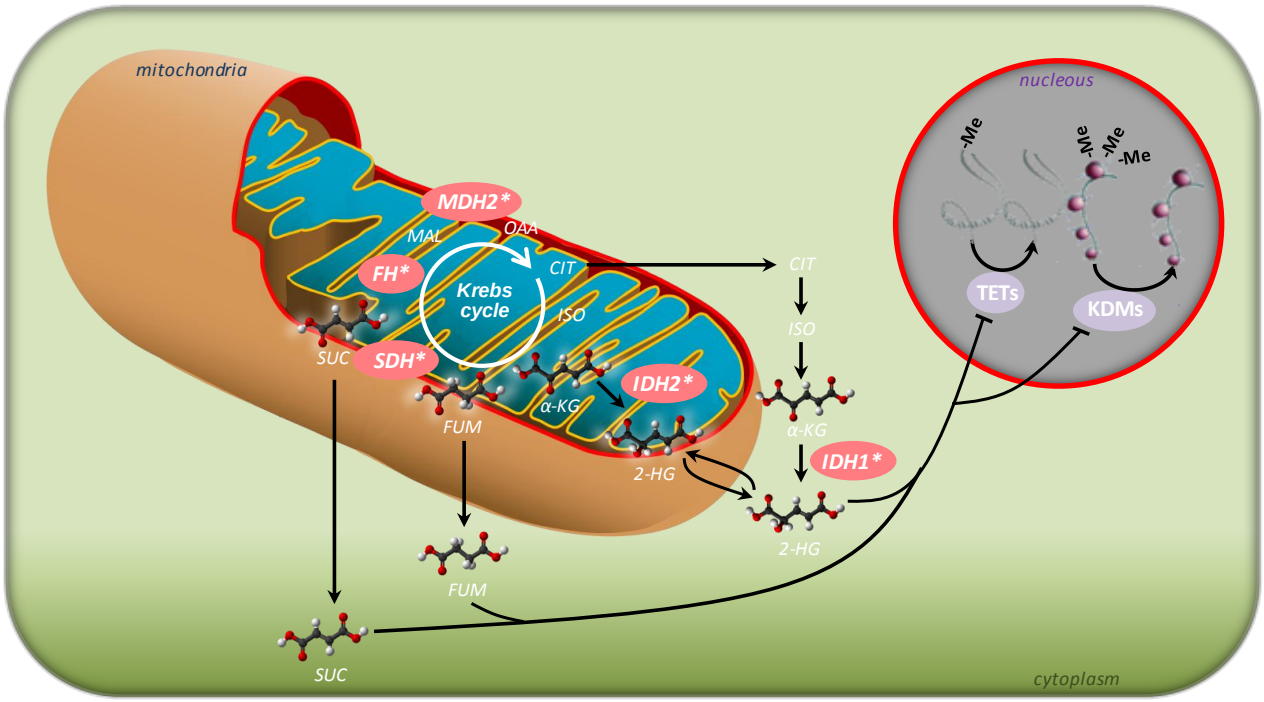

Figure 4. Representation of the oncogenic effect of the accumulation of Krebs cycle intermediates, 2-HG, succinate and fumarate, due to mutations in *IDH1/2*, SDH and *FH*, respectively.

The physiological consequences of disruption of the MDH2 enzyme in mammals have not been described. However, a *Drosophila* pupae-based model revealed the accumulation of late-stage Krebs cycle intermediates, such as malate, succinate, and fumarate, after MDH2 abrogation[166]. We demonstrated in this study that stable abrogation of MDH2 activity in HeLa cells leads to the expected accumulation of krebs cycle intermediates fumarate and malate, a condition reverted by transient introduction of wild-type *MDH2*. Although we did not observed the expected accumulation of malate in *MDH2*-mutated tumors, the high fumarate:succinate ratio observed in the *MDH2*-mutated tumors suggested an excess of fumarate, and pointed to this metabolite as the cause of the CIMP-like profile observed. Neither MDH1 activity nor the expression of other malate-related enzymes, such as the malic enzymes in frozen *MDH2*-mutated tumors, explained the absence of malate accumulation in the tumors. While we cannot rule out that malic enzyme-dependent conversion of malate to pyruvate and NADPH are responsible for the absence of malate accumulation in *MDH2*-mutated tumors, the mechanism behind this controversial result remains unknown.

The detection of two additional mutation carriers within the patient's pedigree, allowed us to confirm the deleterious effect of the heterozygous splicing *MDH2* mutation in established lymphoblastoid cell lines. Moreover, subsequent clinical testing detected high levels of normetanephrine for one of the mutation carriers, confirming the presence of the disease in this relative and the segregation of the mutation with the disease in the pedigree. The norepinephrine secretion profile observed for the two *MDH2* mutation carriers matched that described for PCC/PGL patients carrying Krebs cycle mutations. Moreover, the incomplete penetrance found for the *MDH2* mutation (i.e. one of the two mutation carriers did not show evidence of disease) also agreed with that observed for *SDHB, SDHA, SDHC* and *FH* mutations[15,46,82,170]. No other *MDH2* mutation carriers were detected amongst a selected series (n=29) of patients with clinical features of a hereditary disease. The susceptibility genes most recently described, *TMEM127*[98], *MAX*[140] or *FH*[82], each explain 1 to 2% of cases. Moreover, a previous screening for *FH* mutations in 239 Spanish PCC/PGL patients did not revealed any mutation carrier. Therefore, it seems that finding additional *MDH2*-mutated patients amongst patients in order to establish the prevalence of alterations in this gene, and the associated clinical presentation of the disease will require the screening of a larger series of patients.

In summary, as a result of this study we propose *MDH2* as a new PCC/PGL tumor suppressor susceptibility gene, once again suggesting a link between Krebs cycle disruption and PCC/PGL development. Moreover, our data suggest a possible involvement of other still unknown Krebs cycle-related genes in PCC/PGL cases without known genetic predisposition and showing a CIMP-like profile.

• General discussion of WES applications to the discovery of cancer predisposition genes.

Over the last decade, research into Mendelian disorders has been eclipsed by efforts to dissect the genetic bases of complex traits using GWAS. In addition, the success of investigations focused on deciphering the molecular basis of monogenic disorders has shrunk substantially, probably because of the lack of newer and more powerful methods. Previously, linkage studies had been demonstrated to be the most useful tool in the discovery of new genes playing a role in Mendelian disorders. However the absence of highly informative families, a common scenario in PCC/PGL pedigrees and the major limitation of this approach, has slowed the number of findings during recent years. In the case of PCC/PGL, the genetic and phenotypic heterogeneity of the disease makes the identification of a causal gene even more difficult. Nowadays, high-throughput techniques, especially WES, have emerged as a panacea and the most cost-effective method to discover new candidate genes and causal variants. Early studies have shown the effectiveness of applying WES to unrelated patients who share phenotypic similarities[131,134,135]. Collectively, these studies have demonstrated the advantages of WES over the linkage study design in situations where only a small number of unrelated samples, or sporadic cases, are available. In the case of genetically heterogeneous diseases, such as PCC/PGL, stratifying the patients by focusing on a specific molecular feature or any singular phenotype can help in the selection of informative individuals for WES.

In this thesis we have developed three projects applying WES to a very low number of unrelated individuals, all of them selected because they presented phenotypic characteristics suggesting a hereditary genetic condition. That selection, based on similarities in the transcriptional profile of tumors or on clinical features of heritability, allowed us to identify two new PCC/PGL susceptibility genes: *MAX*, the first cancer susceptibility gene discovered by WES [49], and *MDH2*, another gene encoding a Krebs cycle enzyme (in press). In addition, the *EPAS1* WES project exemplifies that, while the sampling process is crucial, the inheritance model included in the pipeline may be no less important. In conclusion, in this thesis we have demonstrated the success of using WES to identify new susceptibility PCC/PGL genes when an adequate and rational selection of cases and pipeline is applied.

CONCLUSIONES/CONCLUSIONS

CONCLUSIONES

1- La secuenciación masiva del exoma constituye una técnica eficaz para el descubrimiento de nuevos genes de susceptibilidad implicados en el desarrollo de enfermedades que siguen un modelo de herencia mendeliano, como es el caso de los PCCs/PGLs. La técnica debe apoyarse en una adecuada selección de los candidatos, así como en el correcto filtrado de las variantes detectadas con el fin de obtener unos resultados óptimos. Es fundamental tener en cuenta todos los modelos de herencia posibles durante el diseño del proyecto.

2- Las mutaciones germinales en el gen *MAX* confieren susceptibilidad hereditaria a desarrollar PCC/PGL. *MAX*, se comporta como un gen supresor tumoral clásico; se produce LOH del alelo silvestre en los tumores de los pacientes portadores de mutación (debida frecuentemente a una disomía uniparental paterna) y ausencia de proteína MAX funcional.

3- La prevalencia de las mutaciones patogénicas en el gen *MAX* en pacientes con la enfermedad, tanto con PCC como en menor medida con PGL, es de un 1,12% y la implicación del gen en la enfermedad esporádica explica hasta un 1,65% de los casos. Sin embargo, esta proporción aumenta hasta un 66% en pacientes sin mutaciones en otros genes y con PCC bilateral o multifocal y antecedentes familiares de la enfermedad.

4- Un modelo funcional desarrollado en células PC12, permite establecer de manera robusta el potencial patogénico de la mayor parte de las VUS encontradas en el gen *MAX* en pacientes con PCC/PGL. Los resultados funcionales, que guardaban una gran concordancia con los obtenidos a partir del consenso de varias predicciones *in silico* y venían refrendados por la información clínica disponible de los pacientes, son por tanto de clara aplicación en el consejo genético que se ofrece a estas familias.

5- Las mutaciones en el gen *EPAS1* se pueden producir tanto durante el desarrollo embrionario, dando lugar a casos con PCC/PGL múltiple y policitemia, como somáticamente en formas esporádicas de la enfermedad. La ganancia específica del cromosoma 2p constituye un rasgo diferencial de los tumores con mutación en *EPAS1* y puede utilizarse como marcador para la búsqueda de alteraciones en este gen.

6- El gen *MDH2* es un gen supresor tumoral asociado al desarrollo de PCCs/PGLs hereditarios, lo cual supone un nuevo ejemplo de cómo defectos en el ciclo de Krebs tienen un efecto oncogénico. La ausencia de *MDH2* en los tumores, está asociada con un fenotipo hipermetilador similar al descrito en PCCs con mutaciones en los genes *SDH* o en *FH*, causado posiblemente por la acumulación de intermediarios del ciclo de Krebs. La penetrancia incompleta de la mutación encontrada, así como la ausencia de más casos con alteraciones en *MDH2*, sugieren la necesidad de reclutar un gran número de pacientes para determinar la relevancia del gen en la enfermedad.

CONCLUSIONS

1- Whole exome sequencing constitutes an efficient technique to discover susceptibility genes involved in the development of Mendelian hereditary diseases, such as PCCs/PGLs. This technique should be complemented by appropriate filtering of the detected variants and selection of candidates, in order to obtain optimal results. It is crucial to take into consideration in the design of the project all possible inheritance models.

2- Germline mutations in the *MAX* gene confer hereditary susceptibility to develop PCC/PGL. *MAX* behaves as a classical tumor suppressor gene. Absence of the functional protein and LOH of the wild type allele is observed in the tumors of these patients, the latter frequently due to uniparental disomy.

3- The estimated prevalence of pathogenic *MAX* mutations in patients is 1.12%, presenting more often in PCC than PGL. On the other hand, mutations in the gene explain an estimated 1.65% of sporadic cases. This percentage is 66% in patients negative for mutation in other PCC susceptibility gene, with bilateral or multifocal PCC and a family history of the disease.

4- By means of a functional model developed from PC12 cells, the pathogenic potential of the majority of the VUS found in the *MAX* gene in patients presenting PCC/PGL was established. Results from functional assays are concordant with those obtained from the consensus of several *in silico* prediction algorithms and are supported by the clinical information from the patients. This model has a clear application in the genetic counseling offered to these patients.

5- Mutations in the gene *EPAS1* can appear during embryonic development, giving rise either to cases presenting multiple tumors and polycythemia or to sporadic presentation of the disease. The specific gain of the chromosome 2p constitutes a differential feature of tumors harboring *EPAS1* mutations and can be used as a marker for directed genetic screening.

6- The *MDH2* gene is a tumor suppressor gene associated to the development of hereditary PCC/PGL and constitutes a novel example of the oncogenic properties of Krebs cycle inactivation. The absence of MDH2 in tumors is associated with a hypermethylator phenotype, similar to the previously described in PCCs harboring mutations in *FH* or the SDH genes, probably caused by the accumulation of Krebs cycle metabolites. The incomplete penetrance of the mutation, as well as the absence of more cases carrying alterations in the gene, highlight the need to recruit larger series of patients in order to determine the relevance of *MDH2* to the development of disease.

BIBLIOGRAPHY

1. Elakovic, D., Manojlovic, D. & Milovic, N. [Surgical treatment of pheochromocytoma--personal experience]. *Srp Arh Celok Lek* **130 Suppl 2**, 31-7 (2002).
2. Fraenkel, F. & University of Freiburg im Breisgau. Thesis (doctoral), University of Freiburg im Breisgau, 1886. (1886).
3. Neumann, H.P. et al. Evidence of MEN-2 in the original description of classic pheochromocytoma. *N Engl J Med* **357**, 1311-5 (2007).
4. Manger, W.M. An overview of pheochromocytoma: history, current concepts, vagaries, and diagnostic challenges. *Ann N Y Acad Sci* **1073**, 1-20 (2006).
5. Kaltsas, G.A., Papadogias, D. & Grossman, A.B. The clinical presentation (symptoms and signs) of sporadic and familial chromaffin cell tumours (phaeochromocytomas and paragangliomas). *Front Horm Res* **31**, 61-75 (2004).
6. Chen, H. et al. The North American Neuroendocrine Tumor Society consensus guideline for the diagnosis and management of neuroendocrine tumors: pheochromocytoma, paraganglioma, and medullary thyroid cancer. *Pancreas* **39**, 775-83 (2010).
7. McNeil, A.R., Blok, B.H., Koelmeyer, T.D., Burke, M.P. & Hilton, J.M. Phaeochromocytomas discovered during coronial autopsies in Sydney, Melbourne and Auckland. *Aust N Z J Med* **30**, 648-52 (2000).
8. Mannelli, M., Lenders, J.W., Pacak, K., Parenti, G. & Eisenhofer, G. Subclinical phaeochromocytoma. *Best Pract Res Clin Endocrinol Metab* **26**, 507-15 (2012).
9. Pacak, K., Lenders, J.W.M. & Eisenhofer, G. *Pheochromocytoma : diagnosis, localization, and treatment*, vi, 172 p. (Blackwell Pub., Malden, MA, 2007).
10. Cascon, A. et al. Genetics of pheochromocytoma and paraganglioma in Spanish pediatric patients. *Endocr Relat Cancer* **20**, L1-6 (2013).
11. King, K.S. et al. Metastatic pheochromocytoma/paraganglioma related to primary tumor development in childhood or adolescence: significant link to SDHB mutations. *J Clin Oncol* **29**, 4137-42 (2011).
12. Barontini, M., Levin, G. & Sanso, G. Characteristics of pheochromocytoma in a 4- to 20-year-old population. *Ann N Y Acad Sci* **1073**, 30-7 (2006).
13. Lenders, J.W., Eisenhofer, G., Mannelli, M. & Pacak, K. Phaeochromocytoma. *Lancet* **366**, 665-75 (2005).
14. Lack, E.E., Armed Forces Institute of Pathology (U.S.) & Universities Associated for Research and Education in Pathology. *Tumors of the adrenal gland and extra-adrenal paraganglia*, 468 p. (Armed Forces Institute of Pathology, Washington, D.C., 1997).
15. Dahia, P.L. Pheochromocytoma and paraganglioma pathogenesis: learning from genetic heterogeneity. *Nat Rev Cancer* **14**, 108-19 (2014).
16. Schulz, C., Eisenhofer, G. & Lehnert, H. Principles of catecholamine biosynthesis, metabolism and release. *Front Horm Res* **31**, 1-25 (2004).
17. Eisenhofer, G., Goldstein, D.S., Kopin, I.J. & Crout, J.R. Pheochromocytoma: rediscovery as a catecholamine-metabolizing tumor. *Endocr Pathol* **14**, 193-212 (2003).
18. Grossman, A. et al. Biochemical diagnosis and localization of pheochromocytoma: can we reach a consensus? *Ann N Y Acad Sci* **1073**, 332-47 (2006).
19. Robledo, M., Cascon, A. & Curras, M. *The Hereditary Basis of Childhood Cancer*. (2014).
20. Poirier, E., Thauvette, D. & Hogue, J.C. Management of exclusively dopamine-secreting abdominal pheochromocytomas. *J Am Coll Surg* **216**, 340-6 (2013).
21. Sahdev, A. et al. CT and MR imaging of unusual locations of extra-adrenal paragangliomas (pheochromocytomas). *Eur Radiol* **15**, 85-92 (2005).
22. Havekes, B., Romijn, J.A., Eisenhofer, G., Adams, K. & Pacak, K. Update on pediatric pheochromocytoma. *Pediatr Nephrol* **24**, 943-50 (2009).
23. Taieb, D. et al. EANM 2012 guidelines for radionuclide imaging of phaeochromocytoma and paraganglioma. *Eur J Nucl Med Mol Imaging* **39**, 1977-95 (2012).

24. Fikri, A.S. et al. Localization and prediction of malignant potential in recurrent pheochromocytoma/paraganglioma (PCC/PGL) using 18F-FDG PET/CT. *Acta Radiol* **55**, 631-640 (2013).
25. Leung, K., Stamm, M., Raja, A. & Low, G. Pheochromocytoma: the range of appearances on ultrasound, CT, MRI, and functional imaging. *AJR Am J Roentgenol* **200**, 370-8 (2013).
26. King, K.S. et al. Functional imaging of SDHx-related head and neck paragangliomas: comparison of 18F-fluorodihydroxyphenylalanine, 18F-fluorodopamine, 18F-fluoro-2-deoxy-D-glucose PET, 123I-metaiodobenzylguanidine scintigraphy, and 111In-pentetreotide scintigraphy. *J Clin Endocrinol Metab* **96**, 2779-85 (2011).
27. Waguespack, S.G. et al. A current review of the etiology, diagnosis, and treatment of pediatric pheochromocytoma and paraganglioma. *J Clin Endocrinol Metab* **95**, 2023-37 (2010).
28. Darr, R. et al. Pheochromocytoma - update on disease management. *Ther Adv Endocrinol Metab* **3**, 11-26 (2012).
29. Fanti, S. et al. Evaluation of unusual neuroendocrine tumours by means of 68Ga-DOTA-NOC PET. *Biomed Pharmacother* **62**, 667-71 (2008).
30. Kroiss, A. et al. Functional imaging in phaeochromocytoma and neuroblastoma with 68Ga-DOTA-Tyr 3-octreotide positron emission tomography and 123I-metaiodobenzylguanidine. *Eur J Nucl Med Mol Imaging* **38**, 865-73 (2011).
31. Mazza, A. et al. Anti-hypertensive treatment in pheochromocytoma and paraganglioma: current management and therapeutic features. *Endocrine* **45**, 469-78 (2014).
32. Pacak, K. Preoperative management of the pheochromocytoma patient. *J Clin Endocrinol Metab* **92**, 4069-79 (2007).
33. Conzo, G. et al. Laparoscopic adrenalectomy, a safe procedure for pheochromocytoma. A retrospective review of clinical series. *Int J Surg* **11**, 152-6 (2013).
34. Jimenez, C. et al. Current and future treatments for malignant pheochromocytoma and sympathetic paraganglioma. *Curr Oncol Rep* **15**, 356-71 (2013).
35. Matro, J., Giubellino, A. & Pacak, K. Current and future therapeutic approaches for metastatic pheochromocytoma and paraganglioma: focus on SDHB tumors. *Horm Metab Res* **45**, 147-53 (2013).
36. Li, M., Kong, Z.M. & Liu, Z.L. Antioxidant enzyme activities and lipid peroxidation induced by eicosapentaenoic acid (EPA) in PC12 cells. *Cell Biol Toxicol* **22**, 331-7 (2006).
37. Menda, Y. et al. Phase I trial of 90Y-DOTATOC therapy in children and young adults with refractory solid tumors that express somatostatin receptors. *J Nucl Med* **51**, 1524-31 (2010).
38. Martiniova, L. et al. Increased uptake of [(1)(2)(3)I]meta-iodobenzylguanidine, [(1)(8)F]fluorodopamine, and [(3)H]norepinephrine in mouse pheochromocytoma cells and tumors after treatment with the histone deacetylase inhibitors. *Endocr Relat Cancer* **18**, 143-57 (2011).
39. Pacak, K. et al. NF-kappaB inhibition significantly upregulates the norepinephrine transporter system, causes apoptosis in pheochromocytoma cell lines and prevents metastasis in an animal model. *Int J Cancer* **131**, 2445-55 (2012).
40. Park, H.K. et al. Combination treatment with doxorubicin and gamitrinib synergistically augments anticancer activity through enhanced activation of Bim. *BMC Cancer* **14**, 431 (2014).
41. Powers, J.F. et al. Cytocidal activities of topoisomerase 1 inhibitors and 5-azacytidine against pheochromocytoma/paraganglioma cells in primary human tumor cultures and mouse cell lines. *PLoS One* **9**, e87807 (2014).
42. Pappachan, J.M., Raskauskiene, D., Sriraman, R., Edavalath, M. & Hanna, F.W. Diagnosis and management of pheochromocytoma: a practical guide to clinicians. *Curr Hypertens Rep* **16**, 442 (2014).
43. Ayala-Ramirez, M. et al. Treatment with sunitinib for patients with progressive metastatic pheochromocytomas and sympathetic paragangliomas. *J Clin Endocrinol Metab* **97**, 4040-50 (2012).

44. Cassol, C.A. et al. Tyrosine kinase receptors as molecular targets in pheochromocytomas and paragangliomas. *Mod Pathol* **27**, 1050-62 (2014).
45. Mannelli, M. et al. Clinically guided genetic screening in a large cohort of italian patients with pheochromocytomas and/or functional or nonfunctional paragangliomas. *J Clin Endocrinol Metab* **94**, 1541-7 (2009).
46. Cascon, A. et al. Genetics of pheochromocytoma and paraganglioma in Spanish patients. *J Clin Endocrinol Metab* **94**, 1701-5 (2009).
47. Welander, J., Soderkvist, P. & Gimm, O. Genetics and clinical characteristics of hereditary pheochromocytomas and paragangliomas. *Endocr Relat Cancer* **18**, R253-76 (2011).
48. Qin, Y. et al. Germline mutations in TMEM127 confer susceptibility to pheochromocytoma. *Nat Genet* **42**, 229-33 (2010).
49. Comino-Mendez, I. et al. Exome sequencing identifies MAX mutations as a cause of hereditary pheochromocytoma. *Nat Genet* **43**, 663-7 (2011).
50. Letouze, E. et al. SDH mutations establish a hypermethylator phenotype in paraganglioma. *Cancer Cell* **23**, 739-52 (2013).
51. Yang, C. et al. Germ-line PHD1 and PHD2 mutations detected in patients with pheochromocytoma/paraganglioma-polycythemia. *J Mol Med (Berl)* (2014).
52. Eisenhofer, G. et al. Distinct gene expression profiles in norepinephrine- and epinephrine-producing hereditary and sporadic pheochromocytomas: activation of hypoxia-driven angiogenic pathways in von Hippel-Lindau syndrome. *Endocr Relat Cancer* **11**, 897-911 (2004).
53. Dahia, P.L. et al. A HIF1alpha regulatory loop links hypoxia and mitochondrial signals in pheochromocytomas. *PLoS Genet* **1**, 72-80 (2005).
54. Favier, J. et al. The Warburg effect is genetically determined in inherited pheochromocytomas. *PLoS One* **4**, e7094 (2009).
55. Lopez-Jimenez, E. et al. Research resource: Transcriptional profiling reveals different pseudohypoxic signatures in SDHB and VHL-related pheochromocytomas. *Mol Endocrinol* **24**, 2382-91 (2010).
56. Semenza, G.L. HIF-1, O(2), and the 3 PHDs: how animal cells signal hypoxia to the nucleus. *Cell* **107**, 1-3 (2001).
57. Gruber, M. & Simon, M.C. Hypoxia-inducible factors, hypoxia, and tumor angiogenesis. *Curr Opin Hematol* **13**, 169-74 (2006).
58. Shen, C. & Kaelin, W.G., Jr. The VHL/HIF axis in clear cell renal carcinoma. *Semin Cancer Biol* **23**, 18-25 (2013).
59. Kaelin, W.G., Jr. The von Hippel-Lindau tumour suppressor protein: O2 sensing and cancer. *Nat Rev Cancer* **8**, 865-73 (2008).
60. Latif, F. et al. Identification of the von Hippel-Lindau disease tumor suppressor gene. *Science* **260**, 1317-20 (1993).
61. Lonser, R.R. et al. von Hippel-Lindau disease. *Lancet* **361**, 2059-67 (2003).
62. Gimenez-Roqueplo, A.P., Dahia, P.L. & Robledo, M. An update on the genetics of paraganglioma, pheochromocytoma, and associated hereditary syndromes. *Horm Metab Res* **44**, 328-33 (2012).
63. Zhuang, Z. et al. Somatic HIF2A gain-of-function mutations in paraganglioma with polycythemia. *N Engl J Med* **367**, 922-30 (2012).
64. McDonough, M.A. et al. Cellular oxygen sensing: Crystal structure of hypoxia-inducible factor prolyl hydroxylase (PHD2). *Proc Natl Acad Sci U S A* **103**, 9814-9 (2006).
65. Min, J.H. et al. Structure of an HIF-1alpha -pVHL complex: hydroxyproline recognition in signaling. *Science* **296**, 1886-9 (2002).
66. Lorenzo, F.R. et al. A novel EPAS1/HIF2A germline mutation in a congenital polycythemia with paraganglioma. *J Mol Med (Berl)* **91**, 507-12 (2013).
67. Comino-Mendez, I. et al. Tumoral EPAS1 (HIF2A) mutations explain sporadic pheochromocytoma and paraganglioma in the absence of erythrocytosis. *Hum Mol Genet* **22**, 2169-76 (2013).

68. Cecchini, G. Respiratory complex II: role in cellular physiology and disease. *Biochim Biophys Acta* **1827**, 541-2 (2013).
69. Baysal, B.E. et al. Mutations in SDHD, a mitochondrial complex II gene, in hereditary paraganglioma. *Science* **287**, 848-51 (2000).
70. Niemann, S. & Muller, U. Mutations in SDHC cause autosomal dominant paraganglioma, type 3. *Nat Genet* **26**, 268-70 (2000).
71. Astuti, D. et al. Gene mutations in the succinate dehydrogenase subunit SDHB cause susceptibility to familial pheochromocytoma and to familial paraganglioma. *Am J Hum Genet* **69**, 49-54 (2001).
72. Burnichon, N. et al. SDHA is a tumor suppressor gene causing paraganglioma. *Hum Mol Genet* **19**, 3011-20 (2010).
73. Hao, H.X. et al. SDH5, a gene required for flavination of succinate dehydrogenase, is mutated in paraganglioma. *Science* **325**, 1139-42 (2009).
74. Jaakkola, P. et al. Targeting of HIF-alpha to the von Hippel-Lindau ubiquitylation complex by O2-regulated prolyl hydroxylation. *Science* **292**, 468-72 (2001).
75. Ivan, M. et al. HIFalpha targeted for VHL-mediated destruction by proline hydroxylation: implications for O2 sensing. *Science* **292**, 464-8 (2001).
76. Lee, F.S. & Percy, M.J. The HIF pathway and erythrocytosis. *Annu Rev Pathol* **6**, 165-92 (2011).
77. Burnichon, N. et al. Integrative genomic analysis reveals somatic mutations in pheochromocytoma and paraganglioma. *Hum Mol Genet* **20**, 3974-85 (2011).
78. Selak, M.A. et al. Succinate links TCA cycle dysfunction to oncogenesis by inhibiting HIF-alpha prolyl hydroxylase. *Cancer Cell* **7**, 77-85 (2005).
79. Xiao, M. et al. Inhibition of alpha-KG-dependent histone and DNA demethylases by fumarate and succinate that are accumulated in mutations of FH and SDH tumor suppressors. *Genes Dev* **26**, 1326-38 (2012).
80. Noushmehr, H. et al. Identification of a CpG island methylator phenotype that defines a distinct subgroup of glioma. *Cancer Cell* **17**, 510-22 (2010).
81. Schmidt, L.S. & Linehan, W.M. Hereditary leiomyomatosis and renal cell carcinoma. *Int J Nephrol Renovasc Dis* **7**, 253-60 (2014).
82. Castro-Vega, L.J. et al. Germline mutations in FH confer predisposition to malignant pheochromocytomas and paragangliomas. *Hum Mol Genet* **23**, 2440-6 (2014).
83. Segouffin-Cariou, C. & Billaud, M. Transforming ability of MEN2A-RET requires activation of the phosphatidylinositol 3-kinase/AKT signaling pathway. *J Biol Chem* **275**, 3568-76 (2000).
84. Johannessen, C.M. et al. The NF1 tumor suppressor critically regulates TSC2 and mTOR. *Proc Natl Acad Sci U S A* **102**, 8573-8 (2005).
85. Cox, A.D. & Der, C.J. Ras history: The saga continues. *Small GTPases* **1**, 2-27 (2010).
86. de Groot, J.W., Links, T.P., Plukker, J.T., Lips, C.J. & Hofstra, R.M. RET as a diagnostic and therapeutic target in sporadic and hereditary endocrine tumors. *Endocr Rev* **27**, 535-60 (2006).
87. Neumann, H.P. et al. Consequences of direct genetic testing for germline mutations in the clinical management of families with multiple endocrine neoplasia, type II. *JAMA* **274**, 1149-51 (1995).
88. Richardson, D.S., Lai, A.Z. & Mulligan, L.M. RET ligand-induced internalization and its consequences for downstream signaling. *Oncogene* **25**, 3206-11 (2006).
89. Mulligan, L.M. et al. Germ-line mutations of the RET proto-oncogene in multiple endocrine neoplasia type 2A. *Nature* **363**, 458-60 (1993).
90. Karagiannis, A., Mikhailidis, D.P., Athyros, V.G. & Harsoulis, F. Pheochromocytoma: an update on genetics and management. *Endocr Relat Cancer* **14**, 935-56 (2007).
91. Kloos, R.T. et al. Medullary thyroid cancer: management guidelines of the American Thyroid Association. *Thyroid* **19**, 565-612 (2009).
92. Asai, N., Iwashita, T., Matsuyama, M. & Takahashi, M. Mechanism of activation of the ret proto-oncogene by multiple endocrine neoplasia 2A mutations. *Mol Cell Biol* **15**, 1613-9 (1995).
93. Santoro, M. et al. Activation of RET as a dominant transforming gene by germline mutations of MEN2A and MEN2B. *Science* **267**, 381-3 (1995).

94. Boyd, K.P., Korf, B.R. & Theos, A. Neurofibromatosis type 1. *J Am Acad Dermatol* **61**, 1-14; quiz 15-6 (2009).
95. Kehrer-Sawatzki, H. & Cooper, D.N. Mosaicism in sporadic neurofibromatosis type 1: variations on a theme common to other hereditary cancer syndromes? *J Med Genet* **45**, 622-31 (2008).
96. Burnichon, N. et al. Somatic NF1 inactivation is a frequent event in sporadic pheochromocytoma. *Hum Mol Genet* **21**, 5397-405 (2012).
97. Welander, J. et al. Integrative genomics reveals frequent somatic NF1 mutations in sporadic pheochromocytomas. *Hum Mol Genet* **21**, 5406-16 (2012).
98. Yao, L. et al. Spectrum and prevalence of FP/TMEM127 gene mutations in pheochromocytomas and paragangliomas. *JAMA* **304**, 2611-9 (2010).
99. Blackwood, E.M., Luscher, B. & Eisenman, R.N. Myc and Max associate in vivo. *Genes Dev* **6**, 71-80 (1992).
100. Grandori, C., Cowley, S.M., James, L.P. & Eisenman, R.N. The Myc/Max/Mad network and the transcriptional control of cell behavior. *Annu Rev Cell Dev Biol* **16**, 653-99 (2000).
101. Cascon, A. & Robledo, M. MAX and MYC: a heritable breakup. *Cancer Res* **72**, 3119-24 (2012).
102. Karnoub, A.E. & Weinberg, R.A. Ras oncogenes: split personalities. *Nat Rev Mol Cell Biol* **9**, 517-31 (2008).
103. Baines, A.T., Xu, D. & Der, C.J. Inhibition of Ras for cancer treatment: the search continues. *Future Med Chem* **3**, 1787-808 (2011).
104. Yoshimoto, K. et al. ras mutations in endocrine tumors: mutation detection by polymerase chain reaction-single strand conformation polymorphism. *Jpn J Cancer Res* **83**, 1057-62 (1992).
105. Crona, J. et al. Somatic mutations in H-RAS in sporadic pheochromocytoma and paraganglioma identified by exome sequencing. *J Clin Endocrinol Metab* **98**, E1266-71 (2013).
106. Oudijk, L. et al. H-RAS mutations are restricted to sporadic pheochromocytomas lacking specific clinical or pathological features: data from a multi-institutional series. *J Clin Endocrinol Metab* **99**, E1376-80 (2014).
107. Nikiforov, Y.E. & Nikiforova, M.N. Molecular genetics and diagnosis of thyroid cancer. *Nat Rev Endocrinol* **7**, 569-80 (2011).
108. Agrawal, N. et al. Exomic sequencing of medullary thyroid cancer reveals dominant and mutually exclusive oncogenic mutations in RET and RAS. *J Clin Endocrinol Metab* **98**, E364-9 (2013).
109. Ciampi, R. et al. Evidence of a low prevalence of RAS mutations in a large medullary thyroid cancer series. *Thyroid* **23**, 50-7 (2013).
110. Schlisio, S. et al. The kinesin KIF1Bbeta acts downstream from EglN3 to induce apoptosis and is a potential 1p36 tumor suppressor. *Genes Dev* **22**, 884-93 (2008).
111. Yeh, I.T. et al. A germline mutation of the KIF1B beta gene on 1p36 in a family with neural and nonneural tumors. *Hum Genet* **124**, 279-85 (2008).
112. Welander, J. et al. Rare germline mutations identified by targeted next-generation sequencing of susceptibility genes in pheochromocytoma and paraganglioma. *J Clin Endocrinol Metab* **99**, E1352-60 (2014).
113. Ladroue, C. et al. PHD2 mutation and congenital erythrocytosis with paraganglioma. *N Engl J Med* **359**, 2685-92 (2008).
114. Schussheim, D.H. et al. Multiple endocrine neoplasia type 1: new clinical and basic findings. *Trends Endocrinol Metab* **12**, 173-8 (2001).
115. Denes, J. et al. Heterogeneous genetic background of the association of pheochromocytoma/paraganglioma and pituitary adenoma - results from a large patient cohort. *J Clin Endocrinol Metab*, jc20143399 (2014).
116. Gaal, J. et al. Isocitrate dehydrogenase mutations are rare in pheochromocytomas and paragangliomas. *J Clin Endocrinol Metab* **95**, 1274-8 (2010).
117. Rahman, N. Realizing the promise of cancer predisposition genes. *Nature* **505**, 302-8 (2014).
118. Antonarakis, S.E. & Beckmann, J.S. Mendelian disorders deserve more attention. *Nat Rev Genet* **7**, 277-82 (2006).

119. Lander, E.S. et al. Initial sequencing and analysis of the human genome. *Nature* **409**, 860-921 (2001).
120. Finishing the euchromatic sequence of the human genome. *Nature* **431**, 931-45 (2004).
121. Wheeler, D.A. et al. The complete genome of an individual by massively parallel DNA sequencing. *Nature* **452**, 872-6 (2008).
122. Levy, S. et al. The diploid genome sequence of an individual human. *PLoS Biol* **5**, e254 (2007).
123. Bentley, D.R. et al. Accurate whole human genome sequencing using reversible terminator chemistry. *Nature* **456**, 53-9 (2008).
124. McKernan, K.J. et al. Sequence and structural variation in a human genome uncovered by short-read, massively parallel ligation sequencing using two-base encoding. *Genome Res* **19**, 1527-41 (2009).
125. Schuster, S.C. et al. Complete Khoisan and Bantu genomes from southern Africa. *Nature* **463**, 943-7 (2010).
126. Wang, J. et al. The diploid genome sequence of an Asian individual. *Nature* **456**, 60-5 (2008).
127. Ahn, S.M. et al. The first Korean genome sequence and analysis: full genome sequencing for a socio-ethnic group. *Genome Res* **19**, 1622-9 (2009).
128. Kim, J.I. et al. A highly annotated whole-genome sequence of a Korean individual. *Nature* **460**, 1011-5 (2009).
129. Ley, T.J. et al. DNA sequencing of a cytogenetically normal acute myeloid leukaemia genome. *Nature* **456**, 66-72 (2008).
130. Mamanova, L. et al. Target-enrichment strategies for next-generation sequencing. *Nat Methods* **7**, 111-8 (2010).
131. Ng, S.B. et al. Targeted capture and massively parallel sequencing of 12 human exomes. *Nature* **461**, 272-6 (2009).
132. Choi, M. et al. Genetic diagnosis by whole exome capture and massively parallel DNA sequencing. *Proc Natl Acad Sci U S A* **106**, 19096-101 (2009).
133. Ng, S.B. et al. Exome sequencing identifies the cause of a mendelian disorder. *Nat Genet* **42**, 30-5 (2010).
134. Hoischen, A. et al. De novo mutations of SETBP1 cause Schinzel-Giedion syndrome. *Nat Genet* **42**, 483-5 (2010).
135. Ng, S.B. et al. Exome sequencing identifies MLL2 mutations as a cause of Kabuki syndrome. *Nat Genet* **42**, 790-3 (2010).
136. Stenson, P.D. et al. The Human Gene Mutation Database: providing a comprehensive central mutation database for molecular diagnostics and personalized genomics. *Hum Genomics* **4**, 69-72 (2009).
137. Bamshad, M.J. et al. Exome sequencing as a tool for Mendelian disease gene discovery. *Nat Rev Genet* **12**, 745-55 (2011).
138. Burnichon, N. et al. Somatic NF1 Inactivation is a Frequent Event in Sporadic Pheochromocytoma. *Hum Mol Genet* (2012).
139. Wallace, M.R. et al. Type 1 neurofibromatosis gene: identification of a large transcript disrupted in three NF1 patients. *Science* **249**, 181-6 (1990).
140. Burnichon, N. et al. MAX mutations cause hereditary and sporadic pheochromocytoma and paraganglioma. *Clin Cancer Res* **18**, 2828-37 (2012).
141. Romero, O.A. et al. MAX inactivation in small-cell lung cancer disrupts the MYC-SWI/SNF programs and is synthetic lethal with BRG1. *Cancer Discov* (2013).
142. Atchley, W.R. & Fitch, W.M. Myc and Max: molecular evolution of a family of proto-oncogene products and their dimerization partner. *Proc Natl Acad Sci U S A* **92**, 10217-21 (1995).
143. Vervoorts, J. & Luscher, B. DNA binding of Myc/Max/Mad network complexes to oligonucleotides containing two E box elements: c-Myc/Max heterodimers do not bind DNA cooperatively. *Biol Chem* **380**, 1121-6 (1999).

144. Beaulieu, M.E. et al. New structural determinants for c-Myc specific heterodimerization with Max and development of a novel homodimeric c-Myc b-HLH-LZ. *J Mol Recognit* **25**, 414-26 (2012).
145. Gallant, P. & Steiger, D. Myc's secret life without Max. *Cell Cycle* **8**, 3848-53 (2009).
146. Rattenberry, E. et al. A comprehensive next generation sequencing-based genetic testing strategy to improve diagnosis of inherited pheochromocytoma and paraganglioma. *J Clin Endocrinol Metab* **98**, E1248-56 (2013).
147. Kumar, P., Henikoff, S. & Ng, P.C. Predicting the effects of coding non-synonymous variants on protein function using the SIFT algorithm. *Nat Protoc* **4**, 1073-81 (2009).
148. Adzhubei, I.A. et al. A method and server for predicting damaging missense mutations. *Nat Methods* **7**, 248-9 (2010).
149. Li, B. et al. Automated inference of molecular mechanisms of disease from amino acid substitutions. *Bioinformatics* **25**, 2744-50 (2009).
150. Calabrese, R., Capriotti, E., Fariselli, P., Martelli, P.L. & Casadio, R. Functional annotations improve the predictive score of human disease-related mutations in proteins. *Hum Mutat* **30**, 1237-44 (2009).
151. Bendl, J. et al. PredictSNP: robust and accurate consensus classifier for prediction of disease-related mutations. *PLoS Comput Biol* **10**, e1003440 (2014).
152. Capriotti, E., Altman, R.B. & Bromberg, Y. Collective judgment predicts disease-associated single nucleotide variants. *BMC Genomics* **14 Suppl 3**, S2 (2013).
153. Emsley, P., Lohkamp, B., Scott, W.G. & Cowtan, K. Features and development of Coot. *Acta Crystallogr D Biol Crystallogr* **66**, 486-501 (2010).
154. Brownlie, P. et al. The crystal structure of an intact human Max-DNA complex: new insights into mechanisms of transcriptional control. *Structure* **5**, 509-20 (1997).
155. Nair, S.K. & Burley, S.K. X-ray structures of Myc-Max and Mad-Max recognizing DNA. Molecular bases of regulation by proto-oncogenic transcription factors. *Cell* **112**, 193-205 (2003).
156. Thusberg, J., Olatubosun, A. & Vihinen, M. Performance of mutation pathogenicity prediction methods on missense variants. *Hum Mutat* **32**, 358-68 (2011).
157. Olatubosun, A., Valiaho, J., Harkonen, J., Thusberg, J. & Vihinen, M. PON-P: integrated predictor for pathogenicity of missense variants. *Hum Mutat* **33**, 1166-74 (2012).
158. Gonzalez-Perez, A. & Lopez-Bigas, N. Improving the assessment of the outcome of nonsynonymous SNVs with a consensus deleteriousness score, Condel. *Am J Hum Genet* **88**, 440-9 (2011).
159. Kenna, K.P., McLaughlin, R.L., Hardiman, O. & Bradley, D.G. Using Reference Databases of Genetic Variation to Evaluate the Potential Pathogenicity of Candidate Disease Variants. *Hum Mutat* (2013).
160. Gouet, P., Courcelle, E., Stuart, D.I. & Metoz, F. ESPript: analysis of multiple sequence alignments in PostScript. *Bioinformatics* **15**, 305-8 (1999).
161. Nagy, E. & Maquat, L.E. A rule for termination-codon position within intron-containing genes: when nonsense affects RNA abundance. *Trends Biochem Sci* **23**, 198-9 (1998).
162. Xu, W. et al. Oncometabolite 2-hydroxyglutarate is a competitive inhibitor of alpha-ketoglutarate-dependent dioxygenases. *Cancer Cell* **19**, 17-30 (2011).
163. Chou, A.P. et al. Identification of retinol binding protein 1 promoter hypermethylation in isocitrate dehydrogenase 1 and 2 mutant gliomas. *J Natl Cancer Inst* **104**, 1458-69 (2012).
164. Tomlinson, I.P. et al. Germline mutations in FH predispose to dominantly inherited uterine fibroids, skin leiomyomata and papillary renal cell cancer. *Nat Genet* **30**, 406-10 (2002).
165. Castro-Vega, L.J. et al. Germline mutations in FH confer predisposition to malignant pheochromocytomas and paragangliomas. *Hum Mol Genet* (2014).
166. Wang, L., Lam, G. & Thummel, C.S. Med24 and Mdh2 are required for Drosophila larval salivary gland cell death. *Dev Dyn* **239**, 954-64 (2010).
167. Frezza, C. et al. Haem oxygenase is synthetically lethal with the tumour suppressor fumarate hydratase. *Nature* **477**, 225-8 (2011).

168. Philip, B., Ito, K., Moreno-Sanchez, R. & Ralph, S.J. HIF expression and the role of hypoxic microenvironments within primary tumours as protective sites driving cancer stem cell renewal and metastatic progression. *Carcinogenesis* **34**, 1699-707 (2013).
169. Pan, Y. et al. Multiple factors affecting cellular redox status and energy metabolism modulate hypoxia-inducible factor prolyl hydroxylase activity in vivo and in vitro. *Mol Cell Biol* **27**, 912-25 (2007).
170. Schiavi, F. et al. Are we overestimating the penetrance of mutations in SDHB? *Hum Mutat* **31**, 761-2 (2010).
171. Clark, G.R. et al. Germline FH mutations presenting with pheochromocytoma. *J Clin Endocrinol Metab*, jc20141659 (2014).
172. Schimke, R.N., Collins, D.L. & Stolle, C.A. Paraganglioma, neuroblastoma, and a SDHB mutation: Resolution of a 30-year-old mystery. *Am J Med Genet A* **152A**, 1531-5 (2010).
173. van Nederveen, F.H. et al. An immunohistochemical procedure to detect patients with paraganglioma and phaeochromocytoma with germline SDHB, SDHC, or SDHD gene mutations: a retrospective and prospective analysis. *Lancet Oncol* **10**, 764-71 (2009).
174. Sambrook, J., Maniatis, T. & Fritsch, E.F. *Molecular cloning : a laboratory manual*, 3 v. (Cold Spring Harbor Laboratory, Cold Spring Harbor, N.Y., 1989).
175. Livak, K.J. & Schmittgen, T.D. Analysis of relative gene expression data using real-time quantitative PCR and the 2(-Delta Delta C(T)) Method. *Methods* **25**, 402-8 (2001).
176. Reich, M., Ohm, K., Angelo, M., Tamayo, P. & Mesirov, J.P. GeneCluster 2.0: an advanced toolset for bioarray analysis. *Bioinformatics* **20**, 1797-8 (2004).
177. Bergmeyer, H.U., Bergmeyer, J. & Grabl, M. *Methods of enzymatic analysis. III, Enzymes 1,. Oxireductases, transferases*, XXVI, 605 p. (Verlagchemie, Weinheim [etc.], 1983).
178. Bergmeyer, H.U., Bergmeyer, J. & Grabl, M. *Methods of enzymatic analysis. IV, Enzymes 2,. Esterases, glycosidases, lyases, ligases*, XIII, 426 p. (Verlagchemie, Weinheim [etc.], 1984).
179. Barrientos, A. In vivo and in organello assessment of OXPHOS activities. *Methods* **26**, 307-16 (2002).
180. Ausubel, F.M. Current protocols in molecular biology. v. (loose-leaf) (Greene Pub. Associates ; Wiley-Interscience, New York, 1988).
181. Heyn, H. et al. DNA methylation profiling in breast cancer discordant identical twins identifies DOK7 as novel epigenetic biomarker. *Carcinogenesis* **34**, 102-8 (2013).
182. Golub, T.R. et al. Molecular classification of cancer: class discovery and class prediction by gene expression monitoring. *Science* **286**, 531-7 (1999).
183. Alizadeh, A.A. et al. Distinct types of diffuse large B-cell lymphoma identified by gene expression profiling. *Nature* **403**, 503-11 (2000).
184. Perou, C.M. et al. Molecular portraits of human breast tumours. *Nature* **406**, 747-52 (2000).
185. Bittner, M. et al. Molecular classification of cutaneous malignant melanoma by gene expression profiling. *Nature* **406**, 536-40 (2000).
186. Sorlie, T. et al. Repeated observation of breast tumor subtypes in independent gene expression data sets. *Proc Natl Acad Sci U S A* **100**, 8418-23 (2003).
187. Hu, Z. et al. The molecular portraits of breast tumors are conserved across microarray platforms. *BMC Genomics* **7**, 96 (2006).
188. Parker, J.S. et al. Supervised risk predictor of breast cancer based on intrinsic subtypes. *J Clin Oncol* **27**, 1160-7 (2009).
189. Hopewell, R. & Ziff, E.B. The nerve growth factor-responsive PC12 cell line does not express the Myc dimerization partner Max. *Mol Cell Biol* **15**, 3470-8 (1995).
190. Ribon, V., Leff, T. & Saltiel, A.R. c-Myc does not require max for transcriptional activity in PC-12 cells. *Mol Cell Neurosci* **5**, 277-82 (1994).
191. Knudson, A.G., Jr. Mutation and cancer: statistical study of retinoblastoma. *Proc Natl Acad Sci U S A* **68**, 820-3 (1971).

192. Seeger, R.C. et al. Association of multiple copies of the N-myc oncogene with rapid progression of neuroblastomas. *N Engl J Med* **313**, 1111-6 (1985).
193. Zhu, J., Blenis, J. & Yuan, J. Activation of PI3K/Akt and MAPK pathways regulates Myc-mediated transcription by phosphorylating and promoting the degradation of Mad1. *Proc Natl Acad Sci U S A* **105**, 6584-9 (2008).
194. Jimenez, R.H. et al. Regulation of gene expression in hepatic cells by the mammalian Target of Rapamycin (mTOR). *PLoS One* **5**, e9084 (2010).
195. Kohl, N.E. et al. Transposition and amplification of oncogene-related sequences in human neuroblastomas. *Cell* **35**, 359-67 (1983).
196. Romero, O.A. et al. MAX inactivation in small cell lung cancer disrupts MYC-SWI/SNF programs and is synthetic lethal with BRG1. *Cancer Discov* **4**, 292-303 (2014).
197. Favier, J., Buffet, A. & Gimenez-Roqueplo, A.P. HIF2A mutations in paraganglioma with polycythemia. *N Engl J Med* **367**, 2161; author reply 2161-2 (2012).
198. Neumann, H.P. et al. Germ-line mutations in nonsyndromic pheochromocytoma. *N Engl J Med* **346**, 1459-66 (2002).
199. Eisenhofer, G. et al. Catecholamine metabolomic and secretory phenotypes in phaeochromocytoma. *Endocr Relat Cancer* **18**, 97-111 (2011).
200. Suls, A. et al. De novo loss-of-function mutations in CHD2 cause a fever-sensitive myoclonic epileptic encephalopathy sharing features with Dravet syndrome. *Am J Hum Genet* **93**, 967-75 (2013).
201. Hunt, D. et al. Whole exome sequencing in family trios reveals de novo mutations in PURA as a cause of severe neurodevelopmental delay and learning disability. *J Med Genet* **51**, 806-13 (2014).
202. Tatton-Brown, K. et al. Mutations in the DNA methyltransferase gene DNMT3A cause an overgrowth syndrome with intellectual disability. *Nat Genet* **46**, 385-8 (2014).
203. Michaud, J.L. et al. The genetic landscape of infantile spasms. *Hum Mol Genet* **23**, 4846-58 (2014).
204. Youssoufian, H. & Pyeritz, R.E. Mechanisms and consequences of somatic mosaicism in humans. *Nat Rev Genet* **3**, 748-58 (2002).
205. Hsu, L.Y. et al. Proposed guidelines for diagnosis of chromosome mosaicism in amniocytes based on data derived from chromosome mosaicism and pseudomosaicism studies. *Prenat Diagn* **12**, 555-73 (1992).
206. Menten, B. et al. Emerging patterns of cryptic chromosomal imbalance in patients with idiopathic mental retardation and multiple congenital anomalies: a new series of 140 patients and review of published reports. *J Med Genet* **43**, 625-33 (2006).
207. Lu, X.Y. et al. Genomic imbalances in neonates with birth defects: high detection rates by using chromosomal microarray analysis. *Pediatrics* **122**, 1310-8 (2008).
208. Conlin, L.K. et al. Mechanisms of mosaicism, chimerism and uniparental disomy identified by single nucleotide polymorphism array analysis. *Hum Mol Genet* **19**, 1263-75 (2010).
209. Solomon, D.A. et al. Mutational inactivation of STAG2 causes aneuploidy in human cancer. *Science* **333**, 1039-43 (2011).
210. Kaelin, W.G., Jr. Cancer and altered metabolism: potential importance of hypoxia-inducible factor and 2-oxoglutarate-dependent dioxygenases. *Cold Spring Harb Symp Quant Biol* **76**, 335-45 (2011).
211. Hu, C.J., Wang, L.Y., Chodosh, L.A., Keith, B. & Simon, M.C. Differential roles of hypoxia-inducible factor 1alpha (HIF-1alpha) and HIF-2alpha in hypoxic gene regulation. *Mol Cell Biol* **23**, 9361-74 (2003).
212. van Wijk, R. et al. Erythrocytosis associated with a novel missense mutation in the HIF2A gene. *Haematologica* **95**, 829-32 (2010).
213. Huang, S.C. et al. Duplication of the mutant RET allele in trisomy 10 or loss of the wild-type allele in multiple endocrine neoplasia type 2-associated pheochromocytomas. *Cancer Res* **60**, 6223-6 (2000).

214. Lo, R.K. & Wong, Y.H. Signal transducer and activator of transcription 3 activation by the delta-opioid receptor via Galpha14 involves multiple intermediates. *Mol Pharmacol* **65**, 1427-39 (2004).
215. Bassi, D.E. et al. PACE4 expression in mouse basal keratinocytes results in basement membrane disruption and acceleration of tumor progression. *Cancer Res* **65**, 7310-9 (2005).
216. Wang, Y. et al. PCSK6 regulated by LH inhibits the apoptosis of human granulosa cells via activin A and TGFbeta2. *J Endocrinol* **222**, 151-60 (2014).
217. Delic, S., Lottmann, N., Jetschke, K., Reifenberger, G. & Riemenschneider, M.J. Identification and functional validation of CDH11, PCSK6 and SH3GL3 as novel glioma invasion-associated candidate genes. *Neuropathol Appl Neurobiol* **38**, 201-12 (2012).
218. Hinoue, T. et al. Genome-scale analysis of aberrant DNA methylation in colorectal cancer. *Genome Res* **22**, 271-82 (2012).
219. Toyota, M. et al. CpG island methylator phenotype in colorectal cancer. *Proc Natl Acad Sci U S A* **96**, 8681-6 (1999).

APPENDIX: OTHER PUBLICATIONS

1. Pharmacogenomics J. 2014 Nov 4.

High frequency and founder effect of the CYP3A4*20 loss-of-function allele in the Spanish population classifies CYP3A4 as a polymorphic enzyme.

Apellániz-Ruiz M, Inglada-Pérez L, Naranjo ME, Sánchez L, Mancikova V, Currás-Freixes M, de Cubas AA, Comino-Méndez I, Triki S, Rebai A, Rasool M, Moya G, Grazina M, Opocher G, Cascón A, Taboada-Echalar P, Ingelman-Sundberg M, Carracedo A, Robledo M, Llerena A, Rodríguez-Antona C.

Cytochrome P450 3A4 (CYP3A4) is a key drug-metabolizing enzyme. Loss-of-function variants have been reported as rare events, and the first demonstration of a CYP3A4 protein lacking functional activity is caused by CYP3A4*20 allele. Here we characterized the world distribution and origin of CYP3A4*20 mutation. CYP3A4*20 was determined in more than 4000 individuals representing different populations, and haplotype analysis was performed using CYP3A polymorphisms and microsatellite markers. CYP3A4*20 allele was present in 1.2% of the Spanish population (up to 3.8% in specific regions), and all CYP3A4*20 carriers had a common haplotype. This is compatible with a Spanish founder effect and classifies CYP3A4 as a polymorphic enzyme. This constitutes the first description of a CYP3A4 loss-of-function variant with high frequency in a population. CYP3A4*20 results together with the key role of CYP3A4 in drug metabolism support screening for rare CYP3A4 functional alleles among subjects with adverse drug events in certain populations.

2. Genes Chromosomes Cancer. 2011 Nov;50(11):922-9.

VEGF, VEGFR3, and PDGFRB protein expression is influenced by RAS mutations in medullary thyroid carcinoma.

Mancikova V, Inglada-Pérez L, Curras-Freixes M, de Cubas AA, Gómez Á, Letón R, Kersten I, Leandro-García LJ, Comino-Méndez I, Apellaniz-Ruiz M, Sánchez L, Cascón A, Sastre-Marcos J, García JF, Rodríguez-Antona C, Robledo M.

BACKGROUND:

Tyrosine kinase inhibitors (TKIs) have achieved remarkable clinical results in medullary thyroid carcinoma (MTC) patients. However, the considerable variability in patient response to treatment with TKIs remains largely unexplained. There is evidence that it could be due, at least in part, to alterations in genes associated with the disease via their effect on the expression of TKI targets. The objective of this study was to evaluate the influence of RAS mutations on the expression levels in MTC tumors of eight key TKI target proteins.

METHODS:

We assessed by immunohistochemistry the expression of EGFR, KIT, MET, PDGFRB, VEGF, VEGFR1, VEGFR2, and VEGFR3 in a series of 84 primary MTC tumors that had previously been molecularly characterized, including 14 RAS-positive, 18 RET(M918T)-positive, and 24 RET(C634)-positive tumors, as well as 15 wild-type tumors with no mutations in the RET or RAS genes.

RESULTS:

In contrast to RET-positive tumors, RAS-positive tumors expressed neither PDGFRB nor MET (p=0.0060 and 0.047, respectively). Similarly, fewer RAS-positive than RET-related tumors expressed VEGFR3 (p=0.00062). Finally, wild-type tumors expressed VEGF more often than both RAS- and RET-positive tumors (p=0.0082 and 0.011, respectively).

CONCLUSIONS:

This is the first study identifying that the expression of TKI targets differs according to the presence of RAS mutations in MTC. This information could potentially be used to select the most beneficial TKI treatment for these patients.

3. Endocr Relat Cancer. 2013 Jul 12;20(4):611-9.

Influence of RET mutations on the expression of tyrosine kinases in medullary thyroid carcinoma.

Rodríguez-Antona C, Muñoz-Repeto I, Inglada-Pérez L, de Cubas AA, Mancikova V, Cañamero M, Maliszewska A, Gómez A, Letón R, Leandro-García LJ, Comino-Méndez I, Sanchez L, Alvarez-Escolá C, Aller J, Cascón A, Robledo M.

The therapeutic options for patients with metastatic medullary thyroid carcinoma (MTC) have recently increased due to the development of tyrosine kinase inhibitors (TKIs), some of which have achieved remarkable clinical responses in MTC patients. However, the molecular basis for the large variability in TKI responses is unknown. In this exploratory study, we investigated the expression of eight key TKI target proteins (EGFR, KIT, MET, PDGFRB, VEGF (VEGFA), VEGFR1 (FLT1), VEGFR2 (KDR), and VEGFR3 (FLT4)) by immunohistochemistry in 103 molecularly characterized MTC samples and identified the associated clinical and molecular features. A number of MTC samples exhibited a high expression of VEGFR2 and VEGFR3, which were overexpressed in 57 and 43% of the MTC samples respectively. VEGFR1, PDGFRB, VEGF, KIT, and MET were present in 34-20% of the cases, while EGFR was highly expressed in only 10% of the MTC samples. Some proteins exhibited large differences in expression between sporadic and familial cases, suggesting that different RET mutations may be associated with the immunohistochemical profiles. MTC samples with the C634 RET mutation exhibited a higher expression of VEGFR3 and KIT than the M918T RET-mutated and non-mutated RET tumor samples (P=0.005 and P=0.007 respectively) and a lower expression of VEGFR1 (P=0.04). Non-mutated RET MTC cases exhibited a lower expression of PDGFRB (P=0.04). Overall, this is the first study, to our knowledge, to show that multiple TKI targets are highly expressed in a subset of MTCs, suggesting that molecular stratification of patients may have the potential to improve TKI therapies for MTC.

4. Endocr Relat Cancer. 2013 Jun 24;20(4):477-93.

Integrative analysis of miRNA and mRNA expression profiles in pheochromocytoma and paraganglioma identifies genotype-specific markers and potentially regulated pathways.

de Cubas AA, Leandro-García LJ, Schiavi F, Mancikova V, Comino-Méndez I, Inglada-Pérez L, Perez-Martinez M, Ibarz N, Ximénez-Embún P, López-Jiménez E, Maliszewska A, Letón R, Gómez Graña A, Bernal C, Alvarez-Escolá C, Rodríguez-Antona C, Opocher G, Muñoz J, Megias D, Cascón A, Robledo M.

Pheochromocytomas (PCCs) and paragangliomas (PGLs) are rare neuroendocrine neoplasias of neural crest origin that can be part of several inherited syndromes. Although their mRNA profiles are known to depend on genetic background, a number of questions related to tumor biology and clinical behavior remain unanswered. As microRNAs (miRNAs) are key players in the modulation of gene expression, their comprehensive analysis could resolve some of these issues. Through characterization of miRNA profiles in 69 frozen tumors with germline mutations in the genes SDHD, SDHB, VHL, RET, NF1, TMEM127, and MAX, we identified miRNA signatures specific to, as well as common among, the genetic groups of PCCs/PGLs. miRNA expression profiles were validated in an independent series of 30 composed of VHL-, SDHB-, SDHD-, and RET-related formalin-fixed paraffin-embedded PCC/PGL samples using quantitative real-time PCR. Upregulation of miR-210 in VHL- and SDHB-related PCCs/PGLs was verified, while miR-137 and miR-382 were confirmed as generally upregulated in PCCs/PGLs (except in MAX-related tumors). Also, we confirmed overexpression of miR-133b as VHL-specific miRNAs, miR-488 and miR-885-5p as RET-specific miRNAs, and miR-183 and miR-96 as SDHB-specific miRNAs. To determine the potential roles miRNAs play in PCC/PGL pathogenesis, we performed bioinformatic integration and pathway analysis using matched mRNA profiling data that indicated a common enrichment of pathways associated with neuronal and neuroendocrine-like differentiation. We demonstrated that miR-183 and/or miR-96 impede NGF-induced differentiation in PC12 cells. Finally, global proteomic analysis in SDHB and MAX tumors allowed us to determine that miRNA regulation occurs primarily through mRNA degradation in PCCs/PGLs, which partially confirmed our miRNA-mRNA integration results.

5. Endocr Relat Cancer. 2013 May 30;20(3):L1-6.

Genetics of pheochromocytoma and paraganglioma in Spanish pediatric patients.

Cascón A, Inglada-Pérez L, Comino-Méndez I, de Cubas AA, Letón R, Mora J, Marazuela M, Galofré JC, Quesada-Charneco M, Robledo M.

(LETTER TO THE EDITOR)

6. Cancer Res. 2012 Sep 15;72(18):4744-52.

Hematologic β-tubulin VI isoform exhibits genetic variability that influences paclitaxel toxicity.

Leandro-García LJ, Leskelä S, Inglada-Pérez L, Landa I, de Cubas AA, Maliszewska A, Comino-Méndez I, Letón R, Gómez-Graña Á, Torres R, Ramírez JC, Álvarez S, Rivera J, Martínez C, Lozano ML, Cascón A, Robledo M, Rodríguez-Antona C.

Cellular microtubules composed of α-β-tubulin heterodimers that are essential for cell shape, division, and intracellular transport are valid targets for anticancer therapy. However, not all the conserved but differentially expressed members of the β-tubulin gene superfamily have been investigated for their role in these settings. In this study, we examined roles for the hematologic isoform β-tubulin VI and functional genetic variants in the gene. β-tubulin VI was highly expressed in blood cells with a substantial interindividual variability (seven-fold variation in mRNA). We characterized DNA missense variations leading to Q43P, T274M, and R307H, and a rare nonsense variant, Y55X. Because variations in the hematologic target of microtubule-binding drugs might alter their myelosuppressive action, we tested their effect in cell lines stably expressing the different β-tubulin VI full-length variants, finding that the T274M change significantly decreased sensitivity to paclitaxel-induced tubulin polymerization. Furthermore, patients treated with paclitaxel and carrying β-tubulin VI T274M exhibited a significantly lower thrombocytopenia than wild-type homozygous patients (P = 0.031). Together, our findings define β-tubulin VI as a hematologic isotype with significant genetic variation in humans that may affect the myelosuppresive action of microtubule-binding drugs. A polymorphism found in a tubulin isoform expressed only in hemapoietic cells may contribute to the patient variation in myelosuppression that occurs after treatment with microtubule-binding drugs.

7. Clin Cancer Res. 2012 Aug 15;18(16):4441-8.

Regulatory polymorphisms in β-tubulin IIa are associated with paclitaxel-induced peripheral neuropathy.

Leandro-García LJ, Leskelä S, Jara C, Gréen H, Avall-Lundqvist E, Wheeler HE, Dolan ME, Inglada-Perez L, Maliszewska A, de Cubas AA, Comino-Méndez I, Mancikova V, Cascón A, Robledo M, Rodríguez-Antona C.

PURPOSE:

Peripheral neuropathy is the dose-limiting toxicity of paclitaxel, a chemotherapeutic drug widely used to treat several solid tumors such as breast, lung, and ovary. The cytotoxic effect of paclitaxel is mediated through β-tubulin binding in the cellular microtubules. In this study, we investigated the association between paclitaxel neurotoxicity risk and regulatory genetic variants in β-tubulin genes.

EXPERIMENTAL DESIGN:

We measured variation in gene expression of three β-tubulin isotypes (I, IVb, and IIa) in lymphocytes from 100 healthy volunteers, sequenced the promoter region to identify polymorphisms putatively influencing gene expression and assessed the transcription rate of the identified variants using luciferase assays. To determine whether the identified regulatory polymorphisms were associated with paclitaxel neurotoxicity, we genotyped them in 214 patients treated with paclitaxel. In addition, paclitaxel-induced cytotoxicity in lymphoblastoid cell lines was compared with β-tubulin expression as measured by Affymetrix exon array.

RESULTS:

We found a 63-fold variation in β-tubulin IIa gene (TUBB2A) mRNA content and three polymorphisms located at -101, -112, and -157 in TUBB2A promoter correlated with increased mRNA levels. The -101 and -112 variants, in total linkage disequilibrium, conferred TUBB2A increased transcription rate. Furthermore, these variants protected from paclitaxel-induced peripheral neuropathy [HR, 0.62; 95% confidence interval (CI), 0.42-0.93; P = 0.021, multivariable analysis]. In addition, an inverse correlation between TUBB2A and paclitaxel-induced apoptosis (P = 0.001) in lymphoblastoid cell lines further supported that higher TUBB2A gene expression conferred lower paclitaxel sensitivity.

CONCLUSIONS:

This is the first study showing that paclitaxel neuropathy risk is influenced by polymorphisms regulating the expression of a β-tubulin gene.

8. Genes Chromosomes Cancer. 2011 Nov;50(11):922-9.

Detection of the first gross CDC73 germline deletion in an HPT-JT syndrome family.

Cascón A, Huarte-Mendicoa CV, Javier Leandro-García L, Letón R, Suela J, Santana A, Costa MB, Comino-Méndez I, Landa I, Sánchez L, Rodríguez-Antona C, Cigudosa JC, Robledo M.

Hereditary primary hyperparathyroidism (HPT) may develop as a solitary endocrinopathy (FIHP) or as part of multiple endocrine neoplasia Type 1, multiple endocrine neoplasia Type 2A, or hereditary HPT-jaw tumor syndrome. Inactivating germline mutations of the tumor suppressor gene CDC73 account for 14 and 50% of all FIHP and HPT-JT patients, respectively, and have also been found in almost 20% of apparently sporadic parathyroid carcinoma patients. Although more than 60 independent germline mutations have been described, to date no rearrangement affecting the CDC73 locus has been identified. By means of multiplex-PCR we found a large germline deletion affecting the whole gene in a two-generation HPT-JT family. Subsequently array-CGH and specific PCR analysis determined that the mutation spanned ~ 547 kb, and included four additional genes: TROVE2, GLRX2, B3GALT2, and UCHL5. Although no clear mutation-specific phenotype was found associated to the presence of the mutation, further studies are needed to assess whether the loss of the neighboring genes could modify the phenotype of carriers. There was complete absence of nuclear staining in the two HPT-JT-related tumors available. The finding of the first rearrangement affecting the CDC73 gene warrants screening for this tumor suppressor gene inactivation mechanism not only in high-risk CDC73 point mutation-negative HPT-JT families, but also in FIHP patients.